The Role of 6-O-Sulphated Heparan Sulphate in Chronic Renal Fibrosis

Abd Alrasol Alhasan

A thesis submitted in partial fulfillment of the requirements for the degree Doctor of Philosophy

Institute of Cellular Medicine (ICM)
Newcastle University, UK

2012

The Role of 6-O-Sulphated Heparan Sulphate in Chronic Renal Fibrosis

Abd Alrasol Alhasan

A thesis submitted in partial fulfilment of the requirements for the degree Doctor of Philosophy

Institute of Cellular Medicine (ICM)
Newcastle University, UK

2012

Abstract

Heparan sulphate (HS) plays crucial roles during the genesis and resolution of inflammation by sequestration, stabilization and presentation of proinflammatory cytokines and growth factors. The interaction between many of these factors and HS is critically dependent on the variable distribution of anionic 6-O-sulphated glucosamine residues within the structure of HS. The pattern of 6-O-sulphation is generated during HS biosynthesis by HS-6-O-sulphotransferases (HS6STs) but can be modified later by cell-surface HS-6-O-endosulphatases (SULFs). This study was designed to examine the potential contribution of these enzyme families to renal fibrosis following chronic inflammation.

Initial experiments showed that the fibrogenic cytokine TGF-β induced SULF2 expression by renal tubular epithelial cells. Immortalized renal tubular epithelial cells were transfected to constitutively overexpress either HS6ST1 or SULF2 in order to examine the effect of these enzymes on cytokine function. Cells which overexpressed HS6ST1 showed increased binding of FGF2 compared to mock transfected control cells; this FGF2 binding correlated with increased pERK expression and enhanced cell proliferation. The requirement for HS for these processes was validated by inhibition of FGF2 binding with soluble HS, heparin or heparitinase III, whilst the importance of HS sulphation for increased binding was demonstrated after treatment of the cells with chlorate. Structural analysis of ^{35}S-labelled HS from HS6ST1 overexpressing cells demonstrated an increase in mono-6-O-sulphated disaccharides accompanied by a decrease in 2-O-sulphated iduronic acid. By contrast, SULF2 transfectants showed reduced FGF2 binding, ERK activation and proliferation. Structural analysis of ^{35}S-labelled HS from these cells showed a 50% reduction in 6-O-sulphation with a parallel increase in mono-2-O-sulfated iduronic acid.

The significance of the in vitro study for renal fibrosis was then examined using a murine unilateral ureteric obstruction (UUO) model. Immunochemical analysis of UUO kidney sections showed a significant increase in expression of epitopes containing N- and 6-O sulphated HS around the renal tubules. This change was accompanied by a 5-fold increase in expression of the SULF1 gene. In summary, this study suggests that modulation of the expression of sulphate at the 6-O position in HS plays a significant role in the progression of chronic renal fibrosis by alteration of the biological activity of fibrogenic growth factors.

Acknowledgments

The work presented in this thesis was generously funded by Aleppo University and the ministry of Higher Education at the Syrian Arab Republic. Research Fund, without whose support my studies would have been impossible. I would like to take the opportunity to thank those people who were really real family to me and surrounded me with every support and encouragement. In the first instance my supervisors Professor Simi Ali and Professor John Kirby for the opportunity to join the Applied Immunology group and their endless support. They always gave encouragements and never hesitated to give all kind of support inside and outside the laboratory. Their family-atmosphere helped me always to overcome all obstacles during my research period.

Many thanks also to all members of the group Maureen Kirkley, Graeme O'Boyle, Yulia Spielhofer, Watchara Pichitsiri, David Swan and Fatmah Naemi for their help. Thanks also to Dr. Jeremy Palmer, Dr. Helen Robertson, Dr. Trevor Booth, Xin Xu and Dr. Daniel Richard. Many thanks also to Professor Marion Kusche-Gullberg, in Norway for her help in HS structure analyses. Many thanks to Professor van Kuppevelt and Arie Osdterhof for generous gift of phage display antibodies.

Thanks also go to my office members who were always helpful and supportive: Marzena Ciechomska, Dominic Hine, Karim Bennaceur and Eirini Giannoudaki. Many thanks also to my supervisor in Aleppo University Dr. Omar Balach for his support.

Many thanks to all friends and family members for help and support. THANK YOU ALL

Table of contents

1 General introduction 1

1.1 Background to this study 2

1.2 Transplantation and inflammatory response 2

1.3 Transplant rejection 2

1.3.1 Hyperacute rejection 3

1.3.2 Acute rejection 3

1.3.3 Chronic rejection (CR) 3

1.4 The extracellular matrix 9

1.5 Heparan sulphate proteoglycans (HSPG) 9

1.6 Heparan sulphate (HS) 11

1.6.1 Initiation 11

1.6.2 Elongation and polymerization 12

1.6.3 Modification 12

1.6.4 HS modifying enzymes 13

1.6.5 HS sulphation 19

1.6.6 HS-protein interactions 20

1.7 Chemokines 21

1.7.1 Chemokine-HS interaction 22

1.7.2 Leucocyte extravasation 23

1.8 Fibroblast growth factors (FGF) 25

1.8.1 FGF2 and renal fibrogenesis 25

1.8.2 FGF-HS interaction 26

1.8.3 FGF-HS binding epitope 28

1.9 The Role of HS in the regulation of transplant rejection 29

1.9.1 HS in kidney 29
1.9.2 HS in inflammation 30
1.9.3 Role of HS in chronic rejection 31
1.10 Hypothesis 33
1.11 Specific Aims 33
Chapter two 34
2 General materials and methods 34
2.1 Laboratory procedure 35
2.2 Culture media 35
2.2.1 Dulbecco's Modified Eagle Medium (DMEM) 35
2.2.2 DMEM-ham's F12 medium 35
2.2.3 MCDB-131 medium 35
2.2.4 Propagation of cell lines 36
2.3 Cell lines 36
2.3.1 Human kidney (HK2) 36
2.3.2 Human kidney (HKC8) 36
2.3.3 Human microvascular endothelial cell line (HMEC-1) 36
2.3.4 Chinese hamster ovary cells (CHO) 36
2.3.5 EAhy.926 37
2.4 Sub-culture work 37
2.4.1 Adherent cells 37
2.4.2 Cell counting and viability 37
2.4.3 Cryopreservation of cells in liquid nitrogen 37
2.4.4 Mycoplasma screening test 38
2.5 General Molecular Biology 38

2.5.1 RNA isolation 38
2.5.2 Nucleotide quantification 39
2.5.3 RNA separation by gel electrophoresis 39
2.5.4 Synthesis of cDNA 39
2.5.5 Transformation 40
2.5.6 DNA transfection 44
2.5.7 DNA sequencing and alignment 46
2.5.8 Conventional PCR 47
2.5.9 Quantitative PCR (qPCR) 49
2.6 Protein chemistry 54
2.6.1 Protein extraction 54
2.6.2 Protein assay 54
2.6.3 SDS-PAGE 55
2.6.4 Western blotting 56
2.7 Flow Cytometry 57
2.7.1 General principles 57
2.7.2 Immunofluorescence antibody labelling 57
2.7.3 Cell stimulation and phenotyping 58
2.7.4 Antibody labelling 59
2.7.5 Phage display antibody 59
2.8 Statistical analysis 60
3 The Effect of HS6ST1 on HS Structure and Biological Activity 61
3.1 Introduction 62
3.1.1 HS6ST modifying enzyme 62
3.1.2 HS detecting antibodies 62

3.1.3 HS6ST function and physiological role 63
3.1.4 Specific aims 65
3.2 Specific materials and methods 66
3.2.1 FGF2 binding assay 66
3.2.2 CCL5 binding assay 66
3.2.3 Proliferation assay 67
3.2.4 Isotope ^{35}S labelling 68
3.2.5 HS-Heparitinase III treatment 70
3.3 Results 70
3.3.1 Cell Phenotyping 70
3.3.2 Expression of HS6ST1 by conventional PCR 74
3.3.3 Cell stimulation and FGF2 binding 77
3.3.4 Cell stimulation and 10E4 binding 78
3.3.5 Generating of stable HS6ST1 transfectants 79
3.3.6 Transfection procedure 80
3.3.7 Interactions of HS6ST1 transfectant 83
3.3.8 HS6ST1 transfectant binding with FGF2 88
3.3.9 HS structural analysis 97
3.3.10 HS6ST1 and proliferation assay 99
3.3.11 HS6ST1 overexpression and ERK phosphorylation 101
3.4 Discussion 103
3.4.1 Characterization of cell lines 103
3.4.2 Observations of HS6ST1 expression 104
3.4.3 Observation of HS epitopes 104
3.4.4 Observations with FGF2 106

3.4.5 Observation of HS structure....108
4 The Process of HS Degradation....110
4.1 Introduction....111
4.2 HS degradation....111
4.2.1 Sulphatase enzymes....111
4.2.2 Aims....115
4.3 Specific materials and methods....116
4.3.1 SULF2 sequencing and alignment....116
4.3.2 Cell stimulation....117
4.3.3 RT-PCR....118
4.4 Results....120
4.4.1 Cell stimulation and HS degradation enzymes....120
4.4.2 Generation of stable transfectants of SULF2....126
4.4.3 Characterization of SULF-2 transfectants....129
4.4.4 Analysis of the structure of ^{35}S labelled HS....136
4.4.5 Proliferation of the SULF-2 transfectants....138
4.4.6 SULF2 transfectants and ERK activation....139
4.5 Discussion....141
4.5.1 Observation of gene expression following cytokine stimulation....141
4.5.2 Observation of changes in HS epitope expression....143
4.5.3 Physiological changes after SULF2 transfection....144
4.5.4 Examination of HS structure....145
5 HS Changes in UUO Mouse Model....148
5.1 Introduction....149
5.1.1 UUO kidney and chronic rejection....149

5.1.2 Fibrosis markers 150
5.2 Aims 151
5.3 Specific materials and methods 152
5.3.1 Mice maintenance 152
5.3.2 RNA extraction from mouse kidney 153
5.3.3 Frozen sections 154
5.3.4 Primer probes 154
5.3.5 RT-PCR validity test 155
5.3.6 Haematoxylin and Eosin staining (H&E) 156
5.3.7 Immunohistochemistry 156
5.3.8 Mouse on mouse (M.O.M) staining 157
5.4 Results 159
5.4.1 Haematoxylin and eosin staining (H&E) 159
5.4.2 Fibrosis markers 159
5.4.3 Staining with 10E4 antibody 163
5.4.4 Staining with phage display antibodies 163
5.4.5 Gene expression of HS modifying enzymes 170
5.5 Discussion 171
5.5.1 Observation on fibrosis markers 171
5.5.2 Observation on HS changes 171
5.5.3 Observation on mRNA level 173
6 General discussion and conclusion 175
6.1 Summary of findings 176
6.1.1 Introduction 176
6.1.2 Effect of HS6ST1 on FGF2 binding 176

6.1.3 The effect of HS6ST1 over-expression on HS structure 178
6.1.4 The biological effect of SULF2 overexpression 178
6.1.5 Effect of SULF2 overexpression on HS structure 180
6.1.6 Changes of HS sulphation in the UUO mouse model.....180
6.2 Implication of this study.....182
6.3 Future work 183
Chapter Seven 185
7 References and Appendices 185
Appendices.....215
A. Verification of HS6ST1 sequence cloned in vector with HS6ST1 transfectants using reverse BGH primers 215
B. Insert SULF2 align with human SULF2 using –bGHR.....216
C. HS structure analysis (S^{35}) 219
D. HS6ST1 transfectants binding to CCL5 222
E. Publication arising from this study…….. 224
F. Prizes 224

LIST OF FIGURES

Figure 1.1. Model of proteoglycan structure. 10
Figure 1.2. Heparan sulphate modifying. 14
Figure 1.3. Disaccharide structure of heparan sulphate. 17
Figure 1.4. Leucocyte extravasation. 24
Figure 1.5. The ternary complex of FGF-HS-FGFR. 27
Figure 2.1. Drawing of the plasmid vector (pcDNA3.1/zeo+) and HS6ST1 insert. 47
Figure 2.2. Diagram showing primer probes fluorescence during real time PCR. 50
Figure 2.3. Efficiency of qPCR reaction for human GAPDH and HS6ST1 genes. 54
Figure 3.1. HK2 cells stained with anti E-cadherin antibody. 71
Figure 3.2. Flow cytometric demonstration of MHC-II expression after stimulation with IFN-γ. 72
Figure 3.3. Expression of class II MHC antigen after stimulation with IFN-γ 73
Figure 3.4. EAhy-926 cells stained with anti CD31 antibody. 74
Figure 3.5. Agarose gel electrophoresis of RNAs from different cell lines.. 75
Figure 3.6. Agarose gel electrophoresis of HS6ST1 expression by reverse transcription PCR. 76
Figure 3.7. Stimulation of HS6ST1 expression by cytokines.. 77
Figure 3.8. Binding of FGF2 following cytokine stimulation. 78
Figure 3.9. Binding of 10E4 antibody to HK2 cells after cytokine stimulation.. 79
Figure 3.10. Agarose gel electrophoresis of restriction digested plasmids. 80
Figure 3.11. Determination of the transfection efficiency for HK2 cells transfected with GFP. 82
Figure 3.12. HS6ST1 expression of HK2 stable transfectants using qPCR. 83
Figure 3.13. Representative HS6ST1 transfectant binding to 10E4 antibody. 84
Figure 3.14. Binding of HS6ST1 transfectants to 10E4. 84
Figure 3.15. Binding of HS3A8 phage display antibody to HS6ST1 transfectants. 85
Figure 3.16. Representative histogram showing the binding of HS4C3 to HS6ST1 transfected cells. 86
Figure 3.17. Representative histogram of HS6ST1 transfectant binding to RB4EA12. 87
Figure 3.18. Analyses of HS4C3 and RB4EA12 binding to HS6ST1 transfectants. 87
Figure 3.19. Representative histograms showing optimization of the FGF2 binding assay. 88

Figure 3.20. Optimization of the biotinylated FGF2 binding assay. 89
Figure 3.21. Optimization of FGF2 and effect on specificity. 90
Figure 3.22. Analysis of 10E4 binding to chlorate-treated wild-type and HS6ST1 transfected cells. 91
Figure 3.23. FGF2 binding to WT-CHO, CHO-745 (GAG mutant) and CHO-677 (HS mutant) cells. 92
Figure 3.24. FGF2 binding in presence of sodium chlorate. 93
Figure 3.25. FGF2 binding after incubation with heparitinase III. 94
Figure 3.26. Representative histogram of flow cytometry for FGF2 binding to HS6ST1 transfectants. 95
Figure 3.27. The effect of HS6ST1 overexpression on FGF2 binding. 95
Figure 3.28. FGF2 binding in presence of inhibitors. 96
Figure 3.29. FGF2 binding in presence of heparin. 97
Figure 3.30. HS disaccharide composition in HS6ST1 transfectants. 98
Figure 3.31. Sulphate group changes produced by HS6ST1 overexpression.. 99
Figure 3.32. Representative figure showing a proliferation assay by cell counting.. 100
Figure 3.33. Representative results of colourimetric proliferation assay for HS6ST1 transfectants. A, Cells were seeded in 96 well plates in triplicates with 0.05%FCS and incubated for 24, 48, 72 and 96 hours. 101
Figure 3.34. Representative Western blot of pERK1,2 in HS6ST1 and mock transfectants.. 102
Figure 4.1. Drawing of plasmid pcDNA3.1/Myc-His- (vector) and SULF2 gene (insert).....116
Figure 4.2. Plasmid encoding SULF2 digested with *XhoI* and *HindIII*. 117
Figure 4.3. RT-PCR efficiency with specific primer/probe combinations 118
Figure 4.4. Expression of heparanase (HPSE) by EAhy.926 after stimulation with cytokines. 121
Figure 4.5. Expression of HPSE by HK2 cells after stimulation. 122
Figure 4.6. Expression of SULF1 by EAhy.926 after stimulation. 123
Figure 4.7. Expression of SULF1 by HK2 cells after stimulation. 124
Figure 4.8. Expression of sulphatase 2 (SULF2) by EAhy.926 after stimulation. 125
Figure 4.9. Expression of SULF2 by HK2 cells after stimulation. 126
Figure 4.10. Representative histogram of GFP transfection efficiency.. 127

Figure 4.11. Expression of SULF2 in renal epithelial (HKC8) stable transfectants.....128
Figure 4.12. Characterization of HS sulphation of SULF2 transfectants binding to 10E4. 129
Figure 4.13. Representative image of SULF2 transfectants stained with 10E4 antibody 130
Figure 4.14. Quantitative analysis of SULF2 transfectants stained with 10E4 antibody. 131
Figure 4.15. Phage display antibody HS3A8 binding to SULF2 transfectants. 132
Figure 4.16. Phage display antibody HS4C3 binding to SULF2 transfectants.....133
Figure 4.17. Phage display RB4EA12 binding to renal epithelial SULF2 transfectants. 134
Figure 4.18. Binding of FGF2 to SULF2 transfectants. 135
Figure 4.19. SULF2 transfectants binding to CCL5. 136
Figure 4.20. HS disaccharides analysis of SULF2 transfectants. 137
Figure 4.21. Sulphate group changes in SULF2 transfectants. 138
Figure 4.22. Representative proliferation assay for SULF2 transfectants.. 139
Figure 4.23. Western blotting of pERK1,2 for SULF2 transfectants in presence of FGF2...140
Figure 5.1. Unilateral ureteral obstruction mice kidney. 152
Figure 5.2. Representative gel photograph showing RNA extracted from frozen UUO kidney. 154
Figure 5.3. Efficiency of qPCR reaction for murine HPRT1,SULF1and SULF2 genes. 156
Figure 5.4. Staining of mice kidney sections with haematoxylin and eosin (H&E).....160
Figure 5.5. Staining of mice kidney sections with Collagen-1. 161
Figure 5.6. Quantitative analyses of tubular collagen-1 staining of UUO mice kidney.....161
Figure 5.7. Representative image of UUO kidney staining with anti α-SMA antibody.....162
Figure 5.8. Quantitative analysis of mean fluorescence intensity of UUO staining with.....163
Figure 5.9. Representative staining of mice kidney with 10E4 antibody.. 164
Figure 5.10. Quantitative analyses of UUO sections staining with 10E4 antibody.....164
Figure 5.11. Representative staining of murine kidney with phage display HS3A8 antibody. 165
Figure 5.12. Quantitative analyses of UUO section staining with phage display HS3A8 antibody.....166
Figure 5.13. Representative staining of mice kidney with phage display HS4C3 antibody..167
Figure 5.14. Quantitative analyses of UUO sections stained with HS4C3 antibody.....168
Figure 5.15. Representative mice kidney sections stained with RB4EA12 phage display antibody.....169

Figure 5.16. Quantitative analyses of UUO section staining with phage display RB4EA12 antibody.....169
Figure 5.17. Quantitative RT-PCR analyses of gene expression in UUO kidney. 170
Figure 6.1. A summary of the effect of changes in HS sulphation on the biology of renal epithelial cells and the development of UUO pathology. 181

LIST OF TABLES

Table 1.1, Mechanisms of fibrosis (table adapted from Strutz et al., 2003). 5
Table 2.1. Agar plates distribution in transformation. 41
Table 2.2. Transfection reagent optimization (Qiagen). 45
Table 2.3. Thermal cycler conditions for conventional PCR. 48
Table 2.4. Optimal concentrations of PCR mix components. 48
Table 2.5. Primer sequences for conventional PCR amplification. 49
Table 2.6. Real time PCR conditions. 51
Table 2.7. Contents of qPCR tube reaction. 52
Table 2.8. Primer probes for RT-PCR 53
Table 2.9. Components of 10% resolving and stacking acrylamide gels. 55
Table 2.10. Epitopes of HS antibody specific antibodies. 60
Table 3.1. Optimization of transfection procedure. 81
Table 6.1. A summary of FGF2 and phage display antibody binding with HS6ST1 and SULF2 transfectants FGF2 and phage display antibodies. 179

ABBREVIATIONS

APS	Ammonium Persulphate
AT-III	Antithrombin-III
BCA	Bicinochoninic Acid
BSA	Bovine Serum Albumin
CHO	Chinese Hamster Ovary
CR	Chronic Rejection
DAPI	4, 6-Diamidino-2-Phenylindole
DMEM	Dulbecco's Modified Eagle Medium
DEPC	Diethyl Percarbonate
DMSO	Dimethyl Sulphoxide
DNA	Deoxyribonucleic Acid
DTT	Dithiotheritol
ECM	Extracellular Matrix
EDTA	Ethylenediamintetraacetic Acid
ERK	Extracellular Regulated Kinase
EXT	Exostoses
FBS	Fetal Bovine Serum
FCS	Fetal Calf Serum
FGF	Fibroblast Growth Factor
FGFR	Fibroblast Growth Factor Receptor
GAG	Glycosaminoglycan
GAPDH	Glyceraldehyde 3 phosphate dehydrogenase
GBM	Glomerulus Basement Membrane
GFP	Green Fluorescent Protein

GlcA	Glucuronic Acid
GPCR	G-protein Coupled Receptor
H&E	Haematoxylin and Eosin
HCC	Hepatic carcinoma cell line
HCL	Hydrochloric Acid
HGF	Hepatocyte Growth Factor
HK2	Human Kidney
HMEC	Human Microvascular Endothelial cells
HMC	Human Mesangial Cells
HLA	Human Leucocyte Antigen
HS	Heparan Sulphate
HS6ST	Heparan Sulphate 6-sulphotransferase
HPLC	High performance Liquid Chromatography
HPSE	Heparanase
HPRT1	Hypoxanthine phosphoribosyltransferase 1
HSPG	Heparan Sulphate Proteoglycan
HSV	Herpes Simplex Virus
ICAM	Intracellular Adhesion Molecule
IdoA	Iduronic Acid
IFN	Interferon
IL	Interleukin
LPS	Lipopolysaccharide
MHC	Major Histocompatibility Complex
MCP-1	Monocyte Chemoattractant Protein-1
NDST	N-deacetylase/N-sulphotransferase

OST	O-Sulphotransferase
PAGE	Polyacrylamide Gel Electrophoresis
PAPS	3'Phosphoadenosine 5'-Phosphosulphate
PBMC	Peripheral Blood Mononuclear Cells
PBS	Phosphate buffered Saline
PCR	Polymerase Chain Reaction
PDGF	Platelet Derived Growth Factor
PFA	Paraformaldehyde
PMA	Phorbol Myristate Acetate
RNA	Ribonucleic Acid
SDS	Sodium Dodecyl Sulphate
SMA	Smooth Muscle Actin
siRNA	Short Interfering RNA
SULF	Sulphatase
SV40	Simian Virus 40
TA/IF	Tubular atrophy/ interstitial fibrosis
TBS	Tris Buffered Saline
TBST	Tris Buffered Saline Tween-20
TEMED	Tetramethylethylenediamine
TGF-ß	Transforming Growth Factor beta
TNF	Tumour Necrosis Factor
UDP	Uridine Diphosphate
UUO	Unilateral Ureteral Obstruction
VCAM-1	Vascular Cell Adhesion Molecule-1
VEGF	Vascular Endothelial Growth Factor

Chapter One

1 General introduction

1.1 Background to this study

This thesis addresses the role of heparan sulphate (HS) in the etiology of chronic renal allograft rejection. The main reason for losing a transplanted kidney is chronic rejection which is a complex process that involves inflammation and ends in graft dysfunction. Infiltrating leucocytes, endothelial and epithelial cells, cytokines and chemokines all play key role in this process. Heparan sulphate is ubiquitously expressed on all mammalian cell surfaces and the extracellular matrix. Heparan sulphate can interact with many factors of relevance to graft failure. The sulphation of heparan sulphate plays a crucial role in determining its biological activity. Sulphation of heparan sulphate is a multi-step process which is performed specifically by different modifying enzymes. Loss or gain of sulphation affects the binding, binding affinity and signalling pathway of growth factor-receptor interactions. Better understanding of the roles of heparan sulphate in allograft dysfunction might help in improving and maintaining long term allograft survival.

1.2 Transplantation and inflammatory response

Allogenic transplantation initiates a complex and multi-level immune response which recognizes the non-self organ in an initial step that precedes graft damage and rejection. Renal transplantation may result in severe inflammatory response because of ischemia–reperfusion injury despite recipient-donor major histocompatibility complex (MHC) matching (Ysebaert *et al.*, 2000). Graft damage can be classified into several levels depending on time and type of immune response.

1.3 Transplant rejection

Organ allogenic transplantation is the final therapy for end-stage organ failure. Many organs can be transplanted including kidney, liver, heart and pancreas. The first successful human kidney transplant operation took place in 1954 between identical twin brothers in Boston, USA and was performed by Dr. J Murray (Murray, 2002). Organ transplantation is now performed more routinely between genetically different recipients and donors. Although cross-matching tests are performed before transplantation, several anti-mitotic and immunosuppressive drugs need to be given to recipients in order to avoid rejection. The transplanted organ is

susceptible to different types of rejection depending on time of rejection, mechanisms and mediators involved (Terasaki, 2003).

1.3.1 Hyperacute rejection

Hyperacute rejection occurs minutes after transplantation, and is usually mediated by pre-formed anti-donor human leucocyte antigen (HLA)-specific antibodies (Kissmeyer-Nielsen *et al.*, 1966; Sumitran-Holgersson, 2001). These antibodies recognize graft antigens and activate the complement system. Due to cross matching and tissue typing of major histocompatibility molecules (MHC) and ABO, this type of rejection is limited nowadays.

1.3.2 Acute rejection

Acute allograft rejection takes place weeks after transplantation due to mismatching between recipient anti-HLA antibodies and donor tissues. Acute renal allograft rejection is considered both a T cell-mediated (cellular response) and an antibody-mediated process (humoral response) (Le Moine *et al.*, 2002; Terasaki, 2003).

Graft cells are exposed to a specific T-cell mediated immune response initiated by the release of a range of pro-inflammatory cytokines such as interferon-γ (IFN-γ), interleukin-2 (IL-2) and IL-4. After recognizing allograft antigens, $CD4^+$ T cells can differentiate into Th1, Th2 or Th17 subsets which secrete pro-inflammatory cytokines that stimulate additional activities such as T cell proliferation and antibody secretion. These activities consistently lead to an inflammatory response, leukocyte infiltration and tissue damage (Flach *et al.*, 1998).

The humoral response produces alloantibodies against mismatched MHC molecules, ABO antigens and endothelial cells (Win and Pettigrew, 2010). Antibodies against donor tissue are involved in acute and chronic rejection (Terasaki and Cai, 2008).

1.3.3 Chronic rejection (CR)

Chronic allograft rejection constitutes the primary cause of graft loss which often occurs even in cases of high compatibility between donor and recipient. Chronic

rejection takes place months or years after transplantation due to the effect of factors which lead to a loss of graft function.

Recognition of donor antigens leads to a severe reaction towards graft cells and causes decreased long-term survival. The incidence of acute rejection and intratubular infiltration of T cells constitutes one of the most serious reasons for CR (Robertson *et al.*, 2004). Graft damage is usually accompanied by T cell infiltration and proinflammatory cytokine secretion (Waaga *et al.*, 2000).

Chronic renal rejection constitutes the end stage of chronic vascular, glomerular and interstitial inflammation. Tubules and the interstitium form about 90% of the kidney volume, which correlates with kidney function (Nath, 1998). A transplanted graft undergoing chronic rejection displays features similar to what is seen in wound healing. These include epithelial cell proliferation, collagen deposition, tubular atrophy (TA) and interstitial fibrosis (IF) which lead finally to the loss of graft function (Racusen *et al.*, 2002; Cornell and Colvin, 2005; Solez *et al.*, 2007). In addition to tubulointerstitial fibrosis, loss of nephrons and intimal thickening of small arteries has been observed (Gourishankar and Halloran, 2002). Renal fibrosis is divided into three phases: the induction, inflammation and post-inflammatory phase as summarized in table 1.1 (Strutz and Neilson, 2003).

Induction phase	Inflammatory phase	Post-inflammatory phase
Infiltration of mononuclear cells	Increased matrix synthesis and deposition	End of inflammatory stimulus
Release of profibrogenic cytokines	Release of cytokines by infiltrating cells	Release of profibrogenic cytokines by tubular epithelial cells
Activation and proliferation of resident fibroblasts EMT		Proliferation of activated fibroblasts

Table 1.1, Mechanisms of fibrosis (table adapted from Strutz et al., 2003).

1.3.3.1 **Induction phase**

In the induction phase, the main feature is the infiltration of mononuclear cells into the interstitial space. These cells can be located either between tubular epithelial cells or between the epithelial cells and the tubular basement membrane causing tubulitis (Ivanyi and Olsen, 1995). The level of infiltration is correlated with renal function in many diseases (Alexopoulos *et al.*, 1990). T cell influx is supported by a variety of chemokines and proinflammatory cytokines which are secreted by renal epithelial cells. For example, the expression of TNF-α and IL-1 is upregulated in glomerular inflammatory diseases and interstitial fibrosis (Strutz and Neilson, 1994).

1.3.3.2 **Inflammatory phase**

The basic feature of this phase is the secretion of profibrotic cytokines by infiltrated cells leading to matrix synthesis and graft fibrosis. Various cytokines have been shown to promote fibrogenic mechanisms during chronic rejection. These include angiotensin II, fibroblast growth factor 2 (FGF2) and TGF-β along with additional cytokines such as platelet derived growth factor (PDGF) and epidermal growth factor (EGF) (Strutz and Neilson, 2003).

The most important factor in chronic rejection is TGF-β. This plays significant roles in stimulation of epithelial mesenchymal transformation (EMT), transformation of fibroblasts to myofibroblasts and synthesis of extracellular matrix (ECM) proteins such as fibronectin and collagen-I. An experimental model of TGF-β transgenic mice developed glomerulosclerosis and interstitial fibrosis (Kopp *et al.*, 1996). A high concentration of TGF-β is always accompanied by fibrosis in solid organs such as kidney, liver and lung (Border and Noble, 1994). TGF-β gene expression is increased in acute rejection and chronic allograft nephropathy (Pribylova-Hribova *et al.*, 2006). One important cytokine is angiotensin II which induces TGF-β synthesis in renal epithelial cells and fibroblasts (Eddy, 2000). Angiotensin II has the capability to induce ECM proteins such as collagen in interstitial fibrosis *in vitro* (Ruiz-Ortega and Egido, 1997).

In addition, FGF2 constitutes an important mitogen for renal fibroblasts. Induction of FGF2 produces glomerulosclerosis and interstitial fibrosis in rats (Kriz *et al.*, 1995).

1.3.3.3 **Post-inflammatory phase**

In this phase the inflammatory process is limited to a few areas whereas matrix synthesis and deposition is still in progress. The main feature is the proliferation of interstitial fibroblasts. The origin of fibroblasts in the kidney has been a matter of controversy. There is strong evidence that these cells originate from bone marrow derived precursors (Pereira *et al.*, 1998; Abe *et al.*, 2001). However, some of these cells are derived from resident renal epithelial cells which are undergoing mesenchymal transition (Ng *et al.*, 1998; Lan, 2003). It has been demonstrated that about 12% of fibroblasts originate from bone marrow, 30% are derived as a consequence of EMT in mice kidney, about 35% from endothelial to mesenchymal cell transformation and the remaining are thought to originate from resident fibroblasts or other mesenchymal cells (Kalluri and Neilson, 2003; Zavadil and Bottinger, 2005). Fibrogenesis continues during this phase by various mechanisms including ongoing stimulation of fibroblasts by an autocrine loop between fibroblasts and cytokines (Lonnemann *et al.*, 1995). Interaction between epithelial cells and fibroblasts may provide an additional driver of the fibrogenesis process.

Several factors have been shown to play a major role in the etiology of tubular atrophy/interstitial fibrosis (TA/IF) including TGF-β, tumor necrosis factor-α (TNF-α) and FGF2 (Mohamed *et al.*, 2000; Waaga *et al.*, 2000). TGF-β is upregulated during renal rejection; indeed TGF-β plays a major role in the induction of EMT in the kidney in association with FGF2 which stimulates the proliferation of renal fibroblasts (Robertson *et al.*, 2001; Strutz *et al.*, 2001). Furthermore, FGF2 expression has been increased in fibrotic kidney particularly in interstitial and tubular cells (Strutz *et al.*, 2000; Strutz *et al.*, 2002). FGF2 stimulates the release of latent TGF-β from proximal tubules (Phillips *et al.*, 1997). In turn TGF-β stimulates the synthesis and secretion of FGF2 from cortical fibroblasts (Strutz *et al.*, 2001). The main pathology in chronic rejection is tubulointerstitial fibrosis (IF) in association with loss of nephrons and intimal thickening of small arteries (Gourishankar and Halloran, 2002). This fibrosis results mainly from the effect of fibroblasts which in turn, result from epithelial cells undergoing EMT (Lan, 2003).

1.3.3.4 **Epithelial mesenchymal transition (EMT)**

Epithelial mesenchymal transition is a process that involves transformation of polarized epithelial cells into migratory mesenchymal cells. Epithelial cells loose many of their phenotyping features such as polarity and exhibit reduced expression of E-cadherin. At the same time these cells acquire a new mesenchymal phenotype such as spindle-shaped morphology and become more isolated and motile, invasive and more resistant to apoptosis with increased production of ECM molecules (Kalluri and Neilson, 2003; Klymkowsky and Savagner, 2009). At the end of EMT, newly transformed cells migrate through the underlying basement membrane and accumulate in the interstitial spaces of tissues (Okada *et al.*, 1996).

The EMT process is crucial for biological activities such as embryonic development, wound healing and tissue repair (type-I EMT), (Acloque *et al.*, 2009). Another kind of EMT is involved in cancer progression and metastasis (type-III EMT) (Brabletz *et al.*, 2001; Thiery, 2002; Fidler and Poste, 2008). In fibrosis, epithelial cells undergo type-II EMT and become fibroblasts after chronic inflammation accompanied with the effects of several cytokines. Endothelial cells can also undergo type-II EMT in the heart and kidney (Zeisberg *et al.*, 2007a; Zeisberg *et al.*, 2008). For example, endothelial cells from microvasculature were

shown to undergo mesenchymal transformation (EndMT) during fibrosis (Potenta *et al.*, 2008).

EMT is induced by stimulation by several factors which lead to the expression of specific proteins on the cell surface, activation of transcription factors, production of ECM degradation enzymes and expression of cytoskeletal proteins (Kalluri and Weinberg, 2009). Several antigens have been used to characterize type-II EMT. These include fibroblast-specific protein 1 (FSP1), α-smooth muscle actin (α-SMA) and collagen-I (Strutz *et al.*, 1995; Zeisberg *et al.*, 2003).

FSP1 is considered a typical marker of EMT in fibrogenesis (Iwano *et al.*, 2002). FSP1 (also known as S100A4 in human), a member of Ca^{+2} binding S100 family, is considered a cytoskeletal marker for EMT (Rygiel *et al.*, 2010). This marker is expressed early in epithelial cells undergoing EMT. It has been shown that more than one third of FSP1, in transgenic mice, is produced in EMT-derived cells in kidney or liver fibroblasts (Iwano *et al.*, 2002; Zeisberg *et al.*, 2007b). α-SMA also constitutes a marker which is normally expressed in vascular smooth muscles and myoepithelial cells (Gabbiani *et al.*, 1981). In type-II EMT, α-SMA is generally associated with myofibroblasts (Zeisberg and Neilson, 2009).

1.3.3.5 **Renal epithelial cells in chronic rejection**

Renal epithelial cells play pivotal roles in renal function in both health and disease. These cells are found in the lining layer of tubules, collecting ducts and urinary tracts. There is strong evidence that proximal tubular epithelial cells constitute a source of FGF2 and TGF-β (Phillips *et al.*, 1997; Jones *et al.*, 1999). In fibrogenesis, epithelial cells are exposed to the effects of proteinuria and cytokines.

Increased tubular expression of adhesion molecules such as intracellular adhesion molecule-1 (ICAM-1) and/or vascular cell adhesion molecule-1 (VCAM-1) is correlated with interstitial infiltrates in the context of inflammatory response and renal fibrosis (Roy-Chaudhury *et al.*, 1996). Stimulation of renal epithelial cells with IFN-γ induces the expression of MHC-II molecules (Wuthrich *et al.*, 1990). Tubular epithelial cells are able to stimulate T cells by expressing MHC-II molecules and thereafter, working as antigen presenting cells (Banu and Meyers,

1999). MHC-II expression was shown to localize specifically in areas of mononuclear infiltration and damage (Halloran *et al.*, 1988; Wuthrich *et al.*, 1989).

Activated fibroblasts are essential effectors in renal fibrogenesis. These cells can be converted to contractile myofibroblasts which express α-SMA (Okada *et al.*, 1997).

Epithelial cells have the ability to synthesize chemoattractants such as RANTES (Regulated on Activation Normal T Cell Expressed and Secreted) and monocyte chemoattractant protein-1 (CCL2) which facilitate macrophage infiltration into the tubulointerstitial space (Remuzzi and Bertani, 1998). By production of these factors, epithelial cells are an essential component in the pathogenesis of renal inflammation and fibrosis (Phillips *et al.*, 1997).

1.4 The extracellular matrix

Renal fibrosis is characterized by excessive deposition and accumulation of extracellular matrix components such as collagen, fibronectin, laminin and proteoglycans (Eddy, 2000). Cytokines involved in chronic renal dysfunction are also involved in generating ECM components such as TGF-β (Creely *et al.*, 1992). ECM components are generated by cytokine-stimulated mesangial cells, fibroblasts and tubular epithelial cells (Okada *et al.*, 2000). The increase in collagens and fibronectin is also accompanied by increased proteoglycan secretion following stimulation of keratocytes with TGF-β (Funderburgh et al., 2001).

1.5 Heparan sulphate proteoglycans (HSPG)

Proteoglycans are complex molecules composed of central domains called core proteins which are covalently attached to one or more oligosaccharide chains of glycosaminoglycan (GAGs). The core protein has crucial role in determining proteoglycan functions and regulation of activities such as cell adhesion and HS shedding (Bernfield *et al.*, 1999; Saoncella *et al.*, 1999). Depending on the core proteins and GAG chains, proteoglycans are divided into three major groups: chondroitin/dermatan sulphate proteoglycans (CSPGs), heparin /heparan sulphate proteoglycans (HSPGs) and keratan sulphate proteoglycans (KSPGs).

CS-GAGs are composed of galactosamine (GalN) and either glucuronic or iduronic acid (IdoA) whereas the basic component of HS is glucosamine (GlcN) and

glucuronic/iduronic acid. KS is composed of disaccharide units of glucosamine and galactose (Gal) (Gallagher *et al.*, 1990).

HSPGs are categorized in three subfamilies:

The first group contains membrane spanning proteoglycans such as syndecans, betaglycans and CD44. The second group contains membrane associated proteoglycans such as glypicans, whereas the third group contains extracellular matrix (secreted) proteoglycans such as agrin, collagen XVIII and perlecan (Jackson *et al.*, 1991; Bishop *et al.*, 2007).

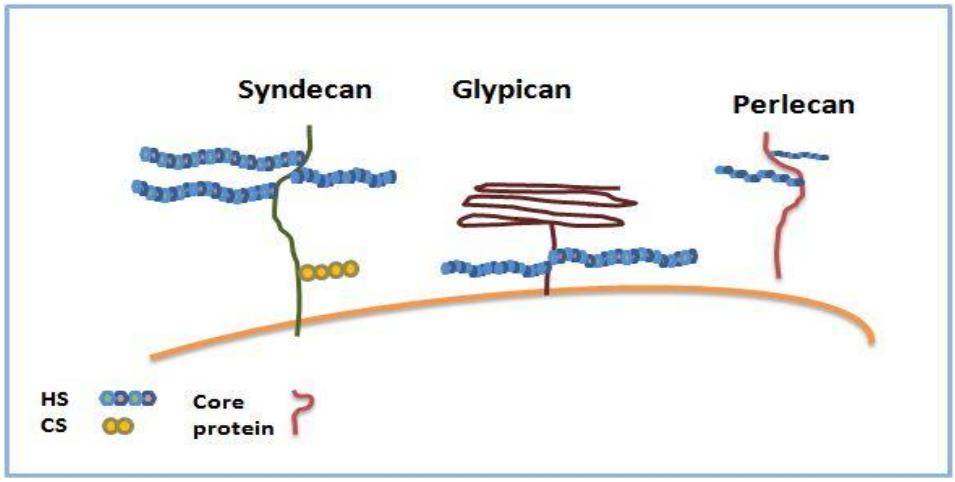

Figure 1.1. Model of proteoglycan structure. Syndecans have trans-membrane core proteins with HS- or CS-GAG chains. Glypicans have GPI core protein with only HS-GAG chains whereas perlecan is a secreted HSPG. Figure adapted from (Lin, 2004)

HSPG consist of a core protein and 2-3 covalently attached GAG chains. Core proteins generally determine the localization of HSPG on cell surface or ECM. Syndecans and glypicans constitute two major groups of core proteins on cell surfaces (Figure 1.1). Syndecans consist of 4 family members (syndecans 1-4) which are expressed differentially in mature tissues. Syndecan 1, for instance, is abundant in epithelial cells whereas syndecan 2 is highly expressed in endothelial cells and fibroblasts (Bernfield *et al.*, 1992; Gotte, 2003).

Syndecans usually bind three GAG chains close to the N termini. These chains, in the case of syndecans 2 and 3 for instance, are exclusively HS-GAGs whereas they may have CS as well in case of syndecans 1 and 4, (Figure 1.1), (Shworak *et al.*, 1994; Rapraeger and Ott, 1998).

In contrast, glypicans are cell-surface glycosylphosphatidylinositol (GPI) bound proteoglycans with six different mammalian members (1-6) and one Drosophila homologue (Lander *et al.*, 1996; Bandtlow and Zimmermann, 2000). All glypicans share a distinctive structure of 14 conserved cysteine residues mainly located in the extracellular domain and exclusively substituted with HS chains (Chen and Lander, 2001).

Heparan sulphate is found on GBM as ECM components such as perlecan, agrin and collagen XVIII (Noonan and Hassell, 1993; Groffen *et al.*, 1998; Halfter *et al.*, 1998). HS is also found at the cell surface of leucocytes, endothelial and epithelial cells in different types such as glypicans, syndecans, betaglycans and CD44 (Carey, 1997; Filmus and Selleck, 2001; Eickelberg *et al.*, 2002). Betaglycan, a receptor for TGF-β, is mainly found in cortical renal interstitium and on microvascular endothelial cells (Eickelberg *et al.*, 2002). Syndecans 1, 2, and 4 are generally expressed at basolateral surfaces of vascular endothelial cells (Bernfield *et al.*, 1992; Rosenberg *et al.*, 1997). Syndecan 1 and 4 are expressed in kidney with various distribution pattern; syndecan 1 for instance, is predominant on basolateral surface of the renal epithelial cells (Cook *et al.*, 1996) whereas syndecan 4 is mainly found on endothelial cells (Kim *et al.*, 1994).

1.6 Heparan sulphate (HS)

HS proteoglycans (HSPGs) are located on cell surfaces and extracellular matrices (ECM) in all mammalian cells. HS concentration may reach up to 200 µg/ml within a thin proteoglycan layer including 50-90% of endothelial cell surfaces (Ali *et al.*, 2003). HS synthesis undergoes a series of steps before reaching its final and functional form.

1.6.1 Initiation

HS synthesis is initiated after binding xylose from uridine-diphospho-D-xylose (UDP-Xylose) to a core protein serine by UDP-xylosyltransferase in Golgi apparatus. Then a molecule of galactose is transferred to the xylose by UDP-Galactosyl (UDP-Gal) transferase I followed by another galactose by UDP-Gal transferase II. The final saccharide (glucoronic acid) of the linkage is added by UDP-Glucuronic acid (UDP-GlcA) transferase I (Esko and Zhang, 1996; Kitagawa

et al., 1998). Following synthesis of this tetrasaccharide linkage, the HS chain is ready to be extended by the addition of repeated glucuronic acid and glucosamine units.

1.6.2 Elongation and polymerization

HS is synthesized as a repeating disaccharide unit composed of N-acetylglucosamine (GlcNAc) and glucuronic acid (GlcA) joined by 1-4 linkage tetrasaccharides (Kjellen and Lindahl, 1991). Elongation of the GAG chain occurs by adding GlcNAc and GlcA to the linkage region by the GlcNAc transferase I enzyme and GlcA transferase II enzyme respectively (Lind *et al.*, 1998; McCormick *et al.*, 2000). These enzymes are products of tumor (exostoses) suppressor genes EXT1 and EXT2 and constitute a part of a hetero-oligomeric complex in the Golgi apparatus that is responsible of HS chain polymerase activity (Munro, 1998; Wei *et al.*, 2000). In the case of addition of GalNAc (instead of GlcNAc) to the tetrasaccharide linkage, a chondroitin sulphate (CS) chain will be created. GAG chains can reach a total length of between 30-200 saccharides (Kjellen and Lindahl, 1991).

Humans with mutations in either gene of EXT1 or EXT2 suffer from benign bone tumours known as exostoses. Mutation in EXT1 and EXT2 results in neonatal lethality at gastrulation due to lack of organized mesoderm and extracellular embryonic tissue (Forsberg and Kjellen, 2001), whereas partial mutation of EXT1 was found to cause truncated HS chains (30% of normal length) and consequent biological activity (McCormick *et al.*, 1998; Lin *et al.*, 2000; Kitagawa *et al.*, 2001).

1.6.3 Modification

HS modification is not random but a controlled and specific process. Each enzyme affects its substrate in a way that allows the next step to take place (Kusche-Gullberg and Kjellen, 2003). HS structure is modified by a range of enzymes beginning with N-deacetylase N-sulphotransferase enzyme (NDST) which replaces the N-acetyl group of GlcNAc with sulphate groups from nucleotide sulphate 3'-phosphoadenosine-5'phosphosulphate (PAPS) donors creating a highly sulphated domain (GlcNS), (Orellana *et al.*, 1994). The PAPS is a general sulphate donor

which is located in the cytoplasm and transferred to the Golgi compartment by nucleotide transporters. This vital molecule is synthesized by the act of PAPS synthetase 1 and 2 (ATP sulphurylase/APS kinase) which combines adenosine triphosphate (ATP) with the adenosinephosphosulphate (APS) kinase enzyme (Venkatachalam *et al.*, 1998).

D-glucuronic acid residues adjacent to GlcNS are epimerized to L-iduronic acid (IdoA) residues by the C5 epimerase enzyme (Li *et al.*, 1997). Additional sulphate groups to IdoA and/or GlcA at 2-O position are added by heparan sulphate 2-O sulphotransferase (HS2ST). Further sulphation takes place by transferring sulphate groups to 6-0 position of GlcNAc and GlcNS by heparan sulphate 6-O sulphotransferase (HS6ST) and, to a lesser extent, to the 3-O position by heparan sulphate 3-O sulphotransferase (HS3ST), (Lindahl *et al.*, 1998), (Figure 2.1).

Polymerization and modification of the HS chain results in a more mature and complicated HS structure. This structure contains three types of sequences: non-sulphated regions with N-Acetyl (NA), mixed regions with N-sulphated (NS) and NA (NA/NS), and N-sulphated regions NS (Gallagher *et al.*, 1992). NS domains extend from 2-9 disaccharides which are flanked by 16-18 disaccharides of NA/NS domains.

Variation of HS structure is attributed, in addition to HS chain length, to the content of O-sulphation imposed on N-sulphated regions (Lyon and Gallagher, 1998). It has been suggested that NA domains at the beginning of HS chains (contiguous with the protein linkage) provide a "flexible non-interactive arm" with more free rotational freedom. This may help in HS interaction with extracellular and cell surface proteins and ligands (Turnbull and Gallagher, 1991; Lyon *et al.*, 1994a).

1.6.4 HS modifying enzymes

The HS chain undergoes a series of modification following chain polymerization. Modification reactions are performed by four sulphotransferase enzymes and an epimerase. The modifying enzymes are generally expressed in a tissue specific and developmentally regulated pattern. Except for HS2ST and C5 epimerase, sulphotransferase enzymes have several isoforms which catalyze the same reaction but with different chemical contexts.

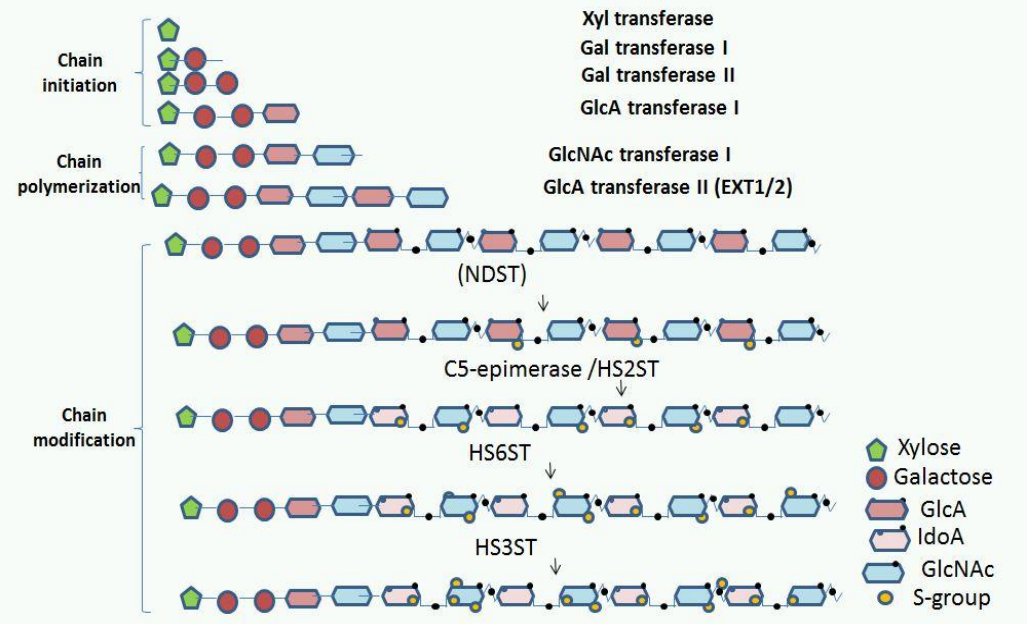

Figure 1.2. Heparan sulphate modifying. The NDST enzyme removes acetyl and adds sulphate group to the GlcNAc. HS2ST transfers S group to the GlcA/IdoA whereas HS6ST and HS3ST transfer S groups the 6-O and 3-O positions of glucosamine respectively, figure adapted from Esko et al. (Esko and Selleck, 2002)

1.6.4.1 **NDST**

The NDST enzyme has 4 mammalian isoforms (1, 2, 3 and 4) with similar sequence homology of 65-80% and different tissue expression (Aikawa *et al.*, 2001; Esko and Selleck, 2002). The sulphotransferase domain of NDST1 contains two highly conserved structural motifs which have the ability to interact with PAPS (Kakuta *et al.*, 1999). The NDST enzyme catalyzes the first modification reaction in HS structure in the Golgi compartment by removing N-acetyl from glucosamine residues and transferring sulphate group to the N position. This modification was shown as a prerequisite for further N- sulphation and all additional modifications including C5 epimerization and O sulphation (Esko and Selleck, 2002; Bengtsson *et al.*, 2003). However, further studies have shown that epimerization or O-sulphation might take place in absence of N-sulphation. This phenomenon was attributed to the presence of a complex of HS modifying enzymes known as GAGosome. In this model, several biosynthetic enzymes work on the same polysaccharide substrate in a flexible manner (Esko and Selleck, 2002). For example, HS synthesized by mice stem cells with a complete absence of N-sulphate groups was shown to have 6-O

sulphate groups; this rules out the requirement for a mandatory N-sulphation step for subsequent HS sulphation (Holmborn *et al.*, 2004).

NDST1 and 2 have a wide tissue distribution whereas NDST3 and 4 are expressed in a more restricted manner. It has been shown that NDST3 and 4 are more abundant in human fetal liver, kidney or brain than NDST1 or NDST2 (Kusche and Lindahl, 1990; Toma *et al.*, 1998; Aikawa *et al.*, 2001). These isoforms are also different in N-deacetylase/N-sulphotransferase activity. For example, NDST1 has higher N-deacetylase activity than N-sulphotransferase activity compared to NDST2 (Aikawa *et al.*, 2001). Additionally the isoform of NDST4 has weak deacetylase activity with high sulphotransferase activity, whereas NDST3 has the reverse properties (Aikawa *et al.*, 2001).

Cells overexpressing NDST exhibit an increase in N-sulphation. NDST2 overexpressing cells express more N-sulphated groups and more extended NS domains compared to cells overexpressing NDST1, which are primarily involved in NA/NS domains (Pikas *et al.*, 2000).

Knock-out of NDST isoforms in experimental animal models produces different phenotypes. Knock-out of NDST1 produces an increased incidence of lethality shortly after birth due to respiratory defects. However, mice with NDST2 knocked-out are viable and fertile but have reduced connective-tissue-type mast cells, which play an important role in heparin synthesis (Forsberg *et al.*, 1999; Fan *et al.*, 2000).

NDST1 is involved in several systems including the nervous system, digestive system and immune system. In an inflammatory response, Wang et al. showed that disruption of NDST1 in endothelial cells reduced chemokine-mediated neutrophil infiltration (Wang *et al.*, 2005). Stimulation of endothelial cells with TNF-α and IFN-γ increased expression of NDST-1 at the mRNA level (Klein *et al.*, 1992; Carter *et al.*, 2003).

1.6.4.2 **GlcA C5 epimerase**

HS chain epimerization usually takes place after N sulphation, where D-glucuronic acid is converted into L-iduronic acid by C5 epimerase, which causes the carboxyl group (C5) of GlcA to locate below the hexose ring. The absence of 2-OS at surrounding GlcA residues is necessary for this reaction (Jacobsson *et al.*, 1984).

Epimerization of HS chains releases conformational forces which facilitate the binding of various factors and ligands to specific sites with the HS chain (Mulloy and Forster, 2000).

Mice lacking the GlcA C5 epimerase enzyme exhibit neonatal lethality which sheds more light on the important role of this enzyme in modifying HS structure with consequent effect on biological and developmental biology (Li *et al.*, 2003).

1.6.4.3 **HS2ST**

The HS2ST enzyme transfers sulphate groups to the 2-O position of GlcA/IdoA. No isoforms for this enzyme have been found. The HS2ST transfers sulphates to substrate including GlcA/IdoA with GlcNS (IdoA-GlcNS), however, this does not include O-sulphated residues or that are adjacent to O-sulphated residues (IdoA-GlcNS6S), (Kobayashi *et al.*, 1996; Kobayashi *et al.*, 1997).

The 2-O sulphation usually occurs after the glucosamine N-sulphation. The C5 epimerase and HS2ST have a kind of interconnection between each other. HS2ST has higher affinity to an iduronic acid than to glucuronic acid (Rong *et al.*, 2001). It has been shown that 50-90% of the 2-O sulphation occurs at the IdoA residue which increases along with NS domain length (Safaiyan *et al.*, 2000).

In 1998, Bullock et al. showed that homozygous mice with HS2ST knockout died during the neonatal period and exhibited bilateral renal agenesis as well as skeletal defects; these defects indicate significant role for HS2ST in HS regulation of morphogenesis during embryonic development (Bullock *et al.*, 1998).

1.6.4.4 **HS6ST**

The HS6ST enzyme transfers sulphate groups to the 6-O position of glucosamine in the HS chain; this role has been described in many species including Drosophila, *C.elegans* and Zebrafish.

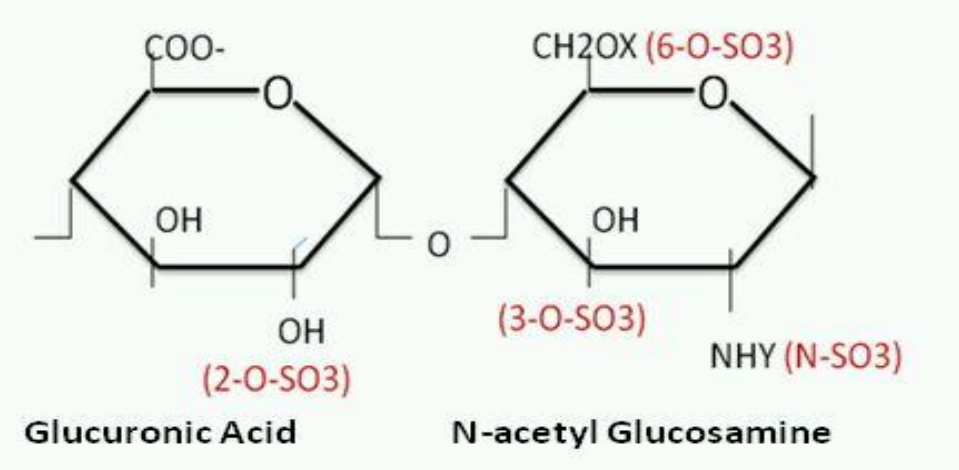

Figure 1.3. Disaccharide structure of heparan sulphate. Repeated disaccharide units contain Glucuronic acid and N- Acetyl glucosamine.

HS6ST has three isoforms which have specific substrates and different tissue distributions. These isoforms generally transfer sulphate groups to the 6-O position of glucosamine substrates varying in concentration, level of sulphation and adjacent sulphated units (Habuchi *et al.*, 2000). Sulphate groups are generally transferred to substrates containing GlcNS-GlcA-GlcNS, GlcNS-IdoA-GlcNS and GlcA-GlcNS3S units with preference for targets containing IdoA in the presence or absence of 2-O sulphation (Smeds *et al.*, 2003). Habuchi et al showed that each isoform is more specific for hexuronic acid (GlcA or IdoA) adjacent to targeted GlcNS. The HS6ST1 enzyme was found to catalyze the sulphation at residues containing GlcA/IdoA rather than 2-O sulphated residues. HS6ST2 catalyzes sulphate transferase to different substrates depending on concentration. For example GlcA-GlcNS substrate is favored at a high concentration while IdoA-GlcNS is preferred at a low concentration (Habuchi *et al.*, 2000). HS6ST3 prefers substrates with higher amount of 2-O sulphation (Jemth *et al.*, 2003), (Figure 1.3).

In addition, the HS6ST isoforms express a variable pattern of tissue expression. Murine HS6ST1 and HS6ST2 are highly expressed in liver and brain respectively, whereas HS6ST3 is ubiquitously expressed (Habuchi *et al.*, 2000). Human HS6ST isoforms have an approximately similar tissue distribution. HS6ST1, for instance, has an abundant distribution pattern (higher expression in liver), whereas HS6ST2 is highly expressed in brain, spleen, placenta and fetal kidney whereas HS6ST3 is ubiquitously expressed in many tissues (Habuchi *et al.*, 2003; Smeds *et al.*, 2003).

The HS6ST expression also varies during development stages; HS6ST1 expression in early mouse embryos is mainly high in neural tissue while in adult mouse this enzyme is mainly expressed in the liver (Sedita *et al.*, 2004).

Sulphation of HS glucosamine at the 6-O position plays a crucial role in the developmental process. In Drosophila, for instance, disruption of HS6ST-RNA expression resulted in remarkable changes in fibroblast growth factor signalling in the tracheal epithelium and affected tracheal morphogenesis (Kamimura *et al.*, 2001) whereas null mutation of the gene encoding HS6ST in *C.elegans* produced defects in the nervous system (Bulow and Hobert, 2004). Habuchi et al. showed that the high percentage of null HS6ST1 mice died between embryonic day 15.5 and the prenatal stage (Habuchi *et al.*, 2007). Additional studies show that mice with mutant HS6ST1 (homozygous) exhibited significant growth retardation, failure to thrive and lethality in early adulthood (Izvolsky *et al.*, 2008). Sulphation at the 6-O position has been involved in development of limbs in the chicken embryo (Nogami *et al.*, 2004; Kobayashi *et al.*, 2010). HS6ST1 and HS6ST2 mutations were found to affect formation of Zebrafish muscles (Bink *et al.*, 2003). In humans, HS6ST mutations cause macular corneal dystrophy (Iida-Hasegawa *et al.*, 2003).

1.6.4.5 **HS3ST**

The HS3ST enzyme transfers sulphate group to the 3-O position of glucosamine in the HS chain. The sulphate group is transferred from PAPS to a substrate such as GlcNS or GlcNS6S (Habuchi *et al.*, 2004). So far, seven HS3ST isoforms have been identified (1, 2, 3A, 3B, 4, 5 and 6) with substrate preferences and more specific biological properties (Shukla *et al.*, 1999; Shworak *et al.*, 1999; Xu *et al.*, 2005). Despite forming only about 1% of the total, sulphation at the 3-O position is crucial for significant biological activities. Late modification of HS by HS3ST isoforms requires generally more specific substrates at various positions. HS3ST2 isoform adds sulphate group to GlcA2S-GlcNS and IdoA2S-GlcNS, while HS3OST-3A transfers sulphate group to IdoA2S-GlcNAc (Liu *et al.*, 1999a).

One pivotal role for 3-O sulphate is formation of the antithrombin-III (AT-III) binding site in HS. HS3ST1 constitutes the predominant isoform involved in the transfer of 3-O sulphate to the AT-III-HS epitope (Liu *et al.*, 1999b). HS can

promote anticoagulation by interacting with AT-III which forms a protease inhibitor of pro-coagulant thrombin (Casu and Lindahl, 2001). HS3ST3B participates in the construction of 3-O sulphated HS binding site of herpes simplex virus type-1 (HSV-1) (Shukla *et al.*, 1999).

Importantly, the HS3ST1 gene is upregulated in rejected (failed) renal allografts compared to non-failed grafts. This result suggests a potential role for HS3ST1 in the pathology of graft rejection, which is accompanied by novel sulphation modulation compared to normal organs or non-failed grafts (Einecke *et al.*, 2010). HS3ST1 knockout mice show no haemostasis defects in coagulation, despite the crucial role of HS3ST1 in synthesis of the HS-AT-III binding site. However, these mice do show retardation of intrauterine development (Shworak *et al.*, 2002).

1.6.5 HS sulphation

HS polymerization and epimerization is crucial for the regulation of HS sulphation and diversity. Availability of the sulphate donor PAPS constitutes an additional factor for the regulation of HS binding efficiency. This is determined by the capacity of PAPS synthesizing enzymes and the PAPS transport system. The concentration of PAPS in the intra-Golgi system is crucial for the sulphation patterns generated by HS modifying enzymes (Wlad *et al.*, 1994; Abeijon *et al.*, 1997). PAPS is synthesized in the cell cytoplasm and transferred to the Golgi compartment by two transporters PAPST1 and PAPST2 (Kamiyama *et al.*, 2003; Kamiyama *et al.*, 2006).

The pattern of HS sulphation is different during carcinogenesis, development and inflammation (Feyzi *et al.*, 1998; Jayson *et al.*, 1998; Carter *et al.*, 2003). HS sulphation also exhibits tissue specificity; indeed, disaccharide analysis of HS chains shows that porcine liver has more heavy sulphated HS than the intestine (Jastrebova *et al.*, 2010). Interestingly, HS sulphation undergoes age-dependent modulations which are accompanied by changes in biological activity, including decreased ability to bind FGF2 (Huynh *et al.*, 2012). In addition, stimulation of endothelial cells with proinflammatory cytokines such as TNF-α and IFN-γ increases expression of the HS modifying enzyme NDST-1 (Klein *et al.*, 1992; Carter *et al.*, 2003). Sections from acutely rejecting human renal biopsies showed

an increase in N-sulphation compared to normal kidney suggesting an important role for HS in regulating the inflammatory response (Ali *et al.*, 2003). Changes in HS expression were also observed in synovial endothelial cells and chemokine binding sites. For example, syndecan 3 is expressed by synovial endothelial cells during normal and rheumatoid inflammatory conditions. However, these cells express HS which selectively binds CXCL8 only during inflammation (Patterson et al., 2005).

1.6.6 HS-protein interactions

HS has polyanionic charges on GAG chains that play a crucial role in binding a wide range of proteins, cytokines and growth factors. Many of these interactions are related to H bonds, van der Waals forces and hydrophobic interaction (Thompson *et al.*, 1994). These interactions allow HS to play an important role in many biological processes including cell adhesion, migration, differentiation, angiogenesis, coagulation, haemostasis, inflammation and proliferation (Wight *et al.*, 1992; Bernfield *et al.*, 1999; Tumova *et al.*, 2000).

The localization of HS on the cell surface enhances the binding of proteins such as growth factors and chemokines, as well as increasing their stability and activity (Lortat-Jacob *et al.*, 1995; Sasisekharan *et al.*, 1997). Interaction between HS and FGF2 for instance, provides protection from thermal and pH denaturation. Binding of HS-FGF2 may also restrict FGF2 diffusion and increase its concentration, which enhances its paracrine mode of activity (Mulloy and Rider, 2006)

Heparin has been used as a highly sulphated model of HS in many studies for HS-protein interactions. Heparin has the same structure as HS, but with more heavily trisulphated disaccharides (Lindahl *et al.*, 1998). Most proteins interact with immobilized heparins via ionic interactions between amino acids such as lysine or arginine which are generally aligned in specific sequences. Consensus sequences suggested for HS/heparin binding proteins include XBBBXXBX, XBBXBX and XBBBXXBBBXXBBX where B and X refer to basic and hydropathic amino acid respectively (Cardin and Weintraub, 1989).

Interaction between cationic binding proteins and negatively charged heparins may indicate relatively nonspecific binding (Salmivirta *et al.*, 1996; Lindahl and Kjellen,

1998). Specific sequences in NA and NA/NS regions of HS provide selective binding domains for various proteins which interact with HS in a biological environment. Additional factors may play roles in generating unique protein binding epitopes, including N-substitution pattern, HS chain length, the number of sulphated domains, the deposition of NS, NS/NA and NA regions, and combination between sulphate groups at N- and O- positions (Lindahl *et al.*, 1998).

A very well studied example of specific HS-protein interaction is between AT-III and HS/heparin. Structural analysis revealed the requirement of a 3-O sulphate group containing pentasaccharide motif (Petitou *et al.*, 2003).

1.7 Chemokines

Chemokines are *chemo*tactic cyto*kines*, a family of homologous proteins with molecular weight between 8-12 kD. These proteins play significant roles in localizing immune cells to the site of tissue damage (inducible) during inflammation or in homing lymphocytes in nonpathological conditions (constitutive) (Rot and von Andrian, 2004). Depending on the presence of cysteine residues (C), chemokines are classified into four families termed: CXC, CC, C and CX3C on the basis of the presence of amino acid X between cysteine residues near the N terminus (Zlotnik and Yoshie, 2000) .

Chemokines signal via specific cell surface G-protein coupled receptors (GPCR); each has seven transmembrane domains (Murdoch and Finn, 2000). Alternatively, GAGs bind to chemokines and have the capability to generate a signal through phosphotyrosine kinase (PTK), even in absence of GPCR. For example CCL5 could signal through HeLa cells stably transfected with CD4 in presence of GAGs even in the absence of GPCR, whereas these cells failed to signal in lacking of cell surface GAGs (Chang *et al.*, 2002).

Chemokines are expressed by a broad spectrum of cells and tissues. CXCL8 and CCL2, for example, are secreted by leucocytes, fibroblasts, platelets, endothelial and epithelial cells. This secretion is mainly maintained by pro-inflammatory cytokines such as TNF-α, IFN-γ, IL-1 and IL-2 (Ward *et al.*, 1998; Hillyer *et al.*, 2003). It has been shown that the CC chemokine family members CCL4 and CCL2

(MCP-1) are upregulated in tubular epithelial cells within rejected renal allografts (Robertson *et al.*, 2000).

1.7.1 Chemokine-HS interaction

Chemokines are anchored and presented by HS on the cell surface in a way that controls their functions. Chemokine-GAG binding domains have been identified by sequence alignment and mutagenesis experiments. These domains consist of basic amino acids (B) and other amino acids (X). The most abundant domain motif for chemokine-GAG binding is XBBXBX and XBBBXXBX (Hileman *et al.*, 1998). For example, HS binding domain in CCL5 (BBXB) includes R44, K45 and R47 which constitute the key HS-CCL5 binding epitope (Proudfoot *et al.*, 2001).

Interaction with HS can protect chemokines from degradation and induces oligomerization (a more active form of chemokines) (Webb *et al.*, 1993; Hoogewerf *et al.*, 1997). This binding is also important for localization of chemokines on endothelial cell surfaces by preventing their displacement by rapid blood flow (Lortat-Jacob *et al.*, 2002).

HS sequesters chemokines at the site of generation, potentially leading to the formation of a chemokine gradient that can play an important role in leucocyte migration (Middleton *et al.*, 2002). HS also plays a significant role in chemokine transport across the endothelial cell layer (transcytosis). CXCL8, for example, is involved in endothelial transcytosis, which is a heparan sulphate dependent process (Middleton *et al.*, 1997). Chemokine gradients influence neutrophil crawling in the extravascular lumen *in vivo*. A macrophage inflammatory protein-2 (MIP-2, CXCL2) releasing gel attracted neutrophils to the vascular endothelia compared to endothelia from heparanase transgenic mice which express short HS chains. This result suggests that an intravascular chemokine gradient is created along endothelial HS which induces neutrophil to crawl towards transmigration sites (Massena *et al.*, 2010).

Chemokine-HS binding is necessary not only for chemokine protection and gradient formation but also for chemokine signalling. HS binding to chemokine allows presentation to GPCRs and, thereafter, chemokine signalling (Hoogewerf *et al.*, 1997; Ali *et al.*, 2000). Mutant CCL7 with an inability to bind HS has a reduced

potential to stimulate transendothelial leucocyte migration in comparison to wild-type chemokine in *in vitro* chemotaxis assay (Ali *et al.*, 2005b). An *in vivo* experiment showed that mutant CCL5 with reduced ability to bind HS is less effective in recruiting leucocytes (Proudfoot *et al.*, 2003). A non-heparin-binding CCL5 mutant (K45A), demonstrated a decreased ability to establish chemokine gradients affecting haptotactic leucocyte transendothelial migration (Ali *et al.*, 2002). Furthermore, heparan sulphate facilitates chemokine transport from tissue to lumen. For example, truncated CCL8 (1-63) with an inability to bind HS, failed to transport through the endothelium to the apical surface (Middleton *et al.*, 1997). The interaction between chemokine and HS has been shown to affect allograft survival; inhibition of chemokine-HS interactions reduced transplant rejection in mice (Dai *et al.*, 2010).

The chemokine-HS interaction exhibits a level of selectivity that has been revealed by identifying the HS binding domain for a limited number of chemokines. Sulphate groups at N- and O- positions are involved in the HS binding site for chemokines such as CCL2, CCL7 and/or CCL8 (Schenauer *et al.*, 2007). Further studies using X-ray diffraction analysis of CCL5 mixed with heparin disaccharides, has shown that N- and 6-O sulphate groups are involved in CCL5-HS interaction (Shaw *et al.*, 2004). The binding site should contain at least 14 monosaccharides in order to allow CCL5 oligomerization which is necessary for affinitive binding and signalling (Rek *et al.*, 2009).

1.7.2 Leucocyte extravasation

During the inflammatory response, leucocytes such as neutrophils migrate into tissues by penetrating the junctions between vascular endothelial cells or by the transcellular pathway. Alternatively, naive lymphocytes can migrate across the high endothelial venules (HEV) in the absence of inflammation (Engelhardt and Wolburg, 2004).

The first step in leucocyte migration is the binding of selectins which mediate attachment to the vascular endothelial wall in the direction of blood flow resulting in leucocyte tethering and rolling (Ley *et al.*, 2007). These cells are recruited to inflammatory sites by binding to three selectins namely: lymphocyte (L), platelet

(P) and endothelial (E) selectins (Lowe, 2003). In the following step, leucocytes firmly adhere to the endothelial surface due to activation of integrins which interact with counter adhesion molecules such as ICAM-1 (Shimizu *et al.*, 2008). This interaction leads to leucocyte arrest in a step that results in activation of a signalling cascade and leucocyte migration (Yadav *et al.*, 2003). In the third step, leucocytes begin to extravasate between or through the endothelial cells towards the tissue. Degradative enzymes, i.e. heparanases facilitate leucocyte release and increase the vascular permeability at the inflammatory endothelial sites (Edovitsky *et al.*, 2006).

Migration of circulating leucocytes towards inflamed tissue is mediated by chemokine-HS binding. This interaction supports the formation of chemokine gradient on endothelial cell surface and ECM which is crucial for leucocyte activation and migration (Middleton *et al.*, 2002; Yadav *et al.*, 2003)

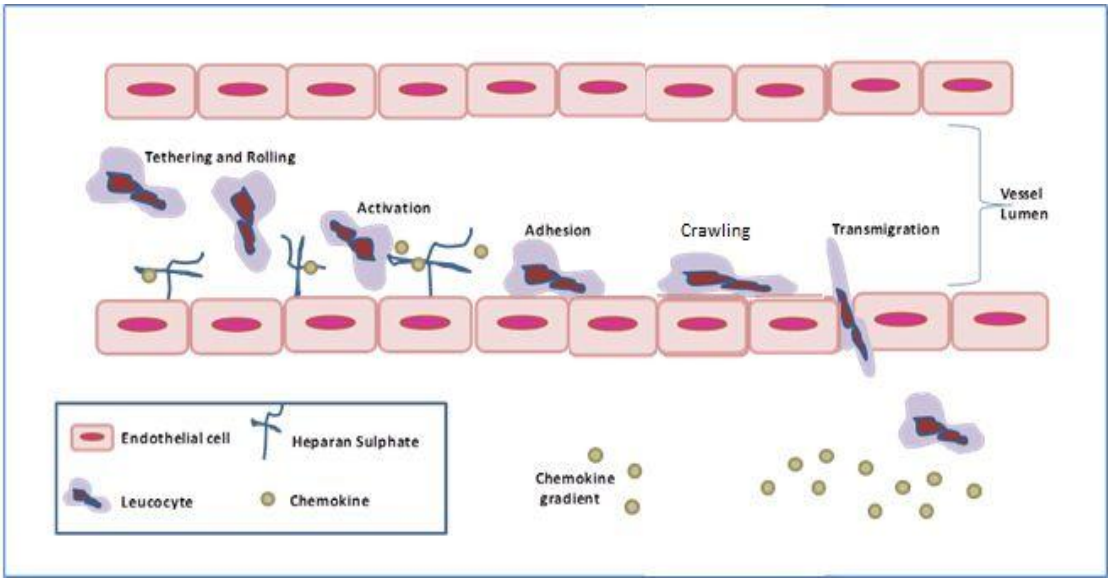

Figure 1.4. Leucocyte extravasation. Leucocytes extravasation can be divided into three main steps. 1, leucocyte rolling involves the binding with selectins. 2, firm adhesion. 3, crawling. 4, diapedesis (transmigration).

However, a recent report has shown that some effector T lymphocytes have the ability to transmigrate via inflamed barriers without surface deposited chemokine or even chemokine gradients (Shulman *et al.*, 2012). This mechanism requires adhesive integrin interaction with inflamed endothelial barriers without the need for integrin-activating chemokines (Figure 1.4).

1.8 Fibroblast growth factors (FGF)

Fibroblast growth factors constitute a family of polypeptides recognized in both vertebrates and invertebrates. In vertebrates the FGFs are categorized into 6 subfamilies that share similar sequences, developmental and biochemical properties. The FGF1 sub family includes acidic and basic FGF members (FGF1 and FGF2 respectively). FGF8 subgroup members (FGF8, FGF17 and FGF18), for instance, have about 80% amino acid sequence similarity and receptor binding identity (Xu *et al.*, 2000; Itoh and Ornitz, 2004). FGF11, FGF12, FGF13 and FGF14 are not classified in subfamilies because they do not activate FGF receptors (Olsen *et al.*, 2003).

1.8.1 FGF2 and renal fibrogenesis

FGF2 is a single-chain polypeptide with a molecular weight of 18 kilo Daltons (kD). FGF2 was first isolated from a kidney homogenate in 1985 (Baird *et al.*, 1985). FGF2 is expressed at different sites in normal human kidney such as distal epithelial and vascular smooth muscle cells (Floege *et al.*, 1999). There is strong evidence that proximal tubular epithelial cells constitute the source of FGF2 and TGF-β (Phillips *et al.*, 1996; Phillips *et al.*, 1997).

FGF2 plays crucial roles in biological activities such as cell proliferation and differentiation. This factor stimulates the proliferation of mesangial, proximal epithelial and endothelial cells *in vitro* and *in vivo* (Zhang *et al.*, 1991; Floege *et al.*, 1993; Klint and Claesson-Welsh, 1999) as well as the production of mesangial cell extracellular matrix (Floege *et al.*, 1992). FGF2 was found to increase the mitogenesis of smooth muscles and fibroblasts (Scholz *et al.*, 2001). Another example of the function of FGF2 is stimulation of the proliferation of smooth muscle cells in asthmatic inflammation (Bosse and Rola-Pleszczynski, 2008).

TGF-β is upregulated during renal rejection; indeed TGF-β plays a major role in the induction of EMT in kidney in association with FGF2 (Robertson *et al.*, 2001; Strutz *et al.*, 2001). FGF2 expression was upregulated in fibrotic kidney, particularly in interstitial and tubular cells. Interestingly, FGF2 stimulated the proliferation of fibroblasts in kidney which indicates the importance of this cytokine in promoting EMT and renal fibrosis (Strutz *et al.*, 2000; Strutz *et al.*, 2002).

Recent reports examined tubular epithelial cells for the expression of syndecan-1 and the heavily sulphated 10E4 epitope alongside FGF2 in renal allograft biopsies. The results show that tubular epithelial cells stained with syndecan-1 and 10E4 antibody failed to stain to FGF2; which explains two levels of regulation for FGF2 binding : the expression of syndecan-1 and sulphation motifs (Celie *et al.*, 2012).

1.8.2 FGF-HS interaction

Interactions between HS and FGFs such as FGF1, FGF2, FGF8 and FGF18 have been extensively studied (Xu *et al.*, 2000; Itoh and Ornitz, 2004; Kreuger *et al.*, 2005). These interactions depend on HS structure and sequences attached to proteoglycans on cell surface (Allen and Rapraeger, 2003).

HS interacts with growth factors via specific binding domains. FGF1 binds to HS via a minimal binding site composed of a tetrasaccharide (Mach *et al.*, 1993), whereas the minimal binding site for FGF2 is a hexasaccharide (Turnbull *et al.*, 1992). The HS interaction with FGF is required for further high affinity binding with FGF specific receptor (FGFR) (Brickman *et al.*, 1995). For example, the FGF2-FGFR signalling requires the presence of the 6-O sulphate group which is necessary for FGF dimerization (Schlessinger, 1988). This interaction enhances the affinity of FGFs for their receptors by forming a trimolecular complex including FGF, FGFR and HS. This complex allows FGFR dimerization and phosphorylation which is necessary for FGFR activation and signalling (Rapraeger *et al.*, 1991; Ornitz *et al.*, 1995). Further studies showed that formation of ternary complex is essential for FGF2 signalling (Ashikari-Hada *et al.*, 2009), (Figure 1.5).

Activation of FGFR leads to phosphorylation of the intracellular signalling pathway of mitogen activating phosphokinase (MAPK), which includes pathways of extracellular regulated kinase (ERK), p38 and c-Jun amino terminal kinase (JNK). Additional pathways were classified under the MAPK group for cell-specific signalling including phospholipase C, phosphoinositol 3 kinase (PI3K) and protein kinase B (Akt) (Dailey *et al.*, 2005; Katz *et al.*, 2007). Crystal structure analysis has shown that FGF2 interacts with its specific receptor in presence of HS in a ternary complex FGF2-HS-FGFR (Pellegrini *et al.*, 2000; Schlessinger *et al.*, 2000).

Sulphation at the O position is crucial for HS binding with fibroblast growth factors. Disruption of specific HS O-sulphotransferase genes during the embryonic stage resulted in significant developmental defects (Ashikari-Hada *et al.*, 2004). Angiogenesis induced by FGF2 was inhibited in presence of 6-O desulphated heparins in chicken embryos (Lundin *et al.*, 2000). Furthermore, double knockout of HS6ST1 and HS6ST2 in murine embryonic fibroblasts exhibited a reduction of FGF4, FGF2 and FGF1 signalling pathways (Sugaya *et al.*, 2008). The role of 2-O and N- sulphate groups as an essential component in the epitope binding as well as the assembly of FGF-HS-FGFR complex was extensively studied (Allen *et al.*, 2001).

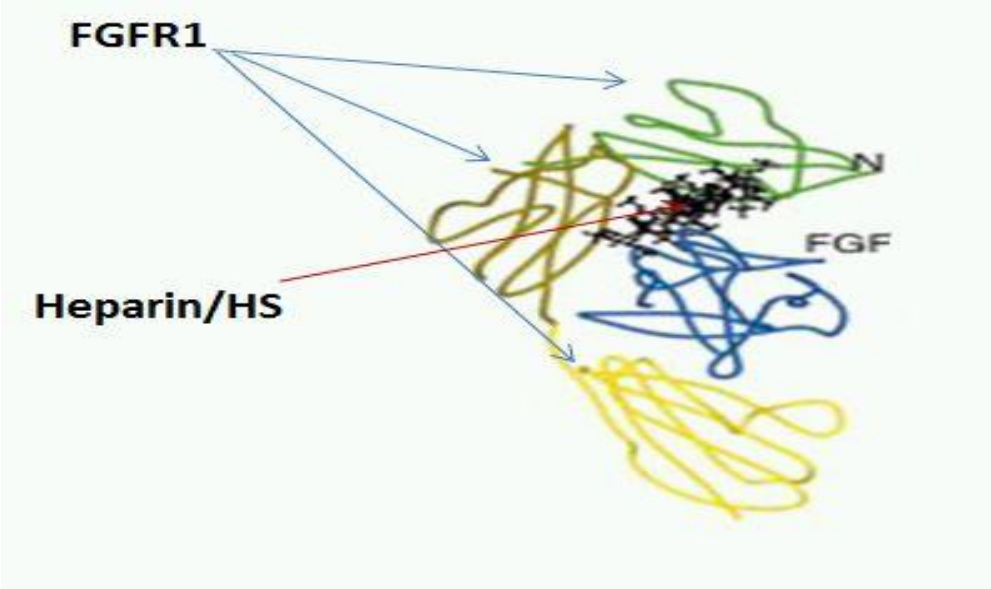

Figure 1.5. The ternary complex of FGF-HS-FGFR. FGF and FGFR have been shown to have a positive charge that binds to negative charged heparin surfaces forming a sandwich model. Figure adapted from (Johnson MS et al, 1999).

Although the trimolecular FGF-HS-FGFR complex is required for complete activation of FGFR, a few cases have shown that FGFs can still bind and activate FGFR in absence of heparin/HS (Roghani *et al.*, 1994). Additionally, Lin et al. demonstrated that in the absence of HS, high levels of FGF can activate FGFR leading to dimerization and signalling (Lin *et al.*, 1999).

1.8.3 FGF-HS binding epitope

HS structural diversity is generated through biosynthesis of polysaccharide units. The nature of HS interaction with FGF2 has been a subject of intense study (Rapraeger *et al.*, 1991; Friedl *et al.*, 2001). Several models have been suggested for FGF-HS-FGFR structure.

Faham et al. were the first group to show that a tetrasaccharide structure of heparin is required for FGF2 binding using crystal diffraction. The FGF-HS binding epitope contains UA2S-GlcNS6S-IdoA2S-GlcNS6S which interact specifically with Aspartic acid-28 (Asp), Arginine-121 (Arg), Lysine-126 (Lys) and Glutamine-135 (Glu) on the FGF2 structure (XBBX), (Faham *et al.*, 1996). This result was confirmed using nuclear magnetic resonance (NMR) spectroscopy (Guglieri *et al.*, 2008). Inclusion of an additional IdoA2S-GlcNS6S domain allowed additional binding to Lys-27, Asn-102 and Lys-136-144 (Faham *et al.*, 1996). Using selectively desulphated disaccharides, it was shown that 2-O sulphate is required for HS-FGF2 binding (Ishihara *et al.*, 1994).

Fragments involved in HS-FGF2 binding were revealed by using binding and elution techniques from FGF2 affinity chromatography columns (Habuchi *et al.*, 1992; Turnbull *et al.*, 1992). Further techniques were used to clarify the HS-FGF2 structure, including x-ray diffraction to resolve crystal structures (Faham *et al.*, 1996; Schlessinger *et al.*, 2000) and affinity analysis of oligosaccharides generated by enzymatically-modified heparin (Jemth *et al.*, 2002; Ashikari-Hada *et al.*, 2004). The crystal structure shows that FGF-HS binding is not just a neutralization of charge but it is also a specific reaction (Waksman and Herr, 1998).

The essential components of the HS-FGF2 epitope are GlcA/IdoA-GlcNS-IdoA2S disaccharide domains (Guimond *et al.*, 1993; Faham *et al.*, 1996; Pye *et al.*, 2000; Kreuger *et al.*, 2001; Loo *et al.*, 2001). Initial experiments showed that five repeating disaccharides of IdoA2S-GlcNS were able to interact with FGF2 (Turnbull *et al.*, 1992). However, the highest binding affinity was observed with 14 dp (degree of polymerization) monosaccharides. Interestingly, 6-O sulphate groups were found in the dp 14 fractions in small amounts. For biological activity, including FGF-FGFR signalling, it was shown that at least 10 monosaccharides are

required, including the 6-O sulphate group (Maccarana *et al.*, 1993; Tyrrell *et al.*, 1993; Ishihara *et al.*, 1994). A good example of the role of 2-O sulphate in FGF2 binding was verified using a specific FGF2 octasaccharides with or without 2-O sulphate groups. Addition of a 2-O sulphated tetrasaccharide resulted in binding of FGF2 (competing) and inhibition of FGFR activation and, thereafter, ERK phosphorylation, whereas in the absence of 2-O sulphates the tetrasaccharide did not inhibit the binding of FGF2 (Ashikari-Hada *et al.*, 2009).

It has been demonstrated that HS-FGF2 binding is correlated to the overall level of HS sulphation. Heavily sulphated heparin oligosaccharides were shown to have more efficient domains compared to sulphated HS (Kreuger *et al.*, 2006). Charge distribution along HS chains is suggested to be the major requisite for HS-protein interaction and to a lesser extent the presence of specific saccharide sequences is required. Accordingly, the importance of specific sulphation of HS with FGF-FGFR binding and signalling was verified in previous reports (Stringer, 2006). However, this interaction is claimed not to depend on a definite sequence of monosaccharide domains or even the presence of a unique component. (Kreuger *et al.*, 2006; Lindahl, 2007). Mulloy et al. have argued that high affinity GAG binding might require specific structural features of oligosaccharides but "does not depend on any single unique sequence, or even a very restricted set of sequences" (Mulloy and Rider, 2006).

1.9 The Role of HS in the regulation of transplant rejection

Heparan sulphate plays various roles in inflammation and fibrosis following kidney transplantation. These roles depend to a large extent on HS structure, sulphation pattern and consequent biological activity.

1.9.1 HS in kidney

The kidney is composed of a large number of functional units called nephrons. Each nephron is composed of a glomerulus, proximal tubule, loop of Henle and distal tubule. The glomerulus basement membrane (GBM), covered by a thin layer of epithelial cells, contains interacting ECM molecules such as collagens, laminins and HSPGs. The GBM plays a key role in glomerular filtration by regulating the access of plasma molecules to the tubular system depending on size, shape and

charge. The GBM has a negative charge, attributed to its content of HS, which forms a selective barrier for plasma proteins (Raats *et al.*, 2000). Therefore, negatively charged proteins will not be able to cross the barrier due to the negative charge of HS in the GBM (Kanwar and Farquhar, 1979).

Glomerular endothelial cells have the capability to produce HS, dermatan sulphate and chondroitin sulphate (Kashihara *et al.*, 1992). Indeed, a study using *in vitro* bovine endothelial cells has shown that IL-1β increases HS expression by glomerular endothelial cells (Sorensson *et al.*, 2003). HS undergoes several modifications in patients with proteinuria such as masking by immune complexes, cleavage, HS depolymerization, or reduced production (Raats *et al.*, 2000). Additionally, HS undergoes changes in sulphation patterns concerning N- and 6-O sulphate groups in systemic lupus erythematic nephropathy. These changes were mainly observed in HS on the endothelium and in the GBM (Rops *et al.*, 2007). HS also facilitates leucocyte infiltration of the tubular epithelium, which causes tubulitis. This role requires interaction between HS and chemokines, cytokines and L-selectins, leading to tubulitis-induced acute rejection (Robertson and Kirby, 2003; Ali *et al.*, 2005a).

1.9.2 HS in inflammation

The immobilization of chemokines by HS leads to the establishment and maintenance of chemokine gradients which are important for leucocyte migration through various tissues and organs (Li *et al.*, 2002). Interestingly, the involvement of HS in chemokine transport across endothelial cell layers (transcytosis) sheds more light on the involvement of HS in the inflammatory response (Gotte *et al.*, 2005). Wang et al. showed that decreased endothelial HS (knock-down of NDST1 and NDST2) caused decreased neutrophil infiltration accompanied with impaired L-selectin binding and reduced chemokine mediated transcytosis through vascular endothelium (Wang *et al.*, 2005).

IFN-γ is a proinflammatory cytokine which plays important roles in the immune response via activating and promoting cell mediated immune response including cytotoxic T cells, NK cells and macrophages (Dalton et al., 1993). IFN-γ is also involved in tissue remodeling, matrix biosynthesis, cell adhesion and cell

differentiation and proliferation (Stark et al., 1998). Binding of IFN-γ to HS provides protection to the cytokine but can modulate its activity (Lortat-Jacob, 2006). Further studies confirmed the role of HS in binding IFN-γ; addition of heparin was shown to block the interaction between endothelial cell HS and IFN-γ by competing with endogenous HS (Douglas et al., 1997). The HS-IFN-γ binding sequence was reported to have NA domains flanked with NS domains (6-8 saccharides) (Lortat-Jacob et al., 1995).

1.9.3 Role of HS in chronic rejection

Heparan sulphate is an essential co-receptor for binding and signalling of various cytokines and growth factors which are involved in the pathology of chronic inflammation of transplanted kidney such as IL-1, IFN-γ, TGF-β and FGFs (Ali *et al.*, 2003).

Acute rejection constitutes a major risk factor for chronic rejection (Waaga et al., 1997). HS undergoes changes in expression and sulphation according to its involvement in inflammatory responses. HS plays significant roles in chronic rejection which are mediated via binding and presenting of factors such as IL-1, IL-6, IL-4, TGF-β, IFN-γ and FGF2 (Phillips et al., 1996; Shirwan, 1999; Valles et al., 1999; Waaga et al., 2000).

TGF-β induces the production of ECM proteins such as collagen-I in rat tubular cells (Creely *et al.*, 1992). TGF-β also stimulates the production of fibronectin and HSPGs in rabbit tubular cells (Humes *et al.*, 1993). Furthermore, HS has the capability to bind and protect TGF-β from degradation leading to high concentration of the cytokine which is necessary for its activity (McCaffrey *et al.*, 1994). Interestingly, selective desulphation of N-, 2-O or 6-O has been shown to affect negatively the TGF-β activity (Lyon *et al.*, 1997).

Recent reports have shown that HS sulphation is modulated in disease along with novel binding roles and activities. In fibrogenic liver disease, HS modifying enzymes showed an increase in their expression at the mRNA level compared to normal tissue. These enzymes included NDST1, sulphatase 1 and 2, HS3ST1, NDST2 and HS6ST1 (Tatrai et al., 2010). Liver fibrosis changed HS expression and sulphation in order to accommodate novel interaction abilities with factors

involved in this process. Increased levels of ECM molecules including collagen XVIII and perlecan were reported in chronic kidney rejection (Joosten *et al.*, 2002). Fragments of perlecan (LG3) were increased in urine as an indicator of chronic kidney disease (O'Riordan *et al.*, 2008); these fragments were also increased in patients serum accompanying with vascular rejection (Soulez *et al.*, 2012). Changes in HS expression levels were also reported in chronic inflamed synovium. Markedly increased expression of syndecans (1, 2 and 3) and glypican 4 was reported in chronic rheumatoid and psoriatic synovia compared to normal joint synovia (Patterson et al., 2008).

1.10 Hypothesis

"The sulphation pattern of HS regulates fibrosis during renal allograft rejection by modulating the biological activity of growth factors".

1.11 Specific Aims

This project aims to achieve the following objectives:

1. To investigate the role of HS6ST1 on HS sulphation and regulation of biological activity of cytokines in renal epithelial cells.
2. To study the effect of endosulphatase 2 (SULF2) expression on HS sulphation and regulation of biological activity of FGF2.
3. To investigate changes in HS sulphation using an *in vivo* model of unilateral ureteral obstruction (UUO) in mouse kidney.

Chapter two

2 General materials and methods

2.1 Laboratory procedure

All experiments were carried out under the safety policy of Newcastle University and the Institute of Cellular Medicine (ICM), in accordance with university rules of 'Safe Working with Biological Hazards', 'Safe Working with Chemicals in the laboratory' and 'A basic Guide for Radiation Workers'. Experiments involving radioisotopes were approved prior to commencement in accordance with rules of 'Local Rules for the Use of Unsealed Sources of Radioactivity in the Medical School-Newcastle University'. For experiments involving the use of potent carcinogens and toxins, a COSHH 'Control of Substances Hazardous to Health' a risk assessment was followed. Tissue culture work was performed in compliance with regulations of BIO-COSHH class II risk assessment with guidelines produced in ICM. Genetic modifications and mammalian cell transfection were approved by the Microbiological Hazards and Genetic Modification Safety Advisory Sub-Committee.

2.2 Culture media

2.2.1 Dulbecco's Modified Eagle Medium (DMEM)

DMEM (Lonza) was supplemented with 100 IU/ml penicillin, 100µg/ml streptomycin, 2mM L-glutamine and 10% heat inactivated fetal calf serum FCS. This medium was used for supporting the growth of EAhy.926 cells.

2.2.2 DMEM-ham's F12 medium

DMEM–Nutrient F12 Ham (DMEM-F12) (Lonza) supplemented with 10% heat inactivated fetal calf serum (FCS), 100IU/ml penicillin, 100µg/ml streptomycin and 2mM of L-glutamine (Sigma-Aldrich). This medium was used for growth of epithelial cell lines HK2, HKC8, CHO, CHO-745 and CHO-677.

2.2.3 MCDB-131 medium

MCDB-131 medium (Sigma-Aldrich) containing 1 ng/ml hydrocortisone (Sigma-Aldrich) and 10 ng/ml human epidermal growth factor (EGF). Complete media

were supplemented with 10% heat inactivated fetal calf serum (FCS), 100 IU/ml penicillin, 100 µg/ml streptomycin and 2mM of L-glutamine (Sigma-Aldrich).

2.2.4 Propagation of cell lines

Adherent cells in this study were grown in 25 and 75 cm^2 flasks horizontally (Griener Bio-One) in humidified 37^oC incubators with 5% CO_2. These cells were harvested every 2-3 days in a ratio of 1:3.

2.3 Cell lines

2.3.1 Human kidney (HK2)

HK2 is a human kidney cell line immortalized from human proximal tubular cells (Ryan *et al.*, 1994). These cells were grown in DMEM-F12 complete medium in horizontal culture flasks. The HK2 cells have adherent and epithelial morphology.

2.3.2 Human kidney (HKC8)

Human kidney proximal tubular epithelial cells (HKC8) were kindly provided by Dr. Lorrain Racusen (Racusen *et al.*, 1997). These cells were grown in complete medium of DMEM–F12.

2.3.3 Human microvascular endothelial cell line (HMEC-1)

This cell line was grown in MCDB-131 medium (Sigma Aldrich) containing 1 ng/ml hydrocortisone (Sigma Aldrich) and 10 ng/ml human epidermal growth factor (EGF) as well as FCS 10% and penicillin-streptomycin as stated above.

2.3.4 Chinese hamster ovary cells (CHO)

CHO-K1 is a wild type Chinese hamster ovary cell line that was grown in complete DMEM-F12 media. Additional mutant cell line known as CHO-745 was used. This mutant cell line is deficient of xylosyltransferase which is an essential enzyme for HS synthesis by transferring xylose to the core protein (serine) of HS which initiates the synthesis of GAG chains. Mutant CHO-745 and CHO-677(a GAG mutant cell line) were grown in DMEM-F12 (Esko *et al.*, 1985).

2.3.5 EAhy.926

EAhy.926 is a hybrid cell line derived by fusion of human umbilical vein endothelial cells HUVEC with human lung carcinoma cell line thioguanine resistant clone A 549. These cells have characteristics of differentiated endothelial cell functions such as haemostasis, inflammation and angiogenesis (Edgell *et al.*, 1983). EAhy.926 cells were grown in complete medium of DMEM.

2.4 Sub-culture work

2.4.1 Adherent cells

Cells were grown till 80% confluence when they were passaged by removing the medium and washed twice with sterile phosphate buffer saline (PBS; Sigma-Aldrich). Cells were detached by incubating with pre-warmed EDTA-Trypsin (Sigma-Aldrich) for 2-3 minutes at 37^{o}C. Following this, the detached cells were neutralized by equal volume of complete medium and transferred to plastic universal tubes (SLS, North Shields, UK) for centrifugation at 500g for 5 minutes. Pellets were resuspended in complete medium and divided into 2-3 flasks.

2.4.2 Cell counting and viability

Cells were counted by using modified Neubauer haemocytometer (Reichert). After being resuspended, 10 µl of cell suspension were put in the counting chamber beneath the coverslip. Cells were counted in at least two of the large squares and the total number was divided by two and multiplied by $1x10^4$ to obtain the final number in ml. Cell viability was examined by mixing one volume of cell suspension with one volume of 0.2% trypan blue (Sigma-Aldrich) and dye-excluding cells were counted as viable.

2.4.3 Cryopreservation of cells in liquid nitrogen

Cells were detached from 80% confluent flasks, spun down at 500g for 5 minutes and resuspended in 0.9ml of complete media, following this 0.1 ml of dimethylsulphoxide (DMSO, Sigma-Aldrich) was added at a final concentration of 10%. The cells were transferred into cryovials (Corning) and put in a freezing

vessel (Nalgene) which contains isopropranol. Cells were then cooled in -80^{o}C at 1 ^{o}C/minute overnight and transferred to liquid nitrogen. These cells were recovered by thawing at 37^{o}C followed by incubation in 5-10 ml of complete medium for 24 hours where medium was replaced with fresh medium to remove any remaining DMSO.

2.4.4 Mycoplasma screening test

Cell contamination with Mycoplasma may affect the cell metabolism, viability, proliferation and function. MycoAlert kit (Lonza) was used for detection of mycoplasma enzymes that catalyze the conversion of adenosine diphosphate (ADP) to adenosine triphosphate (ATP). This conversion can be measured by bioluminescent reaction due to interaction between MycoAlert substrate and ATP. The MycoAlert protocol depends on mixing of 100 µl of supernatant media with 100 µl MycoAlert reagent and the first reading was taken after 5 minutes (A), 10 minutes later the second reading was taken (B). Results were calculated by dividing B/A, and result with less than 1 considered as negative whereas results more than 1 was considered as mycoplasma positive. No positive Mycoplasma results were noticed in this project. However, in case of positive results, cells will be discarded or treated with mycoplasma removal agent (MRA, Serotec) until free of infection.

2.5 General Molecular Biology

2.5.1 RNA isolation

In order to avoid RNA degradation caused by RNase contamination, RNA isolation was carried out under strict rules of high decontamination. These included decontaminating bench, racks, micropipettes, gloves and other equipment with RNase-ZAP (Sigma-Aldrich) followed with alcohol. Cells were grown till 70-80% confluency, washed with PBS and incubated with 1ml RNAzol B reagent (Sigma-Aldrich) for 5 minutes (approximately 1x10^{7}cells). RNAzol B allows cell lysis and solubilization by forming complexes of RNA, water and thiocyanate. Cells were removed by scrapers into 1.7 ml Eppendorf tubes and left at room temperature for 5 minutes. 200 µl (1:5 RNAzol) of pre-chilled chloroform (denatures the protein) was

added and tubes were shaken vigorously for 15 seconds, left on ice 2-3 minutes and centrifuged for 15 minutes at 12000 g in 4^{o}C centrifuge. The upper aqueous layer was gently removed to 1.7 ml Eppendorf tube and mixed well with equal volume of propan2-ol (Isopropranol, BDH LTD, UK) and left on ice for 10 minutes. Tubes were then centrifuged at 12,000g for 10 minutes. Following that, the supernatant was removed and pellets were washed with 1ml of 75% ethanol by centrifugation for 5 minutes at 7500g. Supernatant was removed and pellets were left to air-dry. The RNA was finally reconstituted in 50 µl diethyl pyrocarbonate (DEPC) treated water.

2.5.2 Nucleotide quantification

RNA/DNA was quantified by spectrophotometer (Biophotometer, Nanodrop). One drop (1 µl) of nucleotide was measured at O.D of 260/280 and 230/260. The 260/280 value gives a good clue of the purity of RNA/DNA whereas 260/230 ratio gives an idea about the nucleotide contents. Values of 260/280 more than 2 were considered for good quality and samples were used for further steps. In case of 260/280 value less than 1.8 RNA/DNA sample was discarded and the whole procedure was repeated. 260/280 values lower than 1.8 indicate the presence of proteins, phenol or other contaminants.

2.5.3 RNA separation by gel electrophoresis

To examine its integrity, each RNA sample was run on a 0.8 % Agarose gel with ethidium bromide (final concentration 0.5µg/ml). This gel was electrophoresed in tris-acetate EDTA (TAE) buffer (0.004M Tris-acetate and 0.001M EDTA, pH 8.0) and visualized by UV light. Intact subunits (no smears) of 28s and 18s with a ratio of 2:1 respectively were considered as a good clue of RNA integrity.

2.5.4 Synthesis of cDNA

Complementary DNA (cDNA) is synthesized from RNA by reverse transcription to produce a single strand of DNA. cDNA was obtained from RNA using Superscript III reverse transcriptase (Invitrogen). Each tube contained 5 µg RNA with 1µl oligo $dT_{12\text{-}18}$ primer/random hexameres and 1 µl of dNTP (10mM) in a total volume of 13

µl. Tubes were incubated at 65°C for 5 minutes. The mix was chilled at 4°C for one minute and centrifuged briefly. A master mix of 6 µl was added to each tube (4 µl of 5x First Strand buffer, 1 µl of DTT and 1 µl of Superscript III enzyme) and mixed by gentle pipetting. Tubes were incubated at 50°C for 50 minutes followed by 15 minutes at 70°C before cooling. Incubations were performed in PCR thermal cycler (Hybaid).

2.5.5 Transformation

The cDNA encoding the human HS6ST1 gene (contained in pCR-Blunt II-Topo plasmid) was purchased from Geneservice. This plasmid was cut in order to be ligated to pcDNA3.1/Zeo+. Both plasmids were digested with *Pst* I and *BamH* I resulting in cohesive ends

2.5.5.1 **Bacterial culture**

Escherichia coli (E.coli) were grown in Luria-Bertani (LB) broth (10g/L Bacto-tryptone, 5g/L Bacto-yeast extract, 10g/l sodium chloride and pH:7; Sigma-Aldrich) in different sizes such as universal tubes or glass conical flasks. In case of plasmid-containing bacteria, antibiotics in accordance to the plasmid were added to prevent other clones from growing. In this study, ampicillin (100µg/ml) or kanamycin (50µg/ml) were used for plasmids containing SULF2 or HS6ST1 genes respectively. Bacteria were cryopreserved for longer use by mixing 0.5ml of bacteria broth with 0.5ml of 40 % glycerol (Sigma-Aldrich) in cryovials and kept in -80°C.

Agar plates including ampicillin were also prepared for growing of bacteria after transformation. Antibiotics were necessary to allow only transformed bacteria to grow.

2.5.5.2 **Competent Cells**

Competent cells were made with XL1-Blue, DH5-α or JM83 clones. Bacteria were grown in LB overnight. The next day, 5 ml of bacteria was inoculated in 200 ml of LB and grown in orbital shaking incubator at 37°C till OD_{550} was 0.500. In the following step, cells were chilled at 4°C for 15 minutes, gently mixed with 50 ml of

10 mM $CaCl_2$ and incubated on ice for 10 minutes. Pellets were resuspended in 50ml of cold 75mM $CaCl_2$ and kept on ice for 35 minutes. Tubes were spun down for 15 minutes in cold centrifuge, pellets were suspended in 3 ml of pre-cold 75mM $CaCl_2$ and the resulting content was transferred to a tube containing 0.488 ml of 100% sterile glycerol. Finally, competent bacteria were aliquoted into sterile 1.5 ml tubes and kept in -80^{o}C.

2.5.5.3 **Transformation of competent bacteria**

Plasmids containing the DNA of interest were transformed into competent bacteria in order to obtain a higher quantity of DNA by bacterial growth. In this study DNA insert was ligated in a proper mammalian vector and vector/insert (i.e. HS6ST1-pcDNA3.1/zeo+) was initially transformed into competent cells (DH5-α). First, 10-100ng of plasmid DNA (vector/insert) was incubated with 100µl of competent bacteria (DH5-α) on ice for 30 minutes. The mix was heat-shocked by exposing to temperature of 42^{o}C for 90 seconds in water bath followed by ice cooling for 5 minutes. In the following step, cells were incubated with 20ml LB in shaking incubator at 37^{o}C/150 rpm for 2 hours. The universals were then centrifuged for 5 minutes at 400g and the pellets were gently resuspended in 200 µl of LB medium and spread on LB agar plates (35 g/L of LB Agar) supplied with proper antibiotic. For each experiment, a series of control tubes was included which contained negative and positive controls (Table 2.1).

Number	Agar plate
1	Dish with no bacteria
2	Dish with transformed bacteria and no antibiotics
3	Dish with transformed bacteria and antibiotics
4	Dish with untransformed bacteria with no antibiotics
5	Dish with untransformed bacteria with antibiotics

Table 2.1. Agar plates distribution in transformation.

The plates were incubated overnight at 37^{o}C upside down. Transformed bacteria growing on dishes with antibiotics (Dish-3) were considered positive. For large amounts of DNA, individual colonies were picked up and grown in an antibiotic-containing LB broth in shaking incubator (150 rpm) at 37^{o}C overnight.

2.5.5.4 **DNA precipitation**

DNA precipitation was carried out to increase the DNA concentration for some experiments. Sodium acetate (3M) was added to the DNA to reach a final concentration of (0.3M) and mixed well with 2 volumes of 100% ethanol. The mix was cooled at -80^{o}C for 20 minutes and centrifuged at 15000 g for 10 minutes. DNA pellet was washed with 70% cold ethanol and centrifuged for additional 5 minutes at the same speed. The supernatant was removed and the remaining DNA was air-dried and reconstituted in the appropriate volume of DEPC treated water.

2.5.5.5 **Restriction enzyme digestions**

Restriction enzymes were used in this study depending on the sequence of the plasmid in use. Restriction enzymes can cleave DNA in a sequence specific manner. Plasmid sequence was restriction-mapped using the Invitrogen web site and the restriction enzymes were chosen as needed. Mostly, two restriction enzymes were chosen with unique restriction sites for both of the insert and the vector. One unit of an enzyme is the activity that cleaves 1µg of Lambda-DNA at 37^{o}C in one hour. For each digestion reaction, 1µg of plasmid DNA, 2µl of 10X buffer (Promega), 0.2 µl of BSA and 1 µl (5 units) of restriction enzyme were added in a 20 µl final volume reaction and mixed gently by pipetting. Tubes were incubated at 37^{o}C for 2-3 hours according to the manufacturer's instructions (Promega). For pcDNA3.1/Zeo+ and HS6ST1, both were cut using *Pst I* and *BamH I* that resulted in cohesive ends.

PstI: 5'-CTGCA↓G-3'

BamHI: 5'-G↓GATCC-3'

2.5.5.6 **Ligation Reaction**

DNA coding HS6ST1 was cut using *Pst I* and *BamH* I enzymes and run on an agarose gel (1%) alongside the vector. The insert-DNA was then cut out of the gel and purified. The vector pcDNA3.1/Zeo+ was also digested with restriction enzymes *Pst* I and *BamH,* run on agarose gel and purified as stated above. The DNAs of the insert and the vector were ligated using T4 DNA ligase kit (Invitrogen) following instructions related to cohesive ends. The molar ratio of the insert to the vector was 6:1 respectively. Ligated fragments were tested by digesting with *Pst* I and *BamH* I enzymes and then loaded on 1% agarose gel to visualize the band sizes. Concentration of insert-DNA was calculated according to the equation:

$$\text{Insert mass (ng)} = 6 \times \frac{\textbf{Insert length (bp)}}{\textbf{Vector length (bp)}} \times \text{vector mass (ng)}$$

2.5.5.7 **Gel Electrophoresis**

Agarose gel electrophoresis was carried out to visualize DNA products such as after conventional PCR or following digestion with restriction enzymes. This technique depends on separation of DNA products upon their sizes compared to DNA ladder 100bp (Promega) or 1kbp ladder (Fermentas). The gel is immersed in a TAE buffer where an electric field is applied that allows DNA fragments to migrate towards the positive electrode (according to their negative charges). A definite weight of agarose (w/v), depending on the final concentration required, was dissolved in 50 ml of TAE buffer and boiled in a microwave. The gel was left to cool at room temperature when ethidium bromide (0.5μg/ml) was added. Gels were prepared with different concentrations between (0.7-1.5%) depending on sizes of DNA fragments.

2.5.5.8 **Gel Extraction**

DNA fragments were excised out of the gel and purified following the protocol of QIAquick Gel Extraction Kit (Qiagen). After being electrophoresed, DNA fragments were cut out of the gel using a sterile scalpel. The gel-slice containing the DNA fragment was weighed (mg) and completely dissolved in a binding solution (QG Buffer) at 50^{o}C for 10 minutes. The dissolving mixture was prepared

where 3 volumes (3µl) of QG buffer were mixed with one volume (1mg) of the gel-slice considering that each 1µl of the solution approximately equals to 1mg of gel-slice. The mixture was applied to spin column and washed twice with membrane Wash Solution. In the final step, DNA was eluted using DEPC treated water and stored at -20^{o}C.

2.5.5.9 **DNA extraction**

According to the amount of DNA required, mini, midi or maxi prep kits were used (Qiagen). DNA was isolated from bacteria following the manufacturer's instructions (www.qiagen.com/handbooks). The reaction depends basically on lysis of bacteria under alkaline conditions and adsorbing of DNA to silica in presence of high salt buffer. Transformed bacteria were grown overnight with appropriate antibiotic. The cells were centrifuged and pellets were lysed and neutralized in presence of RNase. Samples were then purified by application of the supernatant to spin columns (silica membrane). The tubes were centrifuged and washed by PB buffer to remove endonucleases. High salt was removed by washing with PE buffer and plasmid DNA was eluted in nuclease free water. DNA was then quantified and stored at -20^{o}C.

2.5.6 DNA transfection

Transfection is a common procedure used to insert a foreign DNA into eukaryotic cells. The DNA is cloned in a vector with the ability to replicate. The plasmid is a double stranded DNA that contains specific promoter with an antibiotic resistance, origin of replication, and cloning sites with different restriction sites.

Transfection is classified into two main types, stable and transient. In transient transfection, the DNA does not integrate in the genome but transfected cells are able to express the gene of interest for several days. In stable transfection the translated DNA is integrated into the genome where it can replicate during cell division.

In this study, stable transfectants were generated by introducing the plasmid with a gene of interest into mammalian cells. Followed by antibiotic selection, single clones were picked and expanded.

The transfection depends on introducing the HS6ST1gene (Gene services) cloned in pcDNA3.1/zeo+ (Invitrogen) into the HK2 cells. The cells were grown to 60% confluence in six-well plates by using lipid-based transfection reagents (Effectene, Qiagen). One day before transfection, cells were seeded in 100 mm dishes and incubated under normal conditions. At the day of transfection cells were confluent by around 70%. For 100 mm dish, 2µg of DNA was dissolved in TE buffer with EC buffer in 300 µl (Table 2.2). DNA was mixed with enhancer at a ratio 1:8. The mixture was left 5-10 minutes at room temperature and 100 µl of Effectene reagent was added, mixed well and left at room temperature for additional 5-10 minutes. Afterwards, cells were washed with PBS and fresh growth medium was added (7 ml). Finally 3 ml of growth medium (DMEM-F12) was added to DNA-Effectene complex and the whole mix was added to the dish and incubated at 37^{o}C with 5% CO_2 for 48 hours. Cells were then passaged at 1:5 to 1:10 ratio and antibiotic (Zeocin, Invitrogen) was added at a final concentration of 400 µg/ml. Antibiotic-containing media was changed at 2-3 days. Colonies were picked and transferred into 48 well plates and grown to confluency before transferring to larger wells or flasks.

2.5.6.1 **Optimization of transfection procedure**

Transfection procedure was optimized using several ratios of Effectene Reagent (ER) to DNA. Best efficiency was noticed at 1: 50 ratio of DNA (µg) and Effectene reagent (µl) respectively.

Culture format	DNA (µg)	Enhancer (µl)	Final volume (µl)	Effectene reagent (µl)	Medium added to transfected reagent (µl)	Medium added to cells (µl)
12-well plate	0.3	2.4	75	6	400	800
6-well plate	0.4	3.2	100	10	600	1600
60 mm dish	1	8	150	25	1000	4000
100 mm dish	2	16	300	60	3000	7000

Table 2.2. Transfection reagent optimization (Qiagen).

2.5.6.2 **Transfection efficiency**

Cells were transfected with green fluorescent plasmid (GFP) (Invitrogen) at the same time and under the same condition as the gene of interest such as DNA concentration and DNA/ER ratio. These cells were examined by flow cytometry after 24 hours in order to estimate the efficiency of transfection. Briefly, GFP transfected cells were washed with PBS twice, detached by EDTA-Trypsin and centrifuged at 500g for 5 minutes. Pellets were resuspended in 2 % BSA-PBS and examined by flow cytometry against wild type cells. Cells that expressed GFP were considered as positively transfected and the ratio of these cells to the whole number of cells was considered as the transfection efficiency.

2.5.6.3 **Antibiotic killing curve**

Zeocin (Invitrogen) is a copper-chelated glycopeptides antibiotic which is isolated from culture broth of *Streptomyces verticillus* mutant. At a toxic level, Zeocin can bind to cell DNA and cleave it causing cell death. HK2 cells were seeded in six-well plates (in duplicates) till 20% confluent where different concentrations of Zeocin were added as follows: 0, 50, 100, 200, 400 and 600 µg/ml in complete media. The cells were left to grow in 37^{o}C, 5% CO_2 and media including antibiotic was changed every two days. The cell confluency was assessed every day for 7-8 days, floating cells were considered as dead. The lowest concentration of antibiotic where cells were completely dead was considered as the toxic dose (400µg/ml). Negative control included cells grown in absence of antibiotics.

2.5.7 DNA sequencing and alignment

Plasmid was supplied from Invitrogen (DNA3.1/zeo+) and cut with *BamHI* and *PstI* which have unique restriction sites, at 929 bp and 961bp respectively (Figure 2.1). HS6ST1 gene was supplied from Geneservice on pCR-Blunt II-TOPO plasmid transformed into bacteria with kanamycin selection antibiotic. HS6ST1 was digested using *PstI* and *BamHI* which produce cohesive ends. The insert (HS6ST1) and the vector (pcDNA3.1zeo+) were ligated using T4 DNA ligase (Invitrogen). Resultant vector-insert was sequenced (Geneservice) and aligned with HS6ST1 in PubMed (see appendices).

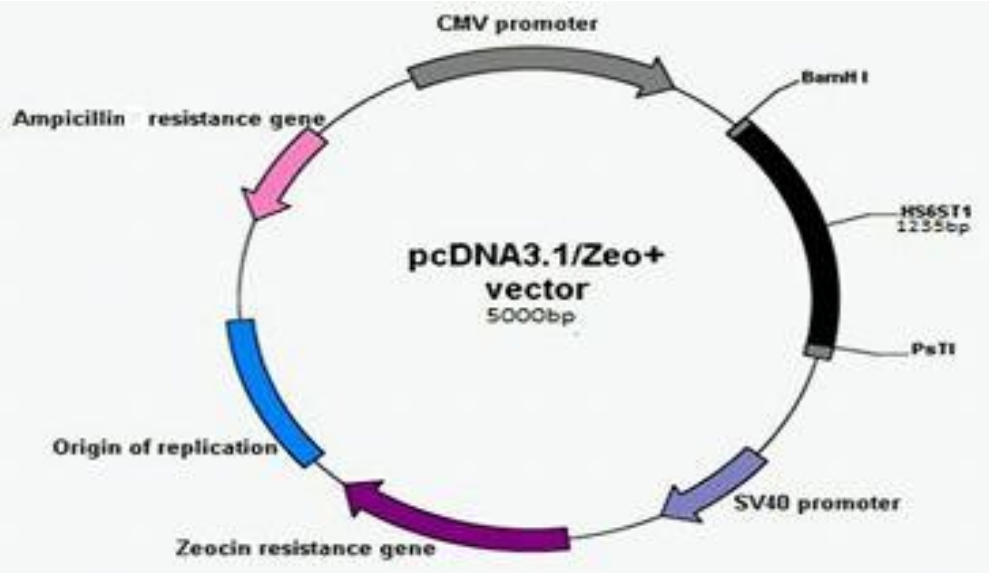

Figure 2.1. Drawing of the plasmid vector (pcDNA3.1/zeo+) and HS6ST1 insert.

2.5.8 Conventional PCR

The polymerase chain reaction (PCR) is used to amplify a target DNA. This reaction requires the presence of oligo nucleotide primers with specific sequence that binds at the beginning of the targeted sequence to be amplified. DNA needs to be denatured into two single chains by increasing temperature up to 94^{o}C which is carried out by thermal cycler. Temperature between 50-60^{o}C is required for primer annealing to the denatured DNA whereas 72^{o}C is required for the Taq polymerase extension (polymerization). Therefore a DNA polymerase chain reaction requires a thermal cycler, oligo nucleotide primers, dNTP and DNA polymerase enzymes with optimal conditions. For primers to anneal to the single stranded DNA, the thermal cycler will bring the temperature down to 50-60 ^{o}C according to the optimum temperature of primer annealing. Taq DNA polymerase enzyme is derived from *Thermus aquaticus* which is active at high temperatures. PCR experiments were performed using ready master mix (VHBio) with primers for house-keeping gene of glyceraldehyde 3-phosphatedehydrogenase (GAPDH) and HS6ST1 gene (VHBio). PCR procedure was optimized by changing temperatures and incubation times as well as concentrations of template DNA and primers. The best conditions for thermal cycler (Hybaid) are summarized in table 2.3.

Step	Duration time	Temperature	Cycles
Initial denaturing	10 minutes	93°C	1 cycle
Denaturing	30 seconds	93 °C	35 cycles
Annealing	30 seconds	55 °C	
Extension	60 minutes	72 °C	
Final extension	10 minutes	72 °C	1 cycle

Table 2.3. Thermal cycler conditions for conventional PCR.

Whereas the optimal concentrations for master mix and primers were as follows for 20 µl reaction tubes (Table 2.4):

Component	Final concentration	Volume (µl)
10x reaction buffer	1x	2
Taq DNA polymerase	0.08	0.2
dNTP	0.2 mM	0.2
primers	0.5 µM	1
$MgCl_2$ (50mM)	1.5 mM	0.8
DEPC-treated H2O		14.5

Table 2.4. Optimal concentrations of PCR mix components.

A plasmid encoding HS6ST1 DNA was used as a positive control (Gene Services) and PCR products were visualized on 1% agarose gel in TAE buffer.

2.5.8.1 **Oligo nucleotide primers**

Oligo primers were designed considering many conditions such as:

- Length between 18-30 bp.

- Primers must not be complementary to each other.
- Melting temperature is between 50°C and 65°C.
- They should bind specifically at the beginning of the target DNA.
- They should have sequence homology with the target DNA.
- CG contents should be around 50-55% of whole nucleotide content.
- Primers for GAPDH and HS6ST1 were designed according to the above conditions and ordered from (VHBio), (Table 2.5).

Primer	Sequence
GAPDH, Forward (F)	5'-ACCCAGAAGACTGTGGATGG-3'
GAPDH, Reward (R)	5'-AGGGGTCTACATGGCAACTG-3'
HS6ST1, F1	5'GCCCATCACACATATGCAAC 3'
HS6ST1, R1	5' GGCAGTCCATGAACTCCTGT 3'
HS6ST1,F2	5' TGATCGTCTTCCTGCACATC 3'
HS6ST1,R2	5'GACGACGTGATCGTCTTCCT 3'

Table 2.5. Primer sequences for conventional PCR amplification.

2.5.9 Quantitative PCR (qPCR)

Real time PCR (RT-PCR or qPCR) is a method developed for quantifying DNA that allows detection of amplified DNA at higher sensitivity compared to conventional PCR. Herein, in qPCR the amount of quantified DNA is linked to fluorescence intensity by binding to a fluorescent reporter molecule. In conventional PCR the amplified DNA is detected at the end of the reaction whereas the quantitative PCR (qPCR) measures the fluorescence at each cycle as the amplification is still in progress (exponential phase) before the consumption of the reagents and the accumulation of inhibitors. Fluorescence reporter molecules such as double-stranded DNA binding-dye or dye-labelled probes are used for monitoring the

progress of amplification reaction. The cycle number where the amplification crosses a definite threshold of fluorescence level is known as threshold cycle (CT). The probes used in this study were hydrolysis probes (TaqMan) which are sequence specific comprised basically of oligonucleotides labelled with FAM dye and TAMRA quencher. TaqMan primers generally contain additional sequence to the primer known as the probe. This probe anneals to the same strand of targeted sequence closely downstream the primer site. The fluorescence reporter dye (FAM) is attached to the 5' end whereas the quencher is attached to the 3' end of the probe. Fluorescence from the reporter is quenched as long as the reporter and the quencher stay close together (Figure 2.2). When polymerization extends, the Taq DNA polymerase encounters the 5' end of the probe. Taq polymerase then degrades the 5' end of the probe releasing the reporter dye and the quencher which results in fluorescence activity.

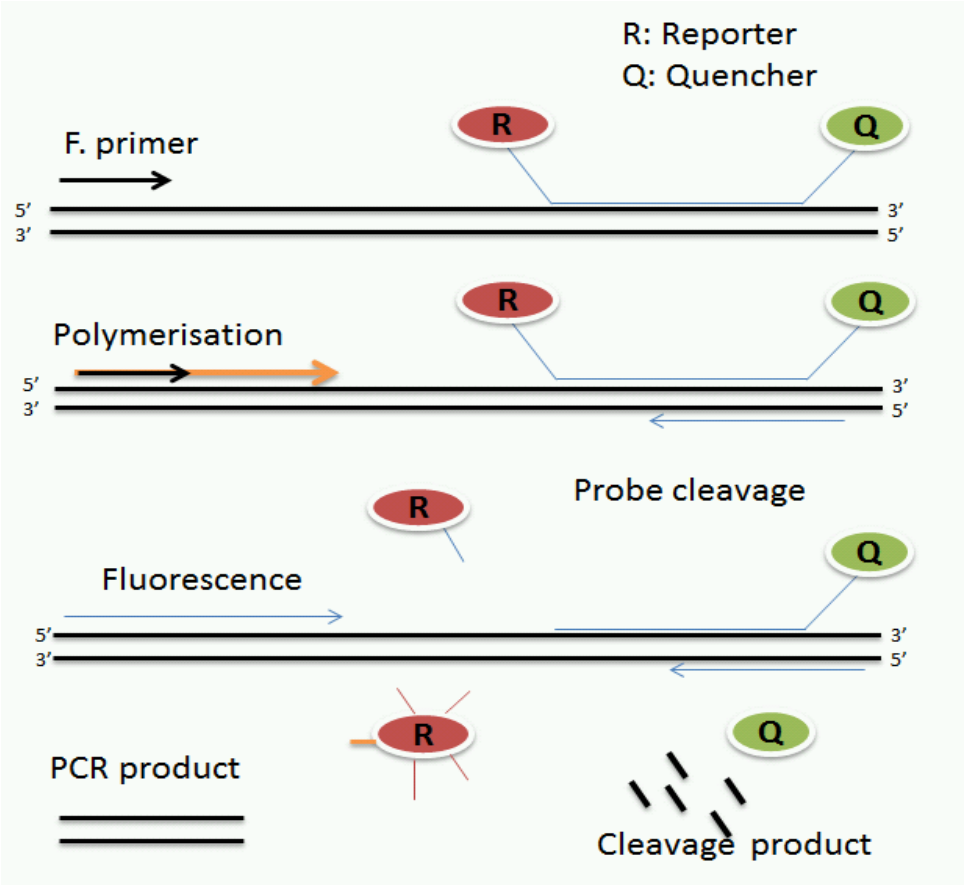

Figure 2.2. Diagram showing primer probes fluorescence during real time PCR.

Real time PCR experiments were performed in 96 well plates using master mix (Stratagene) with high Rox while primer-probes were ordered from TaqMan Gene Expression Assay with FAM dye-labelled probes. Rox dye provides a passive reference dye that helps in fluorescence normalization relating to pipetting errors and instrument limitations.

One tenth of cDNA (2μl) was used as template in each reaction (20μl). QPCR experiments were run in Applied Biosystem Prism 7000 machine with the following conditions (Table 2.6):

Temperature (°C)	Duration (Minutes)	Cycle number
50	2	1
95	10	1
95	15 seconds	40
60	1	40
4	hold	

Table 2.6. Real time PCR conditions.

Each well had a 20 µl reaction volume as follows: 10 µl of 2x master mix (high ROX), 1 µl of primer probe (20 x), 2 µl of cDNA and the volume was completed to 20 µl with RNase free water (7 µl), (Table 2.7).

Component	Volume (µl)
2x master mix	10 µl
cDNA	2 µl
Primer probe	1 µl
H2O	7 µl
Complete volume	20 µl

Table 2.7. Contents of qPCR tube reaction.

2.5.9.1 **Comparative CT method (ΔΔCT)**

For DNA quantification and data analysis, the comparative quantification method was used. This method was chosen to compare large number of targets with a house keeping gene without the need to run a standard curve for each assay. In this method the house keeping gene served as a reference for comparison with a target gene.

QPCR experiments were run in triplicates in 96 well plates and CT values were obtained. ΔΔCT values were calculated for resting (non-stimulated) and stimulated cells for each of the targeted gene and endogenous gene in each experiment. Fold change was expressed as the value of $2^{-\Delta\Delta CT}$ and ΔΔCT values were calculated as follows:

ΔΔCT= ΔCT (calibrator) -ΔCT (unknown).

ΔCT calibrator = (CTTa -CTRa) and

ΔCT unknown= (CTTa -CTRa). Where CTTa is the CT value for targeted gene and CTRa is CT value for reference gene.

ΔCT Data analysis was carried out using REST-2008 software.

2.5.9.2 **Probes**

Human exon junction spanning probes do not detect any amplified genomic DNA. These primer probes were ordered from (Applied Biosystem, TaqMan Gene Expression assay, table 2.8).

Primer-probe	Catalogue Number
GAPDH	Hs0099999905-m1
HS6ST1	Hs00757137-m1
SULF1	Hs00392834-m1
SULF2	Hs00393644-m1
HPSE	Hs00395394-m1

Table 2.8. Primer probes for RT-PCR (Applied Biosystem, TaqMan Gene Expression assay).

2.5.9.3 **Standard curve and Efficiency Test (Validation)**

A standard curve for the reference and targeted genes was made using the same concentration of cDNA. Using 10-fold serial dilutions, the CT numbers and the logarithmic values of RNA concentration (ng) were calculated to express the slope equation and PCR amplification efficiency. The slope of standard curve was used to estimate the PCR amplification efficiency of a real time PCR reaction. The efficiency was calculated from the equation: Exponential amplification=$10^{(-1/slope)}$

Efficiency= $[10^{(-1/slope)}]$-1, i.e. if the slope is -3.3 the amplification will be 2.0092 and efficiency is 1.0092 which means 100% efficiency. The efficiency of an optimal PCR should be between 90 and 110 % i.e. slope value between -3.1 and -3.6. Efficiency of qPCR can be affected by many factors such as amplicon length and primer designs. To achieve valuable results efficiency of qPCR was investigated and the procedure was used only after achieving validity of amplifying of around 100% (Figure 2.3).

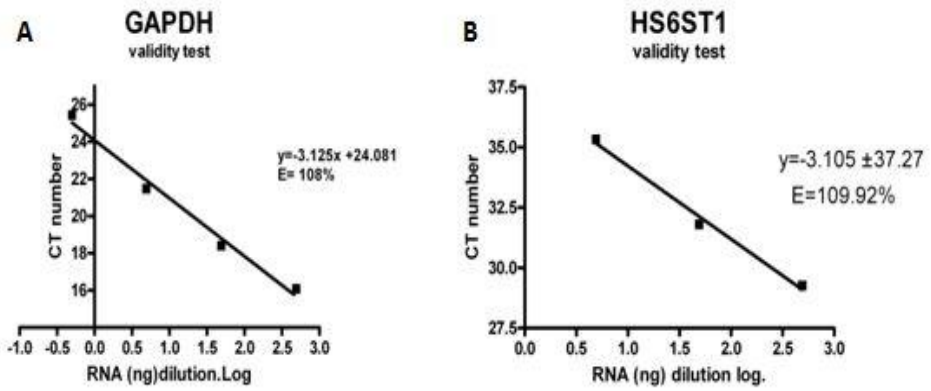

Figure 2.3. Efficiency of qPCR reaction for human GAPDH and HS6ST1 genes. Real time PCR experiment included template cDNA in 10-fold serial dilution in triplicates. CT numbers were calculated and analyzed against logarithms of dilutions. A, efficiency for GAPDH gene. B, efficiency for HS6ST1 gene. (N=2)

2.6 Protein chemistry

2.6.1 Protein extraction

Protein was extracted from cells using a lysis buffer (50mM Tris, 150mM NaCl, 0.5-1% NPO_4, phosphatase inhibitor) which was supplemented with one tablet of protease inhibitor (Complete Mini Protease Inhibitor Cocktail, Roche) for each 10 ml. Cells were grown in 25 cm^2 flasks till 70-80% confluency and medium was removed, cells were washed in PBS and detached by EDTA-Trypsin. Then cells were centrifuged and pellets were treated with 200µl lysis buffer, mixed well and left on ice for 15 minutes. These lysates were sonicated till frothing and centrifuged at 20,000 g for 20 minutes. The supernatant was removed to clean Eppendorf tubes where they were used for protein assay.

2.6.2 Protein assay

Protein concentration was estimated by using Bicinochoninic Acid (BCA) kit (Pierce). The assay basically depends on detecting protein by the Biuret reaction. In this reaction, peptides bind to cupric ions and form a coloured chelate complex under alkaline condition where Cu^{+2} is reduced to Cu^{+}. Then one Cu+ ion reacts with two molecules of BCA forming a purple-coloured product that exhibits absorbance at 562nm wavelength. Protein concentration was estimated in reference

to protein standard curve made using serial dilutions of a known concentration of BSA protein.

2.6.3 SDS-PAGE

SDS-PAGE, sodium dodecyl sulphate polyacrylamide gel electrophoresis, is a procedure that separates different proteins depending on molecular weight instead of negative charge. SDS allows all proteins to have high negative charge so they travel according to their molecular sizes when an electrical field is applied. SDS-PAGE consists of resolving component and stacking component which are prepared as shown in table 2.9. The gel was set up in a running tank with vertical electrophoresis apparatus (Bio-Rad).

Material	Resolving gel 10%	Stacking gel 5%
H2O	4 ml	3.4 ml
30% acrylamide mix	3.3 ml	0.83 ml
1.5 M Tris, pH :8.8	2.5 ml	-
1 M Tris, pH:6.8	-	0.63 ml
10% SDS	0.1 ml	0.05 ml
10% Ammonium persulphate (APS)	0.1 ml	0.05 ml
TEMED	0.004 ml	0.005 ml

Table 2.9. Components of 10% resolving and stacking acrylamide gels.

Acrylamide gel (10%) was used to fractional proteins of molecular sizes between 15 and 170 kD. After sample loading, the gel was immersed in running buffer (25 mM Tris, 250 mM glycine and 0.1%SDS with pH: 8.3) and electrical current of 80-120V was applied. A protein marker (Fermentas) was run with the proteins as a size reference. Equal concentrations of protein samples (10-30µg) were loaded after

being mixed with 1x SDS loading buffer (50mM Tris, 100mM dithiotheritol DTT, 2% SDS, 10% glycerol and 0.1 % Bromophenol blue) and boiled at 100^{o}C for 5 minutes.

2.6.3.1 **Coomassie staining**

Gels were stained with Coomassie blue to visualize the protein bands. Coomassie stain consists of 10% acetic acid (v/v), 10 % isopropanol (v/v) and 0.1 % Coomassie blue powder (w/v).

2.6.4 Western blotting

After running the proteins on acrylamide gel, protein bands were transferred to polyvinylidene difluoride (PVDF, Amersham) membrane by a procedure known as gel transfer. First, the PVDF membrane was immersed in methanol for 30 seconds followed by distilled water for 1-2 minutes. Electrophoresed gel was immersed in transfer buffer which consists of 3.03 g Tris-base, 14.4 g glycine, 200 ml methanol and the mix was made up to 1000 ml in distilled water. The electro-blotting cassette was preassembled in the transfer buffer and PVDF membrane was put over the gel that allows transfer of proteins from the gel to the PVDF membrane. The cassette was then put in transfer tank, immersed with transfer buffer and an electrical field was applied with 30V overnight with the cassette cooled by running water.

The membrane was removed and blocked in 5% non-fatty milk (Marvel) or 5% BSA in TBS-T (5mM Tris, 150mM NaCl, 0.1% Tween-20 with pH: 7.4) for one hour. Primary antibody was added in blocking buffer for at least one hour at room temperature or at 4^{o}C overnight. Then, the membrane was washed three times with TBS-T and incubated with secondary antibody conjugated by horseradish peroxidase (HRP), (Sigma-Aldrich), in blocking reagent for one hour at room temperature. The membrane was then washed in blocking buffer for three times on shaking incubator. The bound antibody was visualized by incubating the membrane with enhanced luminol-based chemiluminescence (ECL) substrate (Pierce, Thermo Scientific). A working reagent was prepared by mixing one volume of reagent A with one volume of reagent B. Appropriate volume (5 ml) of the working reagent was put on the membrane for 5 minutes. This substrate allows the oxidation of

luminol by HRP which results in emission of light. The membrane was then sealed in an appropriate cassette for exposure to X-ray film (Kodak).

2.6.4.1 **Staining of PVDF membrane**

Protein bands on PVDF membrane were visualized after membrane development by staining with copper-phthalocyanine (0.05% copper in 12m HCl).

2.7 Flow Cytometry

2.7.1 General principles

Flow cytometry (FACScan, Becton Dickinson) measures cells quantitatively and qualitatively as the machine recognizes cell numbers and cell types. The cells are forced into a narrow stream so they are counted one at a time. At this point cells are intercepted by a laser beam of known wavelength (generally 488nm) that stimulates the cells to emit light. This light may be scattered at two levels known as forward scatter (FSC) and side scatter (SSC). FSC light is scattered at low angle with laser beam that generates a signal which is proportional to the cell size. SSC light is scattered at 90^{o} angle with the laser beam proportional to the granularity of the cytoplasm. Data from deflected light are collected by a computer unit for each cell which allows determination of cell's number and type. In case of fluorochrome labeling, for example with a FITC-conjugated antibody, light of a different wave length will be emitted after exposure to the laser beam. The emitted light is measured by photomultiplier tubes equipped with filters to measure light at a correct wavelength only. The photomultiplier converts fluorescence into electrical signals which are proportional to the number of excited molecules.

2.7.2 Immunofluorescence antibody labelling

Flow cytometry (BD Biosciences) was used for examining cell fluorescence after using FITC/TRITC-conjugated factors for labelling the molecule of interest. Cells were labelled for intracellular or extracellular antigens. In case of intracellular antigens, cells were treated with detergents such as TritonX-100 (Sigma-Aldrich) to increase permeability allowing dye entry through pores in the plasma membrane.

For labelling cell-surface antigen, cells were detached by incubating with cell dissociation solution (Invitrogen) for 5-10 minutes at 37^{o}C. These cells were then centrifuged at 500g for 5 minutes and pellets resuspended in PBS and counted. Cells were then suspended in 2% BSA-PBS (at 4x10^{6} cell/ml) and a definite number of cells (2x10^{5}) was transferred to Eppendorf tube (50 µl volume). An appropriate volume of primary antibody was added (1:50/100), mixed and incubated on ice (4^{o}C) for 30 minutes. Appropriate isotype-matched control with an irrelevant antibody was used to detect non-specific binding of primary antibody. Unbound antibody was removed by washing the cells for 3 times in PBS. Cells were resuspended in 2%BSA-PBS and fluorochrome-conjugated (FITC) secondary antibody was added for additional 30 minutes and incubated on ice. Secondary antibody is usually produced in different species i.e. rabbit anti mouse and it is specific for the primary antibody. Cells were then washed twice in PBS and resuspended in 200-300 µl of 2%BSA-PBS where they were ready for flow cytometry measurement. Steps that included fluorochrome labelling were performed in the dark. Non-viable cells were excluded by using propidium iodide (PI) at concentration of 5 µg/ml. PI was added immediately to each sample prior to flow cytometry and dead cells were gated out accordingly. Data were analyzed depending on median fluorescence intensity (MFI) measured by flow cytometry. MFI values were determined statistically using WinMDI 2.9 software.

2.7.3 Cell stimulation and phenotyping

Cells were investigated for the expression of specific antigens in order to define their phenotype and examine the activity of stimulators. Endothelial and epithelial cells were examined for the expression of MHC II antigens following stimulation by IFN-γ (R&D). Flow cytometry was used to measuring the expression of MHC II antigens after stimulating cells with interferon gamma IFN-γ (R&D) for different time points. Endothelial and epithelial cells were stimulated with IFN-γ (25 ng/ml) for three and seven days respectively. These cells were detached by trypsin/EDTA, washed three times with PBS and incubated with monoclonal mouse anti-human HLA-DP, DQ, DR, (DAKO Clone CR3/43, FITC-conjugated) for 30 minutes at

4^{o}C. Cells were washed twice, resuspended in 2% BSA- PBS and examined by flow cytometry.

2.7.4 Antibody labelling

Monoclonal antibody 10E4 (Seikagaku-#370255) was used as an anti HS sulphation antibody. Cells were detached using cell dissociation solution (Sigma-Aldrich), washed twice with PBS, counted and suspended in 2% PBS-BSA. 10E4 antibody (mouse anti-human IgM) was added at 1:100 ratios, tubes were then incubated at 4^{o}C for 60 minutes, washed twice with PBS and incubated with FITC-conjugated anti-mouse antibody for additional 30 minutes. Cells were then washed twice with PBS, suspended in 2% PBS-BSA and examined by flow cytometry. Mouse anti-human IgM antibody was used as an isotype.

2.7.5 Phage display antibody

Phage display antibodies are produced in bacteria (generous gift from Prof. T.V. Kuppevelt); these antibodies have the ability to bind to specific epitopes in HS structure. They have been used recently for examining the changes in HS structure over a wide range (table 2.10). For staining with these antibodies, cells were detached using cell dissociation solution (Sigma-Aldrich), washed twice with PBS, counted and suspended in 2% PBS-BSA. Cells were then blocked with 2% BSA-PBS for one hour and incubated with phage display antibody at 1:10 overnight at 4^{o}C. The cells were washed with PBS and incubated with anti-VSV cy3-conjugated antibody (Sigma-Aldrich) at 1:200 on ice for further 30 minutes. Cells were then washed twice with PBS, suspended in 2%PBS-BSA and examined by flow cytometry. Mouse anti-human IgG2 antibody was used as an isotype.

Antibody	GAG used	Specific Epitope	Reference
10E4		N-Acel /N-S	(van den Born et al., 2005; David et al.,1992)
HS3A8	Bovine kidney	N-S, 2-OS, 6-OS and C-5	(Wijinhoven et al.,2007; Dennissen et al., 2002)
HS4C3	Bovine kidney	N-S, 2-OS, 6-OS and 3-OS	(Ten Dam et al.,2006)
RB4EA12	Human skeletal muscle	N-Acel, N-S and 6-OS	(Lensen et al .,2005; Dennissen.,2002)

Table 2.10. Epitopes of HS antibody specific antibodies.

2.8 Statistical analysis

Data were statistically analyzed using Student's (two paired/unpaired) T-test for data with normal distribution. ANOVA for comparing three or more independent groups was used with Tukeys and Bonferroni post tests. Software such as Windows Excel, Prism 3/4, WinMDI 2.9 and REST-2008 were used. P values less than 0.05 were considered significant.

Chapter Three

3 The Effect of HS6ST1 on HS Structure and Biological Activity

3.1 Introduction

Heparan sulphate has a wide range of interactions with a variety of materials such as growth factors, cytokines, viruses, enzymes (Sarrazin *et al.*, 2011). The sulphation of HS undergoes changes in accordance with its involvement in biological activities in health and disease. HS regulation includes sulphation changes at specific sulphate groups by increasing or decreasing the sulphate transferase activities. For example, the stimulation of endothelial cells with cytokines such as IFN-γ resulted in increased expression of NDST1 and NDST2 genes at mRNA level. This increase was shown to enhance the ability of HS to interact and present chemokines such as CCL5 (Carter *et al.*, 2003).

3.1.1 HS6ST modifying enzyme

The HS6ST enzyme transfers sulphate group to the 6-O position of glucosamine of the HS repeated disaccharide units. This enzyme has three isoforms, each with a specific substrate and a different tissue distribution (Habuchi *et al.*, 2000). Changes in sulphation patterns of heparan sulphate can be examined by generating cell lines which overexpress or knock-out a definite sulphate group (Pikas *et al.*, 2000; Do *et al.*, 2006). Overexpression of HS6ST isoforms, for instance, was previously studied by transfecting the human embryonic kidney cell line (HK293) with mice HS6ST isoforms. Structural disaccharide analysis of HS from these cells shows a high concentration of 6-O sulphate groups at GlcA-GlcNS6S and GlcA-GlcNAc6S residues. Additional changes included decreased sulphation at N- and 2-O positions. The HS chains following HS6ST overexpression exhibit further changes in domain distribution including gradual changes from NS, NA/NS and NA domains toward more NS and NA domains along with changes in polyanionic properties and increased chain length (Do *et al.*, 2006).

3.1.2 HS detecting antibodies

Interaction between heparan sulphate and proteins such as growth factors is mediated by specific HS domains. Structural diversity of these domains is often

investigated using the specific HS antibody, 10E4 (David *et al.*, 1992) and additional antibodies produced using phage display technology because of the poor immunogenicity of HS (Dennissen *et al.*, 2002).

Several phage display antibodies are used for the investigation of changes in HS in the context of inflammation, development, carcinogenesis and fibrosis (Gomes *et al.*, 2006; Tatrai *et al.*, 2010). For example, HS4C3 antibody was shown to target a specific HS epitope containing highly sulphated disaccharide of GlcNS3S6S-Ido2S in rat kidney cells (van Kuppevelt *et al.*, 1998; Ten Dam *et al.*, 2006). Incubating cells with FGF2 could inhibit the HS4C3 binding by about 60 % (Lensen *et al.*, 2005).

Staining of renal sections with phage display antibodies showed specific binding to basement membrane epitopes in different renal structures including glomerulus, Bowman's capsule and cortical tubules (Lensen *et al.*, 2005). The RB4EA12 antibody targets an HS epitope composed of IdoA-GlcNS6S (Dennissen *et al.*, 2002). This antibody was used for examining changes in HS in fibrogenesis and carcinogenesis. Interestingly, the HS epitopes for RB4EA12 and HS4C3 were both increased in liver cirrhosis compared to normal liver (Tatrai *et al.*, 2010). However, the fine individual and relative modifications of HS are still a big challenge to resolve (Smits *et al.*, 2006; Rops *et al.*, 2008).

3.1.3 HS6ST function and physiological role

Heparan sulphate is involved in a wide range of biological activities via interaction with many proteins including cytokines, growth factors, morphogens and ECM proteins (Whitelock and Iozzo, 2005). These interactions depend to a large extent on the sulphation pattern of HS including the 6-O position (Esko and Selleck, 2002). HS6-O sulphation is regulated during embryonic development (Allen and Rapraeger, 2003), aging (Feyzi *et al.*, 1998; Huynh *et al.*, 2012) and carcinogenesis (Jayson *et al.*, 1998).

Heparan sulphate interaction with growth factors is dependent on the presence of specific sulphate groups. The role of 6-O sulphation in modulating of HS fine

structure and FGF signalling has been the topic of extensive study. Although 6-O sulphation is not an absolute requirement for FGF2 binding, it constitutes an essential requirement for FGF2-FGFR signalling and mitogenic activity (Sugaya *et al.*, 2008). For example, addition of selective 6-O desulphated heparin blocked the induction of mitogenic activity *in vitro* following FGF2 stimulation (Guimond *et al.*, 1993; Walker *et al.*, 1994). Similarly, disaccharide analyses show that mitogenic activity of FGF2 is correlated with 6-O sulphate content (Pye *et al.*, 1998). Furthermore, Guimond et al. showed that addition of 2-O desulphated heparin, which retains 6-O sulphate groups, has the capability to bind FGF2 with less affinity compared to native heparin. However, removing the 6-O sulphate groups had no effect on FGF2 binding (Guimond *et al.*, 1993). A recent result has shown that GAGs exhibit an age-dependent decrease in FGF2 binding parallel to decreases in N- and 2-O sulphate groups even with increased 6-O sulphate (Huynh *et al.*, 2012). The 6-O sulphate group constitutes an essential component for HS binding with HGF (Lyon *et al.*, 1994a), PDGF (Feyzi *et al.*, 1997), lipoprotein lipase (Parthasarathy *et al.*, 1994) and, interestingly, FGFR1 (Schlessinger *et al.*, 2000).

Additional roles have been reported for 6-O sulphate groups in the inflammatory response. For example, this group is required for HS interaction with L- or E-selectins. This facilitates leucocyte rolling and adhesion to endothelial cells (Wang *et al.*, 2002; Celie *et al.*, 2005).

3.1.4 Specific aims

Definition of the role of HS sulphation is an issue of vital importance due to the involvement of HS in several biological activities in health and disease. This part of the research aims to shed light on changes in HS sulphation. In particular, the role of 6-0 sulphate groups in interaction with cytokines involved in chronic rejection. For further understanding the HS structure modulation and its effect on HS biology, these specific aims are addressed:

- To examine the expression of HS modifying enzymes in human kidney cell lines
- To investigate the changes in sulphation of HS by HS6ST enzyme following cytokine stimulation
- To generate HS6ST1 overexpressing transfectants to:
    - Examine the changes in HS epitopes
    - Study the FGF2 binding to HS6ST1 transfectants
    - Investigate the effect of HS6ST1 overexpression on renal epithelial cell proliferation
    - Study the effect of HS6ST1 on pERK activation
    - Examine the effect of overexpression HS6ST1 on HS structure

3.2 Specific materials and methods

3.2.1 FGF2 binding assay

In this study HS-FGF2 binding was examined using the Fluorokine Biotinylated human basic FGF2 kit (R&D). Cells were detached using cell dissociation solution (Sigma-Aldrich), washed twice with PBS, counted and suspended at $4x10^6$ cells/ml in PBS containing 2% BSA. In Eppendorf tubes, 10 µl of biotinylated FGF2 (final at 570ng/ml) were incubated with 25 µl of cells ($1x10^5$cells) for 60 minutes at 4^oC. Avidin-FITC (10 µl) was then added without wash and the tubes were incubated for another 30 minutes at 4^oC in the dark. Cells were then washed twice with PBS, resuspended in 200µl of PBS containing 2% BSA and investigated by flow cytometry. Biotinylated protein (soybean trypsin inhibitor) to the same level of FGF2 was used as a negative control. The specificity of the reaction was verified using blocking anti-human FGF2 antibody. Negative and specificity controls were carried out with each assay. Median fluorescence intensity (MFI) was used as an expression of fluorescence activity and ΔMFI refers to MFI of sample following subtraction of the control values. Reference values were usually for cells incubated with Avidin-FITC conjugated substrate only (without adding biotinylated factors). The protocol was followed according to manufacturer's instructions.

3.2.2 CCL5 binding assay

A chemokine binding assay (RANTES or CCL5) was developed in order to investigate the effects of sulphation changes of HS on human Fluorokine Biotinylated CCL5 (R&D) in a similar way to FGF2 assay. Fluorokine biotinylated CCL5 was added to $1x10^5$ cells at a final concentration of 100ng/ml and incubated at 4^oC for one hour. Avidin-FITC substrate was added without wash and the mix incubated for 30 minutes at 4^oC. Cells were washed and resuspended in 2% PBS-BSA for flow cytometry analysis. Biotinylated protein (soybean trypsin inhibitor) to the same concentration as CCL5 was used as a negative control. Anti-human CCL5 antibody was used as a blocking control to verify specificity of CCL5 binding. Protocol was followed according to manufacturer's instructions.

(www.rndsystems.com/pdf/nfrn0.pdf)

3.2.3 Proliferation assay

Cell proliferation assays are widely used for studying growth factors or media components that affect cell division and cell biology. In this study, proliferation assay was performed to investigate whether changes in GAG sulphation alter cell proliferation. A non-radioactive, colorimetric proliferation assay (Promega) was used to determine the number of viable cells in proliferation assays. This assay contained a tetrazolium compound (MTS) and electron coupling reagent phenazine methosulphate (PMS). The assay depends on cell bio-reduction of MTS tetrazolium into a formazan product which is soluble in tissue culture medium and can be measured at 490nm. This reduction is performed by dehydrogenase enzymes essentially found in metabolically active cells. Formazan products are proportional to the number of viable cells. The working reagent was prepared in the hood by mixing 2ml of MTS with 0.1 ml of PMS (20:1 ratio) at room temperature.

Cells were harvested, counted and seeded in triplicate in 96 well plates at $5x10^3$ cells/well and cultured with 5% FCS media overnight. The next day, medium was removed and fresh medium with 0.5% FCS was added and the cells were left to grow in normal condition. To examine the effect of FGF2 on proliferation, FGF2 was added at 10ng/ml in separate wells alongside wild type cells. Cells were left to grow according to experimental design for 0, 24, 48, 72 and 96 hours in the same conditions. At the time of assay, medium was removed, 100 µl of fresh 0.5% FCS medium was added with 20 µl of working reagent (MTS/PMS) and mixed gently. The plate was incubated at 37^oC and 5% CO_2 incubator for 1-4 hours. Readings were taken at 490nm wavelength by spectrophotometer at 0, 60,120, 180 and 240 minutes. Wells containing 100 µl of medium only with 20 µl of working reagent (MTS/PMS) were considered as negative controls. Readings were analyzed using Windows Excel and Prism 4.

3.2.4 Isotope ^{35}S labelling

Renal epithelial cells transfected with HS6ST1 and appropriate mock transfectants were labelled with ^{35}S to determine the structure changes of HS. The cells were grown in 25 cm^2 flasks until subconfluent, 5 ml of fresh medium containing 200µCi/ml of $Na_2{}^{35}SO4$ (PerkinElmer Life Sciences) was added at 37^oC for 24 hours. The cells were washed twice with cold PBS and treated with 3 ml of solubilization buffer at 4^oC for 60 minutes in a shaking incubator. The solubilization buffer was prepared in advance and contained 1% Triton X-100, 50 mM Tris, 0.15 M NaCl, pH 7.4 and protease inhibitor (Complete Mini Cocktail, Roche). Lysates were centrifuged at 500g for 15 minutes and the supernatant was transferred into fresh tubes. 100 µl of the supernatant was used for protein estimation by BCA kit (Pierce). The supernatant was used for purification of labelled GAGs.

3.2.4.1 **GAG isolation**

GAGs were isolated by treating supernatants from ^{35}S labelled lysates with Diethylaminoethyl (DEAE) Sephacel (Sigma-Aldrich). DEAE is a weak anion exchange resin based on beaded cellulose. DEAE remains charged and consistently maintains a high capacity in the working range (pH: 2-9). DEAE columns were prepared at least 30 minutes before use. First, the tubes (disposable 2ml polystyrene columns; Thermo Scientific) were set up and washed 2-3 times with equilibration buffer (0.05M Tris/HCl pH: 8.0, 0.15 NaCl and 0.1% TX-100). The liquid inside each tube was held by the bottom cap and a porous floating disc was added on top of the liquid and pushed down avoiding gas bubbles. 500 µl of degassed DEAE slurry was then added and washed 3 times with equilibration buffer; the tube was left for 30 minutes to allow the gel to settle. Labelled supernatant was diluted with equilibration buffer to a final concentration of 0.15 M. The supernatant was then applied to the prepared DEAE column and washed 3 times with 5 ml of equilibration buffer. An additional wash by acetate buffer (0.15M NaCl, 0.05 acetate, 0.1% TX-100, protease inhibitor and pH 4) was performed. The pH was then increased to 7.4 by adding washing buffer (0.05M

Tris pH: 7.4, 0.15 M NaCl, 0.1% TX-100 plus protease inhibitor) and finally the labelled material was eluted by applying high salt elution buffer (0.05 M Tris/pH 7.4, 1.5M NaCl, 0.1%TX-100 and protease inhibitor).

3.2.4.2 **Sample Desalting**

The labelled material containing GAGs were desalted using PD-10 columns (GE Healthcare). PD-10 columns are packed with Sephadex G-25 which allows efficient separation of high molecular weight substances from those with low molecular weight such as NaCl. In this study a protocol was used where the liquid was passed through the column by gravity. The PD-10 columns were prepared in advance by decanting the column storage solution and washing with 25 ml of equilibration buffer (0.5M ammonium bicarbonate). The sample was then applied in a 2.5 ml volume of elution buffer. The sample was collected in the void volume flow through. The samples were then freeze-dried and sent to Prof. Marion Kusche-Gullberg in Norway for further structural analyses.

3.2.4.3 **Experiments performed by Marion Kusche-Gullberg, Bergen, Norway**

The samples were treated with alkaline to release GAGs from the core protein. The GAG chains were then recovered by PD-10 gel filtration and evaporated to smaller volumes. These samples were run on Superose 12 columns before and after degradation of chondroitin sulphate (CS) with ABC chondroitinase to evaluate the HS/CS ratio.

The remaining samples were treated with nitrous acid (pH 1.5) which cleaves the glucosaminidic linkage at GlcNS units. Samples were then reduced by treating with NaBH4 and deamination products (aManR: 2, 5 anhydro-D-mannitol) were fractionated by gel chromatography on Sephadex G-15 equilibrated with 0.2M NH_4CHO_3. Fractions related to di-saccharides and higher saccharides were collected and lyophilized repeatedly. Disaccharides were further separated by high performance anion-exchange liquid chromatography (HPLC).

The ^{35}S-labelled disaccharides were analyzed twice on a Partisil-10 SAX column and eluted at a rate of 1ml/minutes with KH_2PO_4 solutions of stepwise increasing concentration.

Mono-O sulphated and di-O sulphated disaccharides were eluted with 0.026 M and 0.15 M KH_2PO_4 respectively. These disaccharides are GlcA-aManR6S (GMS), IdoA-aManR6S (IMS), IdoA2S-aManR(ISM) and IdoA- aManR6S (ISMS). These correspond to the following disaccharides in the intact chain respectively GlcA-GlcNS6S, IdoA-GlcNS6S, IdoA2S-GlcNS and IdoA2S- GlcNS6S.

3.2.5 HS-Heparitinase III treatment

Heparitinase III is a hydrolysis enzyme produced by *Flavobacterium heparinum* (Sigma-Aldrich). The powder was reconstituted in 20 mM Tris-HCl (pH 7.5) containing 0.1 mg/ml BSA with 4mM CaCl2 according to manufacturer's instructions. Cells were incubated with Heparitinase III at 10 Sigma Unit/ml (one IU=600 Sigma Unit) for 60 minutes at 37 ^{o}C.

3.3 Results

3.3.1 Cell Phenotyping

3.3.1.1 Expression of E-cadherin

E-cadherin is a cell-cell adhesion molecule which is considered a characteristic marker of epithelial cells. Renal epithelial cell phenotype was verified by examining the expression of E-cadherin by immunofluorescence. Cells were stained with anti E-cadherin antibody followed by FITC-conjugated secondary antibody. As shown in figure 3.1, epithelial cells express E-cadherin and show increased fluorescence activity compared to those with secondary antibody only.

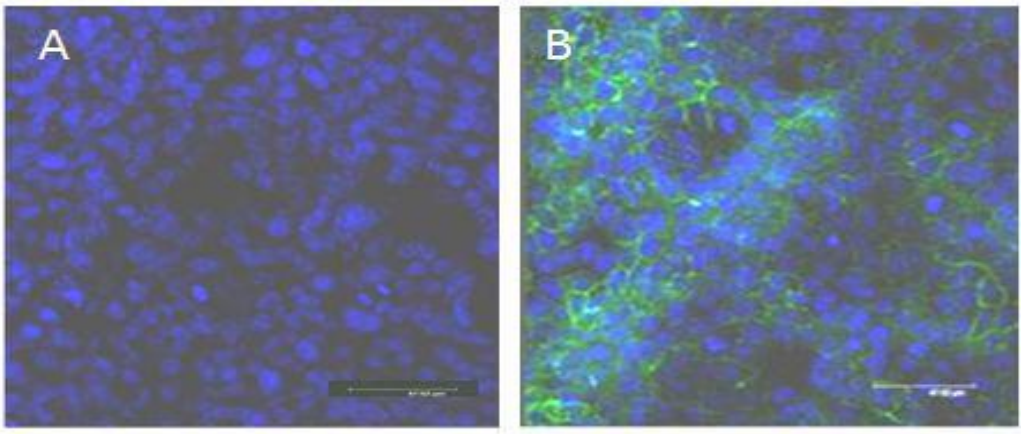

Figure 3.1. HK2 cells stained with anti E-cadherin antibody. A: Cells with no primary antibody (control). B: Cells with E-cadherin antibody and FITC conjugated secondary antibody. Images were taken by scanning fluorescence microscope. The figure is representative of two independent experiments. (Scale bar is 47.62µm)

3.3.1.2 **Expression of MHC-II**

Class-II major histocompatibility complex antigens (MHC-II) are expressed constitutively on the surfaces of antigen presenting cells (APCs) such as macrophages, B cells and dendritic cells. MHC-II antigens are necessary for the presentation of exogenous antigens to CD4+ lymphocytes. These antigens were shown to be upregulated in somatic cells as a consequence of proinflammatory cytokines such as IFN-γ and TNF-α in the context of graft rejection (Pober *et al.*, 1996). IFN-γ is a key proinflammatory cytokine which is upregulated in chronic graft rejection. To investigate the ability of IFN-γ to induce MHC-II molecules in renal epithelial cells, these cells were stimulated with IFN-γ for seven days at 25ng/ml and investigated by flow cytometry. The time and concentration dependency of the response to IFN-γ were optimised earlier within the group (Fritchley *et al.*, 2000). Specificity of antigen labelling was demonstrated by incubating stimulated cells with isotype-matched antibody. As shown in figure 3.2C and 3.3, IFN-γ stimulated cells show significantly increased ($P<0.05$) binding ability to MHC-II antibody compared to resting cells and isotype incubated cells. Epstein-Barr virus transformed lymphoblastoid cell lines (EVB-LCL), express MHC-II molecules, were used in experiments as positive control (Figure 3.2A).

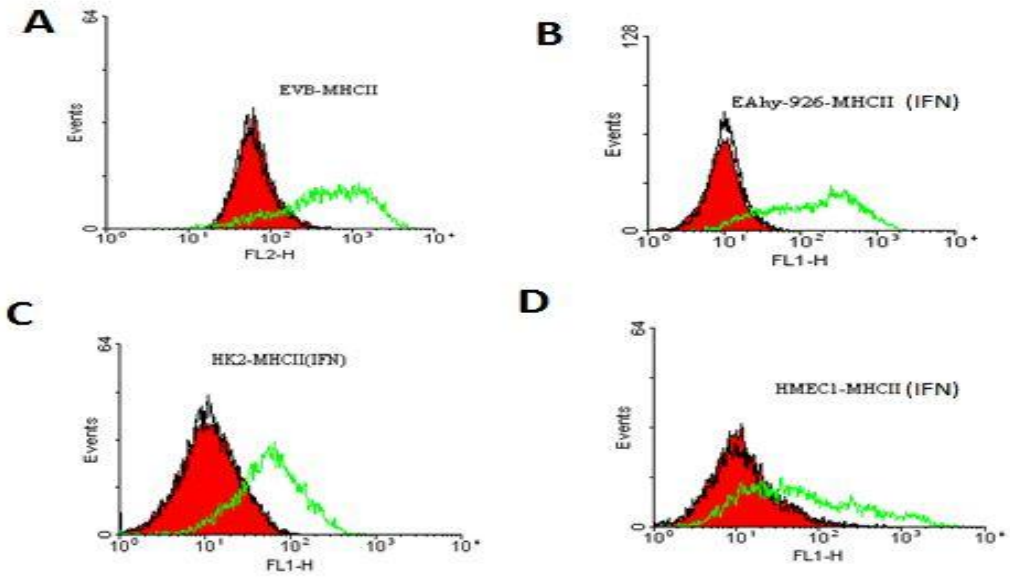

Figure 3.2. Flow cytometric demonstration of MHC-II expression after stimulation with IFN-γ. A, Epstein-Barr transformed virus lymphoblastoid cell lines (EVB) were used as positive control in resting condition. B&D, Endothelial cells (EAhy-926 & HMEC1) were stimulated with IFN-γ (25ng/ml) (green histogram) for 3 days whereas epithelial cells (HK2) were stimulated for 7 days (C). Controls included unstimulated cells (red) and labelling with isotype-matched antibody (black). The data shown is representative of 2 separate experiments (N=2).

Endothelial cells were incubated with IFN-γ for 72 hours and examined for the expression of MHC-II molecules. As shown in Figure 3.2B and D, IFN-γ stimulated EAhy-926 and HMEC-1 cells upregulated MHC-II antigen expression compared to non-stimulated cells. This induction was investigated by flow cytometry with an IFN-γ concentration of 25ng/ml for 72 hours. Median fluorescence intensity showed that MHC-II molecules were significantly upregulated in comparison to unstimulated cells. EVB cells were used as a positive control (Figure 3.3).

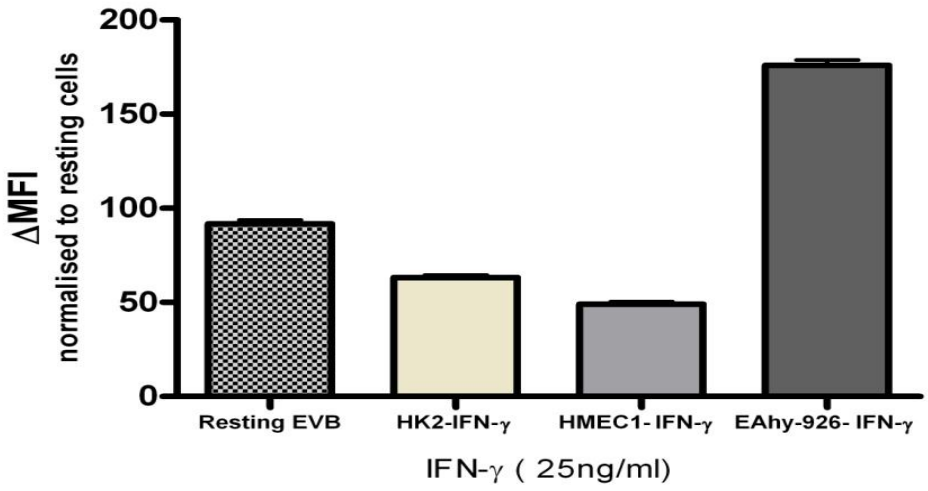

Figure 3.3. Expression of class II MHC antigen after stimulation with IFN-γ. Median fluorescence intensity was measured for the expression of class II MHC antigen. Endothelial cells (HMEC1 and EAhy-926) were stimulated with IFN-γ for 3 days and epithelial cells (HK2) for 7 days. The MHC-II expression was visualized by FITC-conjugated secondary antibody. Epstein-Barr virus lymphoblastoid cell lines (EVB-LCL) at resting condition was used as positive control. Error bars represent the SEM of duplicate determinants (n=2), these data are representative of 2 idependent experiments (N=2).

3.3.1.3 **Expression of CD31**

Endothelial cells (EAhy-926 and HMEC-1) were phenotyped by investigating the expression of CD31 which is also known as platelet endothelial cell adhesion molecule (PECAM-1). CD31 plays a key role in leucocyte transmigration through intracellular junctions. CD31 is found between endothelial cells and considered as a characteristic marker of endothelial cells (Jimenez *et al.*, 2003).

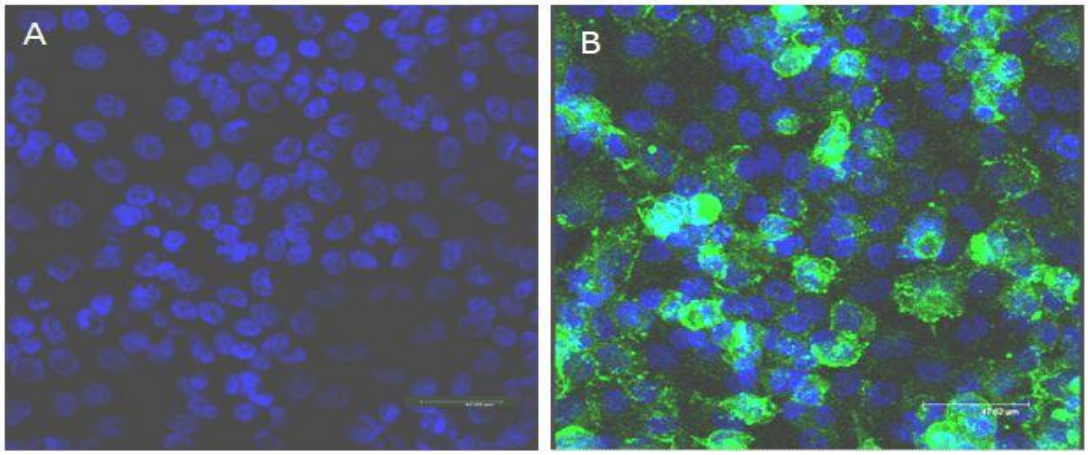

Figure 3.4. EAhy-926 cells stained with anti CD31 antibody. A: Cells with no primary antibody (control). B: Cells with CD31 antibody visualized by FITC conjugated secondary antibody. Images were taken with scanning laser confocal microscope. IgG1 antibody (mouse) was used as a nonspecific binding isotype (not shown). The figure is representative of two independent experiments. (Scale bar is 47.62µm)

Staining of these cells with anti CD31 antibody showed that endothelial cells express significantly levels of CD31 compared to control. Investigations were performed using immunofluorescence confocal microscope (Figure 3.4).

3.3.2 Expression of HS6ST1 by conventional PCR

3.3.2.1 **RNA extraction and gel electrophoresis**

RNA was obtained following cell lysis and its integrity was examined by running defined amount on agarose gels along with RNA ladder. Intact RNA was confirmed by the appearance of sharp bands corresponding to 28S and 18S ribosomal RNA on agarose gel electrophoresis with a ratio of 2:1 respectively.

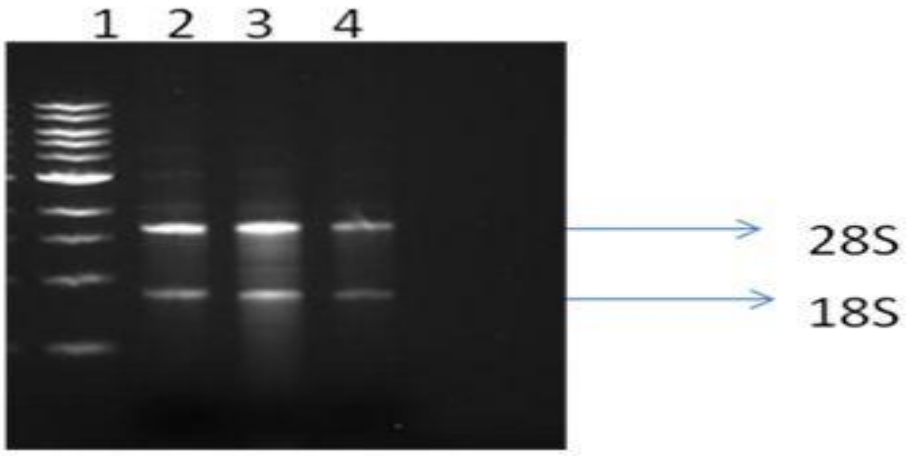

Figure 3.5. Agarose gel electrophoresis of RNAs from different cell lines. For each cell line 0.5 µg of total RNA was loaded on 0.5% agarose gel to examine the integrity of RNA. RNA from HK2, EAhy.926 and HMEC1 were in lanes 2, 3 and 4 respectively.

RNA samples from each of the cell lines used in this study produced well defined 28S and 18S bands with no smearing, indicating little or no degradation (Figure 3.5).

3.3.2.2 **Conventional PCR**

Expression of the HS6ST1 gene was investigated in three cell lines (HK2, EAhy.926 and HMEC1) using the reverse transcription PCR protocol. RNA was obtained from resting cell lines and after stimulation with IFN-γ (25ng/ml) for 24 hours. GAPDH was used as a house keeping gene. Primers for HS6ST1 and GAPDH were designed with product amplicons at 463bp and 590 bp respectively. Plasmid encoding DNA of the HS6ST1 gene was used as a positive control. PCR products were examined by electrophoresis on agarose gels.

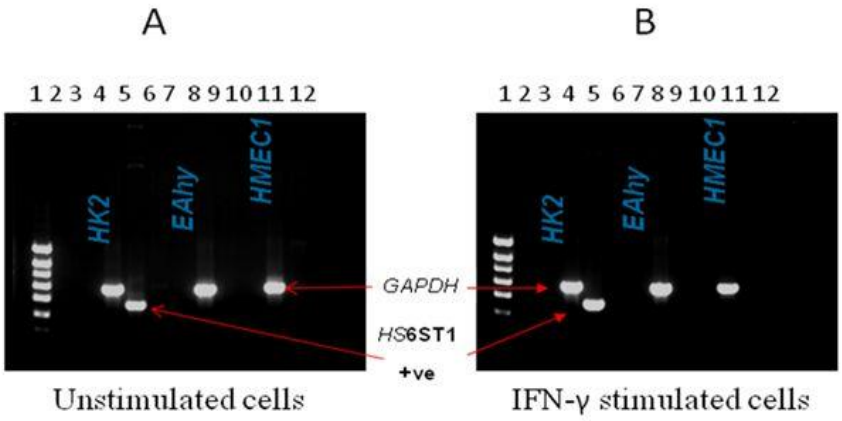

Figure 3.6. Agarose gel electrophoresis of HS6ST1 expression by reverse transcription PCR. PCR was carried out using cDNA from resting and IFN-γ (25ng/ml for 24 hours) stimulated cells. All cells show the expression of GAPDH and HS6ST1 positive control (plasmid encoding HS6ST1). A, Lane-1 (L1) contains 100 bp ladder, L2: PCR mix only, L3: HK2-HS6ST1 (empty), L4: HK2-GAPDH, L5: positive control HS6ST1 plasmid, L6: HK2-HS6ST1 (empty), L7: PCR mix only, L8: EAhy.926-GAPDH, L9; EAhy.926-HS6ST1 (empty), L10: PCR mix only, L11: HMEC1-GAPDH, L12: HMEC1-HS6ST1 (empty). Panel B is the same as A but with IFN-γ stimulated samples.

In figure 3.6 (left panel) the PCR products of resting cells show transcripts for positive control of plasmid HS6ST1 in lane 5 and GAPDH in lanes 4, 8 and 11 from cell lines HK2, EAhy.926 and HMEC1 respectively. No transcripts were seen for HS6ST1 in lanes 6, 9 and 12 that represent HK2, EAhy-926 and HMEC1 respectively. In a similar way the right panel shows lack of expression of HS6ST1 following stimulating with IFN-γ.

3.3.2.3 **Expression of HS6ST1 using quantitative PCR (qPCR)**

Expression of HS6ST1 gene was further investigated by real time PCR which is a more quantitative procedure compared to conventional PCR. HK2, EAhy-926 and HMEC1 were shown to express constitutive levels of HS6ST1. This expression was examined in resting cells and after stimulation with factors such as PMA and cytokines such as TNF-α, IFN-γ and TGF-β. Cytokine concentrations and incubation times were optimised earlier by the group (Fritchley *et al.*, 2000). For HK2 cells, no significant changes in HS6ST1 expression were noticed following

cytokine stimulations for 24 hours. However, IFN-γ significantly ($P<0.05$) downregulated HS6ST1 expression in HMEC1 cells by about 60 % compared to control (Figure 3.7, B).

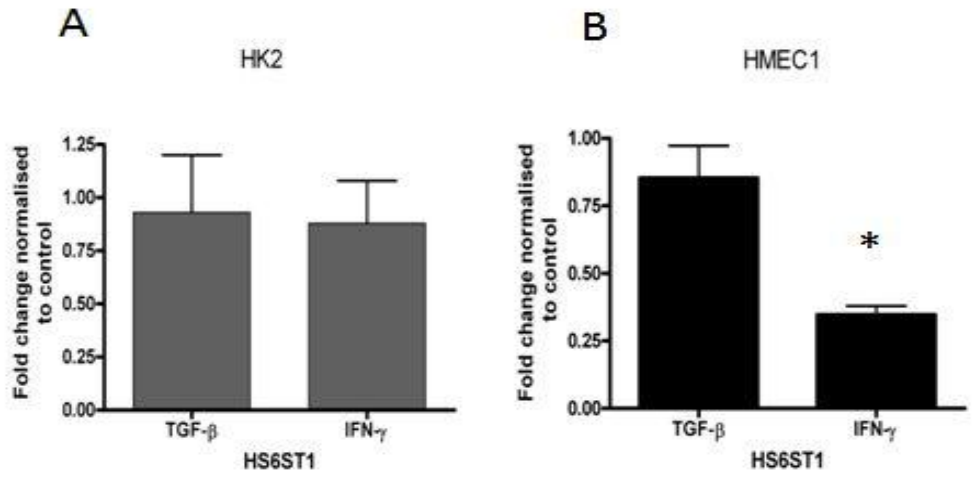

Figure 3.7. Stimulation of HS6ST1 expression by cytokines. A, renal epithelial cells (HK2) were stimulated with TGF-β (10ng/ml) and IFN-γ (25ng/ml) for 24 hours. RNA was extracted and cDNA synthesized and used for qPCR. Each column represents fold change expression of HS6ST1 normalized to control (1). B, endothelial cells HMEC1 were stimulated and screened for HS6ST1 expression after stimulation with TGF-β (10ng/ml) and IFN-γ (25ng/ml) for 24 hours. (N=2, *$P<0.05$).

3.3.3 Cell stimulation and FGF2 binding

To examine the binding of FGF2 to renal epithelial cells, an assay for binding biotinylated FGF2 was designed. Renal epithelial cells (HK2) were shown to bind to FGF2 at a significant level. This binding was further investigated following cell stimulation for 24 hours with cytokines such as IFN-γ and TGF-β. Stimulation of renal epithelial cells with these cytokines produced no significant change ($P > 0.05$) in their binding to FGF2. Unstimulated cells were used as a control (Figure 3.8).

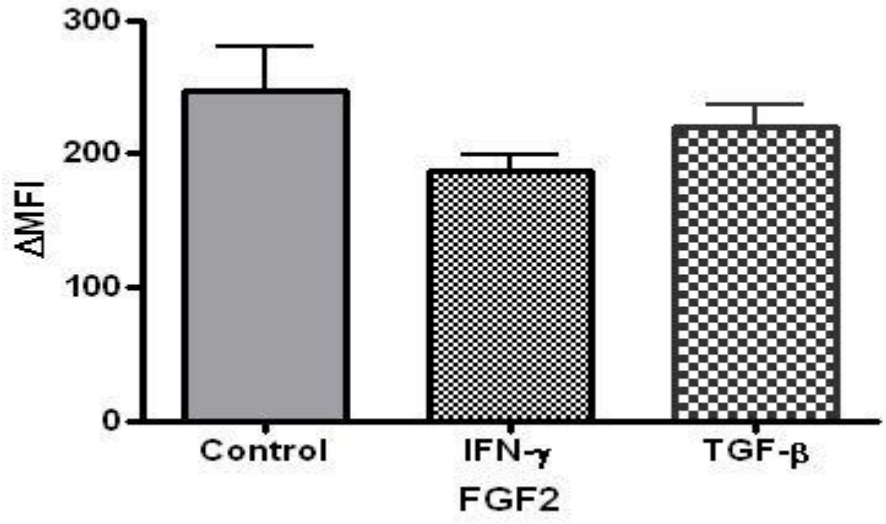

Figure 3.8. Binding of FGF2 following cytokine stimulation. HK2 cells were stimulated with IFN-γ (25ng/ml) and TGF-β (10ng/ml) respectively for 24 hours. Cells were then investigated for their potential to bindFGF2. Flow cytometric results were expressed as median fluorescence intensity (ΔMFI) values and statistics were performed using ANOVA. Stimulated cells were compared to resting cells; error bars show the SEM (N=3, P>0.05).

3.3.4 Cell stimulation and 10E4 binding

To examine the expression of HS on renal epithelial cells, an HS-specific monoclonal antibody was used and cells were investigated by flow cytometry. The 10E4 antibody is a mouse anti-human HS antibody which targets an epitope containing N-acetyl and N-S positions in the structure of HS. Renal epithelial cells (HK2) were shown to bind to 10E4 antibody. This binding ability showed no significant change after stimulation with cytokines such as IFN-γ and TGF-β compared to unstimulated cells as control (Figure 3.9).

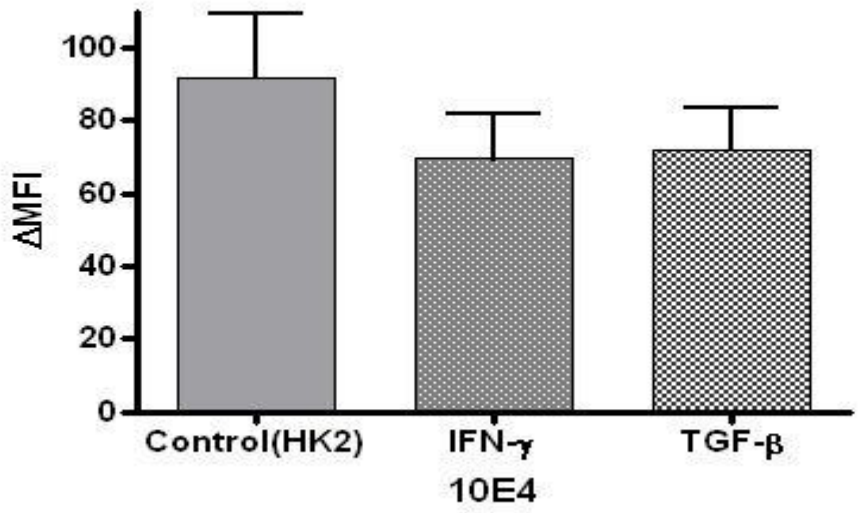

Figure 3.9. Binding of 10E4 antibody to HK2 cells after cytokine stimulation. HK2 cells were stimulated with IFN-γ (25ng/ml) and TGF-β (10ng/ml) for 24 hours. The cells were then investigated for the binding of 10E4 by flow cytometry. The reaction was visualized using a FITC-conjugated secondary antibody. Stimulated cells were compared to resting cells and ΔMFI values were expressed. Error bars show the SEM (N=3, P>0.05).

3.3.5 Generating of stable HS6ST1 transfectants

3.3.5.1 **Cloning of HS6ST1**

The mammalian expression vectors pcDNA3.1/Zeo+ and pCR-Blunt II-Topo coding HS6ST1 were digested with restriction enzymes *Pst I* and *BamH I* to provide unique and specific overhang ends. As a result of digestion, the pcDNA3.1/Zeo vector size was 5 kb and the insert HS6ST1 size was 1321 bp. Both plasmids were analysed by agarose gel electrophoresis (Figure 3.10A).

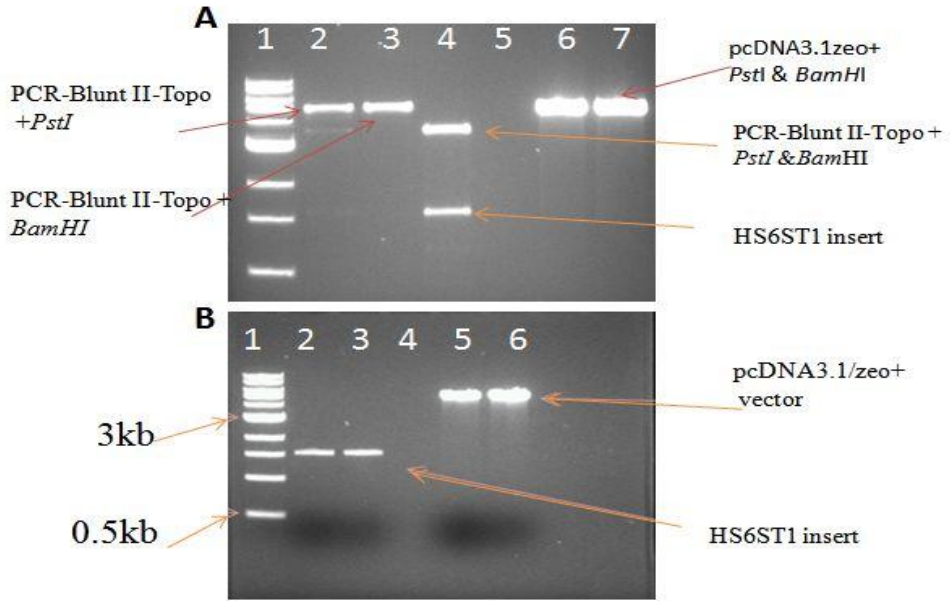

Figure 3.10. Agarose gel electrophoresis of restriction digested plasmids. A, plasmid (PCR-Blunt II-Topo) carrying HS6ST1 and vector pcDNA3.1/Zeo+ were digested with *PstI* and *BamHI*. Both the insert and vector were cut out of the gel and purified. Lane 1: 1 kb ladder, lane 2: Blunt II-Topo + *PstI*, lane 3: Blunt II-Topo +*BamHI*, lane 4: Blunt II-Topo + *PstI* & *BamHI*, lane 6,7 : vector pcDNA3.1/Zeo with *PstI* & *BamHI*. B, Purified HS6ST1 insert and pcDNA3.1/zeo+, digested with *PstI* & *BamHI* and run on the gel. HS6ST1 insert is in lanes 2 and 3 whereas vector pcDNA3.1/Zeo lanes 5 and 6. Lane 1 contains 1kb DNA ladder.

Gel slices were cut out and purified. Purified DNAs for each of the insert (HS6ST1) and the vector were ligated and the resulting vector/insert was amplified and sequenced. The purified DNA was additionally run on the gel for further confirmation of digestion reaction and sizes (Figure 3.10, B).

3.3.6 Transfection procedure

3.3.6.1 **Transfection optimisation**

The transfection procedure involves insertion of DNA within a cell, allowing protein expression. A lipid based transfection protocol was used in this project. The transfection procedure was optimised using different ratios of DNA concentration to Effectene reagent (ER). To obtain best results for transfection efficiency and minimum cell toxicity due to transfection reagents, HK2 cells were

transfected with vector encoding green fluorescent protein (GFP) with different plasmid DNA concentration (µg) to ER (µl) ratios (Table 3.1). The efficiency of transfection was measured by flow cytometry.

DNA concentration	DNA-ER ratio	Efficiency %
0.2µg	1/10	2.3
0.2µg	1/25	1.7
0.2µg	1/50	3
0.4µg	1/10	4.7
0.4µg	1/25	8.3
0.4µg	1/50	21.6

Table 3.1. Optimization of transfection procedure.

Highest transfection efficiency was achieved at a DNA: ER ratio of 1:50 and DNA concentration at 0.4 µg for six well plates (Figure 3.11).

3.3.6.2 **Antibiotic killing curve**

Incubating HK2 cells with different concentrations of antibiotic (Zeocin) showed that the lowest concentration that caused killing of HK2 was 400 µg/ml. Therefore HS6ST1 transfectants were selected in a medium with Zeocin at 400µg/ml and maintained at 300µg/ml, data not shown. .

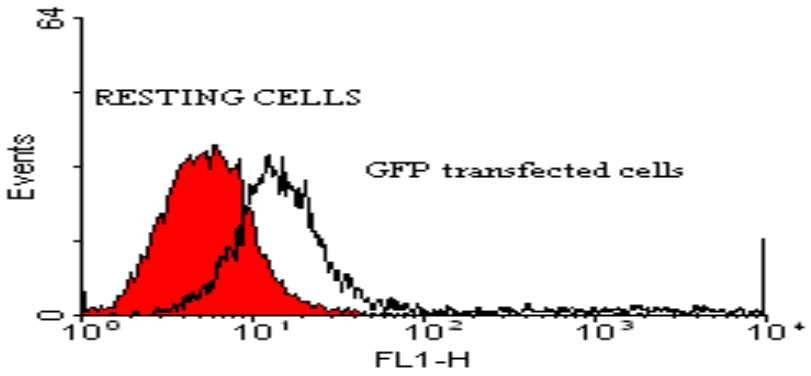

Figure 3.11. Determination of the transfection efficiency for HK2 cells transfected with GFP. Plasmid expressing GFP was transfected into HK2 cells. GFP was transfected at a ratio of 1:50 of DNA to Effectene Reagents respectively. Resting cells showed no fluorescence activity (red histogram) whereas transfected cells showed high fluorescence activity (black line). Investigation was carried out by flow cytometry and data were analysed by WinMDI 2.9.

3.3.6.3 **Generation of HS6ST1 transfectants**

The HS6ST1 insert was ligated to pcDNA3.1/zeo+ and the resultant plasmid was sequenced (see appendices). The HS6ST1 expression vector was transfected into renal epithelial cells using optimised conditions for transfection. Stable clones were created and selected with 400µg/ml Zeocin. Stable clones were grown and screened for the expression of HS6ST1 by real time qPCR. The clones expressing the highest level of HS6ST1 mRNA were selected for further investigation (Figure 3.12). These clones were named as HS6ST1 transfectants and given the initials "T" with a reference number. The highest expressing clones (T4 and T7) were maintained with Zeocin 300µg/ml and used for further investigations. Stable mock transfectants were generated by transfecting HK2 cells with the pcDNA3.1/zeo+ plasmid without the insert. These transfectants were cultured under the same condition as HS6ST1 transfectants (Zeocin, 400µg/ml).

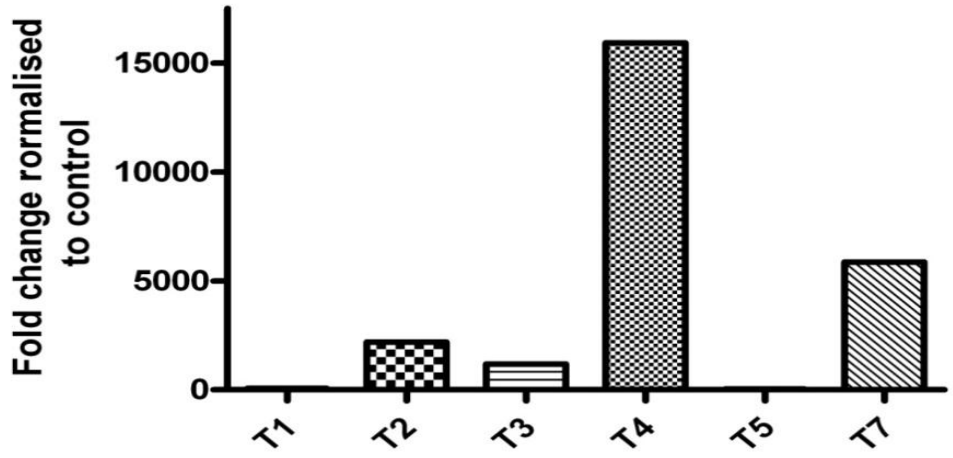

Figure 3.12. HS6ST1 expression of HK2 stable transfectants using qPCR. Total RNA was reverse transcribed and levels measured by qPCR. Values were normalized to GAPDH and reported in relation to wild type HK2 cells. Experiments were performed in duplicate and data represents two independent experiments.

3.3.7 Interactions of HS6ST1 transfectant

3.3.7.1 **Binding to 10E4 antibody (Ab)**

To examine the changes in HS epitopes after HS6ST1 overexpression, renal epithelial transfectants (T7) were investigated for 10E4 antibody binding by flow cytometry. These transfectants were examined in comparison to mock transfectants. HS6ST1 transfectants (T7) showed less binding to 10E4 antibody compared to mock transfectants stained with an isotype-matched control antibody (Figure 3.13).

This reaction was quantified by median fluorescence intensity using flow cytometry. Reaction specificity was examined by incubating cells with isotype (IgM) antibody of the same species (mice). The reduction in 10E4 antibody binding by HS6ST1 transfectants was shown to be statistically significant (Figure 3.14).

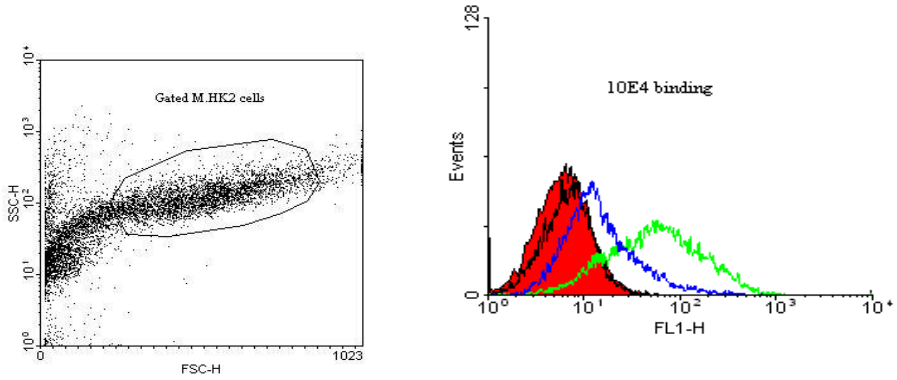

Figure 3.13. Representative HS6ST1 transfectant binding to 10E4 antibody. Left panel represents gated viable cells counted by forward scatter compared to side scatter in flow cytometry. Right panel represents histogram of T7 (blue line) binding to 10E4 in reference to mock transfectants (green line), isotype incubated cells (black line) and cells with secondary antibody only (red histogram).

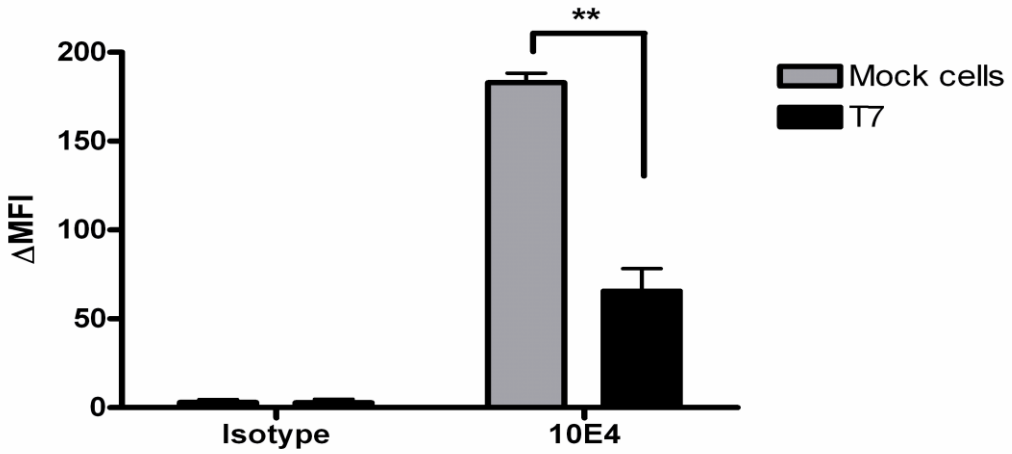

Figure 3.14. Binding of HS6ST1 transfectants to 10E4. 2x104 cells of mock and HS6ST1 transfectants were incubated with 10E4 (1:100) for 60 minutes at 4^{o}C followed by anti-mouse FITC-conjugated antibody. The same number of cells was incubated with IgM isotype antibody. Median fluorescence intensity was measured by flow cytometry. Error bars show the SEM (N=3, **: P < 0.01).

3.3.7.2 **Phage display antibody binding**

A series of experiments was designed to examine the changes in sulphation pattern after HS6ST1 overexpression using HS4C3, RB4EA12 and HS3A8 phage display antibodies (a generous gift from Dr. Van Kuppevelt). Investigations were carried out using flow cytometry.

3.3.7.2.1 Binding to HS3A8 Ab

The HS3A8 antibody targets specific epitope including sulphate groups at N-, 6-O and 2-O positions. As shown in figure 3.15, HS6ST1 transfectants increased the binding of (T7) to HS3A8 antibody compared to mock transfectants (M.HK2). This increase was statistically significant (P<0.05).

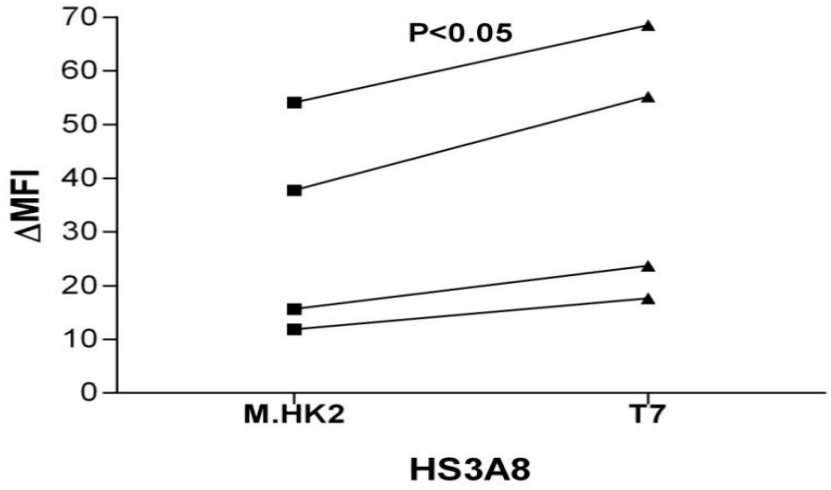

Figure 3.15. Binding of HS3A8 phage display antibody to HS6ST1 transfectants. Cells of mock and HS6ST1 transfectants were incubated on ice with HS3A8 antibody at 1:10 followed by Cy3 labelled anti-VSV secondary antibodies. Fluorescence was investigated by flow cytometry and experiments were performed in duplicates (N=4, P<0.05).

3.3.7.2.2 HS4C3 binding

The HS4C3 phage display antibody targets N-S, 6-OS, 2-OS and 3-OS in the HS structure. Sulphation changes due to HS6ST1 overexpression were investigated by HS4C3 binding with reference to mock transfected cells. Cells with HS6ST1 over expression showed noticeable upregulation of HS4C3 binding compared to mock cells (Figure 3.16). This increase was statistically significant (P<0.05) (Figure 3.18).

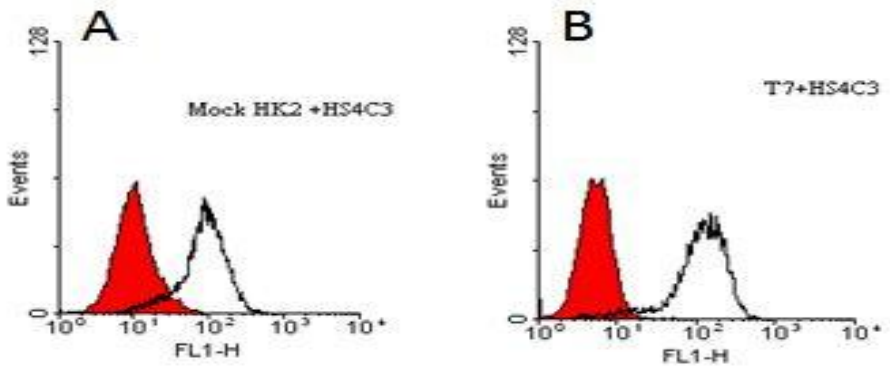

Figure 3.16. Representative histogram showing the binding of HS4C3 to HS6ST1 transfected cells. A, Mock transfectants were incubated with HS4C3 on ice for 60 minutes at 1:10 followed by Cy3 labelled secondary antibody. B, T7 binding to HS4C3 phage display antibody (black line) to T7 transfectants was compared to cells with secondary antibody only (red histogram). Median fluorescence intensity was measured by flow cytometry and the data were analyzed by WinMDI2.9.

3.3.7.2.3 RB4EA12

For further clarification of HS sulphation changes, HS6ST1 expressing transfectants were investigated for the binding of phage display antibody RB4EA12. This antibody targets specifically the N-acetyl, N-S and 6-OS positions on the HS structure. HS6ST1 transfectants showed increased binding to RB4EA12 compared to mock transfectants (Figure 3.17).

HS6ST1 transfectants were shown to upregulate RB4EA12 binding in a significant manner ($P<0.05$), (Figure 3.18).

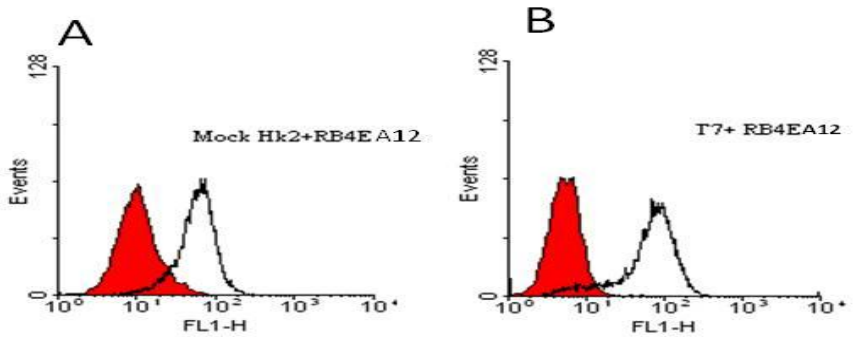

Figure 3.17. Representative histogram of HS6ST1 transfectant binding to RB4EA12. A, Mock transfectant were incubated with RB4EA12 on ice for 60 minutes at 1:10 followed by Cy3 labelled secondary antibody. B, T7 binding to HS4C3 phage display antibody (Black line) compared to T7 cells incubated with secondary antibody only (red line). Median fluorescence intensity was measured by immunofluorescence flow cytometry and data were analyzed by WinMDI2.9.

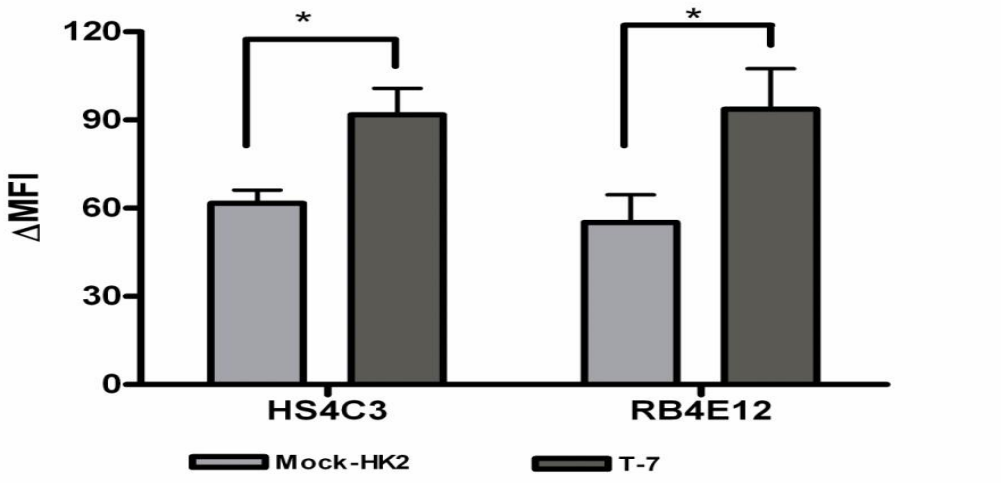

Figure 3.18. Analyses of HS4C3 and RB4EA12 binding to HS6ST1 transfectants. HS4C3 and RB4EA12 antibodies were incubated with mock and HS6ST1 transfectants (T7) for one hour at 4^{o}C followed by addition of monoclonal Cy3-labelled anti-VSV antibody (mouse IgG1 isotype) in 1:200 and incubated for 45 minutes at 4oC. Columns represent mean of median fluorescence intensity of mock and HS6ST1 transfectants (N=2). Error bars represent SEM,*P<0.05.

3.3.8 HS6ST1 transfectant binding with FGF2

3.3.8.1 **Optimisation of FGF2 binding**

3.3.8.1.1 PBS-BSA and RDF1 solution buffer

Biotinylated-FGF2 binding to cell surface HS was optimised in order to obtain best reaction conditions and results. RDF1 is a buffered saline-protein solution provided with the biotinylated FGF2 assay kit. This solution is specifically designed to minimise background staining and stabilise specific binding. Cells were washed and resuspended in PBS-BSA 2% and/or RDF1. Results show that cells washed and suspended in PBS-BSA achieved better binding ratios compared to those with RDF1 (Figure 3.19).

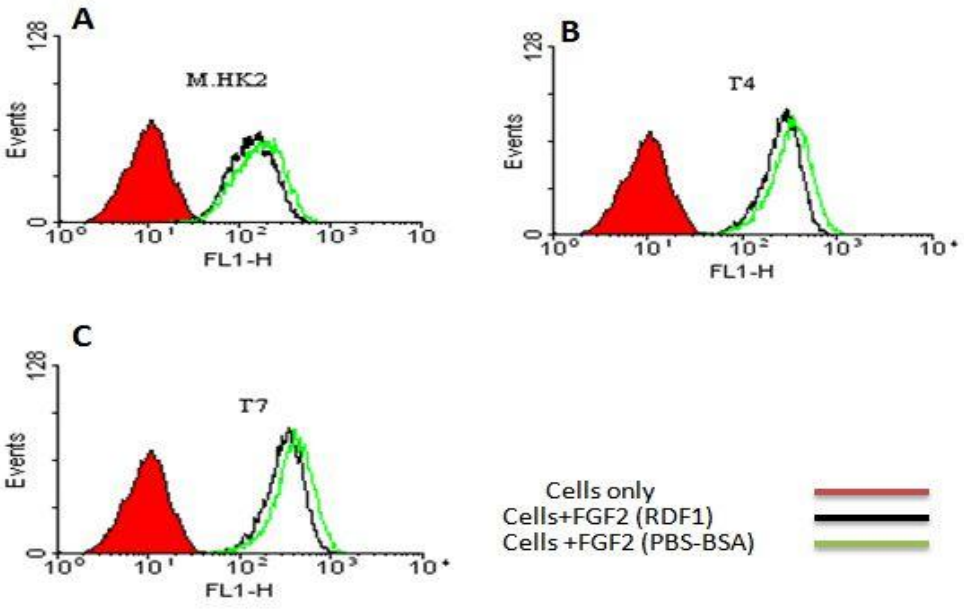

Figure 3.19. Representative histograms showing optimization of the FGF2 binding assay. A, Mock transfectant binding to FGF2 in case of RDF1 (black line) and PBS-BSA (green line) whereas red line represents cells with Avidin-FITC only. B, HS6ST1 transfectants (T4). C, T7 binding to FGF2.

Statistical analysis of MFI values for mock and HS6ST1 transfectants show that PBS-BSA significantly enhanced the binding of FGF2 to all cell lines compared with RDF1(Figure 3.20).

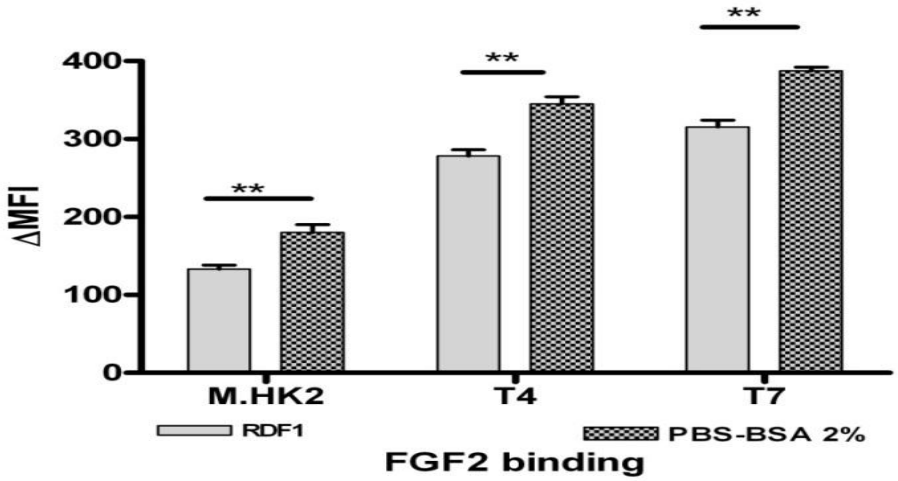

Figure 3.20. Optimization of the biotinylated FGF2 binding assay. Mock HK2 and HS6ST1 transfectants (T4 and T7) were incubated with biotinylated FGF2 followed with the avidin-FITC substrate. Cells were then washed and resuspended in either RDF1 or PBS-BSA2%. Cells were investigated by flow cytometry (N=2, **P<0.01).

This experiment showed that incubation of the FGF2 reaction in RDF1 or PBS-BSA gave similar results in term of specificity (Figure 3.21). No changes were noticed in negative control and anti-FGF2 antibody when using RDF1 or PBS-BSA. This indicates that PBS-BSA has no negative effect on reaction specificity. This result was confirmed in tubes containing mock and two HS6ST1 transfectant clones (T4 and T7).that gave similar results

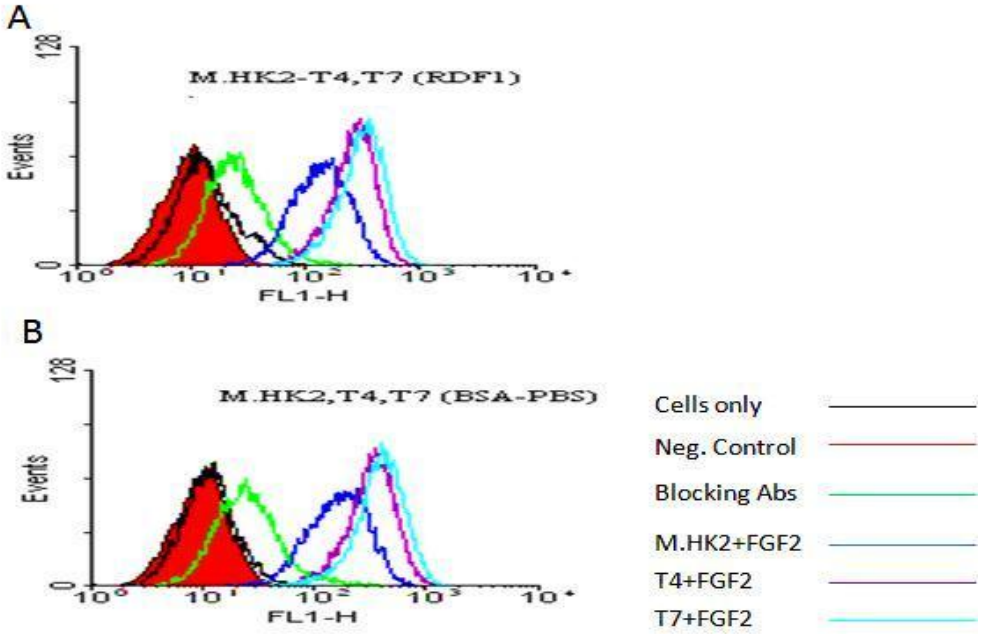

Figure 3.21. Optimization of FGF2 and effect on specificity. A, FGF2 binding assay using RDF1. Negative control appears in black line and blocking with anti FGF2 antibody appears in green. B, FGF2 binding assay with PBS-BSA 2% where negative control appears in black line and blocking antibody in green. Cells were analysed by flow cytometry, N=2.

3.3.8.2 **HS binding to 10E4 in presence of sodium chlorate**

To examine the role of HS in binding the 10E4 antibody, a series of experiments was performed after desulphation of HS by incubating cells with up to 150 mM sodium chlorate for three days. Sodium chlorate inhibits heparan sulphate sulphation by competing with 3'-phosphoadenosine-5'phosphosulphate (PAPS) which constitutes an essential sulphation donor for HS (Safaiyan *et al.*, 1999). Sodium chlorate concentration was optimised in this study for renal epithelial cells, and the higher concentration with viable cells was 150 mM (data not shown). Cells were examined for the 10E4 binding and investigated by flow cytometry. Treating cells with with sodium chlorate will deprive them from sulphation and will give an example of changes of HS sulphation on 10E4 binding epitope following HS6ST1 overexpression. HS6ST1 transfectants in sodium chlorate were examined against wild type and mock transfectants. As shown in figure 3.22, sodium chlorate reduced HS6ST1 transfectants and mock transfectants binding to 10E4 anibody.

This reduction reached up to 50% and 20% respectively compared to non-sodium chlorate treated cells.

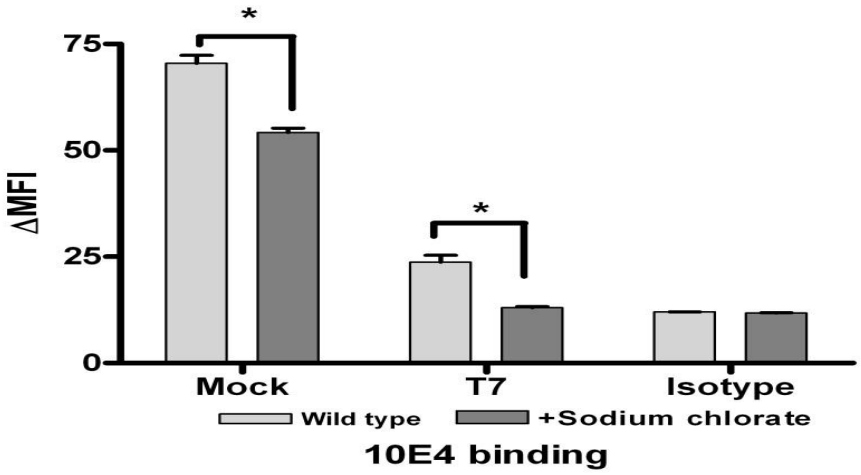

Figure 3.22. Analysis of 10E4 binding to chlorate-treated wild-type and HS6ST1 transfected cells. Cells were incubated with sodium chlorate (150mM) for 72 hours. Cells were then incubated with 10E4 antibody alongside wild type transfectants (without sodium chlorate) at 1:100 at 4^{o}C for 60 minutes. Cells were washed and incubated with FITC-conjugated secondary antibody. Cells were washed and resuspended in PBS containing 2%BSA and examined by flow cytometry. (N=2 with 4 replicates, *: P<0.05)

3.3.8.3 **HS binding to FGF2**

To examine the role of HS in binding FGF2, an assay was designed including wild type Chinese hamster ovary cells (WT-CHO) and 2 mutant cell lines which do not express HS. The mutant cell line CHO-745 lacks the xylosyltransferase activity required to transfer xylose to the core protein (serine); this is necessary to initiate GAG synthesis (Esko *et al.*, 1985). Mutant CHO-677 cells lack HS due to deficient acetyl glucosaminyltransferase and glucorunyltransferase activities; these are vital for HS synthesis (Murphy-Ullrich *et al.*, 1988). Wild type CHO, CHO-745 and CHO-677 were used to examine FGF2 binding to HS and GAGs. The FGF2 assay was carried out by flow cytometry. As shown in figure 3.23, wild-type CHO cells bound more FGF2 than either the CHO mutant cells. This change in FGF2 binding was statistically significant (P<0.01).

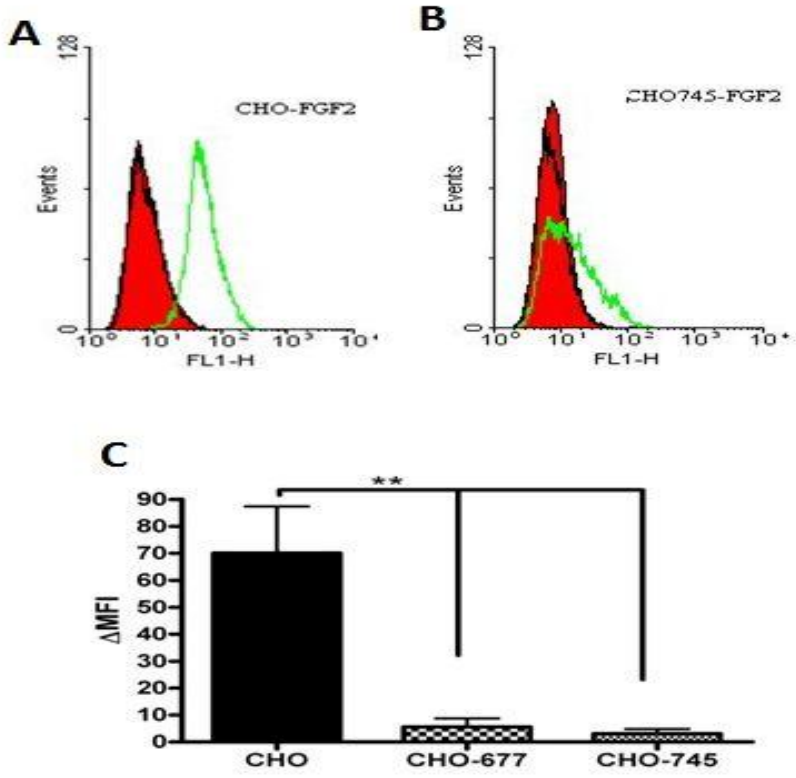

Figure 3.23. FGF2 binding to WT-CHO, CHO-745 (GAG mutant) and CHO-677 (HS mutant) cells. Cells were incubated with biotinylated FGF2 followed by Avidin-FITC and investigated by flow cytometry. A, a representative flow cytometric result showing FGF2 binding to WT-CHO and B, a representative histogram of HS-mutant (CHO-745) cell binding to Bio-FGF2. C, FGF2 binding ability was expressed as ΔMFI. Mean ΔMFI values are shown and error bars represent the SEM. (N=3, **= P<0.01).

3.3.8.4 **FGF2 binding in presence of sodium chlorate**

HS6ST1 transfectants (T7) were incubated with different concentrations of sodium chlorate in a time course of 72 hours followed by FGF2 binding assay. Sodium chlorate was added at 30, 50, 100 or 150 mM. The MFI values for FGF2 binding to the T7 transfectants were markedly decreased at a sodium chlorate concentration of 30 mM compared to mock transfectants. At a sodium chlorate concentration 150mM, FGF2 binding was completely inhibited for both mock and HS6ST1 transfectants, with ΔMFI values of around 20 (Figure 3.24).

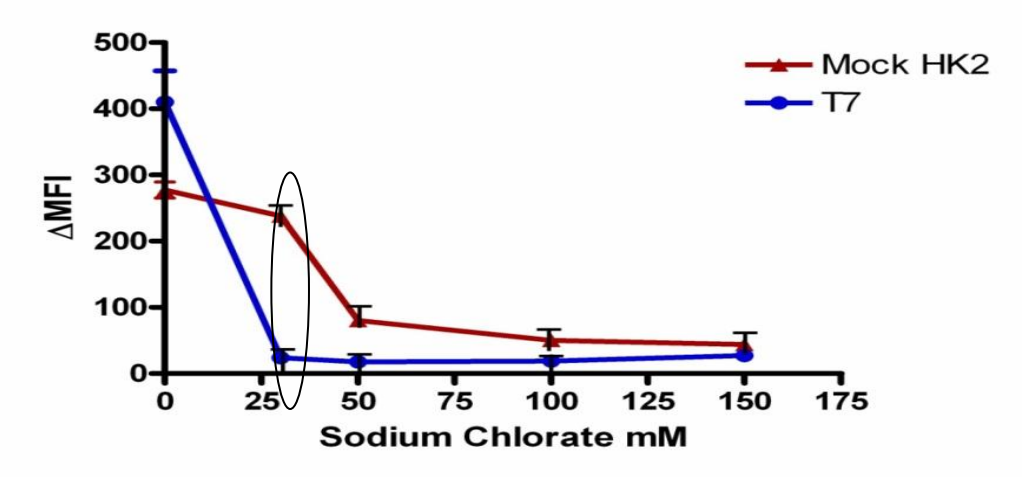

Figure 3.24. FGF2 binding in presence of sodium chlorate. Mock HK2 and HS6ST1 transfectants were incubated with different concentrations of sodium chlorate for 72 hours. Cell viability was determined by Trypan blue. Cells were investigated for FGF2 binding by flow cytometry. The error bars show the SEM (N=3, $P<0.05$).

These results were shown to be statistically significant, with the greatest difference between the cell lines observed at a sodium chlorate concentration 30 mM ($P<0.05$).

3.3.8.5 **FGF2 binding with Heparitinase III**

Heparitinase III is an enzyme known to degrade heparin/HS by cleaving the N-sulphated (NS) domains near iduoronic acid residues (Lohse and Linhardt, 1992). In order to verify the specificity of FGF2 binding to HS, mock and HS6ST1 transfectants were treated with heparitinase III. Figures obtained by flow cytometry showed that ΔMFI values of heparitinase III-treated (mock and HS6ST1 transfectants) were decreased by more than 75% compared to resting cells. Statistical analysis showed that heparitinase III significantly decreased FGF2 binding by both mock and HS6ST1 transfectants ($P<0.05$), (Figure 3.25).

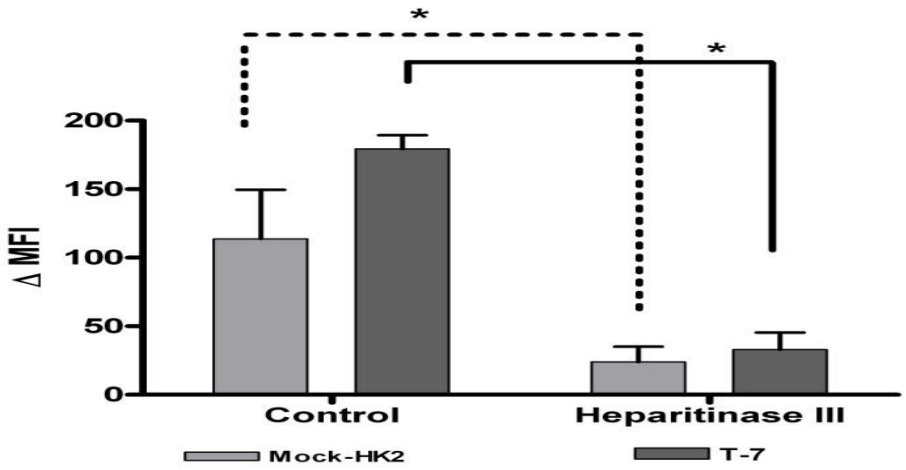

Figure 3.25. FGF2 binding after incubation with heparitinase III. Binding of mock HK2 cells and HS6ST1 overexpressing cells to biotinylated FGF2 before and after application of heparitinase III. Mock and HS6ST1 transfectants were incubated with heparitinase III (10 Sigma unit/ml) for 60 minutes at 37^{o}C. The cells were then incubated with biotinylated FGF2. The results were referenced to cells with no heparitinase III. The error bars show the SEM (N=3, P<0.05).

3.3.8.6 **FGF2 binding with HS6ST1 transfectants**

To examine the effect of HS6ST1 overexpression on HS biology, HS6ST1 transfectants were examined for FGF2 binding and compared to mock transfectants. These cells were incubated with biotinylated FGF2 and the bound factor was quantified by flow cytometry. Flourescence intensity (ΔMFI) values for FGF2 binding by HS6ST1 transfectants (T7) were approximately double those of mock transfectants (Figure 3.27). Statistical analysis showed that HS6ST1 transfection significantly increased the binding of FGF2 (P<0.05). The specificity of this test was verified using a negative control that contains soya bean protein which had been biotinylated to the same extent as FGF2. Additional controls included treating cells with blocking anti-FGF2 antibodies. Low ΔMFI values observed for control cells showed that binding is taking place mainly between HS and FGF2 specifically. Both HS6ST1 clones show increased binding to FGF2 compared to mock transfectants (Figure 3.26).

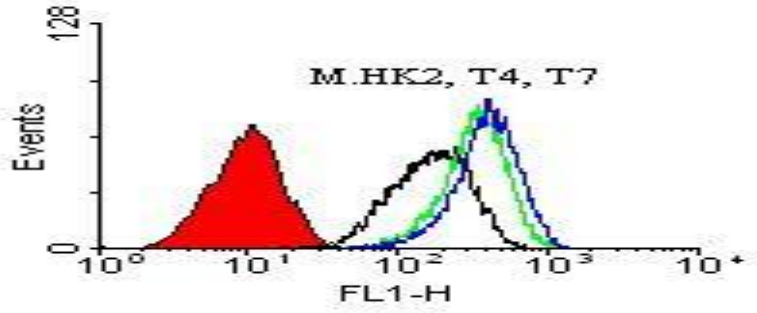

Figure 3.26. Representative histogram of flow cytometry for FGF2 binding to HS6ST1 transfectants. Red histogram represents control cells with Avidin-FITC conjugated substrate, black histogram represents mock transfectants with FGF2, green and blue histograms represent HS6ST1 transfectants (T4 & T7) with FGF2. All cells were incubated with Avidin-FITC substrate, N=3.

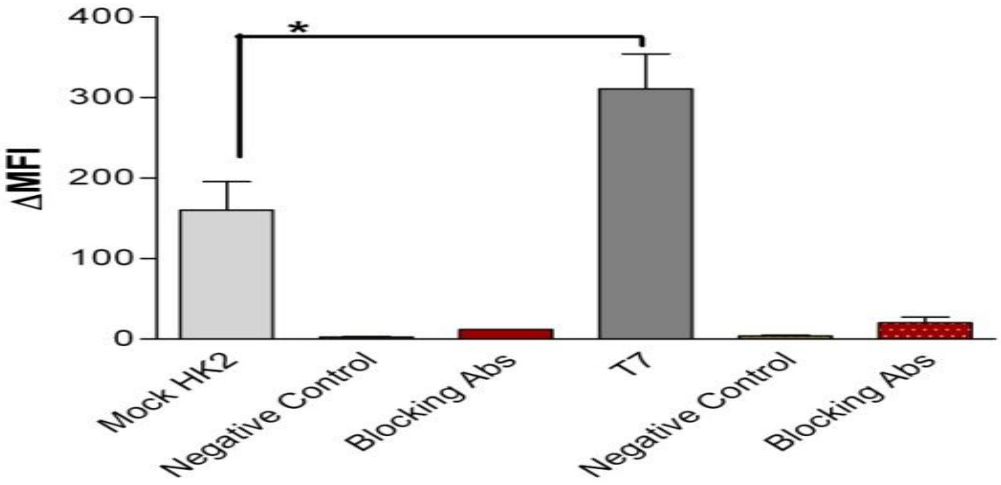

Figure 3.27. The effect of HS6ST1 overexpression on FGF2 binding. Mock HK2 and T7 cells were investigated for binding of biotinylated FGF2, the reaction was verified by FITC-Avidin and fluorescence activity expressed as median fluorescence intensity (MFI) was investigated by flow cytometry. Negative control contained soya bean protein (non HS-binding) biotinylated to the same level as FGF2, whereas specificity was examined by incubating FGF2 with blocking antibodies. Error bars represent the SEM (N=3, * $P<0.05$).

3.3.8.7 **FGF2 binding in presence of inhibitors**

FGF2 binding was further examined in the presence of competitors such as heparan sulphate, heparin, heparin de-O sulphate and heparin de-N sulphate. De-N and de-

O sulphated heparins lack sulphate groups at the N- and O- position respectively. Incubation of FGF2 with de-N or de-O sulphated heparins produced no changes in ΔMFI values for HS6ST1 transfectants compared to control mock and HS6ST1 transfectants (T7). By contrast, incubation of FGF2 with heparin completely inhibited FGF2 binding to both mock and T7 transfectants. Addition of soluble HS to FGF2 inhibited the binding to mock and HS6ST1 transfectant by 90% and 70% respectively. As shown in figure 3.28, heparin and HS significantly competed with mock and T7 transfectants for the binding of FGF2 ($P<0.05$).

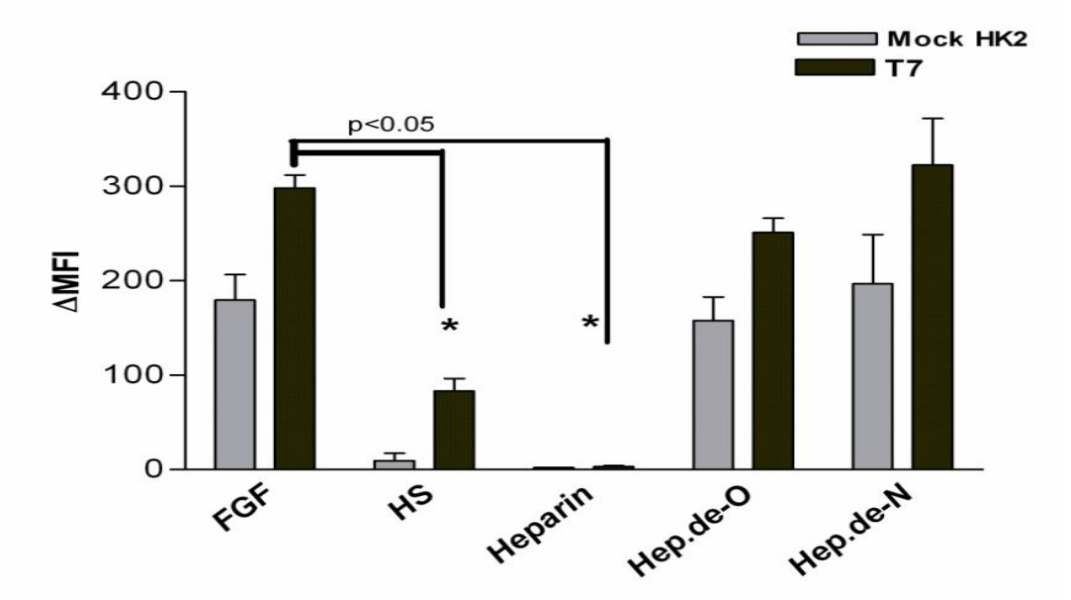

Figure 3.28. FGF2 binding in presence of inhibitors. Heparin de-O sulphate, heparin de-N sulphate, heparin and heparan sulphate were added to FGF2 for 10 minutes prior to cell addition. The assay was run in duplicates under normal conditions. All mediators were added at final concentration of 500μg/ml. Error bars show the SEM (N=2, *: $P<0.05$).

The concentration of heparin that causes 50% inhibition of the FGF2 binding (IC_{50}) was determined by incubating mock and HS6ST1 transfectants with FGF2 in presence of various concentrations of heparin (Figure 3.29). Heparin's IC_{50} for mock transfectants was 0.01 μg/ml compared to 0.1 for HS6ST1 transfectants.

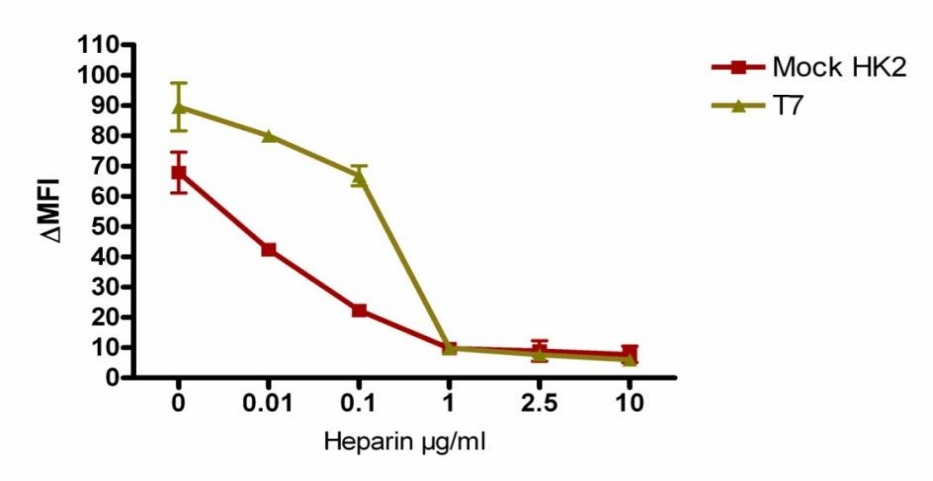

Figure 3.29. FGF2 binding in presence of heparin. Low concentrations of heparin were incubated with FGF2 for 10 minutes at room temperature. Then mock HK2 and T7 cells were added and FGF2 assay was carried out under normal conditions, (N=2).

3.3.9 HS structural analysis

3.3.9.1 **Disaccharide structure**

HS sulphation was examined by using ^{35}S as a source of sulphate to investigate sulphation pattern changes after HS6ST1 transfection. HS structure was fractionated to mono and di-sulphated disaccharides which constitute substrates for the sulphate transferase process performed by HS6ST1 enzyme.

HS6ST1 transfectants showed upregulation of heparan sulphate mono-O sulphated disaccharides such as glucuronic acid-N acetyl glucosamine 6S (GlcA-GNAc6S) and iduronic acid-N acetyl glucosamine (IdoA-GNAc6S) compared to mock transfectants. These disaccharides are represented as GMS and IMS respectively (Figure 3.30). In contrast, HS6ST1 overexpression resulted in decreased concentration of di-sulphated di-saccharides such as IdoA-GlcNS6S and IdoA2S-GlcNS6S (ISM and ISMS) compared to mock transfectants (Figure 3.30). These selective changes in saccharide concentration are statistically significant ($P<0.05$).

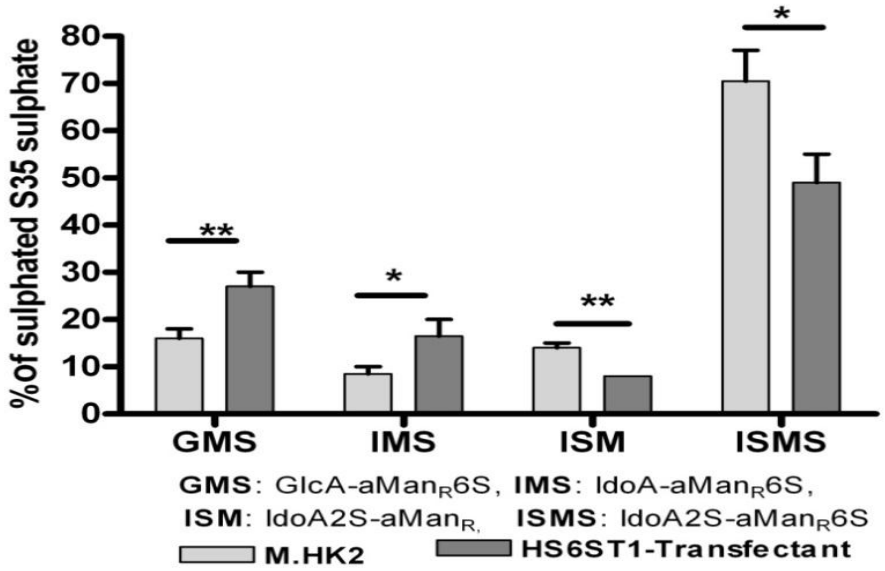

Figure 3.30. HS disaccharide composition in HS6ST1 transfectants. Mock and HS6ST1 transfectants were incubated with ^{35}S at 200μCi/ml for 24 hours. Cells were lysed and GAGs were isolated using DEAE Sephacel columns. Samples were treated with nitrous acid and deaminated products were fractionated by gel chromatography on Sephadex G-15. GAGs were separated using anion-exchange HPLC followed by running and eluting on Partisil 10 SAX columns. (N=2,**P<0.01,*P<0.05), data provided by collaboration with Prof. M. Kusche-Gullberg (Norway)

3.3.9.2 **Sulphate distribution**

The distribution of ^{35}S labelled monosaccharide fractions on the HS structure was examined to further explore the effect of HS6ST1 on the HS sulphation pattern. ^{35}S labelled monosaccharides show that HS6ST1 overexpression changes the total sulphation distribution in the HS structure. Sulphate groups at the 2-O position were downregulated by about 25% in HS6ST1 transfectants compared to mock transfectants. Sulphation at the 6-O and N-S position was not significantly changed (Figure 3.31).

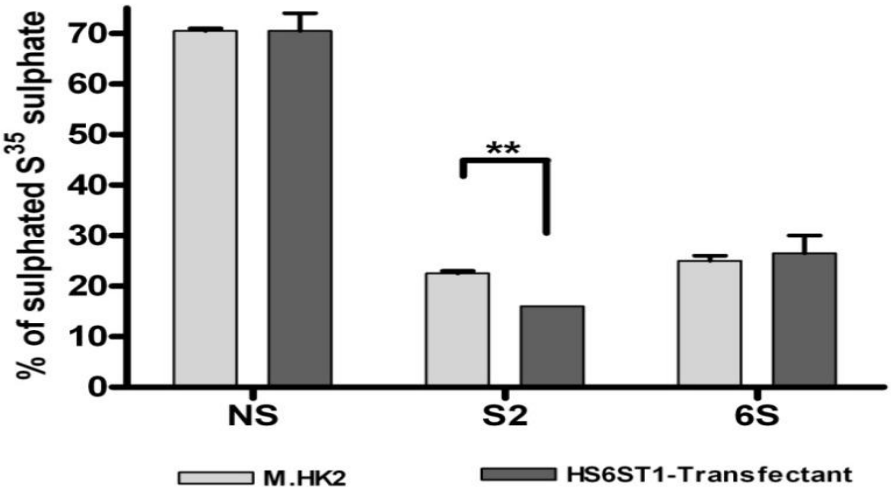

Figure 3.31. Sulphate group changes produced by HS6ST1 overexpression. Samples were isolated from ^{35}S labelled HS chains which were obtained from solubilized cells of mock and HS6ST1 transfectants. GAGs were depolymerized by low pH nitrous acid treatment followed by reduction with $NaBH_4$. Fractions were separated on a Partisil 10-SAX column alongside standard control. Error bars represent SEM, N=2 (4 replicates), **P<0.01).

3.3.10 HS6ST1 and proliferation assay

Measurement of cell proliferation is widely used to examine an increase in the number of viable cells. Non-radioactive proliferation assays depend on the reduction of a tetrazolium substrate into a coloured compound. This reaction takes place due to the effect of dehydrogenase enzymes found in active cells. Mitochondrial dehydrogenases in living cells reduce tetrazolium salts into a coloured formazan compound. To examine the potential role of HS6ST1 in cell biology and proliferation, a series of experiments was set up to measure the proliferation of mock and HS6ST1 transfectants. Proliferation was estimated using two different procedures; cell counting and colormetric proliferation assay. Cell counting showed that cells with HS6ST1 overexpression have higher proliferation ratios than mock transfected cells after few days (Figure 3.32). This result shows that HS6ST1 overexpression increased the number of HS6ST1 transfectants compared to mock transfectants at days 6 and 7 ($P<0.05$).

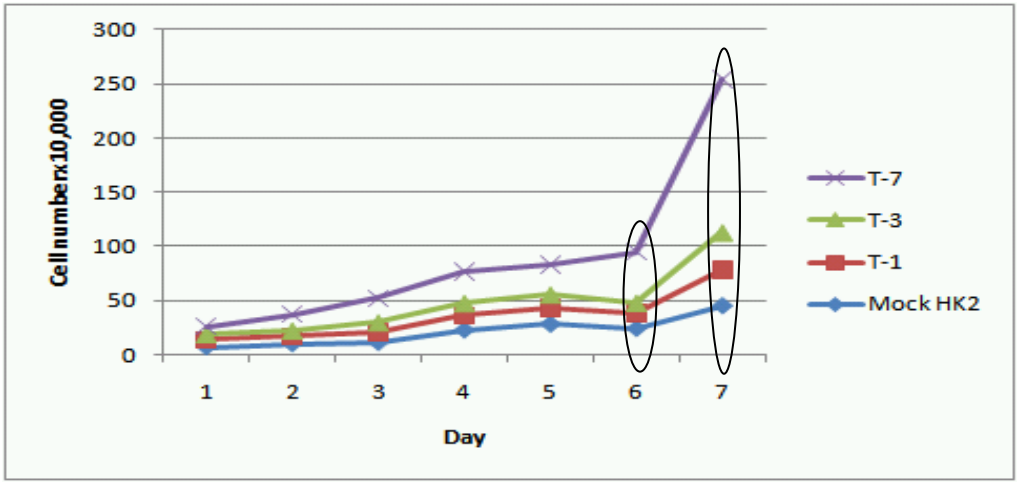

Figure 3.32. Representative figure showing a proliferation assay by cell counting. Equal cell numbers were seeded in 6-well plate with complete media in triplicates. Viable cells (using Trypan blue) were counted by using a Neubauer haemocytometer every 24 hours for 7 days. (N=3, $P<0.05$ between T7 and mock transfectant HK2 at days 6 and 7).

A non-radioactive colourimetric proliferation assay showed that HS6ST1 transfectants were more proliferative than mock transfectants (Figure 3.33, A). To further examine the effect of FGF2 in presence of HS6ST1 overexpression, FGF2 was added to the media and cells were investigated after 24, 48, 72 and 96 hours respectively. FGF2 enhanced the proliferation of HS6ST1 overexpressing cells (Figure 3.33, B). Addition of FGF2 to mock transfectants increased significantly the proliferation ratio compared to untreated mock transfectants.

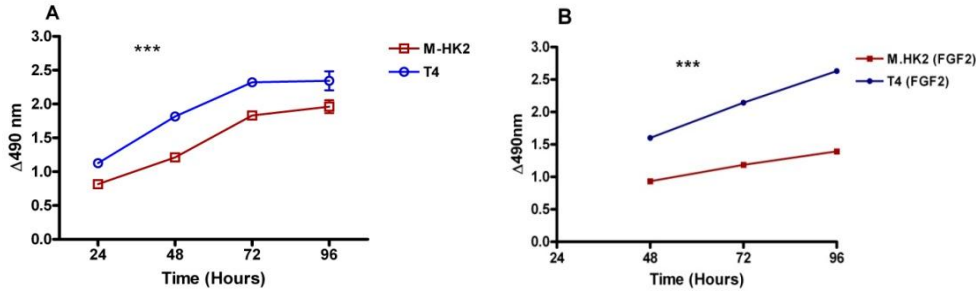

Figure 3.33. Representative results of colourimetric proliferation assay for HS6ST1 transfectants. A, Cells were seeded in 96 well plates in triplicates with 0.05%FCS and incubated for 24, 48, 72 and 96 hours. B, cells were incubated in presence of FGF2 at 10ng/ml. At the time of experiment, fresh medium was added with tetrazolium compound (MTS/PMS) and readings were taken at 490nm after 240 minutes (N=3, P<0.001).

3.3.11 HS6ST1 overexpression and ERK phosphorylation

Binding of FGF2 to its specific receptor, FGFR induces signalling through the intracellular ERK pathway, resulting in phosphorylation of extracellular signal regulated kinase, ERK1,2 to produce pERK1,2 (Loo and Salmivirta, 2002). These proteins are also known as mitogen activated protein (MAP) kinases and play a crucial role in cell proliferation and differentiation. When FGF binds to FGFR, a signal from the cell surface activates several protein mediators and ends in the nucleus resulting in protein transcription or cell division (Klint *et al.*, 1999).

The sulphate group at the 6-O position of HS constitutes a major component in the FGF-FGFR signalling complex. To further examine the role of HS6ST1 in this pathway, a series of experiments was carried out using western blotting to examine the expression of pERK1,2 in HS6ST1 and mock transfectants. Mock and HS6ST1 transfectants were incubated with FGF2 for short periods of time (5-10 minutes) as a stimulator of ERK activation. Western blotting using anti-pERK1,2 antibodies showed that HS6ST1 overexpression increased the production of pERK1,2 in HS6ST1 transfectants compared to mock transfectants. Densitometry of bands representing pERK1,2 showed that HS6ST1 transfectants expressed more than twice the amount of pERK compared to mock transfected cells (P<0.05).

FGF2 stimulation increased the ERK activation in mock transfectants which was proportional to the incubation time. Althogh FGF2 stimulation caused a dramatic increase in pERK1,2 in mock transfectants, this factor had no significant change of pERK1,2 in HS6ST1 transfectants (P>0.05), (Figure 3.34).

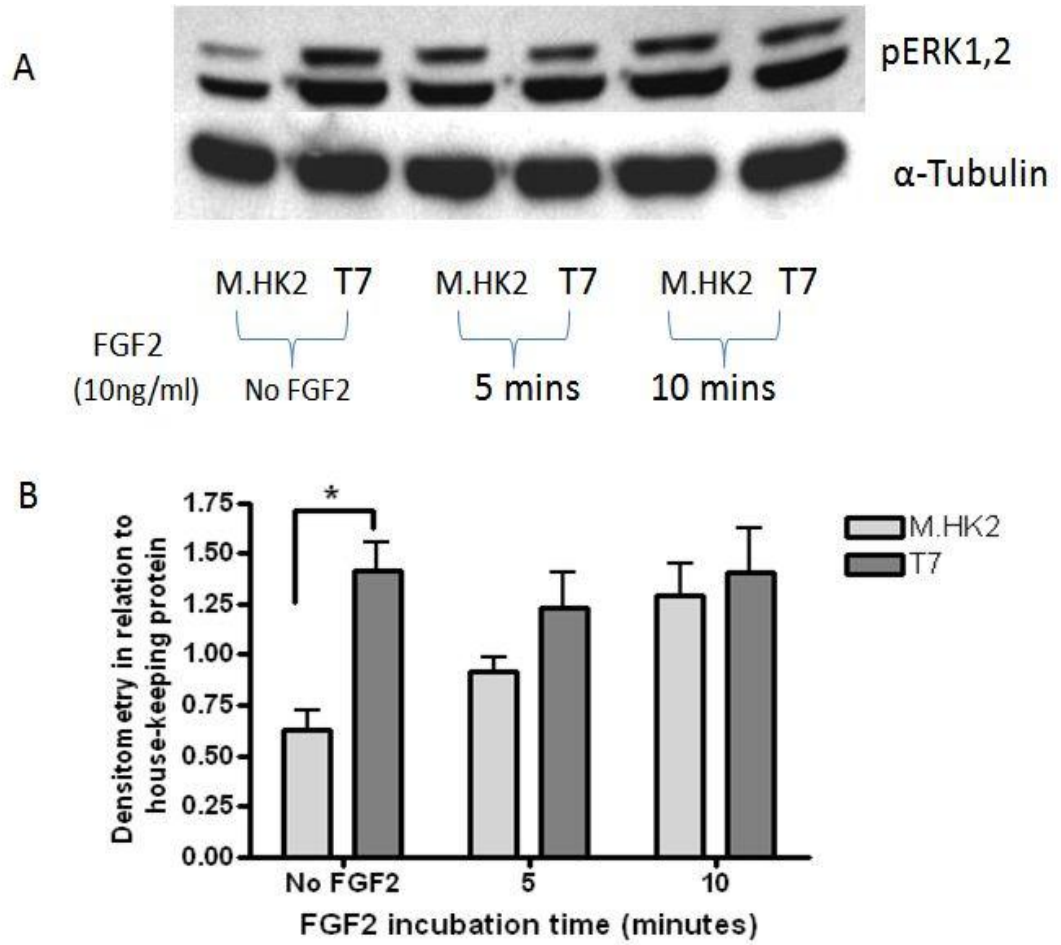

Figure 3.34. Representative Western blot of pERK1,2 in HS6ST1 and mock transfectants. A) Cells were incubated in 0.05% FCS medium for 24 hours. The cells were then exposed to FGF2 (10ng/ml) in 0.05 %FCS media for 5 or 10 minutes. The cells were solubilized and proteins separated on 10% SDS-PAGE at 10 µg protein/well. Phospho-ERK 1,2 antibody (Millipore) was used overnight at 1:1000 (4^{o}C). The same membrane was blotted for α-Tubulin antibody at 1:5000 as a house keeping protein to demonstrate equal protein loading. B) Analysis of densitometry of pERK bands normalized to α–tubulin. These analyses were performed using Image-J and Prism 4 (N=3,*P<0.05).

3.4 Discussion

HS is one of the most abundant GAGs on cell surfaces and within the extracellular matrix. HS undergoes a series of modifications during and after synthesis. These include transferring sulphate groups to specific positions on HS-GAG chains. Specific sulphate domains are required for HS-protein binding and signalling. Sulphate groups at the 6-O position are involved in a variety of interactions and signalling structures (Pye *et al.*, 1998; Wang *et al.*, 2002). HS modifying enzymes have been upregulated following stimulation of endothelial cells with proinflammatory cytokines. This change was accompanied with modulation of presentation and function of mediators such as chemokines (Ali *et al.*, 2005a).

3.4.1 Characterization of cell lines

Phenotyping endothelial and epithelial cells provides a basis for further investigation of these cells. Epithelial and endothelial cell lines in this study were characterized by expressing E-cadherin and CD31 respectively. Epithelial and endothelial cells normally express these markers and can, under particular conditions, lose them for new markers in the context of a transformation process. For example, epithelial cells undergoing EMT can no longer express epithelial markers such as E-cadherin. These cells alternatively express fibrogenic markers such as FSP-1 and α-SMA as signs of transformation (Zeisberg and Neilson, 2009). Similarly, endothelial cells lose the expression of CD31 as a sign of undergoing EndMT (Zeisberg *et al.*, 2007a).

HK2, HMEC1 and EAhy.926 cells were further phenotyped for expression of MHC-II molecules following stimulation with IFN-γ. Induction of MHC-II molecules suggests potential involvement in the pathogenesis of the inflammatory response following graft transplantation. This result supports a previous founding that endothelial and epithelial cells may act as antigen presenting cells in the context of inflammation (Cunningham *et al.*, 1997).

3.4.2 Observations of HS6ST1 expression

This study shows that stimulation of endothelial cells (HMEC1 and Eahy.926) and epithelial cells (HK2) with proinflammatory cytokines has no effect on HS6ST1 expression. Investigation of HS6ST1 expression with conventional PCR exhibited no detectable bands of the agarose gel. Whilst transcripts for HS6ST1 were detected by conventional PCR in HK2 cells they were not identified in HMECs. This is in contrast to the RT-PCR which found HS6ST1 expression in both cell lines. The failure to detect HS6ST1 mRNA in HMECs using conventional PCR may have been due to the relative poor efficiency of this primer combination or the possibility that one of the primer sites in HMECs were mutated. Although using qPCR demonstrated clear expression of the gene in renal epithelial cells, no significant changes in the HS6ST1 gene expression were found following stimulation with cytokines such as IFN-γ or TGF-β. However, IFN-γ caused a significant decrease in the gene expression in endothelial cells (HMEC1).

Additionally, the current study shows that stimulation with these cytokines produces no changes in HS interaction with 10E4 Antibody or biotinylated FGF2. It also seems that treatment with IFN-γ or TGF-β has no effects on HS motif structure or polyanionic charge which are involved in interaction with 10E4 or FGF2. Previously published results show that expression of HS6ST1 and HS6ST2 was upregulated in glomerular endothelial cells following stimulation with TNF-α and/or IL-1β along with NDST1 and 2 on mRNA level (2 fold). Interestingly, this was accompanied with increased 10E4 antibody binding which might be attributed to the increase in NDST1 expression which affects the 10E4 binding site (Rops *et al.*, 2008).

3.4.3 Observation of HS epitopes

In order to examine the changes made by HS6ST1 enzyme on HS structure and biological activity, stable HS6ST1 transfectants were generated. Stable transfectants were examined for HS6ST1 expression and the highest expressing clone (T7) was used for further investigations. This study shows that HS6ST1 transfectants significantly decreased the binding ability to 10E4 antibody compared

to mock transfected cells. The epitope designed for interaction with 10E4 antibody contains a tetrasaccharide domain of N-sulphated and N-acetylated glucosamine (GlcA-GlcNS-GlcA-GlcNAc) (David *et al.*, 1992; Leteux *et al.*, 2001), whereas sulphates at the O-position are not required for this binding (van den Born *et al.*, 2005). However, overexpression of O-sulphation might produce changes in the N-sulphation process, N-acetyl distribution or even overall sulphation which affects 10E4 binding. Unpublished data have shown that overexpressing of NDST1 increases the binding ability of HS-10E4 whereas knock-down of the gene shows the opposite effect (unpublished data by Dr. Spielhofer).

This study shows that HS6ST1 transfectants exhibit a significantly increased ability to bind HS3A8 and HS4C3 antibodies compared to mock transfectants. These antibodies target HS epitopes consisting of trisulphated disaccharides, IdoA2S-GlcNS6S (Dennissen *et al.*, 2002) and GlcNS3S6S respectively (van Kuppevelt *et al.*, 1998). Both epitopes are upregulated in chronic kidney rejection (unpublished data by Dr. Spielhofer, 2010); sections from human kidney undergoing chronic rejection have higher HS3A8 and HS4C3 epitope expression compared to normal, acute or moderately rejected kidney. The increased binding ability of HS3A8 antibody might suggest the involvement of HS6ST1 enzyme in the etiology of renal fibrosis. Similarity between FGF2 and HS4C3 epitopes was shown previously when FGF2-incubated cells blocked the interaction with HS4C3 binding antibody by about 60% (van Kuppevelt *et al.*, 1998). Furthermore, previous addition of HS4C3 antibody completely inhibited the proliferation effect of FGF2 when added to human mesangial cells (HMC) in vitro (Lensen *et al.*, 2005). The increased expression of HS4C3 epitopes in HS6ST1 transfectants can be classified in accordance with possible changes in HS sulphation such as increased FGF2 binding during fibrosis. Similar correlation is shown during development, where cellular response to VEGF was increased with cells showing "higher binding affinity" to HS4C3 (Baldwin *et al.*, 2008). This is important due to the requirement for VEGF signalling (Tessler *et al.*, 1994).

Furthermore, investigations with RB4EA12 show that cells overexpressing HS6ST1 have a higher binding ability to RB4EA12 antibody compared to mock

transfectants. This antibody recognizes an epitope consisting of: N-Acetyl, N-sulphate and 6-O sulphate groups (IdoA-GlcNS6S), whereas 2-O sulphate is not required (Dennissen *et al.*, 2002; Lensen *et al.*, 2005). This result is in line with a previous finding where SULF knock-out mice had higher 6-O sulphation (overexpression) accompanied with increased RB4EA12 binding (Lamanna *et al.*, 2006). Interestingly, HS binding epitopes for HS4C3 and RB4EA12 have been markedly upregulated in human chronic fibrogenic disease (liver cirrhosis), (Tatrai *et al.*, 2010). These observations along with previous literature strongly suggest a possible role for 6-O sulphation in the etiology and development of chronic diseases.

3.4.4 Observations with FGF2

HS binding to FGF2 has been intensively studied from different points of view. HS binds FGF2 via a specific epitope which consists of tetrasaccharide domains of IdoA2S-GlcNS (Habuchi *et al.*, 1992; Turnbull *et al.*, 1992; Guglieri *et al.*, 2008). The 6-O sulphate group is involved in a longer binding site and it is necessary also for receptor activation (Ornitz, 2000).

In this study, biotinylated FGF2 was examined for HS binding using HS6ST1 transfectants. The reaction conditions were optimized and HS-FGF2 binding was investigated using HS and GAG deficient cell lines (CHO-677, 745 respectively) along with wild type CHO cells in a flow cytometric assay (Esko *et al.*, 1985). Two clones of HS6ST1 transfectants were used in the investigations (T4 and T7) to confirm consistency.

The current study shows that incubation with sodium chlorate (30mM) caused a dramatic drop in HS6ST1 transfectants binding to FGF2. The decrease in FGF2 binding is attributed to the HS O-desulphation which constitutes an essential component in HS-FGF2 binding (Kreuger *et al.*, 2001). This result is in agreement with literature where sodium chlorate caused selective O-desulphation (Safaiyan *et al.*, 1999). Indeed, this result shows that the main increase in FGF2 binding might be attributed to the upregulation in O-sulphation occurring due to HS6ST1 overexpression. Similarly, treatment with heparitinase III enzyme resulted in

downregulation of HS-FGF2 binding in both HS6ST1 and mock transfectants. Heparitinase III enzyme has the ability to cleave HS by removing N sulphated residues which is expected to disrupt the HS-FGF2 binding site (Lohse and Linhardt, 1992).

The binding of biotinylated FGF2 was increased (2 fold) by HS6ST1 overexpression compared to mock transfectants; this increase could be for various reasons. Firstly, the 6-O sulphate group is not an essential component in the HS-FGF2 binding epitope, which includes predominantly N-S and 2-OS groups (Guimond *et al.*, 1993; Faham *et al.*, 1996). Although 6-O sulphate is not an essential component for HS-FGF2 binding, small amounts of this group were found in high affinity binding fractions (dp14), (Walker *et al.*, 1994). Secondly, earlier work showed that 2-O desulphated heparin, which retains 6-O sulphate groups, had the capacity to bind FGF2 but with lower affinity than native heparin (Guimond *et al.*, 1993; Ishihara *et al.*, 1997). Thirdly, the increased FGF2 binding might be attributed to the effects of HS6ST1 overexpression on HS sulphation, including increased chain length, HS domain distribution and polyanionic properties (Do *et al.*, 2006). Furthermore, FGF2 increased binding might be attributed to changes in HS chain and overall O-sulphation following HS6ST1 overexpression apart from 6-O sulphate group involvement in the HS-FGF2 binding site in agreement with previous findings (Jastrebova *et al.*, 2006; Mulloy and Rider, 2006). In contrast, overexpression of NDST1 reduced the FGF2 binding of NDST1 transfectants compared to wild type cells, although the N-sulphates play an important role in HS-FGF2 binding epitope (unpublished data by Dr. Spielhofer).

The current study shows that HS6ST1 overexpression has increased FGF-FGFR signalling leading to ERK activation and cell proliferation. Cells with HS6ST1 overexpression increased pERK activation in comparison to mock transfectants. This was noticed in the absence of FGF2; however, addition of FGF2 enhanced the ERK activation in mock transfectants but not in HS6ST1 transfectants. It might be argued that overexpression of HS6ST1 has increased ERK activation to an upper limit in a way that could not be increased even in presence of a high concentration

of FGF2. In agreement with pERK activation, HS6ST1 transfectants expressed higher proliferation ratios than mock transfected cells. This result shows the important role of HS, particularly following HS6ST1 overexpressing in the mitogenic activity of renal epithelial cells. This is in agreement with previous publication which showed involvement of HS in renal cell proliferation (Bokemeyer *et al.*, 1997; Carey, 1997; Raats *et al.*, 2000). Additionally, the current study is in line with the previous notion that ERK activation is increased by HS oligosaccharides containing 2- and 6-O sulphate groups (Jastrebova *et al.*, 2010). In further supporting experiments, an experimental mouse model with HS6ST overexpression exhibited increased FGF2-induced proliferation compared to wild type animals (Lamanna *et al.*, 2006).

3.4.5 Observation of HS structure

Measurement of the expression of HS modifying enzymes has yielded important information in relation to HS structure, sulphation and activity. Enforced expression of individual enzymes is also expected to affect not only the specific substrate but also the overall sulphation, domain distribution and HS chain length.

In this study, disaccharide structural analysis shows that HS6ST1 transfectants exhibit upregulation of 6-O sulphation at mono-O-sulphated disaccharides containing GlcA-GlcNS6S and IdoA-GlcNS6S (GMS and IMS, Figure 3.30) as well as downregulation of heavily sulphated disaccharides GlcA2S-GlcNS6S and IdoA2S-GlcNS6S. Interestingly, HK2 cells express a high level of trisulphated disaccharides (IdoA2S-GlcNS6S) which make these cells more similar to heparin than to HS structure. These findings are in line with previous work which also shows that HS6ST1 overexpression had a relatively high concentration of monosuphated disaccharides GMS and IMS (Do *et al.*, 2006). The current study shows that HS6ST1 transferred sulphate groups to residues containing GlcA/IdoA rather than 2-O sulphated in agreement with previous finding (Habuchi *et al.*, 2000). Furthermore, an increased concentration of 6-O sulphates at monosulphated disaccharides rather than trisulphated disaccharides is consistent with previous

finding which shows that HS6ST1 prefers low sulphated substrates (Habuchi *et al.*, 2007).

This study shows that the overall sulphation at the 6-O position is not increased in HS6ST1 transfectants compared to mock transfectants. This result can be attributed to the high concentration of trisulphated disaccharides (similar to heparin) including 6-O sulphate at the basal level in mock transfectants. Taking into consideration that a highly sulphated substrate does not constitute the preferred substrate for HS6ST1 (Habuchi *et al.*, 2007), it is not surprising that we do not see significant upregulation of 6-O sulphates. This result does not agree with previous published data which showed that overexpression of HS6ST resulted in increased concentration of 6-O sulphation (Do *et al.*, 2006).

Further changes in HS from HS6ST1 transfectants in this study included downregulation of 2-O sulphation with no significant changes in N-sulphation. The decrease in 2-O sulphation was previously accompanied by HS6ST overexpression (Do *et al.*, 2006). The mechanism of compensation by which over-sulphation at one position might affect sulphation at another position is not fully understood. By contrast, it has been shown that double knock-out of sulphatase enzymes which resulted in increased 6-O sulphation was accompanied by an additional increase in 2-O sulphation (Lamanna *et al.*, 2008). It is possible that HS6ST1 overexpression can induce a loss of coordinated activity between HS modifying enzymes which normally function in concert within the gagosome.

In conclusion, HS6ST1 transfectants increased the binding to FGF2 and proliferation of transfected cells. These transfectants exhibited increased binding epitopes against phage display antibodies HS3A8, HS4C3 and RB4EA12. These results show changes in HS sulphation and biological activities which are in line with transplanted kidney undergoing chronic rejection and interstitial fibrosis.

Chapter Four

4 The Process of HS Degradation

4.1 Introduction

HS undergoes various modifications during synthesis in the Golgi system due to different modifying enzymes. HS modifying enzymes such as NDST, HS2ST, HS6ST and HS3ST transfer sulphate groups to the HS chains (see section 1.6.4) which provides complexity and diversity that is needed for the HS function (Habuchi, 2000). HS chains undergo additional modifications due to the effect of hydrolysis enzymes such as heparanase, SULF1 and SULF2. These enzymes further modify the HS structure either by cleaving HS chains or by removing sulphate groups from specific positions (Lamanna *et al.*, 2006). This part of the research aims to shed more light on HS degradation enzymes and the effects on HS interaction and signalling with growth factors involved in the chronic kidney rejection.

HS proteoglycans normally have a half-life of about 1-4 hours on cell surfaces (Yanagishita, 1992). HSPGs are endocytosed or degraded by the action of protease enzymes and lipases. In rat ovary cells for example, the HS chains are transferred after 25 minutes to lysosomes where they are degraded into inorganic sulphate and basic monosaccharides. The HSPGs are recycled 10 times between cell surface and intracellular compartments before degradation in rat parathyroid tissue (Yanagishita, 1992).

4.2 HS degradation

HS chains are degraded after being synthesized, modified and exposed on cells surfaces and extracellular matrices. This process is regulated by sulphatase and heparanase enzymes.

4.2.1 Sulphatase enzymes

Sulphation at the 6-O position is increased by transferring sulphate groups by the action of HS6ST enzymes. However, 6-O sulphate groups can also be removed by the activity of sulphatase enzymes (Dhoot *et al.*, 2001; Lamanna *et al.*, 2007). There are 2 isoforms of relevant sulphatase termed SULF1 and SULF2; these enzymes are members of a family of 17 sulphatase enzymes in humans (Morimoto-Tomita *et al.*, 2002; Sardiello *et al.*, 2005). These members catalyze the hydrolysis of sulphated ester bonds in substrates such as sulpholipids and GAGs.

The endosulphatase enzymes (SULF1 and SULF2) interact with GAG chains via a unique hydrophilic domain (HD) located between N-catalytic domain and the C terminus. The HD has a high content of basic amino acids and therefore a high positive charge at neutral pH which facilities the binding to the anionic heparin/HS structure, anchoring the enzyme to the cell surfaces (Frese *et al.*, 2009). SULF1 was initially discovered in a molecular screen of the sonic hedgehog (Shh) gene in quail embryos; this enzyme is involved in the regulation of cellular differentiation by modulation of the Wnt signalling (Dhoot *et al.*, 2001).

SULF1 and SULF2 have an endosulphatase activity specific for glucosamine containing 6-O sulphate groups on the cell surface (Ai *et al.*, 2006b). These enzymes are considered the final HS modifying enzymes which exist in both cell surface-associated and soluble forms (Morimoto-Tomita *et al.*, 2002). Importantly, SULF2 has been shown to increase the expression of glypican 3 in hepatic cell carcinoma (HCC) and promotes FGF2 signalling (Lai *et al.*, 2008a). Glypican 3 constitutes an important marker for hepatic cell carcinoma metastases (Ning *et al.*, 2012).

4.2.1.1 **SULF enzyme and HS structure**

The SULF enzymes have shown a substrate preference, with 6-O desulphation taking place at UA-GlcNS6S and UA2S-GlcNS-6S residues by 20% and 70% respectively. No sulphatase activity was observed against UA-GlcNAc-6S residues (Lamanna *et al.*, 2008). Heparan sulphate obtained from SULF knockout mice shows various levels of 6-O disaccharide composition. SULF1 knockout mice increase 6-O sulphation in all three HS domains (NS, NA/NS and NA) whereas the SULF2 knockout increases 6-O sulphates in NA only (Lamanna *et al.*, 2007). Although sulphatase enzymes specifically remove 6-O sulphate groups from HS chains, SULF loss was shown to have additional changes on 2-O and N- sulphate groups on different types of HS (Lamanna *et al.*, 2008).

4.2.1.2 **The physiological role of sulphatase**

The interaction between proteins and HS depends on several factors, including chain length, polyanionic charge, and the pattern of sulphation. However, accumulating evidence shows that loss of 6-O sulphation can modify protein binding (Dhoot *et al.*, 2001; Ai *et al.*, 2003a; Wang *et al.*, 2004). One example of the positive effect of sulphatase activity is the Wnt signalling system. The expression of SULF1, by desulphation of the 6-OS group, increased Wnt binding to its cognate receptor Fizzled (Ai *et al.*, 2003a). However, in case of FGF2 the 6-O desulphation leads to deactivation of the signalling pathway (Wang *et al.*, 2004). The removal of 6-O sulphate groups has also been shown to affect the binding of CXCL12 (stromal derived growth factor-1; SDF-1), VEGF and morphogens. These factors play significant roles in activities including development, differentiation and cell growth (Ai *et al.*, 2003a; Wang *et al.*, 2004; Uchimura *et al.*, 2006; Lemjabbar-Alaoui *et al.*, 2010).

Sulphatase gene expression shows differential regulation during health and disease. For instance, the stimulation of human lung fibroblasts with TGF-β induces the upregulation of SULF1 expression. Interestingly, it was suggested that SULF1 might have negative effect on regulation of the fibrogenesis induced by TGF-β (Yue *et al.*, 2008). Expression of the SULF2 gene was increased in breast and lung carcinoma (Morimoto-Tomita *et al.*, 2005; Lemjabbar-Alaoui *et al.*, 2010).

Sulphatase knockout results in mild changes in lung development, growth and viability (Rosen and Lemjabbar-Alaoui, 2007). For example, SULF1 knockout mice show a nearly normal phenotype with higher mortality in the first few months of life whereas SULF2 knockout mice show only mild changes such as weight loss (Lamanna *et al.*, 2006; Lum *et al.*, 2007). Importantly, double knockout of SULF genes results in neonatal lethality accompanied by defects in skeleton, kidney and the nervous system (Holst *et al.*, 2007; Kalus *et al.*, 2009).

4.2.1.3 **Heparanase enzyme (HSPE)**

Mammalian HPSE was first detected in human placenta and a hepatoma cell line (Hulett *et al.*, 1999; Vlodavsky *et al.*, 1999). The HPSE gene was expressed in various cell types and tissues, with relatively high expression in placenta, lymphoid

organs, keratinocytes and carcinoma cells (Dempsey *et al.*, 2000; Parish *et al.*, 2001; Vlodavsky and Friedmann, 2001).

The HPSE is an endoglycosidase involved in HS degradation (Bame, 2001). This enzyme hydrolyses the glucosidic bonds (β 1-4) within the HS chain producing HS fragments of 10-20 sugar units. The suggested cleavage site for HPSE requires the presence of NS and 6-O-S groups in a specific orientation (Pikas *et al.*, 1998; Okada *et al.*, 2002). It has been suggested that the minimum binding site is a trisaccharide domain of two glucosamine units and one UA (GlcN-UA-GlcN), (Okada *et al.*, 2002).

The HPSE enzyme plays important roles in biological activities such as angiogenesis, inflammation, carcinogenesis and metastases (Nasser, 2008). Interestingly, the action of HPSE allows the release of HS fragments, increasing FGF2 binding, dimerization and signalling (Elkin *et al.*, 2001). The HPSE enzyme might also affect the survival of transplanted organs by shedding the HS involved in the AT-III binding site. This effect might be responsible for the intravenous coagulation and fibrin deposits in the graft (Ali *et al.*, 2003). Additionally, HPSE has an essential role in degradation of the vascular basement membrane. This effect facilitates leucocyte passage through basement membrane by increasing barrier permeability during inflammation (Edovitsky *et al.*, 2006). Interestingly, HPSE can regulate syndecan 1 clustering and shedding from tumor cells (Yang *et al.*, 2007). The downregulation of syndecan 1 was shown to result in FGF2-induced EMT (Kato *et al.*, 1995). Importantly, it has been shown recently that HPSE plays a crucial role in regulation and induction of EMT in renal tubular epithelial cells following FGF2 stimulation (Masola *et al.*, 2012).

The expression of HPSE is modulated during inflammatory processes. For example, the expression of heparanase is increased during fibrotic liver disease (Tatrai *et al.*, 2010). The secretion of HPSE is also influenced by proinflammatory cytokines. Stimulation of endothelial cells with proinflammatory cytokines such as TNF-α or IL-1β is known to promote the release of HPSE (Chen *et al.*, 2004).

4.2.2 Aims

Specific aims will be:

- To examine the expression of heparan sulphate degrading enzymes such as sulphatase and heparanase in human kidney epithelial and endothelial cell lines.
- To examine the modulation of sulphatase expression by a wide range of cytokines.
- To generate stable transfectants of SULF2 in order to:
  - Examine the effects on FGF2 binding.
  - Examine the changes in sulphation pattern using phage display antibody.
  - Analyze the changes caused by SULF2 on HS structure using ^{35}S uptake. (This work was carried out in collaboration with Prof. Kusche-Gullberg in Norway)
  - Examine the effects of SULF2 overexpression on CCL5 binding
  - Investigate the effects of SULF2 on cell proliferation.
  - Investigate the effect of SULF2 on ERK activation.

4.3 Specific materials and methods

4.3.1 SULF2 sequencing and alignment

The plasmid was supplied by Addgene with an inserted SULF2 gene into the vector backbone (pcDNA3.1/Myc-His-). The plasmid was transformed into the DH5-α bacteria for DNA amplification and seeded on agar plates with ampicillin. The colonies were used for plasmid DNA isolation (Qiagen) and the DNA was cut by *XhoI* and *HindIII* enzymes which provide unique restriction sites (Figure 4.1).

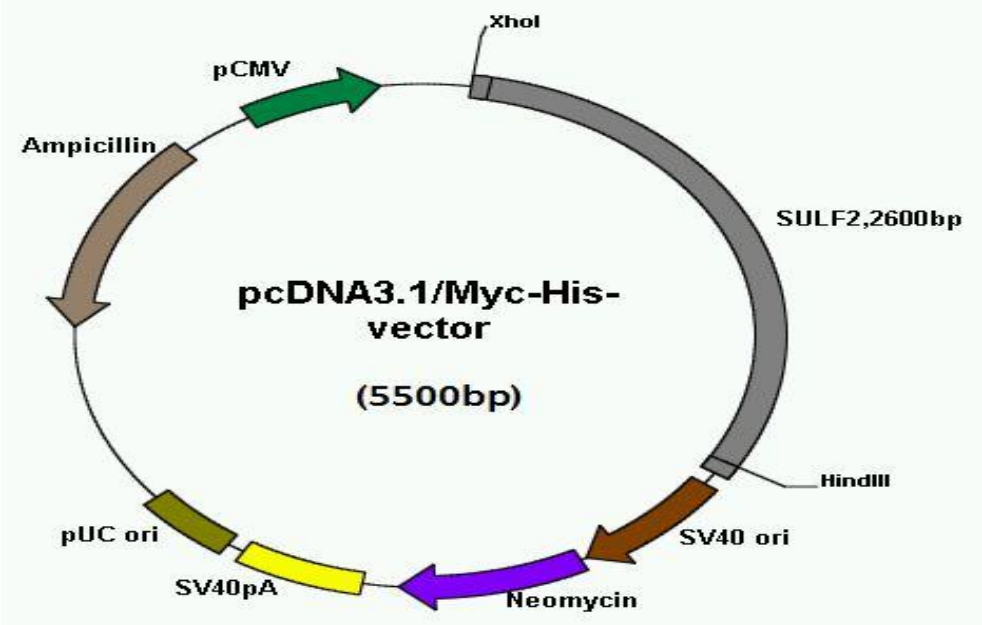

Figure 4.1. Drawing of plasmid pcDNA3.1/Myc-His- (vector) and SULF2 gene (insert).

The restriction enzyme digestion produced two bands of 2600 bp and 5500 bp representing the SULF2 insert and the vector backbone respectively (Figure 4.2). The resultant insert was sequenced (Geneservice) and aligned with the SULF2 gene (Addgene plasmid-13004) in the PubMed-sequence site (see appendices).

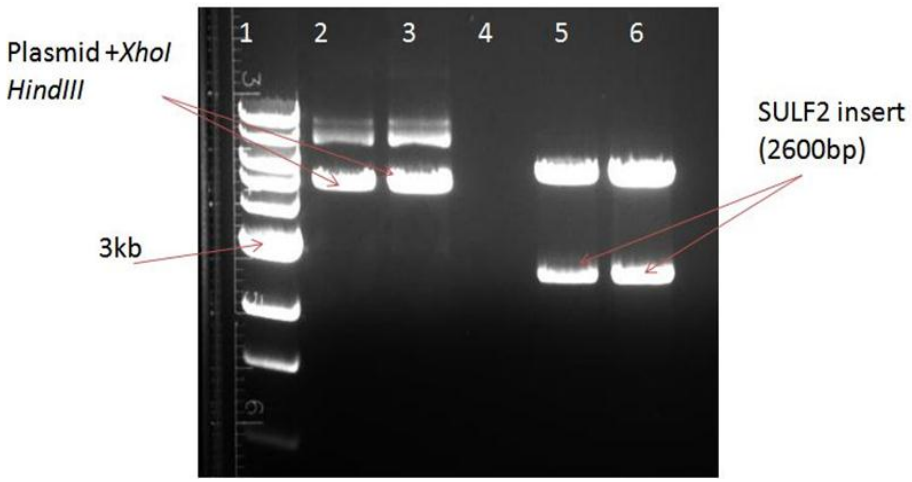

Figure 4.2. Plasmid encoding SULF2 digested with *XhoI* and *HindIII*. The whole (pCDN3.1/his-) plasmid (including SULF2 insert) was digested with restriction enzymes *XhoI* and *HindIII*. The digest reaction was performed at room temperature for 3 hours and the DNA was then run on 0.7% agarose gel alongside 1kb DNA ladder (Lane 1). Lane 2 contains the plasmid with *XhoI*, lane 3 contains plasmid with *HindIII* whereas the lanes 5 and 6 contain plasmid with both enzymes (*XhoI* and *HindIII*) in duplicate.

4.3.2 Cell stimulation

Renal epithelial cells were stimulated with cytokines and changes in HS sulphation were examined for gene expression (qPCR) and antibody interaction. The cells were incubated with different cytokines separately and the RNA was extracted and used for cDNA synthesis and RT-PCR. Renal epithelial cells (HK2) were seeded in six well plates in presence of complete DMEM-F12 medium overnight. Cytokines including IFN-γ, IL-17 or TGF-β were added to the medium in the absence of fetal calf serum (FCS) whereas BSA was added at 1%. After 24 hours, the medium was removed and the cells were washed with PBS and used for RNA extraction by Trizol (Sigma). The resting cells (non-stimulated cells) were considered as control. The stimulated cells were also investigated for interaction with 10E4 antibody and FGF2.

4.3.3 RT-PCR

4.3.3.1 **Testing the efficiency of amplification**

Quantitative PCR was optimized at the beginning of gene expression experiments using specific primer probes (TaqMan) from Applied Biosystem. The cDNA was synthesized and screened for HS degradation enzymes HPSE, SULF1 and SULF2 using exon spanning primer probes (TaqMan) while the GAPDH was used as a house keeping gene. In optimal PCR, DNA amplification should reach 100% when the slope is -3.32. However, an amplification ratio of 90-110% is accepted. For GAPDH, SULF1, SULF2 and HPSE the amplification efficiency (E) values were 108%, 107%, 97.8% and 94.5 % respectively (Figure 4.3).

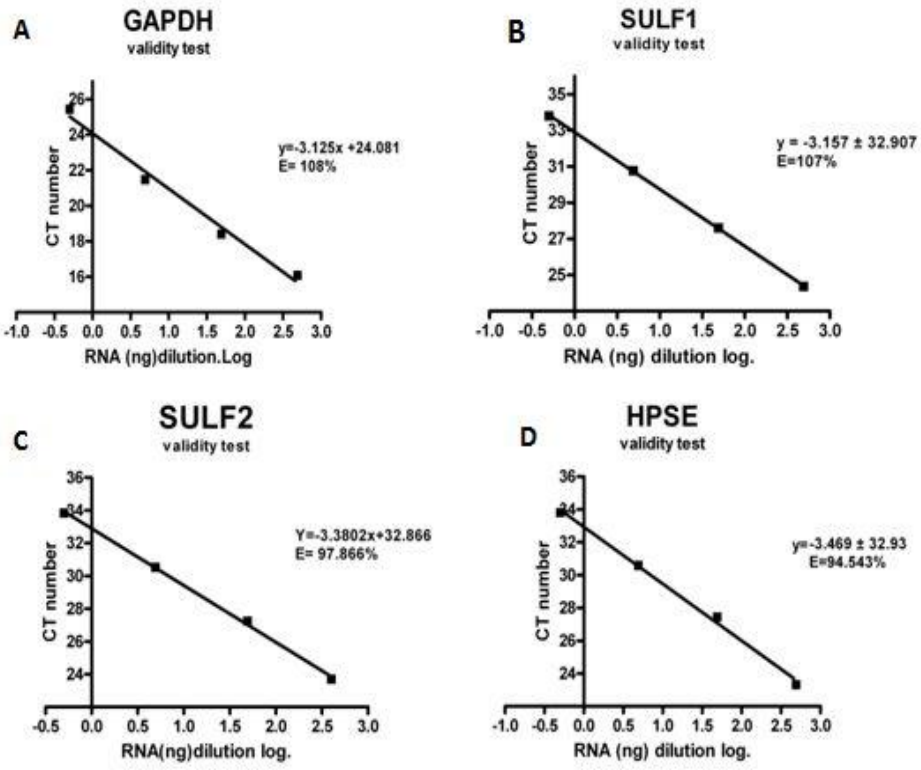

Figure 4.3. RT-PCR efficiency with specific primer/probe combinations. cDNA obtained from HKC8 renal epithelial cells was used as a template for RT-PCR experiment. cDNA was ten-fold diluted in 3 serial dilutions with primer probes of GAPDH, SULF1, SULF2 and HPSE. Cycle threshold (CT) numbers were calculated against logarithm of serial dilution. Statistics were performed by using Excel regression.

4.3.3.2 **PCR primer probes**

Human exon junction spanning probes do not detect any amplified genomic DNA (Applied Biosystem, TaqMan Gene Expression assay).

GAPDH (Hs0099999905-m1)

SULF1 (Hs00392834-m1)

SULF2 (Hs00393644-m1)

HPSE (Hs00395394-m1)

4.4 Results

4.4.1 Cell stimulation and HS degradation enzymes

The expression of HS degrading enzymes was investigated at the mRNA level by stimulating endothelial and epithelial cells with several cytokines. These cytokines were TGF-β, IFN-γ and IL17 at concentrations which include 10ng/ml, 25ng/ml and 100ng/ml respectively; phorbol myristate acetate (PMA) was used at concentration 50ng/ml. The concentrations and time points were optimized in the group earlier. Investigations were performed by qPCR with specific codon-spanning primer probes.

4.4.1.1 **Heparanase (HPSE)**

Heparanase is a glycosidase enzyme which acts as an endo β-D-glucuronidase of HS chain resulting in release of HS fragments of discrete sizes. HPSE expression was investigated in resting cells and after cell stimulation.

4.4.1.1.1 Endothelial cells and HPSE

EAhy.926 cells were stimulated with TGF-β, IFN-γ and IL-17 for 24 hours; PMA was used for control. Cytokine stimulation resulted in no significant changes in HPSE expression on mRNA level compared to resting cells. Figure 4.4 shows that no significant changes were noticed using qPCR assay specific for HPSE ($P>0.05$).

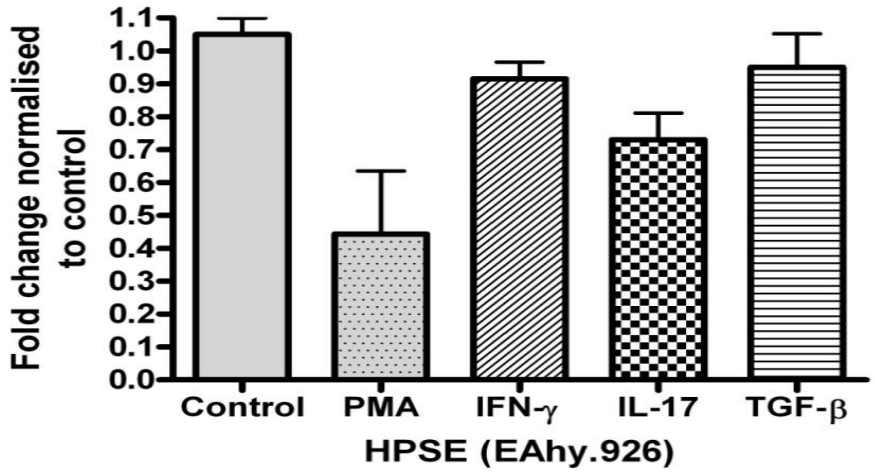

Figure 4.4. Expression of heparanase (HPSE) by EAhy.926 after stimulation with cytokines. Cells were incubated with IFN-γ (25ng/ml), TGF-β (10ng/ml), IL-17 (100ng/ml) and PMA (50ng/ml) for 24 hours. RNA was extracted and used (5µg) for cDNA synthesis. QPCR experiments were performed in triplicates with gene expression assay with specific primer probes. CT values of stimulated cells were calculated and compared to those of resting cells in reference to GAPDH as a house-keeping gene. Data were analysed by ΔΔCT method using REST-2009 software. No significant changes in HPSE expression were observed (N=3), error bars represent the SEM.

4.4.1.1.2 Renal epithelial cells and HPSE

Renal epithelial cells (HK2) were stimulated with cytokines such as TGF-β, IFN-γ and IL-17 for 24 hours whereas PMA was used for control. Then cDNA obtained was examined for the expression of HPSE by real time PCR. Data analyses show that IFN-γ and IL-17 stimulation resulted in no significant changes in HPSE expression compared to resting cells. However TGF-β stimulation significantly downregulated the expression of HPSE by about 50% compared to unstimulated cells. PMA also significantly downregulated HPSE expression by around 25% compared to unstimulated cells (Figure 4.5).

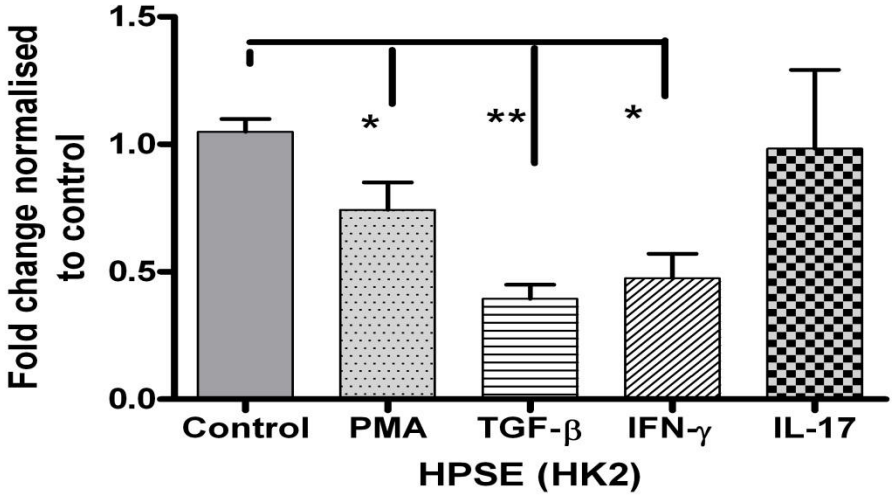

Figure 4.5. Expression of HPSE by HK2 cells after stimulation. Cells were incubated with IFN-γ (25ng/ml), TGF-β (10ng/ml), IL-17 (100ng/ml) and PMA (50ng/ml) for 24 hours. RNA was extracted and used (5μg) for cDNA synthesis. QPCR experiments were performed in triplicates with specific primer probes (TaqMan). CT analysis data were normalized to resting cells in reference to GAPDH as a house-keeping gene. Data were analyzed by ΔΔCT method using REST-2009 software. (N=3, *: P<0.05, **: P<0.01).

4.4.1.1.3 Sulphatase 1 (SULF1)

Sulphatase 1 constitutes a hydrolase enzyme that removes 6-O sulphate groups from the HS chains on cell surfaces. SULF1 gene expression was examined using qPCR after stimulation with a set of cytokines in endothelial and epithelial cell lines. Results were compared to resting cells.

4.4.1.1.4 Endothelial cells and SULF1

SULF1 gene expression in EAhy.926 was examined after stimulation with TGF-β, IFN-γ, and IL17 for 24 hours. As shown in figure 4.6, IL17 stimulation has caused significant (P<0.05) downregulation of SULF1expression by around 60 % compared to resting cells (control). In contrast, TGF-β stimulation has caused significant upregulation of SULF1 expression (P<0.05) by around 2.5 fold compared to resting cells. Changes in SULF1 expression due to the effect of TGF-β and IL17 proved to be statistically significant (Figure 4.6). Stimulation with IFN-γ caused no significant changes on SULF1 expression.

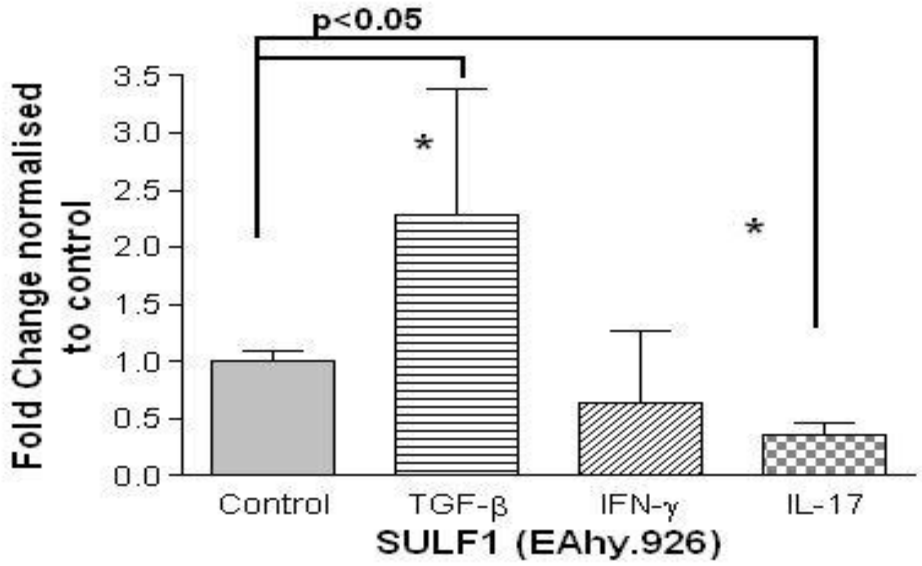

Figure 4.6. Expression of SULF1 by EAhy.926 after stimulation. Cells were incubated with IFN-γ (25ng/ml), TGF-β (10ng/ml) and IL-17 (100ng/ml) for 24 hours. RNA was extracted and used (5μg) for cDNA synthesis. QPCR experiments were performed in triplicates with gene expression assay using specific primer probes. CT values were calculated in reference to GAPDH and resting cells in ΔΔCT method using REST-2009 software. (N=3, *: P<0.05).

4.4.1.1.5 Renal epithelial cells and SULF1

Renal epithelial cells (HK2) were stimulated with TGF-β, IFN-γ, IL17 and PMA for 24 hours and the expression of SULF1 gene was examined. TGF-β and IL17 had no significant effect on SULF1 expression compared to resting cells. Stimulation with IFN-γ, PMA and IL-17 resulted in remarkable downregulation of SULF1 by about 75%, 60% and 30% respectively compared to unstimulated cells (P<0.05). These changes were shown to be statistically significant (Figure 4.7).

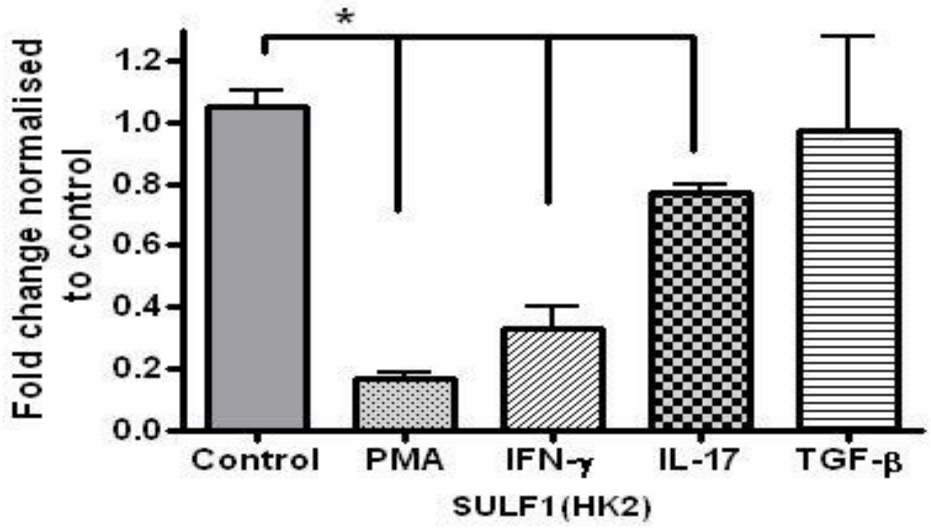

Figure 4.7. Expression of SULF1 by HK2 cells after stimulation. Cells were incubated with IFN-γ (25ng/ml), TGF-β (10ng/ml), IL-17 (100ng/ml) and PMA (50ng/ml) for 24 hours. RNA was extracted and used (5μg) for cDNA synthesis. QPCR experiments were performed in triplicates with specific primer probes (TaqMan). CT values of stimulated cells were calculated and compared to those of resting cells with GAPDH as a house-keeping gene. Data were analyzed by ΔΔCT method using REST-2009 software. (N=3, *: P<0.05).

4.4.1.2 **Sulphatase 2 (SULF2)**

Sulphatase 2 (SULF2) enzyme is an isoform of SULF1 that exists on the cell surface and also in soluble form that hydrolyses the 6-O sulphate of HS chains. SULF2 expression was investigated in endothelial and epithelial cell lines after cytokine stimulation using qPCR.

4.4.1.2.1 Endothelial cells EAhy.926 and SULF2

Endothelial cells EAhy.926 were stimulated with TGF-β, IFN-γ and IL17 for 24 hours; PMA was used for control. As shown in figure 4.8, TGF-β and PMA stimulation caused no significant changes on SULF2 gene expression compared to resting cells. However, stimulation with IFN-γ resulted in upregulation of the SULF2 gene expression by about 3 fold compared to resting cells. In contrast, IL-17 stimulated cells exhibited downregulation of SULF2 by more than 50 % compared to resting cells. Changes due to the effect of IFN-γ and IL-17 have proved to be statistically significant (Figure 4.8).

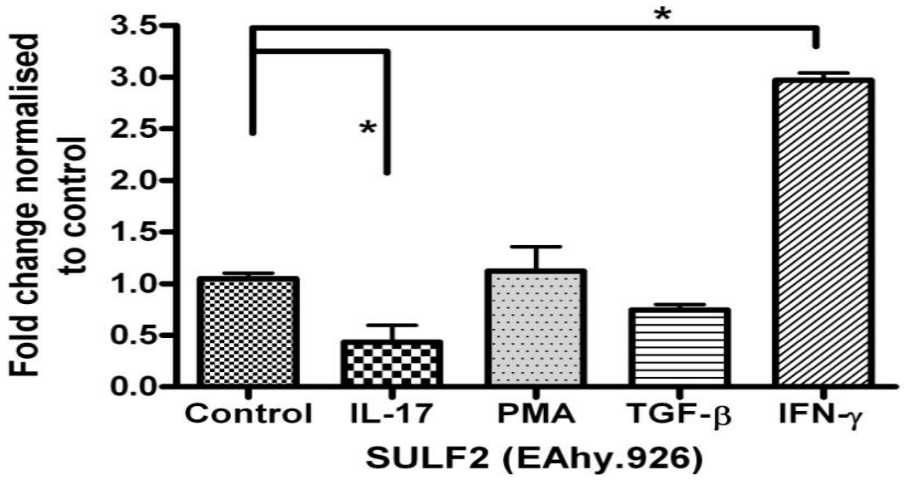

Figure 4.8. Expression of sulphatase 2 (SULF2) by EAhy.926 after stimulation. Cells were incubated with IFN-γ (25ng/ml), TGF-β (10ng/ml), IL-17 (100ng/ml) and PMA (50ng/ml) for 24 hours. RNA was extracted and used (5μg) for cDNA synthesis. QPCR experiments were performed in triplicates with specific primer probes. CT values were analyzed by using REST-2009 software. (N=3, *: P<0.05).

4.4.1.2.2 Renal epithelial cells and SULF2

Renal epithelia cells (HK2) were stimulated with cytokines such as TGF-β, IFN-γ and IL17 for 24 hours; PMA was used for control. The expression of SULF2 gene was then examined. Stimulation with IFN-γ, IL-17 and PMA showed no significant change in the SULF2 gene expression compared to resting cells. Interestingly, stimulation with TGF-β has resulted in gene overexpression of SULF2 by around 5 fold compared to resting cells. This change has been shown to be statistically significant (P<0.01), (Figure 4.9).

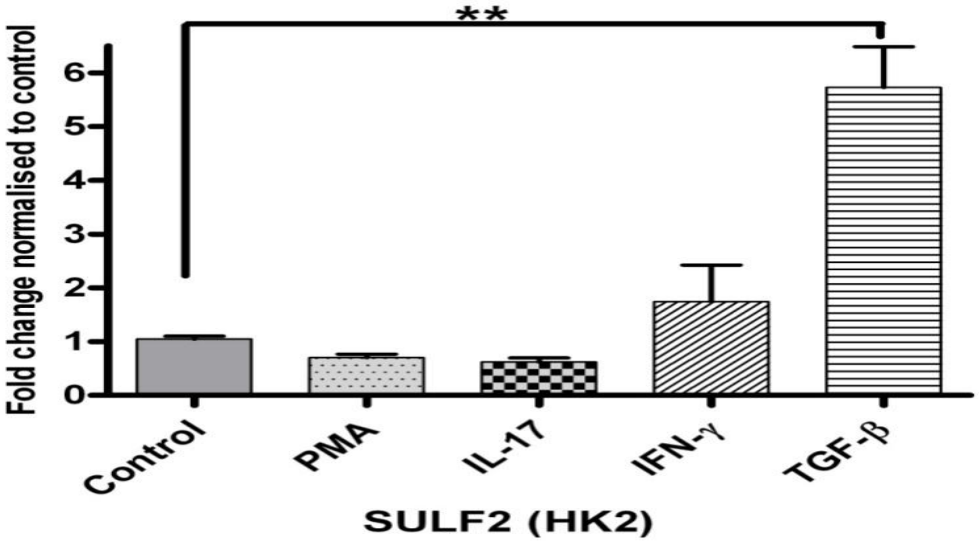

Figure 4.9. Expression of SULF2 by HK2 cells after stimulation. Cells were incubated with IFN- γ (25ng/ml), TGF-β (10ng/ml), IL-17 (100ng/ml) and PMA (50ng/ml) for 24 hours. RNA was extracted and used (5μg) for cDNA synthesis. QPCR experiments were performed in triplicates with specific primer probes (TaqMan). CT values of stimulated cells were calculated and compared to those of resting cells in reference to GAPDH as a house-keeping gene. Data were analyzed by ΔΔCT method using REST-2009 software. (N=3, **: P<0.01).

4.4.2 Generation of stable transfectants of SULF2

Renal epithelial cells stimulated with TGF-β have shown upregulation of SULF2 gene expression by 5 fold as seen above. Due to the role of TGF-β in chronic allograft rejection and in order to shed more light on its role in the sulphation pattern of HS, stable transfectants with SULF2 overexpression were generated. These transfectants were used for further experiments in accordance to chronic rejection and sulphation pattern.

4.4.2.1 **Optimisation of transfection**

Transfection was optimised using a plasmid containing GFP. Reporter plasmid-GFP was transiently transfected into human kidney cell line HKC8 and investigated by flow cytometry. A concentration of 0.4 μg of DNA was used with 50 μl of Effectene reagent (Qiagen), (see 3.3.6.1). 24 hours later, cells expressing GFP formed about 70% of the total transfected cells. This result means that transfection efficiency reached about 70% (Figure 4.10). This ratio constitutes a

good basis for transfection by using the same protocol for transfecting SULF2-containing plasmid into renal epithelial cells.

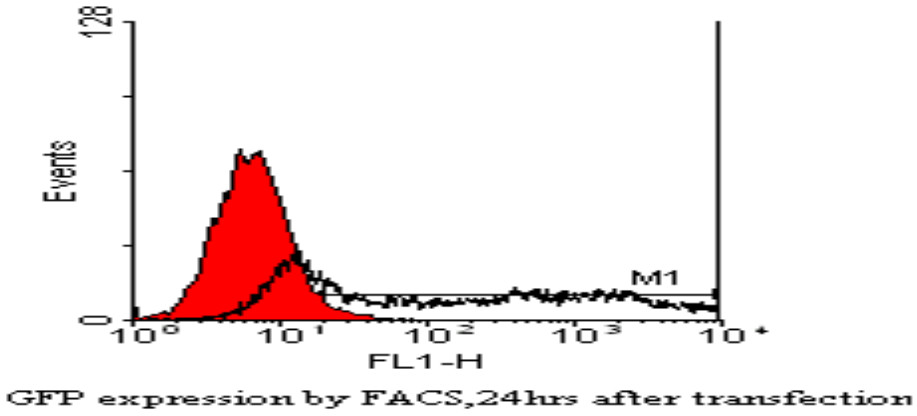

Figure 4.10. Representative histogram of GFP transfection efficiency. Renal epithelial cells were transfected with plasmid encoding GFP. Transfection efficiency was investigated by measuring fluorescence intensity after 24 hours in comparison to non-transfected cells (red line). GFP transfected cells (black line) represented about 70% of total cells. Investigation was carried out by flow cytometry and data were analyzed by WinMDI 2.9.

4.4.2.2 **Antibiotic killing curve**

Incubating HKC8 cells with different concentrations of Geneticin (G418) showed that cells were killed at the lowest concentration starting from 600 μg/ml of G418 in DMEM-F12 complete medium. Transfectants (SULF2) were selected in a medium with G418 at 600μg/ml and maintained at 400μg/ml, data not shown.

4.4.2.3 **SULF2 cloning**

Renal epithelial cells were transfected with plasmid pcDNA3.1/Myc-his- (5500bp) containing SULF2 insert (2600bp). Plasmid-insert was run on agarose gels following digestion with restriction enzymes in order to confirm the size of each component. As shown in figure 4.2, plasmid was digested and run on the gel to confirm the SULF2 insert and vector sizes. The plasmid was sequenced and the results were aligned with the original SULF2 gene sequence (appendices).

4.4.2.4 **Generation of SULF2 transfectants**

A SULF2 expressing plasmid was generated. The sequence was then verified and used for transfecting renal epithelial cells. Resulting clones were selected in presence of G418 (600µg/ml). Selected clones were expanded and screened for the expression of SULF2 by qPCR. Clones were given the initial "S" with a reference number and the highest expression clones (S5 and S11) were used for further investigations. Mock transfectants were generated by transfecting renal epithelial cells with an insert-free plasmid. Mock transfectants were selected and grown under the same conditions as for SULF2 transfectants (Figure 4.11).

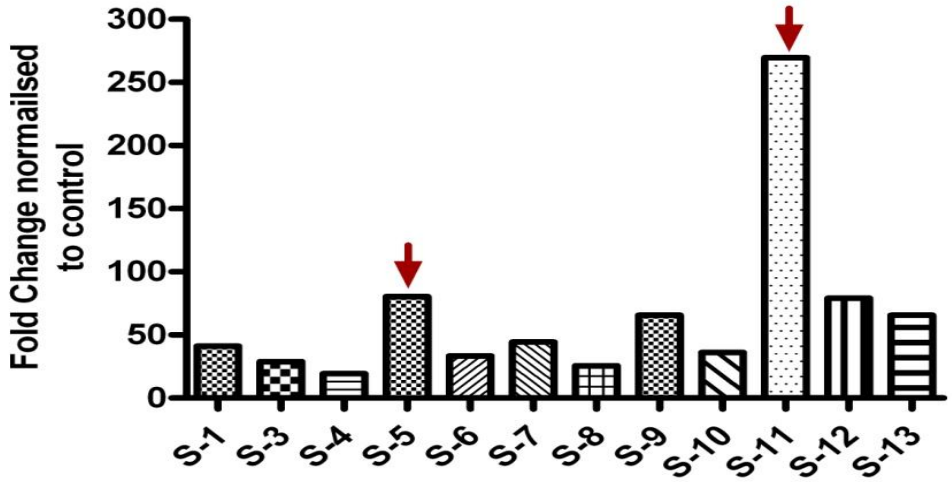

Figure 4.11. Expression of SULF2 in renal epithelial (HKC8) stable transfectants. QPCR experiments were carried out to screen the expression of SULF2 in HKC8-SULF2 transfectants. SULF2 transfectants were grown in presence of G-418 and total RNA was extracted and used for cDNA synthesis for qPCR. GAPDH was used as a house-keeping gene and data were normalized to mock transfected cells. The highest SULF2 expressing clones (S-5 & S-11) were used for further investigations. (N=2)

4.4.3 Characterization of SULF-2 transfectants

4.4.3.1 **Antibody binding to the 10E4 epitope**

In order to investigate changes in HS structure after SULF2 overexpression, a series of experiments were performed to quantify 10E4 antibody binding. These experiments were investigated by immunofluorescence and flow cytometry.

4.4.3.1.1 Flow cytometry

SULF2 transfectants were incubated with 10E4 antibody and the controls included cells incubated with isotype control primary antibody and secondary antibody only (with no primary antibody). These cells were compared to mock transfectants. SULF2 transfectants show a trend to increased binding of the 10E4 antibody compared to mock transfectants (Figure 4.12, A). However, this was not statistically significant (Figure 4.12, B).

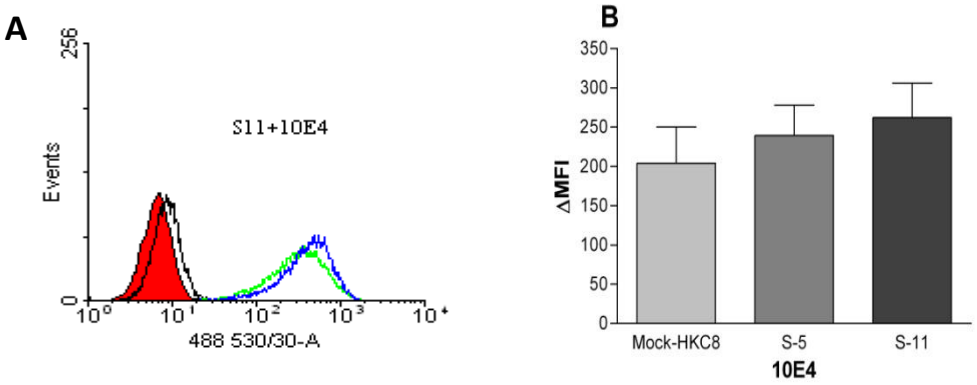

Figure 4.12. Characterization of HS sulphation of SULF2 transfectants binding to 10E4. SULF2 and mock transfectants were incubated with 10E4 antibody at 1:100 for 60 minutes at 4^{o}C followed by FITC-conjugated secondary antibody. A, Histogram representing SULF2 transfectants (S-11) binding to 10E4 (blue) compared to mock transfectants (green), black line represents isotype IgM antibody incubated cells and red line represents cells with secondary antibody only. B, Mean values of median fluorescence intensity (ΔMFI) measured by fluorescence flow cytometry (N=3).

4.4.3.1.2 Immunofluorescence

SULF2 transfectants were stained with anti HS antibody (10E4) by using immunofluorescence technique and investigated by confocal microscopy. The figures produced by this method show that 10E4 binds at a higher level to cells with SULF2 overexpression compared to mock transfectants. Transfectants with less SULF2 expression (S5) showed less antibody binding than cells expressing higher levels of SULF2 (S11). Quantitative analysis by measuring MFI showed significant changes ($P<0.05$), (Figure 4.13, 4.14).

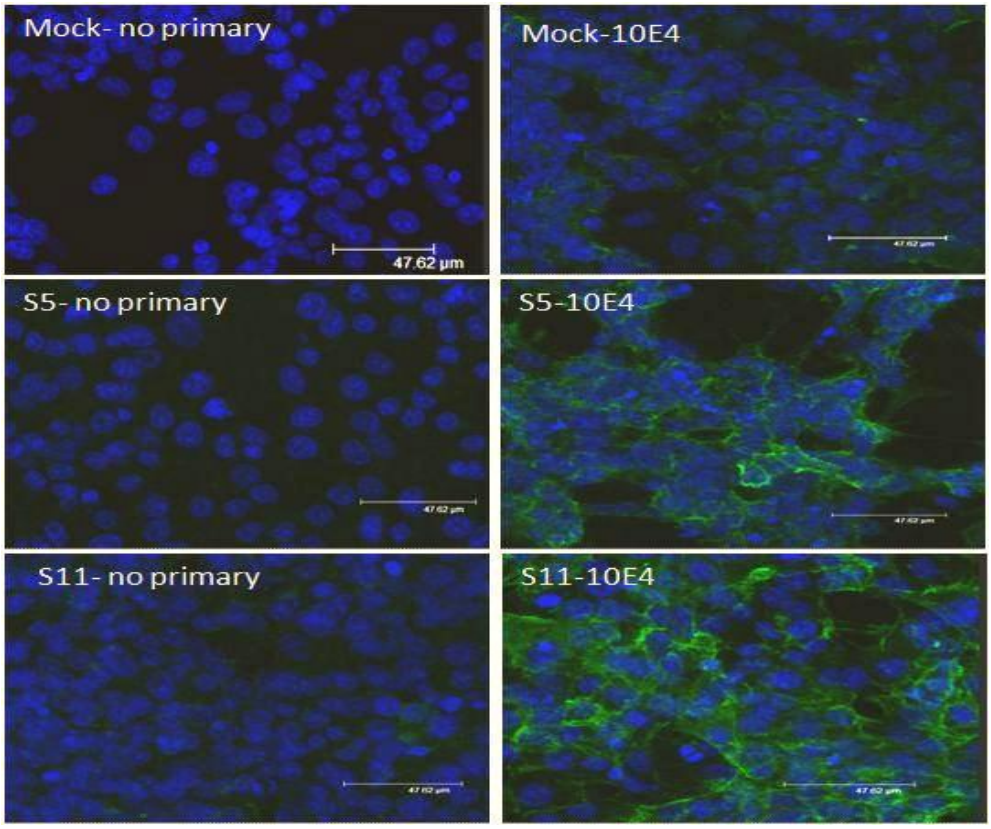

Figure 4.13. Representative image of SULF2 transfectants stained with 10E4 antibody. Cells were seeded in 4 well chamber slides till confluency. Then slides were fixed with cold acetone and blocked with PBS-BSA2% followed by 10E4 antibody at 1:100. FITC-conjugated secondary antibody was added and slides were examined by fluorescence inverted microscope. Scale bar represents 47.62 µm.

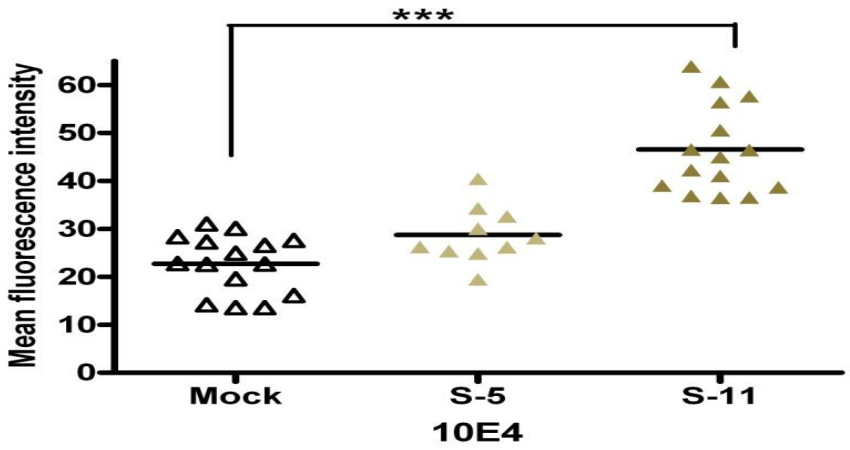

Figure 4.14. Quantitative analysis of SULF2 transfectants stained with 10E4 antibody. Slides of mock and SULF2 transfectants (S5 and S11) were analyzed by Image J to measure mean fluorescence intensity. Three slides from three independent experiments were quantified; each slide was screened for five random and equal areas. (N=3, ***: P<0.001).

4.4.3.2 **Binding to phage display antibodies**

SULF2 removes sulphate group from 6-O position on cell-surface HS. This may also influence the pattern of sulphation at the 3-O, 2-O and N- positions. A series of experiments was carried out using phage display antibodies to investigate changes on HS epitope expression. These experiments were evaluated by flow cytometry.

4.4.3.2.1 Antibody binding to the HS3A8 epitope

HS3A8 antibody targets specific sulphate groups at N-, 6-O and 2-O positions. SULF2 transfectants (S5 and S11) were shown to have a decreased ability to bind HS3A8 antibody compared to mock transfectants. This downregulation was statistically significant (P<0.01) with S11 compared to mock transfectants (Figure 4.15).

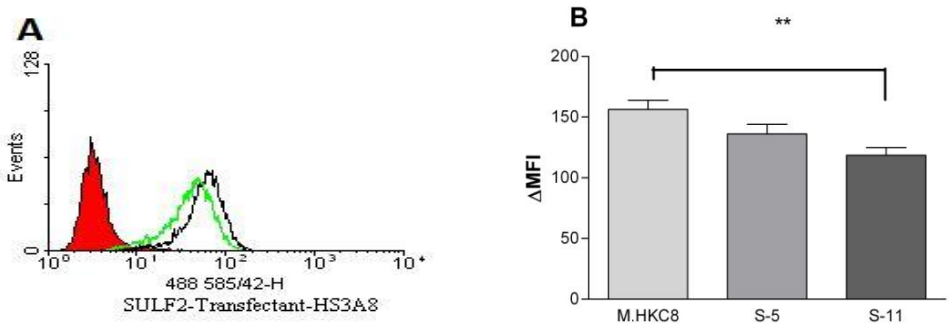

Figure 4.15. Phage display antibody HS3A8 binding to SULF2 transfectants. Mock and transfectants were grown in presence of G-418 until 80% confluency. Cells were detached, washed and incubated with HS3A8 in 1:10 at 4^{o}C for 60 minutes. Secondary anti-VSV-Cy3-conjugated antibody was added (1:200) for additional 30 minutes. Cells were washed, resuspended in 2%FCS-PBS and investigated by flow cytometry. A, representative histogram of SULF2 transfectant (green) binding to HS3A8 compared to Mock transfectant (black). B, Mean values of median fluorescence intensity (ΔMFI) measured by fluorescence flow cytometry (N=3, **: P<0.01).

4.4.3.2.2 Antibody binding to the HS4C3 epitope

SULF2 transfectants and mock transfectants were incubated with HS4C3 phage display antibody. This antibody targets sulphate groups at N- and O- positions. Data from flow cytometry show that cells with SULF2 overexpression had a decreased ability to bind this antibody compared to mock transfectants. This decrease was shown to be statistically significant (P<0.05), (Figure 4.16).

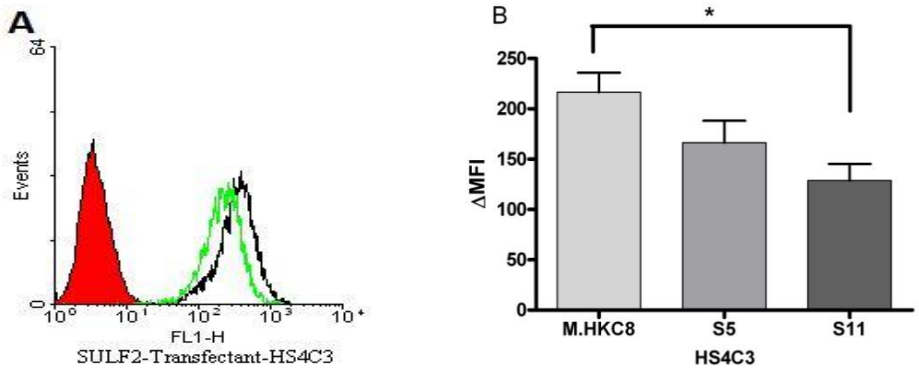

Figure 4.16. Phage display antibody HS4C3 binding to SULF2 transfectants. Mock and transfectants were grown in presence of G-418 until 80% confluent. Cells were detached, washed and incubated with HS4C3 in 1:10 at 4^{o}C for 60 minutes. Secondary anti VSV Cy3-labelled antibody was added (1:200) for additional 30 minutes. Cells were washed, resuspended in 2%FCS-PBS and investigated by flow cytometry. Data were analysed using WinMDI 2.9 and Prism 4 software. A, representative histogram of SULF2 transfectant (green) binding to HS4C3 compared to mock transfectant (black). B, Mean values of median fluorescence intensity (ΔMFI) measured by fluorescence flow cytometry, error bars represent the SEM (N=3, *: P<0.05).

4.4.3.2.3 Antibody binding to the RB4EA12 epitope

The RB4EA12 antibody targets sulphate groups at the N- and 6-O positions. An assay was designed to investigate the changes at sulphate groups following SULF2 overexpression. SULF2 transfectants showed a decreased ability to bind RB4EA12 compared to mock transfectants. This change was statistically significant (P<0.05), (Figure 4.17).

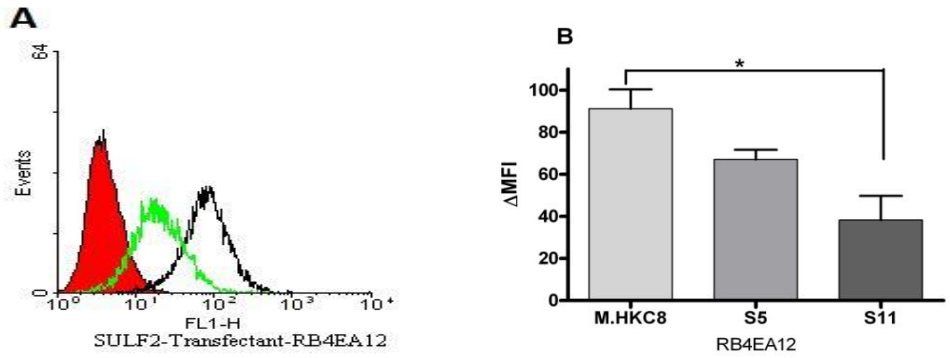

Figure 4.17. Phage display RB4EA12 binding to renal epithelial SULF2 transfectants. Mock and SULF2 transfectants were grown in 600µg/ml G-418 until 80% confluent. Cells were detached, washed and incubated with RB4EA12 in 1:10 at 4^{o}C for 60 minutes. Secondary anti VSV-Cy3 labeled antibody was added (1:200) for additional 30 minutes. Experiments were carried out in duplicates. A, representative histogram of SULF2 transfectant (green) binding to RB4EA12 compared to mock transfectant (black). B, Mean values of median fluorescence intensity (ΔMFI) measured by fluorescence flow cytometry. Data were analysed using WinMDI 2.9 and Prism 4 software. (N=2, *: P<0.05).

4.4.3.3 **Binding of FGF2**

To examine the effect of SULF2 overexpression on FGF2 binding, a series of experiments was carried out to assess the binding of FGF2. Two clones of SULF2 transfectants were used in the assay, one transfectant (S11) showed statistically significant results for binding biotinylated FGF2, whereas the S5 transfectant showed no significant results for FGF2 binding (data not shown). Reaction specificity was verified by using negative control consisting of biotinylated Soya bean protein and anti FGF2 blocking antibodies to block unspecific binding. The reaction was investigated by flow cytometry.

The SULF2 transfectants showed a 30% decreased binding of FGF2 compared to mock transfectants. This change was statistically significant (P<0.05), (Figure 4.18).

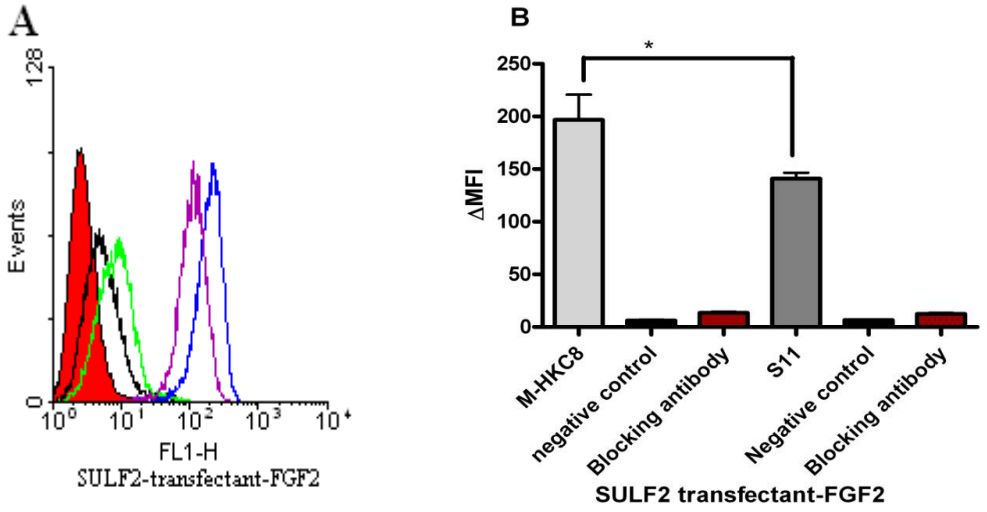

Figure 4.18. Binding of FGF2 to SULF2 transfectants. Mock-HKC8 and SULF2 transfectants (S-11) were incubated with FGF2 on ice for 60 minutes followed by Avidin-FITC substrate for 30 minutes. A, representative histogram of SULF2 transfectant (purple) binding to FGF2 compared to mock transfectant (blue), black line represents negative control (Soya bean protein) and green line represents anti-FGF2 containing tube whereas red histogram represents cells in incubated with secondary FITC-avidin substrate only. B, Mean values of median fluorescence intensity (ΔMFI) measured by fluorescence flow cytometry, error bars represent the SEM (N=3, *P<0.05).

4.4.3.4 **Binding of CCL5**

A series of experiments were carried out to investigating the binding of SULF2 transfectants to RANTES (CCL5). Biotinylated CCL5 was incubated with a defined number of cells, the reaction was visualised by adding Avidin-FITC substrate and the reaction was investigated by flow cytometry. Reaction specificity was verified by using Soya bean protein biotinylated to the same level as CCL5 as a negative control. Anti CCL5 blocking antibody was used as an additional control to confirm the binding specificity. Data analysis shows that SULF2 transfectants decreased the binding of CCL5 by about 40% compared to mock transfectants. This change is statistically significant (P<0.05), (Figure 4.19).

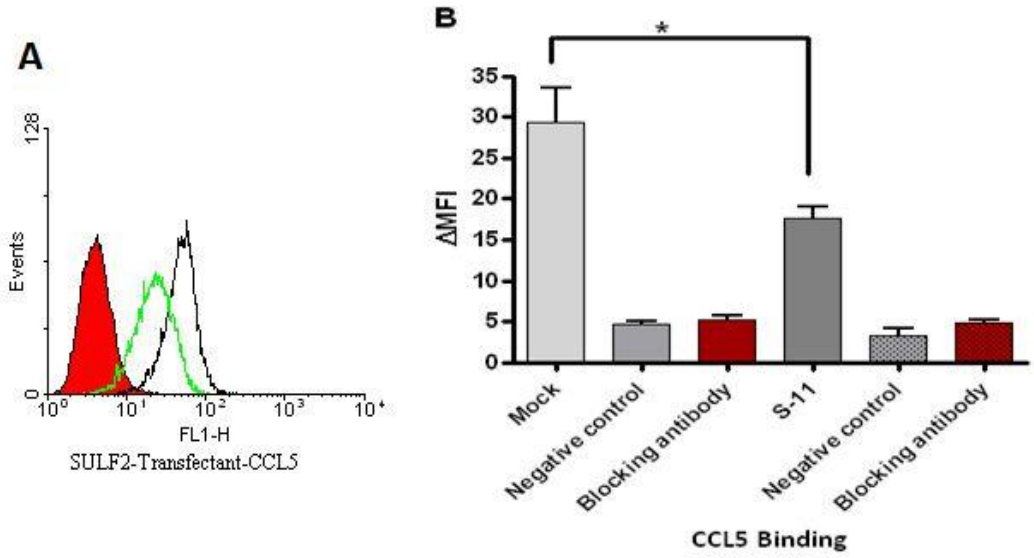

Figure 4.19. SULF2 transfectants binding to CCL5. Mock-HKC8 and SULF2 transfectants (S-11) were incubated with CCL5 at 4^{o}C for 60 minutes followed by Avidin-FITC for 30 minutes. These cells were investigated by immunofluorescence flow cytometry. Fluorescence activity was expressed as ΔMFI and data were analysed by WinMDI 2.9 and Prism 4 software. A, representative histogram of SULF2 transfectant (green) binding to CCL5 compared to mock transfectant (black) whereas red histogram represents cells with secondary substrate only. B, Mean values of median fluorescence intensity (ΔMFI) measured by fluorescence flow cytometry. Error bars represent the SEM, (N=3,*P<0.05).

4.4.4 Analysis of the structure of ^{35}S labelled HS

Heparan sulphate from mock and SULF2 transfected renal epithelial cells were analysed to examine structural changes following SULF2 transfection. Mock and SULF2 transfectants were incubated with ^{35}S as a source of sulphate for 24 hours. The cells were lysed and heparan sulphate was separated by ion-exchange as stated in (3.2.4). Samples were alkali treated and recovered GAGs were filtered by gel filtration. GAGs were treated with nitrous acid and reduced to deaminated products. Deaminated products were fractionated to disaccharides and further separated by anion-exchange HPLC.

SULF2 transfectants show that sulphatase removes 6-O sulphate groups from not only highly sulphated IdoA2S-GlcNS6S (ISMS) but also from mono sulphated disaccharides of GlcA-GlcNS6S (GMS) and IdoA-GlcNS6S (IMS). In contrast, SULF2 transfectants show remarkable increase (more than double) in IdoA2S-

GlcNS (ISM) concentration compared to mock transfectants (P<0.001), (Figure 4.20).

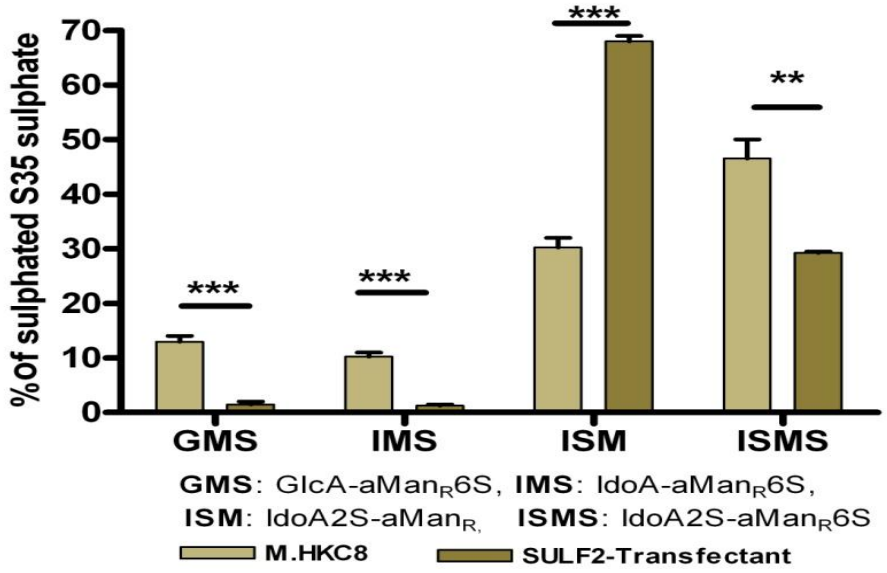

Figure 4.20. HS disaccharides analysis of SULF2 transfectants. Mock and SULF2 transfectants were incubated with ^{35}S 200µCi/ml for 24 hours. Cells were lysed and GAGs were isolated using DEAE Sephacel columns. Samples were treated with nitrous acid and deaminated products were fractionated by gel chromatography on Sephadex G-15. GAGs were separated using anion-exchange HPLC followed by running and eluting on Partisil 10 SAX columns. (N=2, **: P<0.01,*: P<0.05)

Sulphation changes following SULF2 transfection show that HS undergoes downregulation of sulphation at the N-position by about 10% compared to mock transfectants. Sulphate groups at the 6-O position were also downregulated by about 25% in SULF2 transfectants compared to mock transfectants (P<0.01). However, sulphation at the 2-O position was upregulated by two-fold in SULF2 transfectants compared to mock transfectants (Figure 4.21).

Data analysis shows that 6-O containing disaccharides were decreased by about 50% in SULF2 transfectants compared to mock transfectants. 2-O containing disaccharides were upregulated by 25% compared to mock transfectants (Figure 4.21).

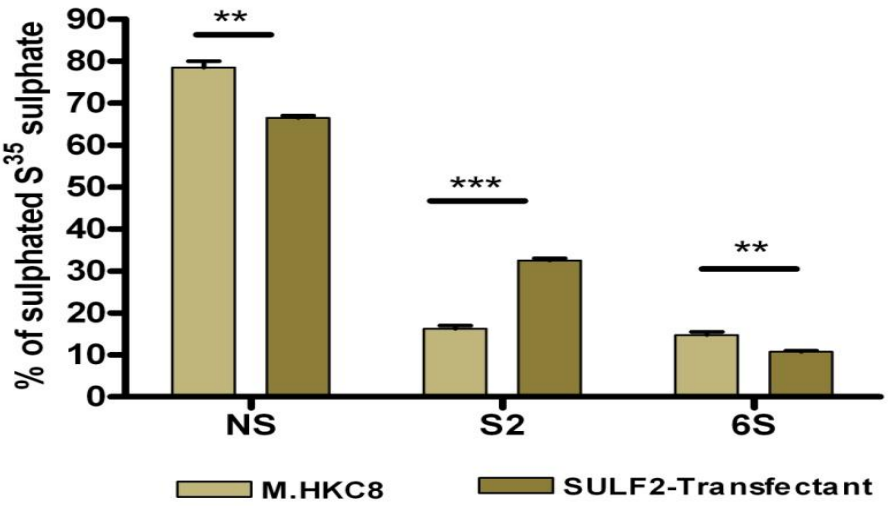

Figure 4.21. Sulphate group changes in SULF2 transfectants. Samples were isolated from ^{35}S labelled HS chains from solubilized cells from mock and SULF2 transfectants. GAGs were depolymerized by low pH nitrous acid treatment followed by reduction with NaBH4. Fractions were separated on Partisil 10-SAX column alongside with standard control. (N=2, *P<0.05).

4.4.5 Proliferation of the SULF-2 transfectants

As stated in 3.3.11, sulphate groups at the 6-O position of HS have been implicated in regulation of the MAP kinase pathway that affects the proliferation of epithelial cells. In this study, renal epithelial cells overexpressing SULF2 and mock transfectants were examined for proliferation by using a non-radioactive colorimetric proliferation assay. As shown in figure 4.22, cells with SULF2 overexpression have lower proliferation after 72 and 96 hours compared to mock transfectants. Despite being small, this difference was found statistically significant (P<0.01). Incubation of these cells with FGF2 enhanced the proliferation of both SULF2 and mock transfectants (Figure 4.22). In all cases, an equal number of cells was seeded into the assay wells at time 0.

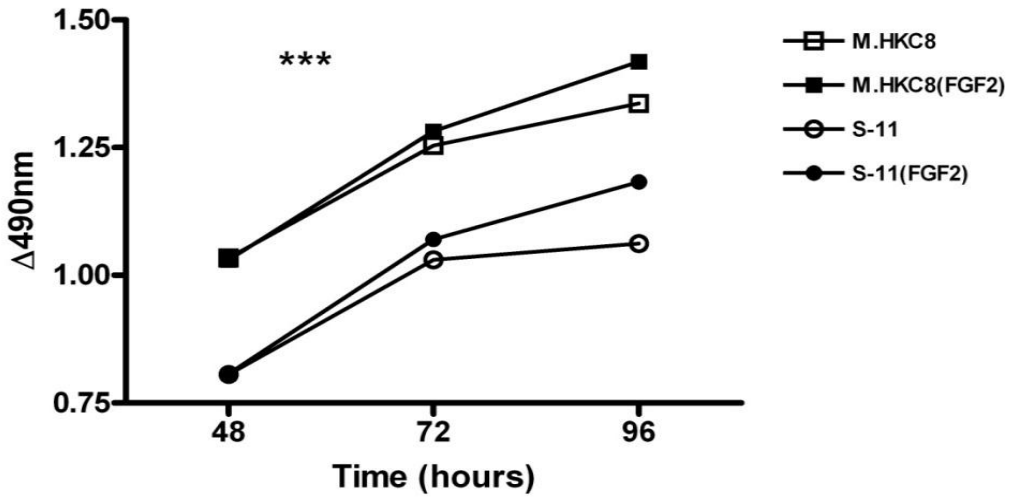

Figure 4.22. Representative proliferation assay for SULF2 transfectants. Mock-HKC8 and SULF2 transfectants were seeded in 96 well plates in triplicates with 0.05%FCS and incubated for 24, 48, 72 and 96 hours. The same mock-HKC8 and SULF2 transfectants were incubated with FGF2 at 10ng/ml. Experiments were carried out by removing the medium and adding fresh medium with tetrazolium compound (MTS/PMS) and the plate was read at 490nm after 4 hours of incubation at 37^{o}C. (N=3, P<0.001).

4.4.6 SULF2 transfectants and ERK activation

Sulphate groups at the 6-O position of HS have been implicated in FGF2-mediated activation of the ERK signaling pathway. FGF2 increases phosphorylation of ERK into pERK. In the previous chapter (3.3.11) it was shown that HS6ST1 transfectants increase the phosphorylation of ERK1,2. To further examine the role of 6-O sulphation on the ERK pathway, a series of experiments was carried out by Western blotting using a specific pERK antibody. Cells were exposed to recombinant FGF2 as a stimulator of pERK activation for several time points. As shown in figure 4.23, SULF2 transfectants demonstrate significantly (P<0.05) reduced pERK activation by about 30% compared to mock transfectants. Addition of FGF2 for 3,5 and 10 minutes increases the pERK activation in both SULF2 and mock transfectants but there was a difference of approximately 30% between mock and SULF2 transfectants. For equal loading, α-tubulin was used as a house-keeping protein.

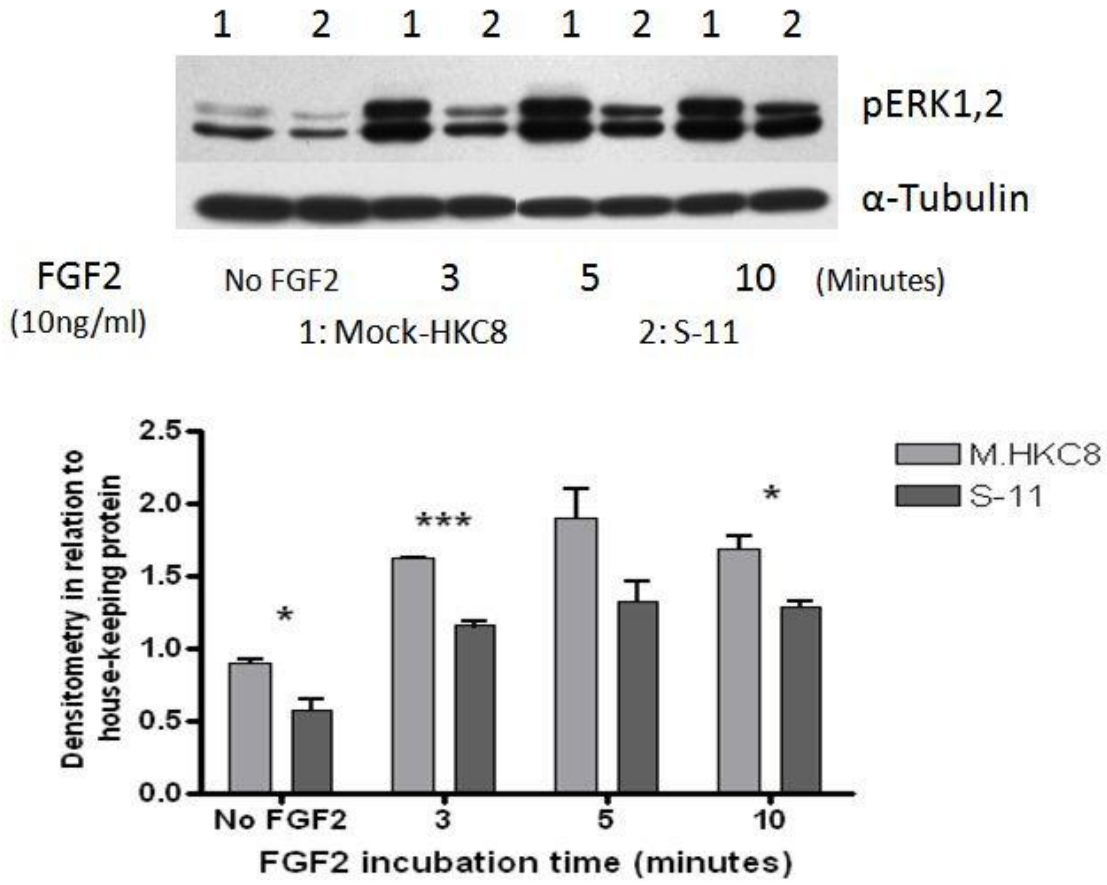

Figure 4.23. Western blotting of pERK1,2 for SULF2 transfectants in presence of FGF2. Mock and SULF2 transfectants (S-11) were seeded in 6 well plates in 0.05% FCS-DMEM-F12. Cells were then incubated with FGF2 at 10ng/ml for 3, 5 and 10 minutes. Medium was removed and lysis buffer was added. Lysates were run on 10% SDS-PAGE and transferred to PVDF membrane. Protein bands were probed by anti pERK1, 2 at 1:1000 overnight at 4^{o}C followed by HRP-secondary antibody. The same membrane was blotted for anti-tubulin-α. Bands were visualized by ECL substrate. Densitometry analyses were performed using Image-J software. (N=2, $p<0.05$).

4.5 Discussion

Heparan sulphate undergoes a process of degradation and desulphation due to the effect of heparanase and sulphatase enzymes. This process allows the HS to change its biological activities in accordance with novel roles to be played. The HS sulphatase activity is influenced by proinflammatory cytokines during inflammation and chronic diseases. Stimulation of specific cell lines with different cytokines mimics the environment of inflammation. Building on stimulation results, stable transfectants of endosulphatase gene were generated in order to examine definite biological activities. These transfectants provide a good model to examine the effect of endosulphatase on HS structure and the potential for interaction between HS and growth factors.

4.5.1 Observation of gene expression following cytokine stimulation

4.5.1.1 Heparanase (HPSE)

Endothelial and epithelial cells were stimulated by several cytokines which are upregulated during inflammation. The stimulated cells were analyzed using qPCR for the expression of specific genes encoding heparanase and sulphate enzymes. These genes were investigated on mRNA level using specific probes and qPCR. This study shows that the heparanase expression is significantly downregulated following stimulation by TGF-β and to a lesser extent by PMA. This result contradicts with a former finding which shows that HPSE expression is upregulated in fibrotic liver disease (6-fold) (Tatrai *et al.*, 2010). The current result also contradicts with previous research which showed that cytokines such as TNF-α or IL-1β could increase HPSE secretion by endothelial cells (Chen *et al.*, 2004).

HPSE has been shown to play significant role in FGF2-induced EMT in association with syndecan accumulation and cleavage, thus the downregulation of the gene observed after stimulation by TGF-β might suggest an autocrine feedback mechanism of HPSE in the regulation of EMT (Masola *et al.*, 2012). However, further investigation including measurement of syndecan1 expression will be required for a better understanding of the consequences of HPSE regulation.

4.5.1.2 **SULF1 and SULF2**

Epithelial and endothelial cells were stimulated by several cytokines in order to examine changes in sulphatase gene expression. For the SULF1 gene, different levels of expression were found in endothelial and epithelial cells following cytokine stimulation. The current study shows that SULF1 expression in epithelial cells was significantly downregulated following stimulation by IFN-γ or PMA whereas, in endothelial cells, it was significantly increased following the TGF-β stimulation (2.5 fold), (Figures 4.6, 4.7). This result is consistent with previously reported results showing that stimulation of fibroblasts with TGF-β increased SULF1 expression *in vitro* and *in vivo* but with no significant changes in SULF2 expression (Yue *et al.*, 2008). Accordingly, SULF1 expression was increased in chronic liver cirrhosis (6 fold) (Tatrai *et al.*, 2010).

Changes in HS sulphation are associated with the level of sulphotransferase and sulphatase enzymes (Tatrai *et al.*, 2010). HS sulphation undergoes various modulations following stimulation with pro-inflammatory cytokines. This study shows that SULF2 expression was dramatically increased (5 fold) following stimulation of renal epithelial cells with TGF-β. This increase is expected to affect the role of HS in chronic inflammation and fibrotic disease. Modulation of HS sulphation has been reported in inflammation and following cytokine stimulation. For example, stimulation of glomerular endothelial cells with TNF-α or IL-1β has produced changes in N- and 6-O sulphation (Rops *et al.*, 2008). Furthermore, stimulation of brain glia with TGF-β/TNF-α has resulted in upregulation of 2S sulphation and HS syndecan-1 synthesis (Properzi *et al.*, 2008). An increase in SULF2 gene expression was also reported in carcinoma cells in human breast cancer (Morimoto-Tomita *et al.*, 2005).

In order to further investigate the role of SULF2, stable transfectants of SULF2 in renal epithelial cells were generated. These transfectants were grown under antibiotic selection alongside mock transfectants. Fifteen clones were selected and two clones with the highest levels of SULF2 expression (S11 and S5) were used for

further investigations. These clones were examined first for SULF2 expression on mRNA level by qPCR.

4.5.2 Observation of changes in HS epitope expression

Changes in the structure of HS produced by SULF2 overexpression were investigated by examining the interaction between SULF2 transfectants and the 10E4 monoclonal antibody by immunofluorescence and flow cytometry. This study shows that SULF2 transfectants had increased expression of the 10E4 epitope by immunofluorescence microscopy but not by flow cytometry. The HS-10E4 epitope includes a tetrasaccharide domain of N-sulphated and N-acetylated glucosamine (GlcA-GlcNS-GlcA-GlcNAc), (David *et al.*, 1992; Leteux *et al.*, 2001). The binding to 10E4 antibody is therefore influenced by N-sulphation, as this constitutes an essential component of the HS-10E4 epitope. The increased expression of 10E4 epitope shown by immunofluorescence might be distributed between changes in extracellular HS compared to cell surface which is mostly affected following cell dissociation in the flow cytometry procedure. It has been shown that a reduction in N-sulphation is accompanied by a reduction in 10E4 antibody binding (Pankonin *et al.*, 2005) and an increase in N-sulphation accompanied by increased 10E4 antibody binding (unpublished data by Dr. Spielhofer 2010), (van den Born *et al.*, 2005). However, a previously published work showed that SULF1 overexpression decreased the 10E4 epitopes in 3T3 cells (Ai *et al.*, 2003b).

The changes in HS sulphation following the SULF2 overexpression were further examined using phage display anti-HS antibodies. These antibodies are widely used due to their interaction with specific sulphated saccharide domains in the HS structure. The current study showed that SULF2 transfection significantly reduced HS3A8 antibody binding. This antibody targets an HS epitope containing trisulphated disaccharides (IdoA2S-GlcNS6S), (Dennissen *et al.*, 2002). The reduction in antibody binding might be attributed to downregulation of the 6-S component in the binding epitope. For example, TGF-β induced overexpression of SULF1caused different changes in HS sulphation, including a reduction in the 6-O

sulphate and increase in the N-S and 2-S groups in the human lung fibroblasts (Yue *et al.*, 2008).

To investigate the changes in HS in more detail, the interaction between SULF2 transfectant cells and the HS4C3 antibody was examined. This antibody targets trisulphated disaccharides with Iduronic acid and Glucuronic acid, i.e. GlcNS6S-GlcA-GlcNS3S6S-IdoA2S-GlcNS3S6S (van Kuppevelt *et al.*, 1998). In the previous chapter, it was shown that cells overexpressing HS6ST1 significantly upregulated the HS4C3 binding epitope. Therefore it is of great importance to determine whether 6-O desulphation has the opposite effect. SULF2 transfectants showed a small but significant decrease in HS4C3 binding ability. It has been previously reported that the binding of HS4C3 is correlated with FGF2 binding (Lensen *et al.*, 2005). Thus, the downregulation of HS4C3 binding observed with SULF2 transfectants in the current study suggests that reduction of 6-O sulphation might inhibit the binding to FGF2.

Additionally, SULF2 transfectants showed increased expression of epitopes which interact with 10E4, whereas HS3A8 and HS4C3 epitopes were reduced. This result is consistent with previously published literature showing that increased 10E4 binding was accompanied by reduced binding to HS3A8 and HS4C3 in glomerular endothelial cells following stimulation by TNF-α (Rops *et al.*, 2008). The current study also showed that SULF2 transfection was associated with a marked reduction in expression of the RB4EA12 epitope. This reduction is mainly attributed to the 6-O content of the RB4EA12 binding epitope, which also contains NS or NAc residues (GlcNS6S/GlcNAc6S) (Dennissen *et al.*, 2002; Lensen *et al.*, 2005).

4.5.3 Physiological changes after SULF2 transfection

4.5.3.1 **FGF2 binding**

Having generated stable SULF2 transfectants, the physiological role of HS was examined by investigating the binding of FGF2. SULF2 transfected cells showed a significant reduction in their potential to bind FGF2 compared to mock transfectants. Earlier results have shown that although 6-O sulphate is not essential for FGF2 binding, this group is crucial for FGF2-mediated receptor signalling and mitogenic activity (Guimond *et al.*, 1993; Dai *et al.*, 2005). The current study

showed that SULF2 overexpression downregulated FGF2-mediated signalling via the ERK pathway as well as reducing cell proliferation. This result is consistent with many previous studies which show a decrease in ERK activation following sulphatase overexpression (Dai *et al.*, 2005; Kamimura *et al.*, 2006). Several researchers have found that SULF1 (but not SULF2) has the ability to reduce the intracellular signalling of many growth factors, including FGF2 (Lai *et al.*, 2003; Lai *et al.*, 2004a; Lai *et al.*, 2004b; Wang *et al.*, 2004). However, it has been reported that SULF2 transfectants can show increased FGF2 binding and signalling in human hepatocellular carcinoma cells (Lai *et al.*, 2008a).

4.5.3.2 **CCL5 presentation**

The current study shows that CCL5 presentation was downregulated following SULF2 overexpression. Unpublished work from this group showed that overexpression of NDST1 increased both CCL5 presentation and binding of the 10E4 antibody (Dr. Spielhofer 2010, PhD thesis). The specific site on HS that binds CCL5 is poorly defined (Vives *et al.*, 2002). However, N- and O-sulphate groups seem to be involved in the binding motif (Shaw *et al.*, 2004; Yamaguchi *et al.*, 2006). This suggests that changes in sulphation following SULF2 overexpression will have a negative effect on CCL5 presentation. An earlier study from this group showed that the presentation of CCL5 by endothelial cells is increased by increased N-sulphation of HS (Carter *et al.*, 2003).

4.5.4 Examination of HS structure

Overexpression of the 6-O endosulphatase, SULF2 has biological effects on the interaction between HS and FGF2 and CCL5, as well as antibody binding to HS. This suggests that these changes in biological activity are accompanied with changes in HS structure. To address this issue HS structure was examined by compositional analysis of disaccharides following deaminative cleavage (aManR) of ^{35}S labelled HS. This work was performed in collaboration with Professor Marion Kusche-Gullberg (Norway).

This study shows that SULF2 overexpression produced significant changes in HS structure, including disaccharide concentration, domain distribution and sulphation pattern. The disaccharide analysis showed a noticeable downregulation of residues

such as GlcA-GlcANS6S (GMS) and IdoA-GlcANS6S (IMS) and the trisulphated disaccharide Ido2S-GlcNS6S (ISMS). By contrast, SULF2 overexpression increased the concentration of IdoA2S-GlcNS (ISM). It is expected that the SULF enzymes target predominantly the HS-trisulphated disaccharide as a favorite substrate (Ai *et al.*, 2006b). Accordingly, the upregulation of ISM (predominant in the NA/NS domain) is consistent with a previously report of overexpression of SULF2 (in 293T cells) *in vitro* (Ai *et al.*, 2006b). This result is in agreement with previously reported changes in the distribution of HS domains following 6-O desulphation, which include greater expression of NA/NS domains than NS domains (Lamanna *et al.*, 2007). The resultant HS domain distribution might explain the changes in HS epitopes and physiological roles observed by interaction with phage display antibodies and FGF2 or CCL5 respectively.

In the current study, the mode of HS sulphation following SULF2 overexpression showed a significant reduction in 6-O and N-sulphates but an increase in 2-O sulphate groups. Similarly, an increase in 2-O sulphation was reported in a previous study with SULF overexpression (Ai *et al.*, 2006b). However, this was not the case in SULF1 overexpression in *Drosophila* where no changes in 2-O sulphation were observed after 6-O desulphation (Kamimura *et al.*, 2006). Interestingly, SULF1 and SULF2 knockout mice have shown that these enzymes can modulate the expression of sulphate groups at the N- and 2-O positions in cell surface and extracellular HS (Lamanna *et al.*, 2008). These non-substrate changes might explain a potential compensatory effect following SULF2 over-expression. However, following TGF-β induced overexpression of SULF1, no changes were found in the N- and 2-O sulphation alongside the 6-O desulphation (Yue *et al.*, 2008). The level of overexpression might be responsible for this variance; in our study the increase in SULF2 gene expression following transfection is about 250-fold.

Although the total decrease in 6-O sulphate concentration was not remarkable, it was accompanied with significant changes in FGF2 and CCL5 binding activities. This can be justified by accompanying changes with additional sulphate positions including N- and 2-O positions. Furthermore, SULF2 overexpression was accompanied with low concentration of GlcA-Glc6S and IdoA-Glc6S which might

explain the reduced binding to FGF2 and CCL5. This result is in agreement with previously shown changes in FGF2 biological activity following modulations of HS sulphation (Huynh *et al.*, 2012).

Taken together, these findings show that the SULF2 enzyme has an important role in regulation of the sulphation of HS which is accompanied by changes in physiological function by modification of the interaction with FGF2 and CCL5. The SULF2 transfectants also showed reduced proliferation and ERK activation compared to mock transfectants. Analysis of the structure of HS isolated from SULF2 overexpressing cells showed decreased expression of substrate disaccharides such as GlcA-GlcANS6S (GMS), IdoA-GlcANS6S (IMS) and Ido2S-GlcNS6S (ISMS) along with increased IdoA2S-GlcNS (ISM).

Chapter Five

5 HS Changes in UUO Mouse Model

5.1 Introduction

Chronic rejection has been the major cause for loss of transplanted organs. Heparan sulphate has a wide range of interaction abilities with proteins, including cytokines and growth factors which are involved in the etiology of chronic fibrosis. Earlier unpublished work in our group has shown that heparan sulphate is upregulated in chronic rejection as well as in acute rejection compared to normal kidney. Phage display antibodies were used in the two previous chapters in order to show modulation of HS sulphation after HS6ST1 or SULF2 overexpression. In this chapter we followed up with an *in vivo* model of renal fibrosis to shed more light on changes in heparan sulphate sulphation. This was performed by generating mice with a unilateral ureteral obstruction (UUO) of kidney. Expression of specific HS epitopes in the UUO kidney will provide a better understanding of the modulations of HS structure during fibrosis.

5.1.1 UUO kidney and chronic rejection

The UUO kidney constitutes an *in vivo* model of experimental renal injury that leads to renal disease and fibrosis. Mouse UUO constitutes an important model for examining renal fibrosis as well as experimental therapy (Chen *et al.*, 2007).

A series of events takes place 24 hours after UUO including reduced renal blood flow and glomerular filtration rate. These changes are generally followed by hydronephrosis, interstitial inflammatory infiltration and tubular cell death (Vaughan *et al.*, 2004). Further changes include increased interstitial myofibroblasts (Hewitson *et al.*, 2001), tubular atrophy (TA), (Gobe and Axelsen, 1987), expansion of renal interstitium, increased ECM proteins and interstitial fibrosis (IF), (Eddy, 1996; Klahr and Morrissey, 2002). Additional structural changes are expected to take place such as tubular dilation (Sunami *et al.*, 2004). The UUO kidney in rabbits shows interstitial deposition of collagen I, III and IV, fibronectin and, interestingly, increased expression of HSPG (Sharma *et al.*, 1993).

Several mechanisms are involved in the etiology and development of IF in the UUO kidney. Macrophage infiltration leads to proliferation and activation of fibroblasts in addition to production of cytokines leading to tubular cell death (apoptosis), (Misseri *et al.*, 2005). The second mechanism includes tubular cell

death by apoptosis and necrosis which may lead to TA. This can be induced by factors including ischemia, hypoxia, oxidative stress and tubular dilation (Chevalier *et al.*, 2009). For example, oxidative radicals have a toxic effect on tubular epithelial cells which may cause apoptosis (Schaaf *et al.*, 2002). Furthermore, oxidative radicals were shown to stimulate the expression of TGF-β1 and the production of ECM proteins during IF (Yuan *et al.*, 2003). The third mechanism is the production of IF following activation of the EMT process. Renal epithelial cells become motile fibroblasts and migrate into the tubular interstitium where they produce extracellular components (Iwano *et al.*, 2002).

5.1.2 Fibrosis markers

Renal fibrosis is characterized by several pathological changes, as stated above, as well as increased expression of significant markers. One of the key markers is the expression of fibroblast specific protein FSP1 (S100-A4). Another marker is increased expression of α-SMA, which constitutes a key marker of myofibroblasts in both human renal IF and UUO models (Essawy *et al.*, 1997; Roberts *et al.*, 1997). Furthermore, accumulation of ECM proteins including fibronectin and collagen (types I, III, IV and V) is considered a good indicator of the fibrogenesis process (Okada *et al.*, 2000). In some cases the loss of expression is considered an indicator of potential changes during fibrosis. For example, the loss of E-cadherin was found in TGF-β induced EMT which indicated a novel phenotype of the transformed cells (Zeisberg *et al.*, 2003). It seems clear that murine UUO provides the best model available for analysis of changes in the sulphation of HS during the development of a renal pathology analogous to the tubular atrophy with IF that is seen during chronic renal allograft rejection.

5.2 Aims

The experiments described in this chapter examine changes in HS sulphation following the induction of murine UUO. The following topics will be addressed:

- Induction of the murine UUO model.
- Immunocytochemical study of post UUO renal fibrosis.
- Immunocytochemical study of changes in the expression of sulphation-dependent epitopes in the mRNA expression levels of HS using specific antibodies.
- Quantitative examination of changes in the expression of HS modifying enzyme (NDST1, SULF1, SULF2 and HS6ST1) in UUO kidney.

5.3 Specific materials and methods

5.3.1 Mice maintenance

All animal handling was performed in accordance with the guidelines of the ethical committee of Newcastle University and Home Office Project License. Wild type C57BL/6N male inbred mice (C57BL/6N, Supplier CRUK) were housed for one week prior to use (age 8-10 weeks). Mice received water and standard mouse chow. These mice were subjected to an abdominal incision where the left ureter was completely double ligated under general anesthesia with isoflurane and oxygen (Figure 5.1). These animals were killed after 7 and 14 days of obstruction and both kidneys were removed. Surgery was performed thankfully by Christopher Fox. The obstructed kidney was referred to as UUO kidney whereas contralateral right kidney was referred as the wild-type kidney. For RNA isolation, one fifth of the kidney was excised and immersed immediately in liquid nitrogen and stored later at -80^{o}C.

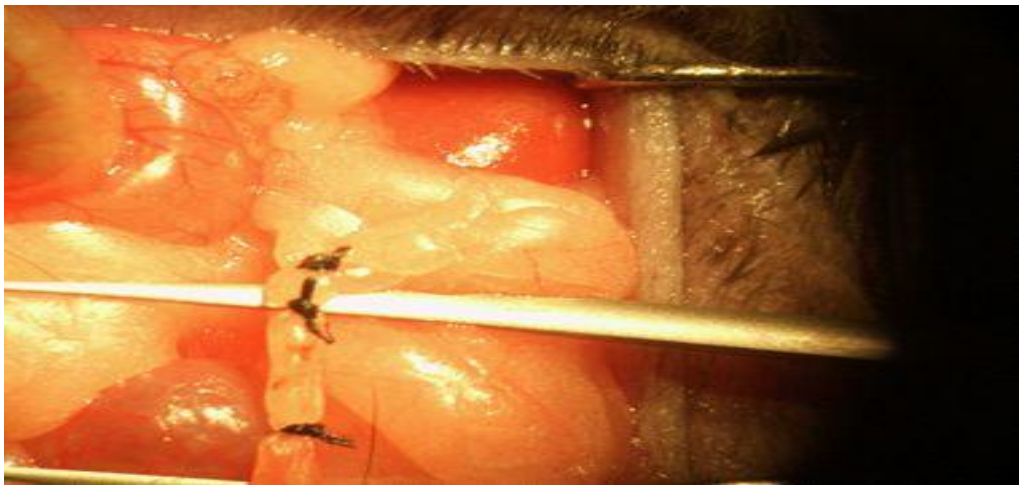

Figure 5.1. Unilateral ureteral obstruction mice kidney. The left ureter was double ligated and cut to generate UUO kidney. Mice were killed after 7 or 14 days and both the kidneys were removed.

For paraffin embedded sections, kidney was sectioned and immersed in Formalin Solution 10% Neutral Buffer (Sigma-Aldrich) for 24 hours before transfer to 70% ethanol. Sections were then dehydrated, embedded in paraffin blocks and stored at room temperature. For frozen sections, kidney sections were immersed

immediately in cold isopentane for few minutes, then in liquid nitrogen and later stored at -80^{o}C.

5.3.2 RNA extraction from mouse kidney

Tissues taken from wild type and UUO kidney were stored in -80^{o}C for RNA isolation. For more productivity and purity, the SV total RNA isolation system (Promega) was used. This system incorporates a DNase treatment step that reduces genomic DNA contamination. This is necessary when using non exon-boundary spanning qPCR primer probes. A ribonuclease free environment was created by cleaning all equipment, racks and surfaces with RNase-Zap (Sigma-Aldrich), diethylpyrocarbonate (DEPC) treated water and alcohol. Tubes were autoclaved in advance and filter tips were used. β-mercaptoethanol (BME) was added to the lysis buffer (Promega) as recommended in the manufacturer instructions.

Kidney tissues were weighed under cold condition and the protocol for weights less that 30mg was followed. This protocol is used for processing small tissue samples. Tissue was mixed with BME-added lysis buffer (175µl) in a clean glass mortar (pre-incubated on ice) and processed with a pestle till completely homogenized. Lysates were transferred to a clean tube, mixed with dilution buffer and incubated on a heat block at 70^{o}C for 3 minutes. The tubes were then centrifuged at 13000g for 10 minutes and supernatants were taken out, mixed with 95% ethanol and transferred to a spin column assembly. The spin columns were centrifuged at 13000g for one minute, ethanol-added RNA Wash Solution was added and the tubes were centrifuged for further 1 minute. Each tube was then incubated with fresh DNase incubation mix (40 µl Yellow Core Buffer, 40 µl 0.09M $MnCl_2$ and 5 µl of DNase enzyme) for 15 minutes at room temperature. The reaction was stopped by adding 200 µl of DNase Stop Solution. Tubes were then washed with RNA Wash Solution and the RNA was eluted by adding 100 µl of nuclease free water. Tubes were centrifuged and the RNA was quantitated, electrophoresed at 0.7% agarose gel and stored at -80 ^{o}C (Figure 5.2).

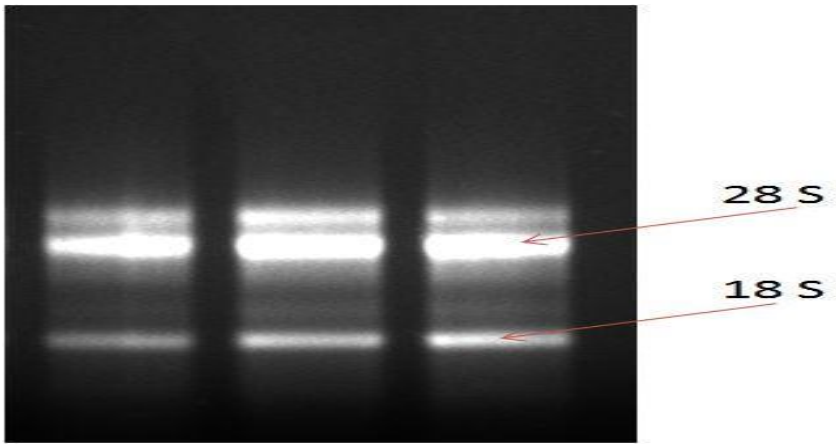

Figure 5.2. Representative gel photograph showing RNA extracted from frozen UUO kidney. Three samples from three animal UUO kidneys were extracted and separated on 0.7% agarose gel.

5.3.3 Frozen sections

Frozen sections from wild type and UUO kidneys were cut into 5 µm thick-cross sections using cryostat at -20^{o}C. Frozen sections were stored at -20^{o}C until needed. These sections were fixed with cold acetone at -20^{o}C for 10 minutes and left for air-dry at room temperature. Sections were then blocked with 2% BSA-PBS for one hour and incubated with phage display antibody at 1:10 overnight at 4^{o}C (generous gift from Prof. van Kuppevelt). Slides were then washed with TBS and incubated with anti-VSV Cy3-conjugated antibody (Sigma-Aldrich). Nuclei were visualized by adding 4-6 diamine-2 phenylindol (DAPI) at 2 µg/ml final concentration (Sigma-Aldrich) and the slides were mounted in fluorescence mounting media (DAKO). Slides were investigated using immunofluorescence microscopy. Slides were prepared from five different animals with a UUO kidney. For each animal, at least three slides were stained and each slide was investigated by quantifying five equal squares $(2.5uM)^2$ from tubular and interstitial spaces. Mean fluorescence intensity was expressed and compared between UUO kidney and normal kidney sections. Slides were quantified using Image-J software.

5.3.4 Primer probes

Primer probes from TaqMan gene expression assay (Applied Biosystem) with FAM dye and TAMRA quencher were used for RNA analysis. All probes except for HS6ST1 were exon boundary spanning preventing detection of genomic DNA.

The primer for HS6ST1 was not exon boundary spanning and could detect genomic DNA. RNA samples were treated with DNase to increase specificity by removing any possible DNA contamination which might be detected by primer probes-s1. Pre-designed primer probes were purchased from Applied Biosystem:

HPRT1 (Mm00446968-m1); m1 indicates that the probe spans an exon junction and it does not detect genomic DNA.

HS6ST1 (Mm 01229698-s1); s1 indicates that the probe is derived from a genomic DNA sequence.

SULF1 (Mm 00552283-m1)

SULF2 (Mm 1248026-m1)

NDST1 (Mm 00447005-m1)

5.3.5 RT-PCR validity test

Hypoxanthine phosphoribosyltransferase 1 (HPRT1) was used as a house keeping gene in mice qPCR experiments. Validity test was performed for investigating the qPCR condition and amplification efficiency. Primers for HPRT1, SULF1, SULF2 and HS6ST1 were investigated. Validity values were calculated as stated before (4.3.3.1) and efficiency values were 106, 103 and 104.4% respectively (Figure 5.3).

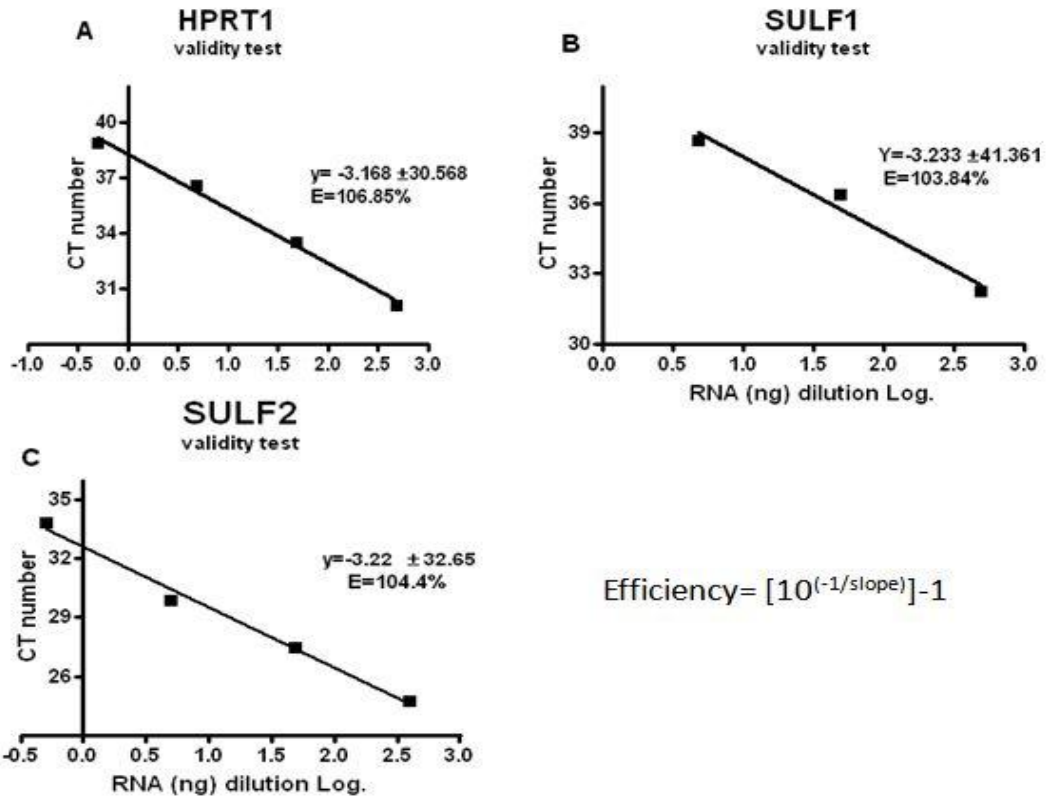

Figure 5.3. Efficiency of qPCR reaction for murine HPRT1,SULF1and SULF2 genes. Real time PCR experiment included cDNA template in serial dilutions in triplicates. Values at X axis represent the logarithm of the RNA concentration (ng). cDNA was synthesized in 5 µg RNA. A, Represents efficiency for house-keeping gene HPRT1. B, represents efficiency for SULF1 gene whereas C represents efficiency for SULF2 amplification. (N=2)

5.3.6 Haematoxylin and Eosin staining (H&E)

Frozen sections were fixed with acetone at -20^{o}C for 10 minutes and left to air-dry at room temperature. Sections were then immersed in haematoxylin for 3 minutes at room temperature, followed by washing with tap water. Slides were dipped in Scott's water for 30 seconds and washed with tap water. In the next step, slides were immersed in eosin for one minute and washed with tap water. Slides were then dehydrated in gradients of alcohol (50%, 75%, 95% and 100%), cleared with xylene, mounted with DPX and left to dry.

5.3.7 Immunohistochemistry

Frozen sections were stained for collagen-1 (Rabbit anti-mouse, Millipore) by immunohistochemistry. Sections were fixed with acetone at -20^{o}C for 10 minutes

and left for air-dry at room temperature before incubation with 0.3 % hydrogen peroxide in PBS-NaN_3 for 10 minutes at room temperature. Sections were then washed in TBS and blocked by Avidin for 15 minutes followed by Biotin for 15 minutes (Vector Blocking Kit). The slides were washed by TBS and blocked with 20% normal swine serum (NSS) for one hour at room temperature. The primary antibody (Millipore) in NSS at 1:150 was added and the sections incubated overnight at 4^{o}C. After washing 3 times in TBS, biotinylated secondary antibody (Goat anti rabbit) in NSS at 1:200 was added and incubated at room temperature for one hour. The slides were then washed in TBS and incubated in ABC (Avidin Biotinylated HRP Complex) for 30 minutes (ABC Vector prepared 30 minutes in advance). During incubation, 2.5 ml of 3, 3-diaminobenzidine (DAB) solution was prepared, mixed with 2 µl H_2O_2 and left in the dark. Slides were covered with DAB solution for at least 2 minutes until they turned brown and washed with tap water. Slides were then counterstained with Mayer's haematoxylin for 5 minutes and "blued" for few seconds in Scott's water. In the final step slides were dehydrated in gradients of alcohol (50%, 75%, 95% and 100%), cleared with xylene, mounted with DPX and left to dry. Images were taken with Leica LCM microscope and data were analyzed with Image-J software.

5.3.8 Mouse on mouse (M.O.M) staining

A mouse on mouse (M.O.M) kit (Vector) was used when staining murine tissues with murine antibodies as anti-mouse secondary antibodies do not distinguish between the mouse primary antibody and the endogenous mouse immunoglobulin (Ig). This results in a high background staining which affects the specific binding. This problem was solved by using Avidin-Biotin blocking agents in the M.O.M protocol. In brief, frozen sections were fixed with cold acetone at -20^{o}C for 10 minutes and left to air-dry at room temperature. Slides were blocked in excess Avidin for 15 minutes followed by Biotin for a further 15 minutes at room temperature. The slides were incubated for one hour in mouse immunoglobulin blocking reagent at room temperature. The slides were then washed with TBS and incubated in primary antibody in M.O.M diluent (Protein concentrate in TBS) overnight at 4^{o}C. After washing, the slides were incubated with biotinylated

secondary anti-mouse IgG reagent for 10 minutes at room temperature. Then the sections were washed and fluorescein Avidin DCS was applied for 5 minutes followed by TBS washing. Finally the slides were incubated with DAPI and mounted with Vectashield mounting medium (Dako).

5.3.8.1 **Data analysis**

Data were statistically analyzed by using Student's unpaired T-test for data with a normal distribution. ANOVA for comparing three or more independent groups with Tukeys and Bonferroni post tests was also used. Software including Windows Excel, Prism 4, Image-J and REST2008 were used. P values < 0.05 were considered significant.

5.4 Results

5.4.1 Haematoxylin and eosin staining (H&E)

Haematoxylin stains basophilic structures a deep purple or blue colour. Eosin is an acidic stain of a red colour which stains acidophilic structures in the cytoplasm a red or pink colour. Frozen sections were stained by H&E to show the pathological changes after UUO. Dilation of the tubule's lumen with increase in ECM spaces was noticed in UUO sections compared to intact kidney sections (Figure 5.4).

5.4.2 Fibrosis markers

Fibrosis is a major consequence of UUO kidney. Several fibrosis markers are upregulated following UUO, including fibronectin, collagens, α-SMA and increased depositions of ECM proteins (Sunami *et al.*, 2004). In order to verify the fibrosis in kidney after 7 days of UUO incidence, the frozen sections were stained with antibodies against collagen-1 and α-SMA.

5.4.2.1 Staining collagen-1

Chronic fibrosis is usually accompanied by pathological changes including epithelial cell proliferation, EMT and deposition of collagen in extracellular spaces (Misseri *et al.*, 2004). Collagen I deposition in the interstitial space is considered a diagnostic marker for tissue fibrosis. Collagen I was observed in the basement membrane and interstitial spaces.

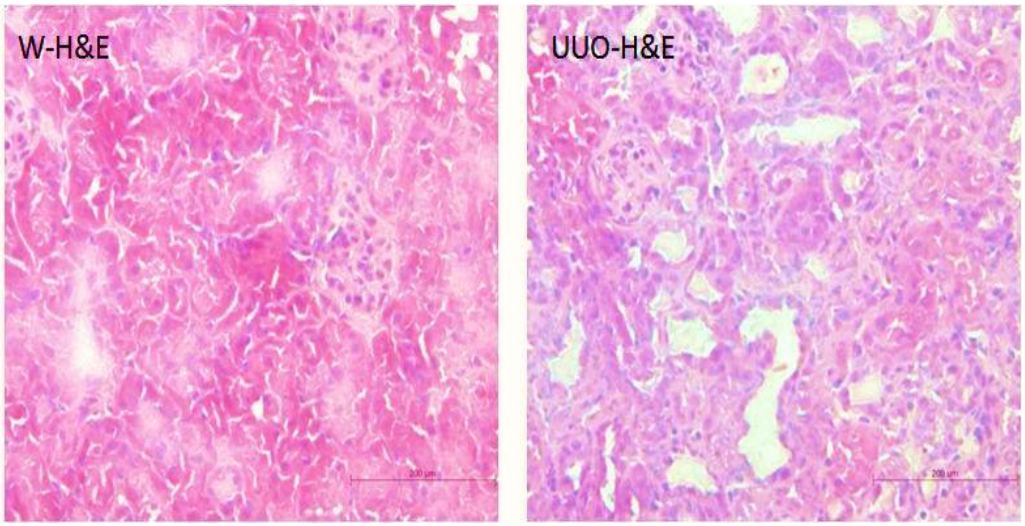

Figure 5.4. Staining of mice kidney sections with haematoxylin and eosin (H&E). Frozen sections from wild type and UUO kidney were fixed with cold acetone and stained with haematoxylin followed by eosin. Sections were then immersed in a gradient of alcohol and xylene. The scale bar represents 100 µM.

Frozen sections were stained with anti-collagen-1 antibody using the immunohistochemistry procedure. Sections show that collagen-1 is upregulated in UUO kidney compared to intact wild type kidney. Data were analyzed by quantitation of stained sections at the tubular and interstitial spaces. These analyses show that collagen-1 was significantly upregulated in interstitial spaces in UUO kidney compared to wild type ($P<0.001$), (Figure 5.5, 5.6).

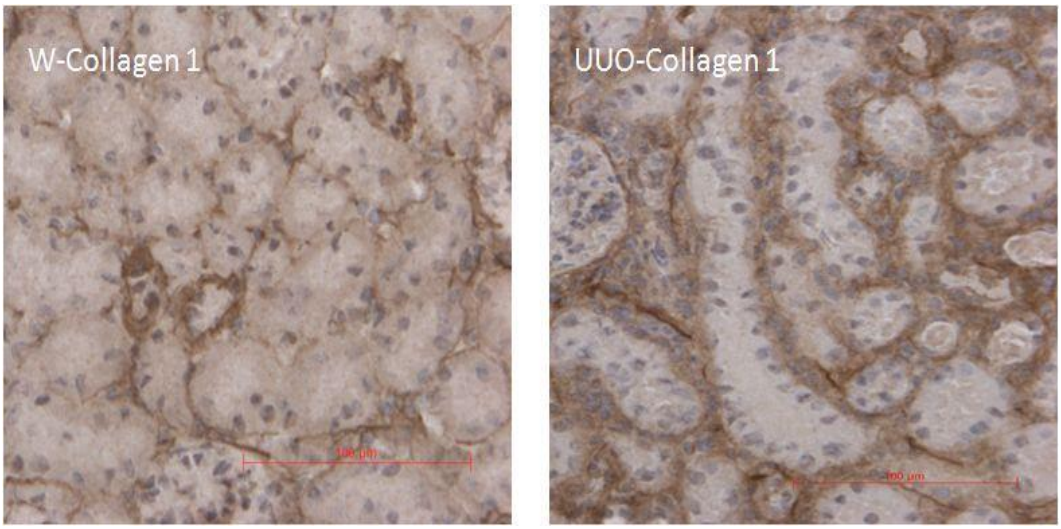

Figure 5.5. Staining of mice kidney sections with Collagen-1. Sections from normal and UUO kidneys were blocked with Avidin-Biotin and incubated with Collagen-1 (1:150) overnight at 4^{o}C followed by incubation with biotinylated secondary antibody. Sections were incubated with Vector ABC and developed with DAB-H_2O_2. Brown color represents collagen-I activity. Scale bar represents 200 µM.

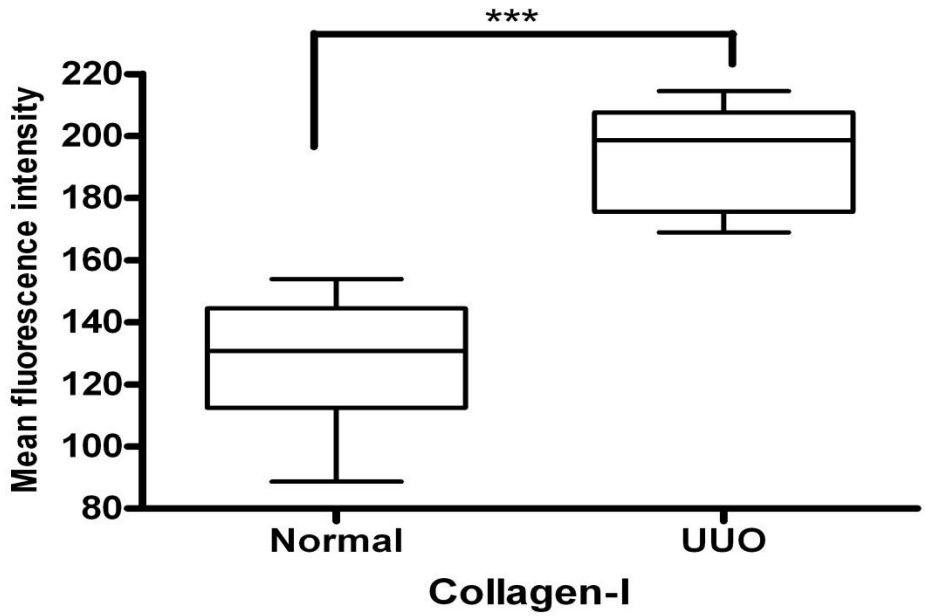

Figure 5.6. Quantitative analyses of tubular collagen-1 staining of UUO mice kidney. Results represent data from three UUO mice and three normal kidneys. At least three sections from each kidney were screened (n=15). Frozen sections were stained with collagen-1 by immunohistochemistry. Random areas (five for each section) from tubules were quantified and analyzed by Image-J software. (N=3, ***P<0.001).

5.4.2.2 **Staining with α-SMA**

Upregulation of α-smooth muscle actin depositions constitutes an additional diagnostic marker of myofibroblasts. In normal kidney, a very limited number of cells with α-SMA is found in the vascular walls. Increasing numbers of α-SMA expressing cells are accompanied by renal disease. Frozen sections were stained with α-SMA antibody in order to confirm the process of fibrosis in these UUO models. Sections were stained with α-SMA antibody using the immunofluorescence technique and investigated by fluorescence microscopy. Results show that UUO kidney has a greater number of cells expressing α-SMA compared to normal kidney. This increase was mainly localized around vascular structures ($P<0.001$), (Figure 5.7, 5.8).

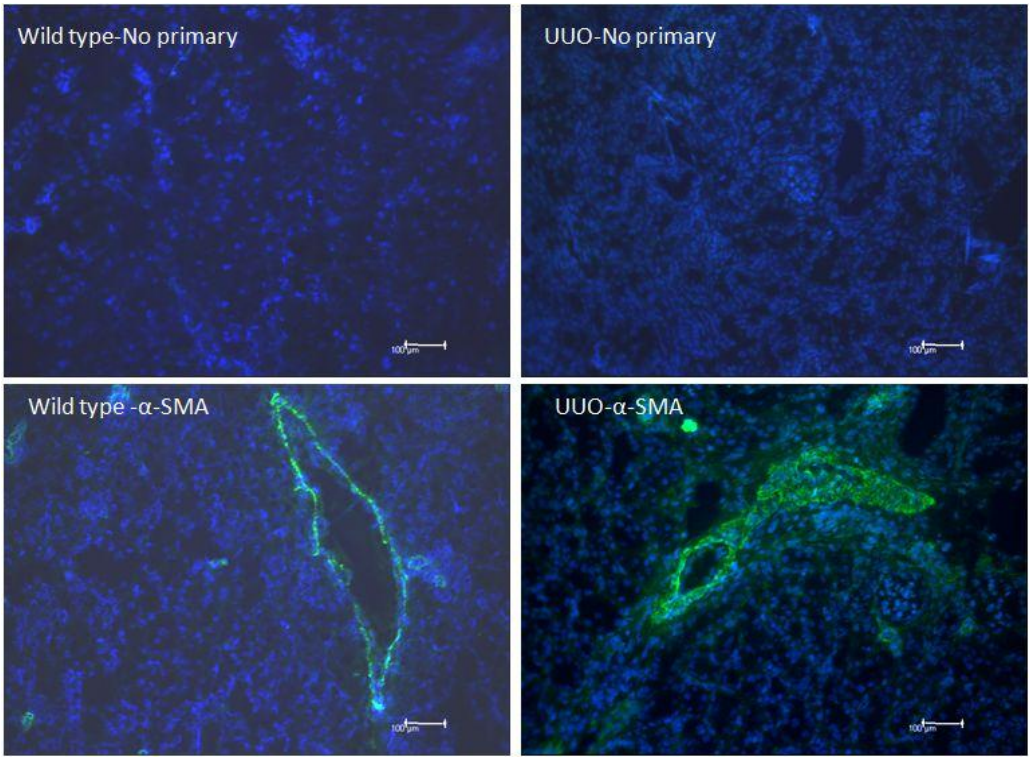

Figure 5.7. Representative image of UUO kidney staining with anti α-SMA antibody. Frozen sections from wild type and UUO kidney were fixed with cold acetone, blocked with PBS-BSA 2% and incubated with anti α-SMA antibody at 4^{o}C overnight. Slides were washed with TBS and stained with FITC-conjugated secondary antibody. Scale bars represent 100 µM.

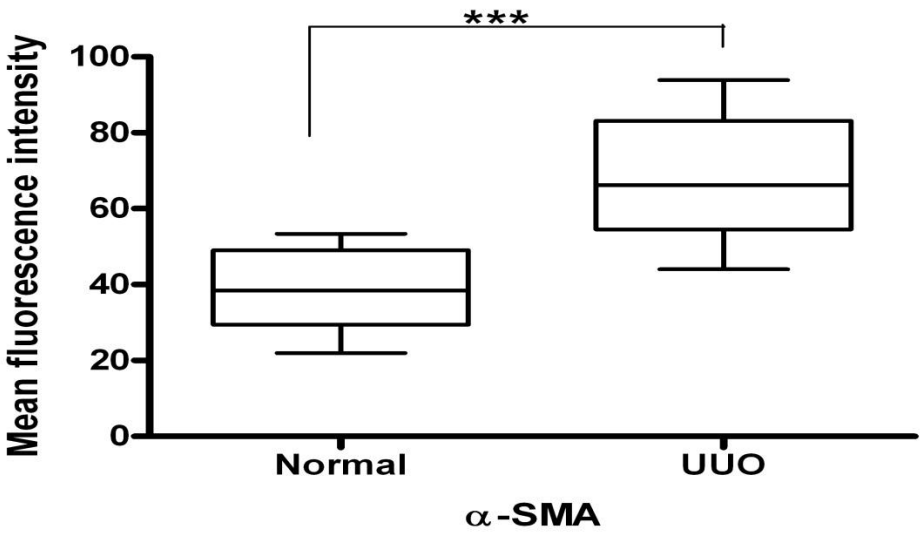

Figure 5.8. Quantitative analysis of mean fluorescence intensity of UUO staining with. Data were taken from three animal kidneys with UUO and compared to three normal kidneys. Sections were taken from three different animals and five sections were screened from each one (n=15). Mean fluorescence intensity was measured using Image-J software. (N=3, ***=P<0.001).

5.4.3 Staining with 10E4 antibody

10E4 antibody targets heparan sulphate epitopes in Bowman's capsule and tubules basement membrane (van Kuppevelt *et al.*, 1998). Frozen sections from UUO and wild type kidney were stained with 10E4 antibody using a mouse on mouse (M.O.M) protocol and investigated by fluorescence microscopy. 10E4 antibody was bound mainly within the tubular basement membrane with increased deposition in UUO sections compared to normal sections. Data analysis using tubular mean fluorescence intensity, show that binding of 10E4 antibody is significantly upregulated (P<0.001) in UUO sections compared to wild type (Figure 5.9, 5.10).

5.4.4 Staining with phage display antibodies

Phage display antibodies have been widely used for investigation of changes in HS structure. These antibodies show selectivity against kidney structures including glomerular basement membrane (GMB), tubules and the interstitium. Three phage display antibodies were used in this study (generous gift from Dr. Van Kuppevelt).

Sections were further examined by fluorescence microscopy. These antibodies were optimised recently in the group by (Dr. Julia Spielhofer).

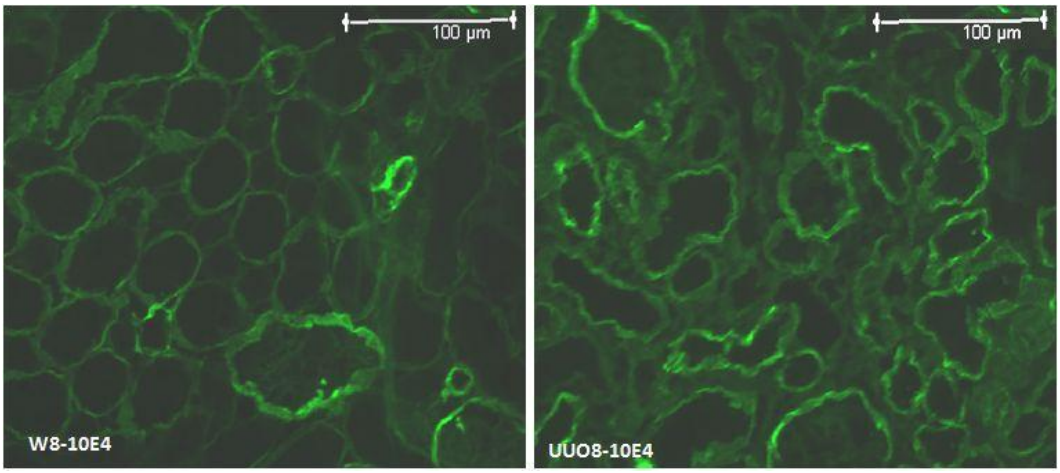

Figure 5.9. Representative staining of mice kidney with 10E4 antibody. Frozen sections from wild type and UUO kidneys were stained with 10E4 antibody by using mouse on mouse (M.O.M) protocol. Sections were fixed by cold acetone and blocked by Avidin-Biotin. Then slides were incubated with mice IgG blocking antibody followed by incubation with 10E4 (1:100) overnight at 4oC. Biotinylated secondary anti-mouse antibody was added and followed by fluorescein Avidin DCS. Slides were visualized by Leica Fluorescein microscopy. Scale bar represents 100 µM.

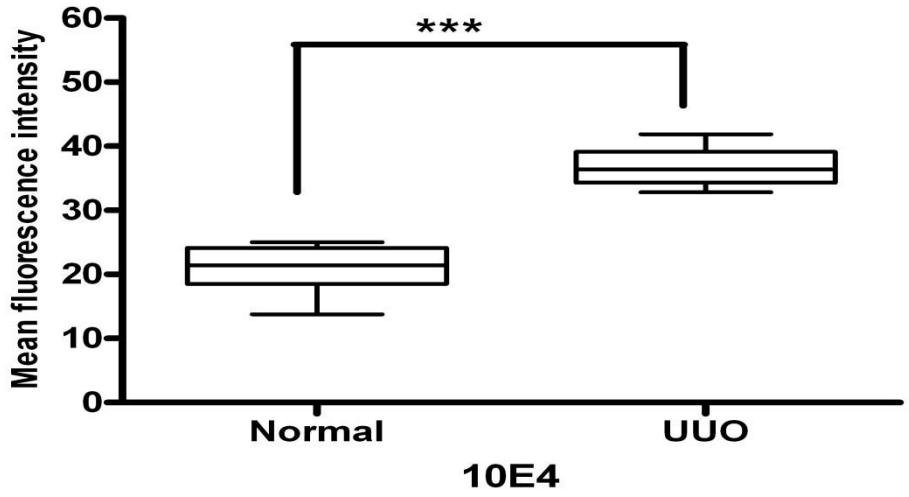

Figure 5.10. Quantitative analyses of UUO sections staining with 10E4 antibody. Frozen sections from three normal and UUO kidneys were stained with 10E4. Sections from each kidney (5 areas, n=15) were analyzed by measuring the density of tubular and interstitial areas randomly by Image-J software. (N=3, ***: P<0.001)

5.4.4.1 **HS3A8**

HS3A8 antibody reacts with highly sulphated oligosaccharides including 6-O and N- sulphate groups (GlcNS6S) and sulphated iduronic acid (IdoA2S) (van de Westerlo et al., 2002). A series of experiments was performed to stain frozen sections from UUO and wild type kidney with HS3A8 antibody for immunofluorescence analysis. The UUO sections show that HS3A8 antibody was most predominant in tubular basement membrane and interstitial spaces (Figure 5.11). Data analysis included mean fluorescence intensity of tubular and interstitial structures and showed that the upregulation of HS3A8 deposition was significant ($P<0.001$), (Figure 5.12).

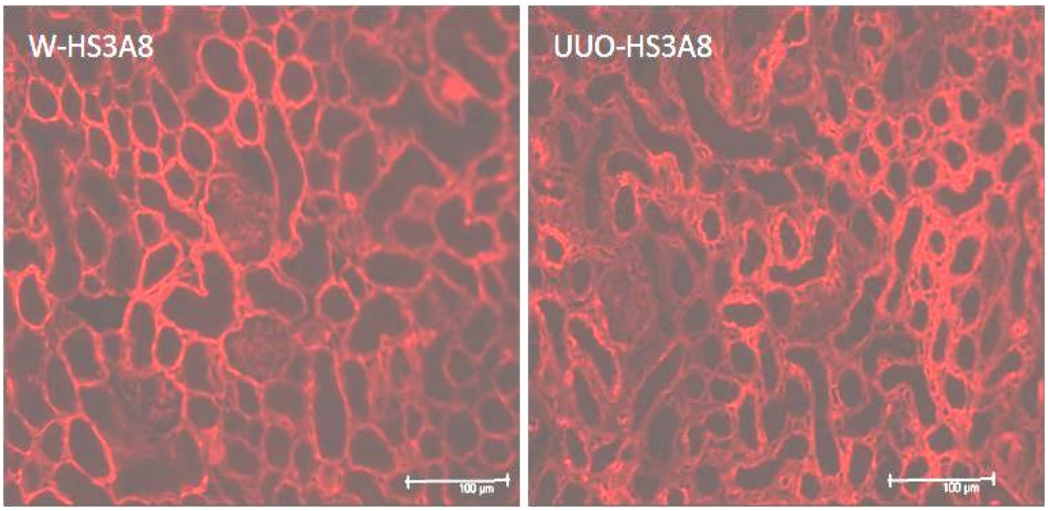

Figure 5.11. Representative staining of murine kidney with phage display HS3A8 antibody. Frozen sections from wild type and UUO kidneys (from animals 4, 6 and 8) were stained with HS3A8 antibody. Sections were fixed by cold acetone and blocked by 2% BSA-PBS. Slides were incubated with HS3A8 antibody at 1:20 overnight at 4^{o}C. Slides were visualized by adding secondary Cy3-labelled anti VSV antibody (1:200). Slides were examined with Leica fluorescence microscopy. Scale bar represents 100 µM.

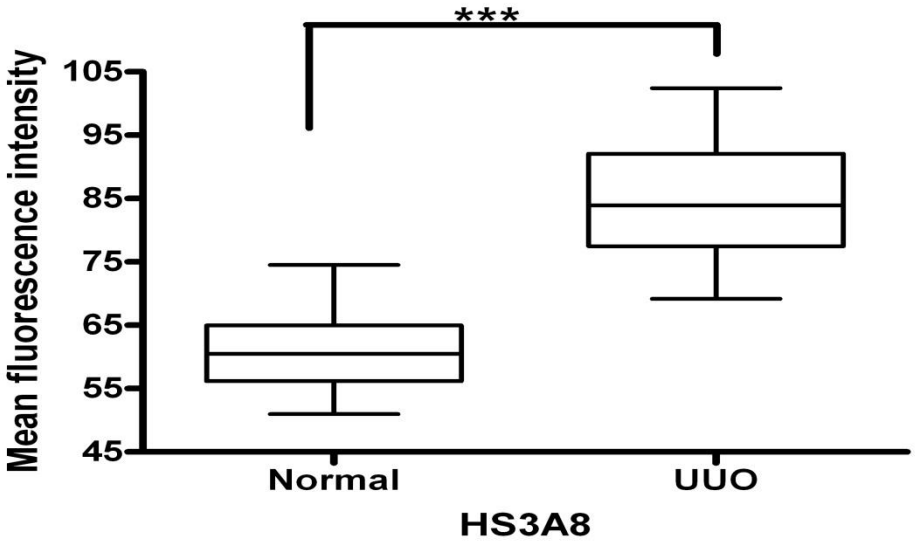

Figure 5.12. Quantitative analyses of UUO section staining with phage display HS3A8 antibody. Three sections from each kidney were analyzed by measuring the density of tubular and interstitial areas (5 areas, n=45) randomly by Image-J software. Three animals were investigated (N=3, ***: P<0.001).

5.4.4.2 **HS4C3**

Phage display antibody HS4C3 targets the IdoA2S-GlcNS3S6S domain on the HS structure. In kidney, HS4C3 predominantly stains peritubular capillaries and GMB (van Kuppevelt et al., 1998). Frozen sections stained with HS4C3 antibody show that glomerular staining was predominant in both wild type and UUO sections. Tubules and interstitium show increased staining in UUO sections compared to wild type (Figure 5.13). These changes were shown to be statistically significant (P<0.001) by measuring mean fluorescence intensity of selective tubular and interstitial structures (Figure 5.14).

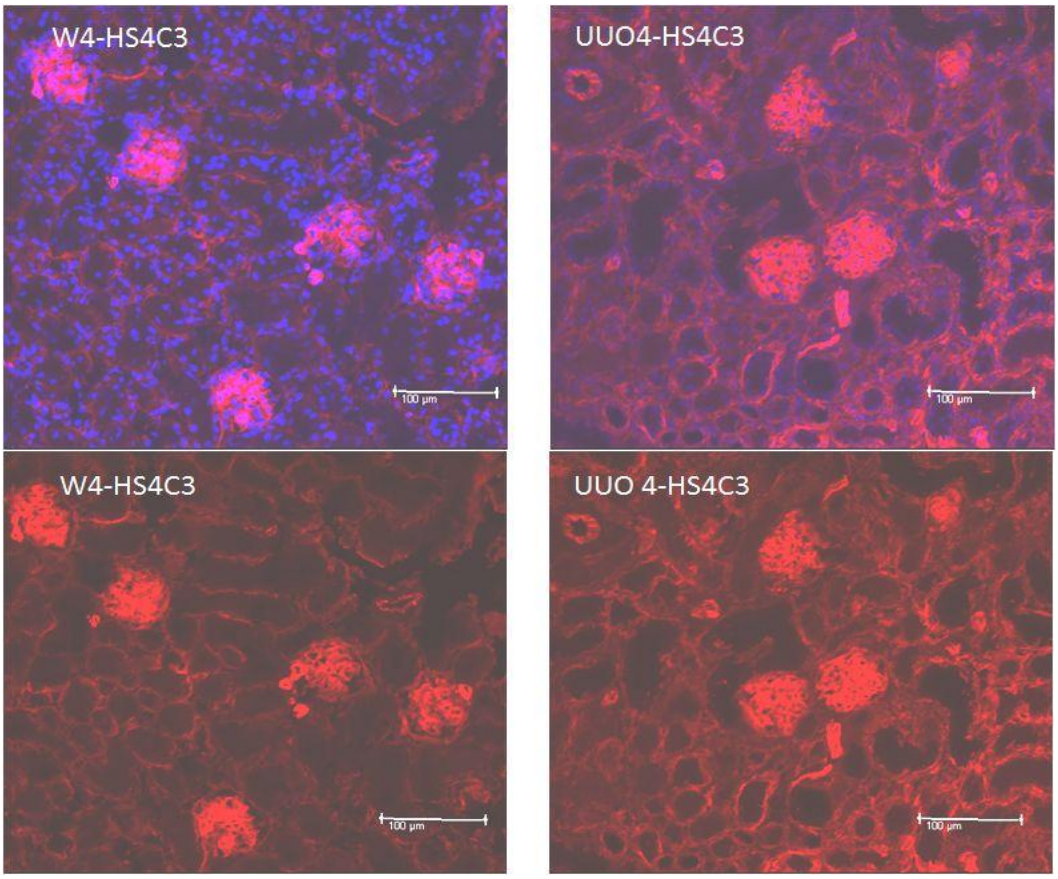

Figure 5.13. Representative staining of mice kidney with phage display HS4C3 antibody. Frozen sections from wild type and UUO kidneys were stained with HS4C3 antibody. Sections were fixed by cold acetone and blocked by 2% BSA-PBS. Then slides were incubated with HS4C3 antibody at 1:20 of 2% BSA-PBS overnight at 4^{o}C. Secondary Cy3-labelled anti VSV antibody was added. Slides were visualized with Leica fluorescence microscopy. Scale bar represents 100 µM.

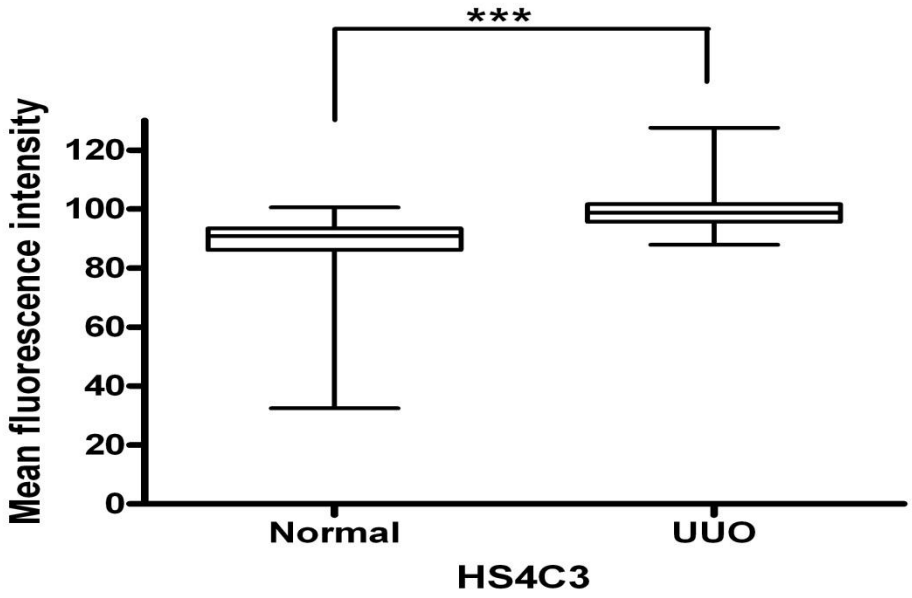

Figure 5.14. Quantitative analyses of UUO sections stained with HS4C3 antibody. Frozen sections from normal and UUO kidneys were stained with phage display HS4C3 antibody. Sections from each kidney were analyzed by measuring the density of tubular and interstitial areas (n=30) randomly by Image-J software. (N=3, ***: P<0.001)

5.4.4.3 **RB4EA12**

The RB4EA12 antibody recognizes mainly IdoA-GlcNS6S on the HS structure, RB4EA12 most strongly stains cortical tubules in kidney structure (Dennissen *et al.*, 2002). Frozen sections stained with RB4EA12 show predominant staining in tubules and to a lesser extent the interstitium or glomerulus (Figure 5.15). Tubular fluorescence intensity shows significant changes (P<0.01) between UUO and wild type sections (Figure 5.16).

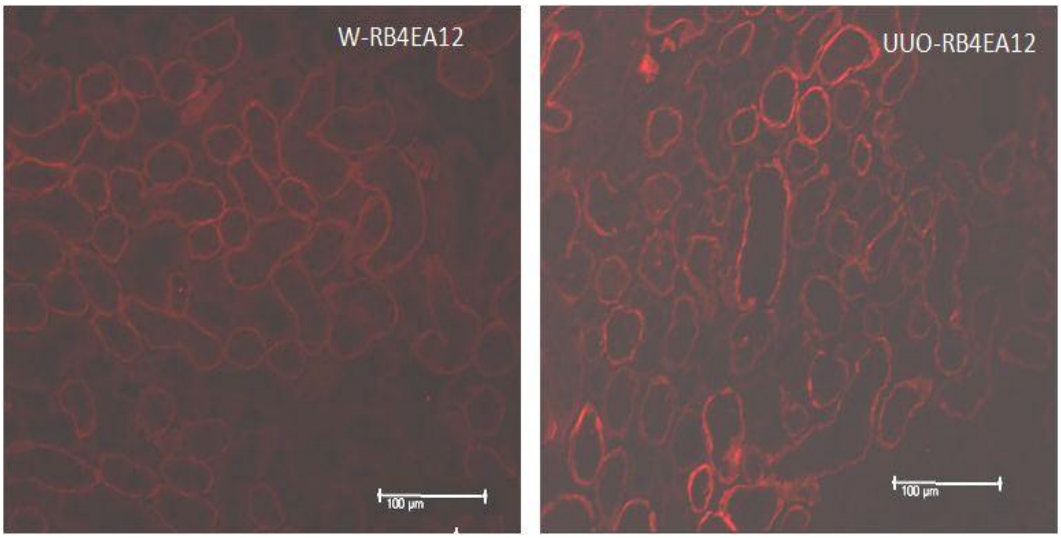

Figure 5.15. Representative mice kidney sections stained with RB4EA12 phage display antibody. Frozen sections from wild type and UUO kidneys (from animals 2 and 6) were stained with RB4EA12 antibody. Sections were fixed by cold acetone and blocked by 2% BSA-PBS. Then slides were incubated with RB4EA12 antibody at 1:20 of 2% BSA-PBS overnight at 4^{o}C. Secondary Cy3-labelled anti VSV antibody was added. Slides were visualized by Leica fluorescence microscopy. Scale bar represents 100 µM.

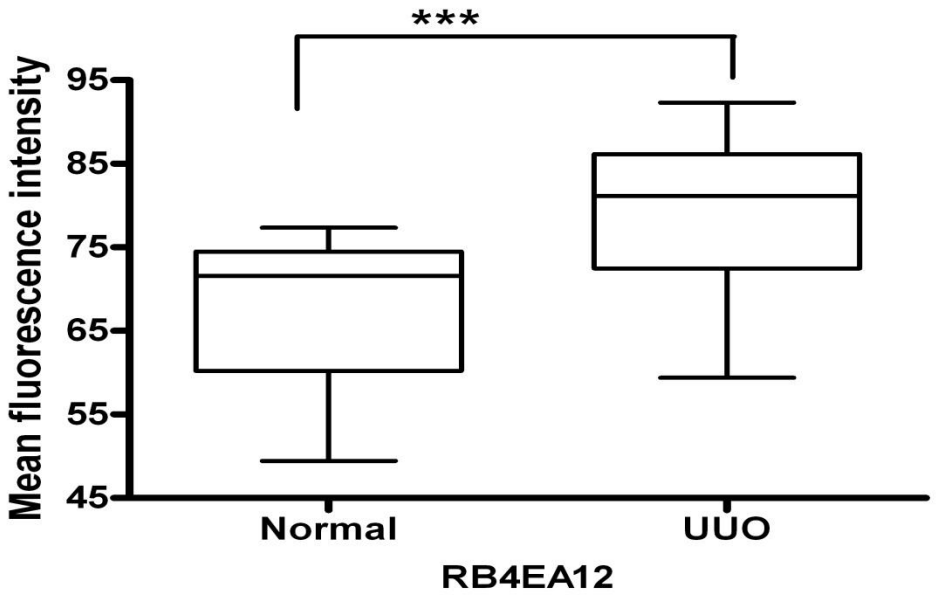

Figure 5.16. Quantitative analyses of UUO section staining with phage display RB4EA12 antibody. Sections from each kidney were analyzed by measuring the density of tubular and interstitial areas (n=30) randomly by Image-J software. (N=3, ***: P<0.001)

5.4.5 Gene expression of HS modifying enzymes

5.4.5.1 **Efficiency test for murine qPCR**

To shed more light on changes taking place in UUO kidneys on the mRNA level, a series of RT-PCR experiments were performed. Using RNA from UUO and wild type kidney, cDNA were synthesized and used for RT-PCR. These experiments were designed to examine the changes on HS gene expression such as mouse NDST1, HS6ST1, SULF1 and SULF2. HPRT1 was used as a house keeping gene. Data analysis using CT numbers and ΔΔCT method show that UUO kidney had significantly ($P<0.01$) upregulated the SULF1 gene expression by about three fold compared to wild type kidney. By contrast, expression of SULF2 gene was downregulated by about 40% in UUO kidney compared to wild type kidney ($p<0.01$). Gene expression of NDST1 and HS6ST1 showed no significant changes (Figure 5.17).

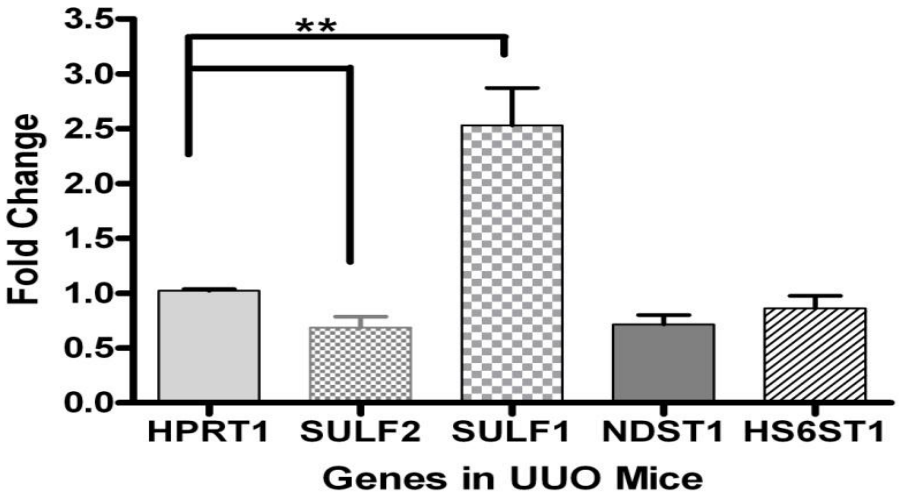

Figure 5.17. Quantitative RT-PCR analyses of gene expression in UUO kidney. cDNA was synthesized following DNase treated RNA from normal and UUO mice kidneys. Expression of genes was investigated using TaqMan gene expression assay in reference to house-keeping HPRT1 gene. Data were analyzed by using ΔΔCT method and REST2008 software. (N=3, **: $P<0.01$)

5.5 Discussion

This chapter aims to compare *in vitro* findings of HS sulphation changes resulted in modulation of interaction with biotinylated FGF2 and phage display antibodies with an *in vivo* model of renal fibrosis. The UUO kidney model was created by double ligation of the left ureter for 7 and 14 days. Changes in UUO kidney were studied using H&E staining, immunofluorescence and immunohistochemistry. Furthermore, expression of HS modifying genes during UUO was examined with qPCR.

5.5.1 Observation on fibrosis markers

Fibrotic markers were investigated in this study in UUO kidney to confirm that fibrosis is induced by day 7 after induction of UUO. In this study, investigation of collagen I and α-SMA showed significant upregulation in UUO kidney compared to normal kidney. The increased expression of collagen I in UUO kidney is considered an indication of fibrosis and renal scarring (Kelynack *et al.*, 1999). The current result is consistent with previous research showing increased collagen deposition in the context of UUO fibrosis (Wright *et al.*, 1996).

Another example of fibrosis development in the UUO kidney was shown by investigation of α-SMA. Results show that UUO kidney significantly increased the expression of α-SMA compared to wild type kidney. This result is in line with previously reported interstitial fibrosis (Alpers *et al.*, 1994). Additionally, this result is in agreement with the involvement of myofibroblasts in the synthesis of α-SMA during interstitial fibrosis (Badid *et al.*, 2002).

5.5.2 Observation on HS changes

The 10E4 monoclonal antibody was used in frozen sections to determine the abundance of N-sulphated epitopes in normal and UUO kidney. This study shows that the 10E4 epitope was significantly increased in the UUO kidney compared to wild type kidney, mainly located in basement membrane and peritubular spaces. The 10E4 antibody targets N-acetyl/N-sulphate domains of HS structure (David *et al.*, 1992). This result is in agreement with literature showing that the 10E4 antibody and N-sulphation epitope were associated with biological activities of

chronic disease such as wound healing and proliferation of epithelial cells (Celie *et al.*, 2008). Furthermore, Morita et al. found that in renal interstitial fibrosis (unlike glomerulosclerosis), the 10E4 epitope was increased alongside FGF2 binding epitope in the expanded peritubular interstitium (Morita *et al.*, 1994a). However, earlier work in our group showed increased expression of 10E4 antibody in acute and moderate rejection of kidney whereas no significant increase in chronic rejection was noticed (Unpublished data from Dr. Spielhofer 2010).

Phage display antibodies were used to increase understanding of HS changes in the UUO model. Frozen sections were stained with HS3A8, HS4C3 and RB4EA12 antibodies. This study showed significantly increased expression of these HS epitopes in UUO kidney compared to wild type kidney. The HS3A8 antibody targets a complex HS epitope composed mainly of trisulphated disaccharides IdoA2S-GlcANS6S (Dennissen *et al.*, 2002), whereas HS4C3 antibody targets a domain of IdoA2S-GlcNS3S6S (van Kuppevelt *et al.*, 1998). This result is in line with earlier unpublished work in our group which showed increased expression of HS3A8 and HS4C3 epitopes in chronic rejection of liver and kidney grafts (Dr. Spielhofer). Importantly, it has been shown recently that HS deposition in liver cirrhosis is correlated with changes in HS modification machinery; the HS4C3 epitope was accumulated in chronic liver disease as well as in rat liver fibrogenesis. This deposition includes in addition to blood vessels, basement membrane and epithelial bile ducts (Tatrai *et al.*, 2010).

Targeting the HS4C3 epitope using a specific antibody resulted in inhibition of the stimulatory effect of FGF2 on human mesangial cell (HMC) proliferation, suggesting a similarity between FGF2 and HS4C3 epitope binding domains of HS (Lensen *et al.*, 2005). Conversely, addition of FGF2 antibodies inhibited the binding of HS4C3 by about 60% (Lensen *et al.*, 2005). These findings support the hypothesis that upregulation of HS4C3 in UUO kidney is an indicator of the regulation of effector factors, such as FGF2, which have a crucial role on graft fibrosis.

The targeting of tubular basement membrane by both FGF2 and the phage display antibodies might indicate increased FGF2 binding alongside increased synthesis of antibody epitopes. FGF2 binding was linked to tubulointerstitial injury in human

kidney, suggesting a further involvement of the effector in tubular epithelial cell growth and proliferation (Morita *et al.*, 1994b). The increased expression of HS4C3 indicates to a potential role of the 3-O sulphate groups in the HS involvement in fibrosis pathology. This is in agreement with previously reported high expression of the HS3ST1 gene in failed grafts compared to non-failed graft or normal kidney (Einecke *et al.*, 2010).

Furthermore, this study shows that staining frozen sections with the RB4EA12 antibody showed increased deposition of a related HS epitope in UUO kidney compared to wild type kidney. The RB4EA12 antibody targets an HS epitope composed of disaccharide with N-Acetyl/N-sulphate with 6-O sulphate (IdoA-GlcNS6S) (Dennissen *et al.*, 2002). The RB4EA12 epitope was mainly localized in the thickened basement membrane and peritubular spaces of dilated ducts in UUO kidney (Figure 5.15). It has been reported that RB4EA12 stains proximal tubules in human kidney (Lensen *et al.*, 2005). The current upregulation reflects a moderate increase in HS 6-O sulphation in UUO kidney. This is in agreement with increased expression of RB4EA12 in human fibrogenic disease including liver cirrhosis and focal nodular hyperplasia (Tatrai *et al.*, 2010). In fact, this increase seems consistent with suggested roles of N- and 6-O sulphation changes in HS regulation during fibrogenic renal disease.

5.5.3 Observation on mRNA level

To further investigate changes in HS in renal fibrosis, additional experiments were performed to measure the expression of HS modifying enzymes at mRNA level using qPCR. Genes encoding NDST1, HS6ST1, SULF1 and SULF2 were investigated in reference to the HPRT1 housekeeping gene. Results show that expression of the 6-O endosulphatase SULF1 and SULF2 are significantly changed by UUO.

The SULF2 gene was downregulated by about 40% whereas SULF1 was upregulated by 3-fold in UUO tissue compared to wild type (Figure 5.17). The sulphatase enzymes remove 6-O sulphate group from a substrate containing Ido2S-GlcNS6S (Dhoot *et al.*, 2001; Ai *et al.*, 2006a). The current result is also in agreement with recent data showing that SULF1 expression is increased (6 fold) in

chronic liver cirrhosis (Tatrai *et al.*, 2010). Interestingly, this study shows no changes in NDST1 and HS6ST1 expression in UUO mice at mRNA level despite the increase in N- and 6-O sulphate epitopes noticed in UUO staining. This can be justified by the presence of three isoforms for HS6ST and four isoforms for NDST which catalyze the same reaction.

Heparan sulphate was shown to undergo changes during acute and chronic diseases. Several publications have reported changes in HS modifying enzymes following cell stimulation by proinflammatory cytokines. For example, stimulation of glomerular endothelial cells with IFN-γ caused increased expression of NDST1 on mRNA level which increased sulphation at the N- position and , thereafter, enhanced the chemokine presentation and leucocyte migration (Carter et al., 2003).

The current study shows differential regulation of SULF1 and SULF2 in the UUO kidney. This is in agreement with a previous research which showed also that each enzyme has independent expression in the same tissue (Lai *et al.*, 2004a; Lai *et al.*, 2008b). These data are further supported by HS regulation in lupus nephritis, where SULF2 expression was decreased by 2 fold with no detectable changes in SULF1expression (Rops *et al.*, 2008).

Taken together, these findings confirm the importance of HS modifying enzymes and demonstrate several manners of regulation of HS biology in health and disease. Although the mechanism of HS regulation is not clear, this molecule exhibits a range of modifications which enhance its cytokine binding and presenting activities. The SULF2 expression following TGF-β stimulation of HK2 cells along with increased SULF1 expression in UUO kidney suggests a potential role for these enzymes in the pathology of kidney fibrosis.

Chapter Six

6 General discussion and conclusion

6.1 Summary of findings

6.1.1 Introduction

Heparan sulphate is involved in a variety of biological activities including development, carcinogenesis and inflammation. It is involved in interaction with a wide range of proinflammatory cytokines and growth factors which play essential roles in the inflammatory response and graft rejection. Interestingly, HS undergoes several modifications during embryonic life, carcinogenesis and inflammation (Hacker *et al.*, 2005; Lai *et al.*, 2008a; Huynh *et al.*, 2012). In chronic rejection, for instance, modification to HS sulphation enhances the binding, concentration and activity of TGF-β, IFN-γ, chemokines and FGF2. The interaction between proteins and HS requires to a large extent specific binding motifs on HS with unique sulphation patterns (Lindahl, 2007). Sulphation of HS undergoes significant changes during acute kidney rejection (Ali *et al.*, 2005a) and chronic liver cirrhosis (Tatrai *et al.*, 2010).

6.1.2 Effect of HS6ST1 on FGF2 binding

Fibroblast growth factor 2 plays a key role in the pathology of renal fibrosis and EMT. This factor stimulates the proliferation of fibroblasts and mesangial cells and induces the secretion of TGF-β, which stimulates the EMT process (Strutz and Zeisberg, 2006).

Many enzymes are involved in HS synthesis and modification. For FGF2 binding, the binding motif on HS must include N-sulphate and 2-O sulphate groups (Guimond *et al.*, 1993; Faham *et al.*, 1996). The HS6ST enzymes transfer 6-O sulphate to the C6 position of glucosamine within the HS structure. This 6-O sulphate plays a significant role in the binding of a variety of cytokines and growth factors to HS (Lyon *et al.*, 1994b; Feyzi *et al.*, 1997). This group is also essential for FGF2-FGFR signalling and subsequent mitogenic activity (Pye *et al.*, 1998).

HS6ST1 is a highly expressed isoform of the HS6ST enzyme (Habuchi *et al.*, 2003; Smeds *et al.*, 2003). Stable transfectants of renal epithelial cells with HS6ST1 overexpression were generated to investigate the changes in HS structure and biological activity produced by this enzyme. These transfectants show for the first

time that overexpression of HS6ST1 significantly increases the binding of FGF2 to these cells. This was accompanied with an increase in ERK activation and proliferation. Although 6-O sulphate is not a major component of the FGF2 binding motif, which also contains NS and 2-OS modifications (Ishihara *et al.*, 1994; Kreuger *et al.*, 2001), the increase in FGF2 binding represents a novel and interesting result.

Despite intensive study of the heparin/HS binding motif for FGF2, no unique binding sequence has been completely described (Esko and Selleck, 2002). In the FGF2 binding domain, the N- and O-sulphate groups are located in a way that allows HS-protein interaction to take place. The location of N- and 2-O sulphate groups along with chain length and overall O-sulphation seems more important for HS interaction than the specific distribution of sulphate groups (Jastrebova *et al.*, 2006). In conclusion, the HS-FGF2 binding does not depend completely on any single unique sequence but on the combination of several components (Mulloy and Rider, 2006).

The increase in FGF2 binding was accompanied with increased expression of HS epitopes specific for the HS3A8, HS4C3 and RB4EA12 monoclonal antibodies. Earlier results have shown competition between HS4C3 antibody and FGF2 binding to HS. Treatment of human mesangial cells (HMC) with the HS4C3 antibody also resulted in inhibition of the stimulatory effect of FGF2 on HMC proliferation. Similarly, treatment of these cells with FGF2 inhibited the binding of HS4C3 (Lensen *et al.*, 2005). Therefore, the increased binding of HS4C3 by HS6ST1 transfectants indicates that the function of HS can change following HS6ST1 overexpression during renal fibrosis.

Upregulation of the HS3A8 and RB4EA12epitopes on the HS6ST1 overexpressing cells suggests that additional changes in HS chemistry can occur following HS6ST1 overexpression during renal fibrosis. An increase in RB4EA12 binding has also been reported in chronic liver cirrhosis and suggests a potential role for increased expression of the 6-O sulphate group in fibrogenesis (Tatrai *et al.*, 2010).

6.1.3 The effect of HS6ST1 over-expression on HS structure

The structure of HS was examined using ^{35}S radioactive isotope and disaccharide analysis following deaminative cleavage (aManR) and HPLC (in collaboration with Prof. Marion Kusche-Gullberg in Norway). The overexpression of HS6ST1 has an important effect on disaccharide structure and distribution. This includes increased mono-O sulphated disaccharides (GlcA-GlcNS6S and IdoA-Glc-NS6S) and decreased trisulphated disaccharides (GlcA2S-GlcNS6S and IdoA2S-Glc-NS6S). This result is consistent with an earlier report describing specific substrates for HS6ST1 enzyme which prefers non-sulphated glucoronic acid (GlcA-GlcNAc) rather than 2-O sulphated iduronic acid residue (IdoA2S-GlcNS) (Habuchi *et al.*, 2000).

The changes observed in HS structure include an increase in NA/NS domains following HS6ST1 overexpression; this is in agreement with earlier literature (Do *et al.*, 2006). Interestingly, no changes in the overall 6-O sulphation were found following HS6ST1 overexpression. This may be attributed to the high degree of sulphation of HS produced by wild-type HK2 cells; hence the addition effect could not be seen.

6.1.4 The biological effect of SULF2 overexpression

Endosulphatase enzymes are the final modifying enzymes in HS synthesis (Lamanna *et al.*, 2006). These enzymes (SULF1 and SULF2) remove 6-O sulphate groups from the HS chain on the cell surface and the extracellular matrix. In order to mimic the role of inflammatory cytokines on HS degradation, renal epithelial cells were stimulated with cytokines and investigated for the expression of HS degrading enzymes by qPCR. Interestingly, stimulation with TGF-β increased the gene expression of SULF2 by 5 fold compared to resting cells. This result is similar to literature previous report that stimulation with TGF-β can induce the expression of SULF1 in lung fibroblasts *in vitro* and *in vivo* (Yue *et al.*, 2008).

To shed more light on HS changes following SULF2 overexpression, stable SULF2 transfectants were generated and investigated for changes in HS biology. These transfectants were examined for binding to biotinylated FGF2. Interestingly, SULF2 transfectants showed reduced FGF2 binding to their cell surface.

Consistently, SULF2 transfectants also showed reduced binding of the HS3A8, HS4C3 and RB4EA12 antibodies. This is consistent with a previous report showing that changes in the expression of the HS4C3 epitope were paralleled by similar changes in FGF2 binding (Lensen *et al.*, 2005). Thus, the reduced binding of FGF2, HS3A8 and HS4C3 to SULF2 transfectants might be consistent with an anti-fibrotic effect of SULF2 overexpression; this is opposite to the effect of HS6ST1 overexpression (Table 6.1).

	HS6ST1 transfectant	SULF2 transfectant	UUO kidney
FGF2	++	- -	N/A
10E4	- -	++	++
HS3A8	+	- -	+ +
HS4C3	+	- -	+
RB4EA12	+ +	- -	+

Table 6.1. A summary of FGF2 and phage display antibody binding with HS6ST1 and SULF2 transfectants FGF2 and phage display antibodies.

In accordance with previous findings, SULF2 transfectants have less ERK activation compared to mock transfectants. Removal of 6-O sulphate groups is expected to affect FGF-FGFR signalling and, consequently, ERK activation (Guimond *et al.*, 1993; Dai *et al.*, 2005). The same can be said about the proliferation of SULF2 transfectants which showed a reduced proliferation rate compared to mock transfectants. Previous researchers have found that 6-O endosulphatase enzymes have a negative effect on proliferation and mitogenic activity (Dai *et al.*, 2005; Kamimura *et al.*, 2006).

HS changes following SULF2 overexpression also resulted in decreased binding and presentation of the chemokine CCL5. Binding of CCL5 to HS depends on N- and O-sulphation. Therefore, changes in HS sulphation can explain the modulation of CCL5 presentation (Shaw *et al.*, 2004).

6.1.5 Effect of SULF2 overexpression on HS structure

The effect of overexpression of SULF2 was examined by incubating SULF2 transfectants with radioactive ^{35}S and analyzing the disaccharide structure using deaminative cleavage (aManR) followed by HPLC. These changes show that SULF2 removes 6-O sulphate groups from trisulphated disaccharides as a substrate target. This is consistent with previous literature (Ai *et al.*, 2003b; Ai *et al.*, 2006b). Additionally, this result shows that the SULF2 enzyme removes the 6-O sulphate from disulphated disaccharides (GlcA-GlcNS6S and IdoA-GlcNS6S).

Interestingly, SULF2 overexpression had a significant effect not only on 6-O desulphation but also on 2-O and N-sulphation. Desulphation of the 6-O group was accompanied by upregulation of 2-O sulphation, which is consistent with previous results (Ai *et al.*, 2006b). This study also shows a mild downregulation of N-sulphation following SULF2 overexpression. By contrast, no significant changes in N- or 2-O sulphation were found in TGF-β induced SULF1 overexpression *in vitro* and *in vivo* in lung fibroblasts (Yue *et al.*, 2008). SULF1 overexpression in *Drosophila* produces no compensatory increase of 2-O sulphation (Kamimura *et al.*, 2006). The effect of 6-O desulphation on N- and 2-O sulphation might be related to the level of expression of the gene. Changes in sulphation and structure are mostly responsible for the changes in physiological functions and antibody binding. These changes explain the different roles that HS might have during inflammation processes and the mechanism which affects HS regulation.

6.1.6 Changes of HS sulphation in the UUO mouse model

UUO mice constitute an *in vivo* model of chronic fibrosis with increased expression of fibrosis markers such as α–SMA and collagen I. UUO mice were generated after 7 days of double ligation of the ureter. Frozen sections of the kidney were stained with phage display antibodies. Results show significant upregulation of HS epitopes required for binding the 10E4, HS3A8, HS4C3 and RB4EA12 antibodies. Upregulation of the binding of these antibodies suggests changes in HS chemistry during kidney fibrosis. HS3A8 and HS4C3 epitopes were also upregulated in fibrotic, rejected renal allografts, as shown earlier in this group (Dr. Spielhofer).

Interestingly, these changes were similar to those observed for HS6ST1 transfectants, whereas the opposite was found in SULF2 transfectants (Table 6.1).

In the case of the 10E4 antibody, UUO sections showed an increase in 10E4 epitope expression whereas HS6ST1 transfectants expressed less of the 10E4 epitope. Earlier work showed that this epitope was upregulated in acute and moderate rejection but not in chronic renal allograft rejection (unpublished data by Dr. Spielhofer). Expression of the 10E4 epitope in chronic fibrotic kidney with interstitial fibrosis (but not with glomerular sclerosis) has also been reported (Morita *et al.*, 1994b).

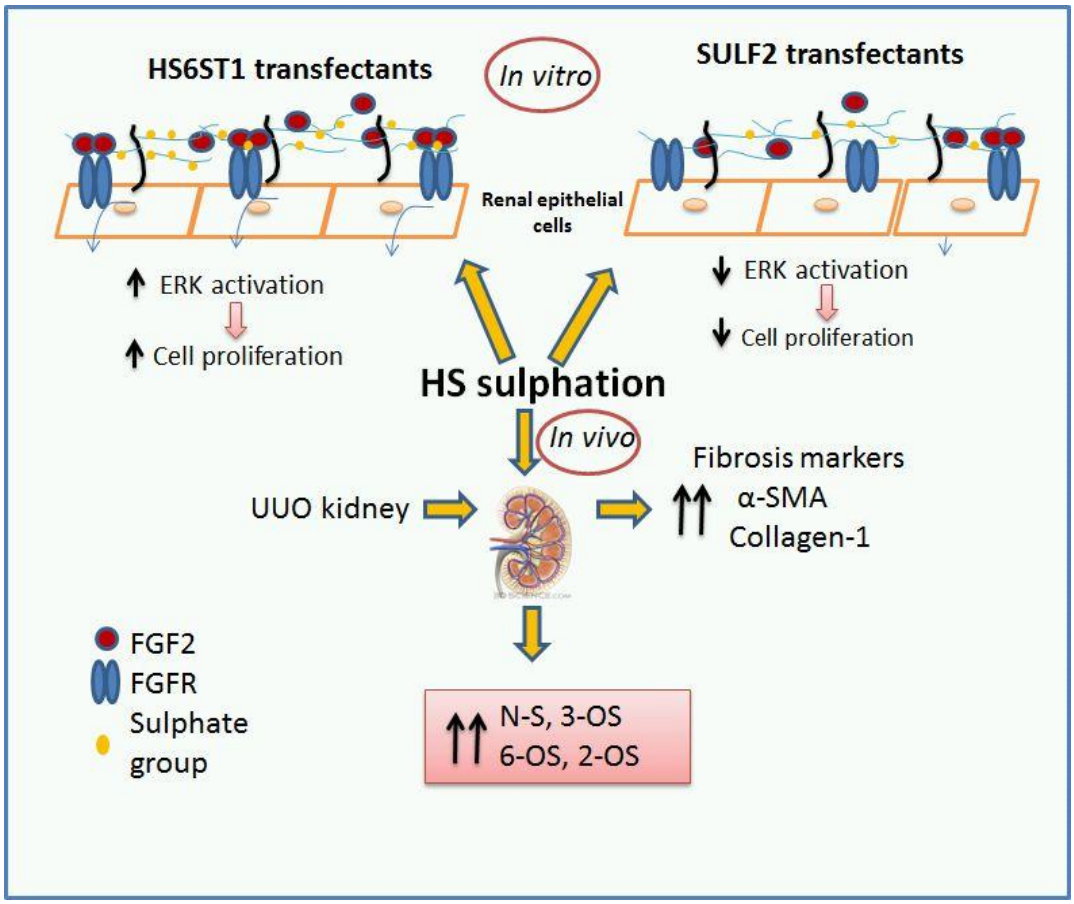

Figure 6.1. A summary of the effect of changes in HS sulphation on the biology of renal epithelial cells and the development of UUO pathology.

Further investigations of the expression of HS modifying enzymes in UUO kidney were performed at the mRNA level by qPCR. These investigations show a significant increase in expression of SULF1 with a decrease in SULF2. However, no significant changes were noticed for NDST1 or HS6ST1. Again, upregulation

of SULF1 highlights the role of this enzyme in regulation of HS biology during chronic renal fibrosis. It seems that tissues undergoing fibrosis have a different response to HS regulation. Stimulation of renal epithelial cells with TGF-β increased the expression of SULF2 with no changes in SULF1 (chapter 4). Interestingly, it has been reported that SULF1 expression is increased following TGF-β stimulation of pulmonary fibroblasts *in vitro* and *in vivo* whereas SULF2 expression did not show any significant changes (Yue *et al.*, 2008).

Therefore, these results suggest that HS undergoes significant changes following the overexpression of HS6ST1 and SULF2. After HS6ST1 overexpression, HS shows an increased ability to bind FGF2 and phage display antibodies (HS3A8, HS4C3 and RB4EA12). The increased expression of these epitopes might lead to a profibrotic environment which is enhanced by the increased anti-coagulant activity associated with the existence of the 3-OS component of the HS4C3 epitope (AT-III binding site), (Girardin *et al.*, 2005). Importantly, the SULF2 transfectants undergo reverse modifications including downregulation of binding to FGF2, HS3A8, HS4C3 and RB4EA12. An *in vivo* model of kidney fibrosis showed significant upregulation of binding properties of HS3A8, HS4C3 and RB4EA12 antibodies accompanied with increased expression of SULF1 on mRNA. These changes did not include HS6ST1 expression which might be related to an increase in alternative isoforms (HS6ST2 or HS6ST3).

Taken together, these results suggest that the 6-O sulphation of HS has an important role in fibrogenesis associated with renal rejection..

6.2 Implication of this study

Specific targeting of HS6ST as a therapeutic intervention might have value for the prolongation of renal allograft survival. For example, blocking the interaction of cytokines such as TGF-β or FGF2 with HS might allow the graft to escape a variety of profibrotic events. HS targeting might include the use of soluble heparin-like molecules with limited anticoagulant activity but high affinity for pro-inflammatory and -fibrotic cytokines. This requires knowledge of the specific HS sequences involved in cytokine binding. Addition of such specific sequences might more potently delay (or even prevent) chronic renal allograft graft fibrosis. This kind of

treatment might also complement the main immunosuppressive drugs which are used after transplantation.

The same can be said for the phage display HS-specific antibodies. Non immunogenic humanized antibodies might be used to block HS domains which bind FGF2; this may reduce FGF2-induced fibrogenic effects. Recent data has shown that an anti-FGF2 antibody has the ability to inhibit the proliferation of hepatocellular carcinoma cells and the growth of carcinoma cell lines in nude mice (Wang *et al.*, 2012).

Exploring the changes in HS during chronic renal rejection could provide prognostic information of relevance for clinical therapy. For example, regular examination of urine-secreted HS fragments in comparison to normal HS shedding might provide a non-invasive early warning of graft pathology.

6.3 Future work

There are a number of questions arising from this study. Answers to these questions will certainly improve our understanding of the role of HS in renal fibrosis.

1. Heparan sulphate undergoes a series of modifications due to the effect of several modifying enzymes. These enzymes transfer sulphate groups to the HS chains which affects their biological activity. This study examined the changes made by overexpression of HS6ST1 and SULF2. Overexpression of additional enzymes will provide more information about HS structure and biological activities.
2. Heparan sulphate plays a crucial role in inflammation and leucocyte migration. 6-O sulphation is known to be crucial for cell adhesion mediated by L- and P-selectin (Wang *et al.*, 2002). Cell lines with overexpression of HS6ST1, SULF1, SULF2 and other modifying enzymes could be used in leucocyte rolling assays under controlled shear pressure (using platforms such as the Cellix system) for examination of the effect of HS modification on leucocyte rolling and adhesion.
3. The effect of HS6ST1 and SULF2 on HS structure might be examined using additional procedures such as NMR and mass spectrometry (MS).

4. Increased expression of 6-O sulphate was shown in fibrotic UUO kidney and accompanied with increased FGF2 binding (Figure 5.11, 5.13 and 5.15). Use of a soluble heparinoid or GAG mimetic with an ability to bind cytokines and growth factors should reduce the biological activity of these factors and inhibit allograft fibrosis. A good example of this strategy is the use of low molecular weight heparin (Tinzaparin) to inhibit the binding between chemokine CXC12 and its receptor CXCR4, which reduced the metastatic spread of human breast cancer (Harvey *et al.*, 2007).

Chapter Seven

7 References and Appendices

References

Abe, R., Donnelly, S.C., Peng, T., Bucala, R. and Metz, C.N. (2001) 'Peripheral blood fibrocytes: differentiation pathway and migration to wound sites', *Journal of Immunology*, 166(12), pp. 7556-62.

Abeijon, C., Mandon, E.C. and Hirschberg, C.B. (1997) 'Transporters of nucleotide sugars, nucleotide sulfate and ATP in the Golgi apparatus', *Trends Biochem Sci*, 22(6), pp. 203-7.

Acloque, H., Adams, M.S., Fishwick, K., Bronner-Fraser, M. and Nieto, M.A. (2009) 'Epithelial-mesenchymal transitions: the importance of changing cell state in development and disease', *Journal of Clinical Investigation*, 119(6), pp. 1438-49.

Ai, X., Do, A.-T., Kusche-Gullberg, M., Lindahl, U., Lu, K. and Emerson, C.P., Jr. (2006a) 'Substrate specificity and domain functions of extracellular heparan sulfate 6-O-endosulfatases, QSulf1 and QSulf2', *Journal of Biological Chemistry*, 281(8), pp. 4969-76.

Ai, X., Do, A.-T., Lozynska, O., Kusche-Gullberg, M., Lindahl, U. and Emerson, C.P., Jr. (2003a) 'QSulf1 remodels the 6-O sulfation states of cell surface heparan sulfate proteoglycans to promote Wnt signaling', *Journal of Cell Biology*, 162(2), pp. 341-51.

Ai, X., Do, A.T., Kusche-Gullberg, M., Lindahl, U., Lu, K. and Emerson, C.P., Jr. (2006b) 'Substrate specificity and domain functions of extracellular heparan sulfate 6-O-endosulfatases, QSulf1 and QSulf2', *Journal of Biological Chemistry*, 281(8), pp. 4969-76.

Ai, X., Do, A.T., Lozynska, O., Kusche-Gullberg, M., Lindahl, U. and Emerson, C.P., Jr. (2003b) 'QSulf1 remodels the 6-O sulfation states of cell surface heparan sulfate proteoglycans to promote Wnt signaling', *Journal of Cell Biology*, 162(2), pp. 341-51.

Aikawa, J., Grobe, K., Tsujimoto, M. and Esko, J.D. (2001) 'Multiple isozymes of heparan sulfate/heparin GlcNAc N-deacetylase/GlcN N-sulfotransferase. Structure and activity of the fourth member, NDST4', *Journal of Biological Chemistry*, 276(8), pp. 5876-82.

Alexopoulos, E., Seron, D., Hartley, R.B. and Cameron, J.S. (1990) 'Lupus nephritis: correlation of interstitial cells with glomerular function', *Kidney Int*, 37(1), pp. 100-9.

Ali, S., Fritchley, S.J., Chaffey, B.T. and Kirby, J.A. (2002) 'Contribution of the putative heparan sulfate-binding motif BBXB of RANTES to transendothelial migration', *Glycobiology*, 12(9), pp. 535-43.

Ali, S., Hardy, L.A. and Kirby, J.A. (2003) 'Transplant immunobiology: a crucial role for heparan sulfate glycosaminoglycans?', *Transplantation*, 75(11), pp. 1773-82.

Ali, S., Malik, G., Burns, A., Robertson, H. and Kirby, J.A. (2005a) 'Renal transplantation: examination of the regulation of chemokine binding during acute rejection', *Transplantation*, 79(6), pp. 672-9.

Ali, S., Palmer, A.C., Banerjee, B., Fritchley, S.J. and Kirby, J.A. (2000) 'Examination of the function of RANTES, MIP-1alpha, and MIP-1beta following interaction with heparin-like glycosaminoglycans', *J Biol Chem*, 275(16), pp. 11721-7.

Ali, S., Robertson, H., Wain, J.H., Isaacs, J.D., Malik, G. and Kirby, J.A. (2005b) 'A non-glycosaminoglycan-binding variant of CC chemokine ligand 7 (monocyte chemoattractant protein-3) antagonizes chemokine-mediated inflammation', *Journal of Immunology*, 175(2), pp. 1257-66.

Allen, B.L., Filla, M.S. and Rapraeger, A.C. (2001) 'Role of heparan sulfate as a tissue-specific regulator of FGF-4 and FGF receptor recognition', *Journal of Cell Biology*, 155(5), pp. 845-58.

Allen, B.L. and Rapraeger, A.C. (2003) 'Spatial and temporal expression of heparan sulfate in mouse development regulates FGF and FGF receptor assembly', *Journal of Cell Biology*, 163(3), pp. 637-48.

Alpers, C.E., Hudkins, K.L., Floege, J. and Johnson, R.J. (1994) 'Human renal cortical interstitial cells with some features of smooth muscle cells participate in tubulointerstitial and crescentic glomerular injury', *J Am Soc Nephrol*, 5(2), pp. 201-9.

Ashikari-Hada, S., Habuchi, H., Kariya, Y., Itoh, N., Reddi, A.H. and Kimata, K. (2004) 'Characterization of growth factor-binding structures in heparin/heparan sulfate using an octasaccharide library', *Journal of Biological Chemistry*, 279(13), pp. 12346-54.

Ashikari-Hada, S., Habuchi, H., Sugaya, N., Kobayashi, T. and Kimata, K. (2009) 'Specific inhibition of FGF-2 signaling with 2-O-sulfated octasaccharides of heparan sulfate', *Glycobiology*, 19(6), pp. 644-54.

Badid, C., Desmouliere, A., Babici, D., Hadj-Aissa, A., McGregor, B., Lefrancois, N., Touraine, J.L. and Laville, M. (2002) 'Interstitial expression of alpha-SMA: an early marker of chronic renal allograft dysfunction', *Nephrol Dial Transplant*, 17(11), pp. 1993-8.

Baird, A., Esch, F., Bohlen, P., Ling, N. and Gospodarowicz, D. (1985) 'Isolation and partial characterization of an endothelial cell growth factor from the bovine kidney: homology with basic fibroblast growth factor', *Regul Pept*, 12(3), pp. 201-13.

Baldwin, R.J., ten Dam, G.B., van Kuppevelt, T.H., Lacaud, G., Gallagher, J.T., Kouskoff, V. and Merry, C.L. (2008) 'A developmentally regulated heparan sulfate epitope defines a subpopulation with increased blood potential during mesodermal differentiation', *Stem Cells*, 26(12), pp. 3108-18.

Bame, K.J. (2001) 'Heparanases: endoglycosidases that degrade heparan sulfate proteoglycans', *Glycobiology*, 11(6), pp. 91R-98R.

Bandtlow, C.E. and Zimmermann, D.R. (2000) 'Proteoglycans in the developing brain: new conceptual insights for old proteins', *Physiol Rev*, 80(4), pp. 1267-90.

Banu, N. and Meyers, C.M. (1999) 'IFN-gamma and LPS differentially modulate class II MHC and B7-1 expression on murine renal tubular epithelial cells', *Kidney Int*, 55(6), pp. 2250-63.

Bengtsson, J., Eriksson, I. and Kjellen, L. (2003) 'Distinct effects on heparan sulfate structure by different active site mutations in NDST-1', *Biochemistry*, 42(7), pp. 2110-5.

Bernfield, M., Gotte, M., Park, P.W., Reizes, O., Fitzgerald, M.L., Lincecum, J. and Zako, M. (1999) 'Functions of cell surface heparan sulfate proteoglycans', *Annu Rev Biochem*, 68, pp. 729-77.

Bernfield, M., Kokenyesi, R., Kato, M., Hinkes, M.T., Spring, J., Gallo, R.L. and Lose, E.J. (1992) 'Biology of the syndecans: a family of transmembrane heparan sulfate proteoglycans', *Annu Rev Cell Biol*, 8, pp. 365-93.

Bink, R.J., Habuchi, H., Lele, Z., Dolk, E., Joore, J., Rauch, G.J., Geisler, R., Wilson, S.W., den Hertog, J., Kimata, K. and Zivkovic, D. (2003) 'Heparan sulfate 6-o-sulfotransferase is essential for muscle development in zebrafish', *J Biol Chem*, 278(33), pp. 31118-27.

Bishop, J.R., Schuksz, M. and Esko, J.D. (2007) 'Heparan sulphate proteoglycans fine-tune mammalian physiology', *Nature*, 446(7139), pp. 1030-7.

Bokemeyer, D., Guglielmi, K.E., McGinty, A., Sorokin, A., Lianos, E.A. and Dunn, M.J. (1997) 'Activation of extracellular signal-regulated kinase in proliferative glomerulonephritis in rats', *Journal of Clinical Investigation*, 100(3), pp. 582-8.

Border, W.A. and Noble, N.A. (1994) 'Transforming growth factor beta in tissue fibrosis', *N Engl J Med*, 331(19), pp. 1286-92.

Bosse, Y. and Rola-Pleszczynski, M. (2008) 'FGF2 in asthmatic airway-smooth-muscle-cell hyperplasia', *Trends Mol Med*, 14(1), pp. 3-11.

Brabletz, T., Jung, A., Reu, S., Porzner, M., Hlubek, F., Kunz-Schughart, L.A., Knuechel, R. and Kirchner, T. (2001) 'Variable beta-catenin expression in colorectal cancers indicates tumor progression driven by the tumor environment', *Proc Natl Acad Sci U S A*, 98(18), pp. 10356-61.

Brickman, Y.G., Ford, M.D., Small, D.H., Bartlett, P.F. and Nurcombe, V. (1995) 'Heparan sulfates mediate the binding of basic fibroblast growth factor to a specific receptor on neural precursor cells', *Journal of Biological Chemistry*, 270(42), pp. 24941-8.

Bullock, S.L., Fletcher, J.M., Beddington, R.S. and Wilson, V.A. (1998) 'Renal agenesis in mice homozygous for a gene trap mutation in the gene encoding heparan sulfate 2-sulfotransferase', *Genes Dev*, 12(12), pp. 1894-906.

Bulow, H.E. and Hobert, O. (2004) 'Differential sulfations and epimerization define heparan sulfate specificity in nervous system development', *Neuron*, 41(5), pp. 723-36.

Cardin, A.D. and Weintraub, H.J. (1989) 'Molecular modeling of protein-glycosaminoglycan interactions', *Arteriosclerosis*, 9(1), pp. 21-32.

Carey, D.J. (1997) 'Syndecans: multifunctional cell-surface co-receptors', *Biochem J*, 327 (Pt 1), pp. 1-16.

Carter, N.M., Ali, S. and Kirby, J.A. (2003) 'Endothelial inflammation: the role of differential expression of N-deacetylase/N-sulphotransferase enzymes in alteration of the immunological properties of heparan sulphate', *J Cell Sci*, 116(Pt 17), pp. 3591-600.

Casu, B. and Lindahl, U. (2001) 'Structure and biological interactions of heparin and heparan sulfate', *Advances in Carbohydrate Chemistry & Biochemistry*, 57, pp. 159-206.

Celie, J.W., Katta, K.K., Adepu, S., Melenhorst, W.B., Reijmers, R.M., Slot, E.M., Beelen, R.H., Spaargaren, M., Ploeg, R.J., Navis, G., van der Heide, J.J., van Dijk, M.C., van Goor, H. and van den Born, J. (2012) 'Tubular epithelial syndecan-1 maintains renal function in murine ischemia/reperfusion and human transplantation', *Kidney Int*.

Celie, J.W., Keuning, E.D., Beelen, R.H., Drager, A.M., Zweegman, S., Kessler, F.L., Soininen, R. and van den Born, J. (2005) 'Identification of L-selectin binding heparan sulfates attached to collagen type XVIII', *Journal of Biological Chemistry*, 280(29), pp. 26965-73.

Celie, J.W., Reijmers, R.M., Slot, E.M., Beelen, R.H., Spaargaren, M., Ter Wee, P.M., Florquin, S. and van den Born, J. (2008) 'Tubulointerstitial heparan sulfate proteoglycan changes in human renal diseases correlate with leukocyte influx and proteinuria', *Am J Physiol Renal Physiol*, 294(1), pp. F253-63.

Chang, T.L., Gordon, C.J., Roscic-Mrkic, B., Power, C., Proudfoot, A.E., Moore, J.P. and Trkola, A. (2002) 'Interaction of the CC-chemokine RANTES with glycosaminoglycans activates a p44/p42 mitogen-activated protein kinase-dependent signaling pathway and enhances human immunodeficiency virus type 1 infectivity', *J Virol*, 76(5), pp. 2245-54.

Chen, C.O., Park, M.H., Forbes, M.S., Thornhill, B.A., Kiley, S.C., Yoo, K.H. and Chevalier, R.L. (2007) 'Angiotensin-converting enzyme inhibition aggravates renal interstitial injury resulting from partial unilateral ureteral obstruction in the neonatal rat', *Am J Physiol Renal Physiol*, 292(3), pp. F946-55.

Chen, G., Wang, D., Vikramadithyan, R., Yagyu, H., Saxena, U., Pillarisetti, S. and Goldberg, I.J. (2004) 'Inflammatory cytokines and fatty acids regulate endothelial cell heparanase expression', *Biochemistry*, 43(17), pp. 4971-7.

Chen, R.L. and Lander, A.D. (2001) 'Mechanisms underlying preferential assembly of heparan sulfate on glypican-1', *J Biol Chem*, 276(10), pp. 7507-17.

Chevalier, R.L., Forbes, M.S. and Thornhill, B.A. (2009) 'Ureteral obstruction as a model of renal interstitial fibrosis and obstructive nephropathy', *Kidney Int*, 75(11), pp. 1145-52.

Cook, D.M., Hinkes, M.T., Bernfield, M. and Rauscher, F.J., 3rd (1996) 'Transcriptional activation of the syndecan-1 promoter by the Wilms' tumor protein WT1', *Oncogene*, 13(8), pp. 1789-99.

Cornell, L.D. and Colvin, R.B. (2005) 'Chronic allograft nephropathy', *Curr Opin Nephrol Hypertens*, 14(3), pp. 229-34.

Creely, J.J., DiMari, S.J., Howe, A.M. and Haralson, M.A. (1992) 'Effects of transforming growth factor-beta on collagen synthesis by normal rat kidney epithelial cells', *Am J Pathol*, 140(1), pp. 45-55.

Cunningham, A.C., Zhang, J.G., Moy, J.V., Ali, S. and Kirby, J.A. (1997) 'A comparison of the antigen-presenting capabilities of class II MHC-expressing human lung epithelial and endothelial cells', *Immunology*, 91(3), pp. 458-63.

Dai, E., Liu, L.Y., Wang, H., McIvor, D., Sun, Y.M., Macaulay, C., King, E., Munuswamy-Ramanujam, G., Bartee, M.Y., Williams, J., Davids, J., Charo, I., McFadden, G., Esko, J.D. and Lucas, A.R. (2010) 'Inhibition of chemokine-glycosaminoglycan interactions in donor tissue reduces mouse allograft vasculopathy and transplant rejection', *PLoS One*, 5(5), p. e10510.

Dai, Y., Yang, Y., MacLeod, V., Yue, X., Rapraeger, A.C., Shriver, Z., Venkataraman, G., Sasisekharan, R. and Sanderson, R.D. (2005) 'HSulf-1 and HSulf-2 are potent

inhibitors of myeloma tumor growth in vivo', *Journal of Biological Chemistry*, 280(48), pp. 40066-73.

Dailey, L., Ambrosetti, D., Mansukhani, A. and Basilico, C. (2005) 'Mechanisms underlying differential responses to FGF signaling', *Cytokine Growth Factor Rev*, 16(2), pp. 233-47.

Dalton, D.K., Pitts-Meek, S., Keshav, S., Figari, I.S., Bradley, A. and Stewart, T.A. (1993) 'Multiple defects of immune cell function in mice with disrupted interferon-gamma genes', *Science*, 259(5102), pp. 1739-42.

David, G., Bai, X.M., Van der Schueren, B., Cassiman, J.J. and Van den Berghe, H. (1992) 'Developmental changes in heparan sulfate expression: in situ detection with mAbs', *Journal of Cell Biology*, 119(4), pp. 961-75.

Dempsey, L.A., Brunn, G.J. and Platt, J.L. (2000) 'Heparanase, a potential regulator of cell-matrix interactions', *Trends Biochem Sci*, 25(8), pp. 349-51.

Dennissen, M.A., Jenniskens, G.J., Pieffers, M., Versteeg, E.M., Petitou, M., Veerkamp, J.H. and van Kuppevelt, T.H. (2002) 'Large, tissue-regulated domain diversity of heparan sulfates demonstrated by phage display antibodies', *Journal of Biological Chemistry*, 277(13), pp. 10982-6.

Dhoot, G.K., Gustafsson, M.K., Ai, X., Sun, W., Standiford, D.M. and Emerson, C.P., Jr. (2001) 'Regulation of Wnt signaling and embryo patterning by an extracellular sulfatase', *Science*, 293(5535), pp. 1663-6.

Do, A.T., Smeds, E., Spillmann, D. and Kusche-Gullberg, M. (2006) 'Overexpression of heparan sulfate 6-O-sulfotransferases in human embryonic kidney 293 cells results in increased N-acetylglucosaminyl 6-O-sulfation', *Journal of Biological Chemistry*, 281(9), pp. 5348-56.

Douglas, M.S., Rix, D.A., Larnkjaer, A., Dark, J.H., Talbot, D. and Kirby, J.A. (1997) 'Blockade of the interaction between interferon-gamma and endothelial glycosaminoglycans: a novel strategy for immunosuppression?', *Transplant Proc*, 29(1-2), pp. 1086-8.

Eddy, A.A. (1996) 'Molecular insights into renal interstitial fibrosis', *J Am Soc Nephrol*, 7(12), pp. 2495-508.

Eddy, A.A. (2000) 'Molecular basis of renal fibrosis', *Pediatr Nephrol*, 15(3-4), pp. 290-301.

Edgell, C.J., McDonald, C.C. and Graham, J.B. (1983) 'Permanent cell line expressing human factor VIII-related antigen established by hybridization', *Proc Natl Acad Sci U S A*, 80(12), pp. 3734-7.

Edovitsky, E., Lerner, I., Zcharia, E., Peretz, T., Vlodavsky, I. and Elkin, M. (2006) 'Role of endothelial heparanase in delayed-type hypersensitivity', *Blood*, 107(9), pp. 3609-16.

Eickelberg, O., Centrella, M., Reiss, M., Kashgarian, M. and Wells, R.G. (2002) 'Betaglycan inhibits TGF-beta signaling by preventing type I-type II receptor complex formation. Glycosaminoglycan modifications alter betaglycan function', *Journal of Biological Chemistry*, 277(1), pp. 823-9.

Einecke, G., Reeve, J., Sis, B., Mengel, M., Hidalgo, L., Famulski, K.S., Matas, A., Kasiske, B., Kaplan, B. and Halloran, P.F. (2010) 'A molecular classifier for predicting future graft loss in late kidney transplant biopsies', *Journal of Clinical Investigation*, 120(6), pp. 1862-72.

Elkin, M., Ilan, N., Ishai-Michaeli, R., Friedmann, Y., Papo, O., Pecker, I. and Vlodavsky, I. (2001) 'Heparanase as mediator of angiogenesis: mode of action', *Faseb J*, 15(9), pp. 1661-3.

Engelhardt, B. and Wolburg, H. (2004) 'Mini-review: Transendothelial migration of leukocytes: through the front door or around the side of the house?', *Eur J Immunol*, 34(11), pp. 2955-63.

Esko, J.D. and Selleck, S.B. (2002) 'Order out of chaos: assembly of ligand binding sites in heparan sulfate', *Annu Rev Biochem*, 71, pp. 435-71.

Esko, J.D., Stewart, T.E. and Taylor, W.H. (1985) 'Animal cell mutants defective in glycosaminoglycan biosynthesis', *Proc Natl Acad Sci U S A*, 82(10), pp. 3197-201.

Esko, J.D. and Zhang, L. (1996) 'Influence of core protein sequence on glycosaminoglycan assembly', *Current Opinion in Structural Biology*, 6(5), pp. 663-70.

Essawy, M., Soylemezoglu, O., Muchaneta-Kubara, E.C., Shortland, J., Brown, C.B. and el Nahas, A.M. (1997) 'Myofibroblasts and the progression of diabetic nephropathy', *Nephrol Dial Transplant*, 12(1), pp. 43-50.

Faham, S., Hileman, R.E., Fromm, J.R., Linhardt, R.J. and Rees, D.C. (1996) 'Heparin structure and interactions with basic fibroblast growth factor', *Science*, 271(5252), pp. 1116-20.

Fan, G., Xiao, L., Cheng, L., Wang, X., Sun, B. and Hu, G. (2000) 'Targeted disruption of NDST-1 gene leads to pulmonary hypoplasia and neonatal respiratory distress in mice', *FEBS Lett*, 467(1), pp. 7-11.

Feyzi, E., Lustig, F., Fager, G., Spillmann, D., Lindahl, U. and Salmivirta, M. (1997) 'Characterization of heparin and heparan sulfate domains binding to the long splice variant of platelet-derived growth factor A chain', *J Biol Chem*, 272(9), pp. 5518-24.

Feyzi, E., Saldeen, T., Larsson, E., Lindahl, U. and Salmivirta, M. (1998) 'Age-dependent modulation of heparan sulfate structure and function', *Journal of Biological Chemistry*, 273(22), pp. 13395-8.

Fidler, I.J. and Poste, G. (2008) 'The "seed and soil" hypothesis revisited', *Lancet Oncol*, 9(8), p. 808.

Filmus, J. and Selleck, S.B. (2001) 'Glypicans: proteoglycans with a surprise', *Journal of Clinical Investigation*, 108(4), pp. 497-501.

Flach, R., Speidel, N., Flohe, S., Borgermann, J., Dresen, I.G., Erhard, J. and Schade, F.U. (1998) 'Analysis of intragraft cytokine expression during early reperfusion after liver transplantation using semi-quantitative RT-PCR', *Cytokine*, 10(6), pp. 445-51.

Floege, J., Eng, E., Lindner, V., Alpers, C.E., Young, B.A., Reidy, M.A. and Johnson, R.J. (1992) 'Rat glomerular mesangial cells synthesize basic fibroblast growth factor. Release, upregulated synthesis, and mitogenicity in mesangial proliferative glomerulonephritis', *J Clin Invest*, 90(6), pp. 2362-9.

Floege, J., Eng, E., Young, B.A., Alpers, C.E., Barrett, T.B., Bowen-Pope, D.F. and Johnson, R.J. (1993) 'Infusion of platelet-derived growth factor or basic fibroblast growth factor induces selective glomerular mesangial cell proliferation and matrix accumulation in rats', *J Clin Invest*, 92(6), pp. 2952-62.

Floege, J., Hudkins, K.L., Eitner, F., Cui, Y., Morrison, R.S., Schelling, M.A. and Alpers, C.E. (1999) 'Localization of fibroblast growth factor-2 (basic FGF) and FGF receptor-1 in adult human kidney', *Kidney Int*, 56(3), pp. 883-97.

Forsberg, E. and Kjellen, L. (2001) 'Heparan sulfate: lessons from knockout mice', *Journal of Clinical Investigation*, 108(2), pp. 175-80.

Forsberg, E., Pejler, G., Ringvall, M., Lunderius, C., Tomasini-Johansson, B., Kusche-Gullberg, M., Eriksson, I., Ledin, J., Hellman, L. and Kjellen, L. (1999) 'Abnormal mast cells in mice deficient in a heparin-synthesizing enzyme', *Nature*, 400(6746), pp. 773-6.

Frese, M.A., Milz, F., Dick, M., Lamanna, W.C. and Dierks, T. (2009) 'Characterization of the human sulfatase Sulf1 and its high affinity heparin/heparan sulfate interaction domain', *Journal of Biological Chemistry*, 284(41), pp. 28033-44.

Friedl, A., Filla, M. and Rapraeger, A.C. (2001) 'Tissue-specific binding by FGF and FGF receptors to endogenous heparan sulfates', *Methods Mol Biol*, 171, pp. 535-46.

Fritchley, S.J., Kirby, J.A. and Ali, S. (2000) 'The antagonism of interferon-gamma (IFN-gamma) by heparin: examination of the blockade of class II MHC antigen and heat shock protein-70 expression', *Clin Exp Immunol*, 120(2), pp. 247-52.

Funderburgh, J.L., Funderburgh, M.L., Mann, M.M., Corpuz, L. and Roth, M.R. (2001) 'Proteoglycan expression during transforming growth factor beta -induced keratocyte-myofibroblast transdifferentiation', *Journal of Biological Chemistry*, 276(47), pp. 44173-8.

Gabbiani, G., Kapanci, Y., Barazzone, P. and Franke, W.W. (1981) 'Immunochemical identification of intermediate-sized filaments in human neoplastic cells. A diagnostic aid for the surgical pathologist', *Am J Pathol*, 104(3), pp. 206-16.

Gallagher, J.T., Turnbull, J.E. and Lyon, M. (1990) 'Heparan sulphate proteoglycans', *Biochem Soc Trans*, 18(2), pp. 207-9.

Gallagher, J.T., Turnbull, J.E. and Lyon, M. (1992) 'Patterns of sulphation in heparan sulphate: polymorphism based on a common structural theme', *Int J Biochem*, 24(4), pp. 553-60.

Girardin, E.P., Hajmohammadi, S., Birmele, B., Helisch, A., Shworak, N.W. and de Agostini, A.I. (2005) 'Synthesis of anticoagulantly active heparan sulfate proteoglycans by glomerular epithelial cells involves multiple 3-O-sulfotransferase isoforms and a limiting precursor pool', *Journal of Biological Chemistry*, 280(45), pp. 38059-70.

Gobe, G.C. and Axelsen, R.A. (1987) 'Genesis of renal tubular atrophy in experimental hydronephrosis in the rat. Role of apoptosis', *Lab Invest*, 56(3), pp. 273-81.

Gomes, R.R., Jr., Van Kuppevelt, T.H., Farach-Carson, M.C. and Carson, D.D. (2006) 'Spatiotemporal distribution of heparan sulfate epitopes during murine cartilage growth plate development', *Histochem Cell Biol*, 126(6), pp. 713-22.

Gotte, M. (2003) 'Syndecans in inflammation', *Faseb J*, 17(6), pp. 575-91.

Gotte, M., Bernfield, M. and Joussen, A.M. (2005) 'Increased leukocyte-endothelial interactions in syndecan-1-deficient mice involve heparan sulfate-dependent and -independent steps', *Curr Eye Res*, 30(6), pp. 417-22.

Gourishankar, S. and Halloran, P.F. (2002) 'Late deterioration of organ transplants: a problem in injury and homeostasis', *Curr Opin Immunol*, 14(5), pp. 576-83.

Groffen, A.J., Ruegg, M.A., Dijkman, H., van de Velden, T.J., Buskens, C.A., van den Born, J., Assmann, K.J., Monnens, L.A., Veerkamp, J.H. and van den Heuvel, L.P. (1998) 'Agrin is a major heparan sulfate proteoglycan in the human glomerular basement membrane', *J Histochem Cytochem*, 46(1), pp. 19-27.

Guglieri, S., Hricovini, M., Raman, R., Polito, L., Torri, G., Casu, B., Sasisekharan, R. and Guerrini, M. (2008) 'Minimum FGF2 Binding Structural Requirements of Heparin and Heparan Sulfate Oligosaccharides As Determined by NMR Spectroscopy (dagger)', *Biochemistry*.

Guimond, S., Maccarana, M., Olwin, B.B., Lindahl, U. and Rapraeger, A.C. (1993) 'Activating and inhibitory heparin sequences for FGF-2 (basic FGF). Distinct requirements for FGF-1, FGF-2, and FGF-4', *J Biol Chem*, 268(32), pp. 23906-14.

Habuchi, H., Habuchi, O. and Kimata, K. (2004) 'Sulfation pattern in glycosaminoglycan: does it have a code?', *Glycoconj J*, 21(1-2), pp. 47-52.

Habuchi, H., Miyake, G., Nogami, K., Kuroiwa, A., Matsuda, Y., Kusche-Gullberg, M., Habuchi, O., Tanaka, M. and Kimata, K. (2003) 'Biosynthesis of heparan sulphate with diverse structures and functions: two alternatively spliced forms of human heparan sulphate 6-O-sulphotransferase-2 having different expression patterns and properties', *Biochem J*, 371(Pt 1), pp. 131-42.

Habuchi, H., Nagai, N., Sugaya, N., Atsumi, F., Stevens, R.L. and Kimata, K. (2007) 'Mice deficient in heparan sulfate 6-O-sulfotransferase-1 exhibit defective heparan sulfate biosynthesis, abnormal placentation, and late embryonic lethality', *Journal of Biological Chemistry*, 282(21), pp. 15578-88.

Habuchi, H., Suzuki, S., Saito, T., Tamura, T., Harada, T., Yoshida, K. and Kimata, K. (1992) 'Structure of a heparan sulphate oligosaccharide that binds to basic fibroblast growth factor', *Biochem J*, 285 (Pt 3), pp. 805-13.

Habuchi, H., Tanaka, M., Habuchi, O., Yoshida, K., Suzuki, H., Ban, K. and Kimata, K. (2000) 'The occurrence of three isoforms of heparan sulfate 6-O-sulfotransferase having different specificities for hexuronic acid adjacent to the targeted N-sulfoglucosamine', *Journal of Biological Chemistry*, 275(4), pp. 2859-68.

Habuchi, O. (2000) 'Diversity and functions of glycosaminoglycan sulfotransferases', *Biochim Biophys Acta*, 1474(2), pp. 115-27.

Hacker, U., Nybakken, K. and Perrimon, N. (2005) 'Heparan sulphate proteoglycans: the sweet side of development', *Nature Reviews Molecular Cell Biology*, 6(7), pp. 530-41.

Halfter, W., Dong, S., Schurer, B. and Cole, G.J. (1998) 'Collagen XVIII is a basement membrane heparan sulfate proteoglycan', *Journal of Biological Chemistry*, 273(39), pp. 25404-12.

Halloran, P.F., Urmson, J., Ramassar, V., Laskin, C. and Autenried, P. (1988) 'Increased class I and class II MHC products and mRNA in kidneys of MRL-lpr/lpr mice during

autoimmune nephritis and inhibition by cyclosporine', *Journal of Immunology*, 141(7), pp. 2303-12.

Harvey, J.R., Mellor, P., Eldaly, H., Lennard, T.W., Kirby, J.A. and Ali, S. (2007) 'Inhibition of CXCR4-mediated breast cancer metastasis: a potential role for heparinoids?', *Clin Cancer Res*, 13(5), pp. 1562-70.

Hewitson, T.D., Kelynack, K.J., Tait, M.G., Martic, M., Jones, C.L., Margolin, S.B. and Becker, G.J. (2001) 'Pirfenidone reduces in vitro rat renal fibroblast activation and mitogenesis', *J Nephrol*, 14(6), pp. 453-60.

Hileman, R.E., Fromm, J.R., Weiler, J.M. and Linhardt, R.J. (1998) 'Glycosaminoglycan-protein interactions: definition of consensus sites in glycosaminoglycan binding proteins', *Bioessays*, 20(2), pp. 156-67.

Hillyer, P., Mordelet, E., Flynn, G. and Male, D. (2003) 'Chemokines, chemokine receptors and adhesion molecules on different human endothelia: discriminating the tissue-specific functions that affect leucocyte migration', *Clin Exp Immunol*, 134(3), pp. 431-41.

Holmborn, K., Ledin, J., Smeds, E., Eriksson, I., Kusche-Gullberg, M. and Kjellen, L. (2004) 'Heparan sulfate synthesized by mouse embryonic stem cells deficient in NDST1 and NDST2 is 6-O-sulfated but contains no N-sulfate groups', *Journal of Biological Chemistry*, 279(41), pp. 42355-8.

Holst, C.R., Bou-Reslan, H., Gore, B.B., Wong, K., Grant, D., Chalasani, S., Carano, R.A., Frantz, G.D., Tessier-Lavigne, M., Bolon, B., French, D.M. and Ashkenazi, A. (2007) 'Secreted sulfatases Sulf1 and Sulf2 have overlapping yet essential roles in mouse neonatal survival', *PLoS One*, 2(6), p. e575.

Hoogewerf, A.J., Kuschert, G.S., Proudfoot, A.E., Borlat, F., Clark-Lewis, I., Power, C.A. and Wells, T.N. (1997) 'Glycosaminoglycans mediate cell surface oligomerization of chemokines', *Biochemistry*, 36(44), pp. 13570-8.

Hulett, M.D., Freeman, C., Hamdorf, B.J., Baker, R.T., Harris, M.J. and Parish, C.R. (1999) 'Cloning of mammalian heparanase, an important enzyme in tumor invasion and metastasis', *Nat Med*, 5(7), pp. 803-9.

Humes, H.D., Nakamura, T., Cieslinski, D.A., Miller, D., Emmons, R.V. and Border, W.A. (1993) 'Role of proteoglycans and cytoskeleton in the effects of TGF-beta 1 on renal proximal tubule cells', *Kidney Int*, 43(3), pp. 575-84.

Huynh, M.B., Morin, C., Carpentier, G., Garcia-Filipe, S., Talhas-Perret, S., Barbier-Chassefiere, V., van Kuppevelt, T.H., Martelly, I., Albanese, P. and Papy-Garcia, D. (2012) 'Age-related changes in glycosaminoglycans from rat myocardium involve altered capacities to potentiate growth factors functions and heparan sulfate altered sulfation', *Journal of Biological Chemistry*.

Iida-Hasegawa, N., Furuhata, A., Hayatsu, H., Murakami, A., Fujiki, K., Nakayasu, K. and Kanai, A. (2003) 'Mutations in the CHST6 gene in patients with macular corneal dystrophy: immunohistochemical evidence of heterogeneity', *Invest Ophthalmol Vis Sci*, 44(8), pp. 3272-7.

Ishihara, M., Kariya, Y., Kikuchi, H., Minamisawa, T. and Yoshida, K. (1997) 'Importance of 2-O-sulfate groups of uronate residues in heparin for activation of FGF-1 and FGF-2', *J Biochem*, 121(2), pp. 345-9.

Ishihara, M., Shaklee, P.N., Yang, Z., Liang, W., Wei, Z., Stack, R.J. and Holme, K. (1994) 'Structural features in heparin which modulate specific biological activities mediated by basic fibroblast growth factor', *Glycobiology*, 4(4), pp. 451-8.

Itoh, N. and Ornitz, D.M. (2004) 'Evolution of the Fgf and Fgfr gene families', *Trends Genet*, 20(11), pp. 563-9.

Ivanyi, B. and Olsen, S. (1995) 'Tubulitis in renal disease', *Curr Top Pathol*, 88, pp. 117-43.

Iwano, M., Plieth, D., Danoff, T.M., Xue, C., Okada, H. and Neilson, E.G. (2002) 'Evidence that fibroblasts derive from epithelium during tissue fibrosis', *Journal of Clinical Investigation*, 110(3), pp. 341-50.

Izvolsky, K.I., Lu, J., Martin, G., Albrecht, K.H. and Cardoso, W.V. (2008) 'Systemic inactivation of Hs6st1 in mice is associated with late postnatal mortality without major defects in organogenesis', *Genesis*, 46(1), pp. 8-18.

Jackson, R.L., Busch, S.J. and Cardin, A.D. (1991) 'Glycosaminoglycans: molecular properties, protein interactions, and role in physiological processes', *Physiol Rev*, 71(2), pp. 481-539.

Jacobsson, I., Lindahl, U., Jensen, J.W., Roden, L., Prihar, H. and Feingold, D.S. (1984) 'Biosynthesis of heparin. Substrate specificity of heparosan N-sulfate D-glucuronosyl 5-epimerase', *Journal of Biological Chemistry*, 259(2), pp. 1056-63.

Jastrebova, N., Vanwildemeersch, M., Lindahl, U. and Spillmann, D. (2010) 'Heparan sulfate domain organization and sulfation modulate FGF-induced cell signaling', *Journal of Biological Chemistry*, 285(35), pp. 26842-51.

Jastrebova, N., Vanwildemeersch, M., Rapraeger, A.C., Gimenez-Gallego, G., Lindahl, U. and Spillmann, D. (2006) 'Heparan sulfate-related oligosaccharides in ternary complex formation with fibroblast growth factors 1 and 2 and their receptors', *Journal of Biological Chemistry*, 281(37), pp. 26884-92.

Jayson, G.C., Lyon, M., Paraskeva, C., Turnbull, J.E., Deakin, J.A. and Gallagher, J.T. (1998) 'Heparan sulfate undergoes specific structural changes during the progression from human colon adenoma to carcinoma in vitro', *J Biol Chem*, 273(1), pp. 51-7.

Jemth, P., Kreuger, J., Kusche-Gullberg, M., Sturiale, L., Gimenez-Gallego, G. and Lindahl, U. (2002) 'Biosynthetic oligosaccharide libraries for identification of protein-binding heparan sulfate motifs. Exploring the structural diversity by screening for fibroblast growth factor (FGF)1 and FGF2 binding', *Journal of Biological Chemistry*, 277(34), pp. 30567-73.

Jemth, P., Smeds, E., Do, A.T., Habuchi, H., Kimata, K., Lindahl, U. and Kusche-Gullberg, M. (2003) 'Oligosaccharide library-based assessment of heparan sulfate 6-O-sulfotransferase substrate specificity', *Journal of Biological Chemistry*, 278(27), pp. 24371-6.

Jimenez, J.J., Jy, W., Mauro, L.M., Horstman, L.L., Soderland, C. and Ahn, Y.S. (2003) 'Endothelial microparticles released in thrombotic thrombocytopenic purpura express von

Willebrand factor and markers of endothelial activation', *Br J Haematol*, 123(5), pp. 896-902.

Jones, S.G., Morrisey, K., Williams, J.D. and Phillips, A.O. (1999) 'TGF-beta1 stimulates the release of pre-formed bFGF from renal proximal tubular cells', *Kidney Int*, 56(1), pp. 83-91.

Joosten, S.A., van Dixhoorn, M.G., Borrias, M.C., Benediktsson, H., van Veelen, P.A., van Kooten, C. and Paul, L.C. (2002) 'Antibody response against perlecan and collagen types IV and VI in chronic renal allograft rejection in the rat', *Am J Pathol*, 160(4), pp. 1301-10.

Kakuta, Y., Sueyoshi, T., Negishi, M. and Pedersen, L.C. (1999) 'Crystal structure of the sulfotransferase domain of human heparan sulfate N-deacetylase/ N-sulfotransferase 1', *Journal of Biological Chemistry*, 274(16), pp. 10673-6.

Kalluri, R. and Neilson, E.G. (2003) 'Epithelial-mesenchymal transition and its implications for fibrosis', *Journal of Clinical Investigation*, 112(12), pp. 1776-84.

Kalluri, R. and Weinberg, R.A. (2009) 'The basics of epithelial-mesenchymal transition', *Journal of Clinical Investigation*, 119(6), pp. 1420-8.

Kalus, I., Salmen, B., Viebahn, C., von Figura, K., Schmitz, D., D'Hooge, R. and Dierks, T. (2009) 'Differential involvement of the extracellular 6-O-endosulfatases Sulf1 and Sulf2 in brain development and neuronal and behavioural plasticity', *J Cell Mol Med*, 13(11-12), pp. 4505-21.

Kamimura, K., Fujise, M., Villa, F., Izumi, S., Habuchi, H., Kimata, K. and Nakato, H. (2001) 'Drosophila heparan sulfate 6-O-sulfotransferase (dHS6ST) gene. Structure, expression, and function in the formation of the tracheal system', *J Biol Chem*, 276(20), pp. 17014-21.

Kamimura, K., Koyama, T., Habuchi, H., Ueda, R., Masu, M., Kimata, K. and Nakato, H. (2006) 'Specific and flexible roles of heparan sulfate modifications in Drosophila FGF signaling', *Journal of Cell Biology*, 174(6), pp. 773-8.

Kamiyama, S., Sasaki, N., Goda, E., Ui-Tei, K., Saigo, K., Narimatsu, H., Jigami, Y., Kannagi, R., Irimura, T. and Nishihara, S. (2006) 'Molecular cloning and characterization of a novel 3'-phosphoadenosine 5'-phosphosulfate transporter, PAPST2', *Journal of Biological Chemistry*, 281(16), pp. 10945-53.

Kamiyama, S., Suda, T., Ueda, R., Suzuki, M., Okubo, R., Kikuchi, N., Chiba, Y., Goto, S., Toyoda, H., Saigo, K., Watanabe, M., Narimatsu, H., Jigami, Y. and Nishihara, S. (2003) 'Molecular cloning and identification of 3'-phosphoadenosine 5'-phosphosulfate transporter', *Journal of Biological Chemistry*, 278(28), pp. 25958-63.

Kanwar, Y.S. and Farquhar, M.G. (1979) 'Anionic sites in the glomerular basement membrane. In vivo and in vitro localization to the laminae rarae by cationic probes', *Journal of Cell Biology*, 81(1), pp. 137-53.

Kashihara, N., Watanabe, Y., Makino, H. and Kanwar, Y.S. (1992) 'Interleukin-1-induced alterations in glomerular proteoglycans: biochemical and tissue autoradiographic aspects', *J Am Soc Nephrol*, 3(2), pp. 203-13.

Kato, M., Saunders, S., Nguyen, H. and Bernfield, M. (1995) 'Loss of cell surface syndecan-1 causes epithelia to transform into anchorage-independent mesenchyme-like cells', *Mol Biol Cell*, 6(5), pp. 559-76.

Katz, M., Amit, I. and Yarden, Y. (2007) 'Regulation of MAPKs by growth factors and receptor tyrosine kinases', *Biochim Biophys Acta*, 1773(8), pp. 1161-76.

Kelynack, K.J., Hewitson, T.D., Pedagogos, E., Nicholls, K.M. and Becker, G.J. (1999) 'Renal myofibroblasts contract collagen I matrix lattices in vitro', *Am J Nephrol*, 19(6), pp. 694-701.

Kim, C.W., Goldberger, O.A., Gallo, R.L. and Bernfield, M. (1994) 'Members of the syndecan family of heparan sulfate proteoglycans are expressed in distinct cell-, tissue-, and development-specific patterns', *Mol Biol Cell*, 5(7), pp. 797-805.

Kissmeyer-Nielsen, F., Olsen, S., Petersen, V.P. and Fjeldborg, O. (1966) 'Hyperacute rejection of kidney allografts, associated with pre-existing humoral antibodies against donor cells', *Lancet*, 2(7465), pp. 662-5.

Kitagawa, H., Egusa, N., Tamura, J.I., Kusche-Gullberg, M., Lindahl, U. and Sugahara, K. (2001) 'rib-2, a Caenorhabditis elegans homolog of the human tumor suppressor EXT genes encodes a novel alpha1,4-N-acetylglucosaminyltransferase involved in the biosynthetic initiation and elongation of heparan sulfate', *Journal of Biological Chemistry*, 276(7), pp. 4834-8.

Kitagawa, H., Tone, Y., Tamura, J., Neumann, K.W., Ogawa, T., Oka, S., Kawasaki, T. and Sugahara, K. (1998) 'Molecular cloning and expression of glucuronyltransferase I involved in the biosynthesis of the glycosaminoglycan-protein linkage region of proteoglycans', *J Biol Chem*, 273(12), pp. 6615-8.

Kjellen, L. and Lindahl, U. (1991) 'Proteoglycans: structures and interactions', *Annu Rev Biochem*, 60, pp. 443-75.

Klahr, S. and Morrissey, J. (2002) 'Obstructive nephropathy and renal fibrosis', *Am J Physiol Renal Physiol*, 283(5), pp. F861-75.

Klein, N.J., Shennan, G.I., Heyderman, R.S. and Levin, M. (1992) 'Alteration in glycosaminoglycan metabolism and surface charge on human umbilical vein endothelial cells induced by cytokines, endotoxin and neutrophils', *J Cell Sci*, 102 (Pt 4), pp. 821-32.

Klint, P. and Claesson-Welsh, L. (1999) 'Signal transduction by fibroblast growth factor receptors', *Front Biosci*, 4, pp. D165-77.

Klint, P., Kanda, S., Kloog, Y. and Claesson-Welsh, L. (1999) 'Contribution of Src and Ras pathways in FGF-2 induced endothelial cell differentiation', *Oncogene*, 18(22), pp. 3354-64.

Klymkowsky, M.W. and Savagner, P. (2009) 'Epithelial-mesenchymal transition: a cancer researcher's conceptual friend and foe', *Am J Pathol*, 174(5), pp. 1588-93.

Kobayashi, M., Habuchi, H., Habuchi, O., Saito, M. and Kimata, K. (1996) 'Purification and characterization of heparan sulfate 2-sulfotransferase from cultured Chinese hamster ovary cells', *J Biol Chem*, 271(13), pp. 7645-53.

Kobayashi, M., Habuchi, H., Yoneda, M., Habuchi, O. and Kimata, K. (1997) 'Molecular cloning and expression of Chinese hamster ovary cell heparan-sulfate 2-sulfotransferase', *J Biol Chem*, 272(21), pp. 13980-5.

Kobayashi, T., Habuchi, H., Nogami, K., Ashikari-Hada, S., Tamura, K., Ide, H. and Kimata, K. (2010) 'Functional analysis of chick heparan sulfate 6-O-sulfotransferases in limb bud development', *Dev Growth Differ*, 52(2), pp. 146-56.

Kopp, J.B., Factor, V.M., Mozes, M., Nagy, P., Sanderson, N., Bottinger, E.P., Klotman, P.E. and Thorgeirsson, S.S. (1996) 'Transgenic mice with increased plasma levels of TGF-beta 1 develop progressive renal disease', *Lab Invest*, 74(6), pp. 991-1003.

Kreuger, J., Jemth, P., Sanders-Lindberg, E., Eliahu, L., Ron, D., Basilico, C., Salmivirta, M. and Lindahl, U. (2005) 'Fibroblast growth factors share binding sites in heparan sulphate', *Biochem J*, 389(Pt 1), pp. 145-50.

Kreuger, J., Salmivirta, M., Sturiale, L., Gimenez-Gallego, G. and Lindahl, U. (2001) 'Sequence analysis of heparan sulfate epitopes with graded affinities for fibroblast growth factors 1 and 2', *Journal of Biological Chemistry*, 276(33), pp. 30744-52.

Kreuger, J., Spillmann, D., Li, J.-p. and Lindahl, U. (2006) 'Interactions between heparan sulfate and proteins: the concept of specificity', *Journal of Cell Biology*, 174(3), pp. 323-7.

Kriz, W., Hahnel, B., Rosener, S. and Elger, M. (1995) 'Long-term treatment of rats with FGF-2 results in focal segmental glomerulosclerosis', *Kidney Int*, 48(5), pp. 1435-50.

Kusche-Gullberg, M. and Kjellen, L. (2003) 'Sulfotransferases in glycosaminoglycan biosynthesis', *Current Opinion in Structural Biology*, 13(5), pp. 605-11.

Kusche, M. and Lindahl, U. (1990) 'Biosynthesis of heparin. O-sulfation of D-glucuronic acid units', *J Biol Chem*, 265(26), pp. 15403-9.

Lai, J., Chien, J., Staub, J., Avula, R., Greene, E.L., Matthews, T.A., Smith, D.I., Kaufmann, S.H., Roberts, L.R. and Shridhar, V. (2003) 'Loss of HSulf-1 up-regulates heparin-binding growth factor signaling in cancer', *J Biol Chem*, 278(25), pp. 23107-17.

Lai, J.P., Chien, J., Strome, S.E., Staub, J., Montoya, D.P., Greene, E.L., Smith, D.I., Roberts, L.R. and Shridhar, V. (2004a) 'HSulf-1 modulates HGF-mediated tumor cell invasion and signaling in head and neck squamous carcinoma', *Oncogene*, 23(7), pp. 1439-47.

Lai, J.P., Chien, J.R., Moser, D.R., Staub, J.K., Aderca, I., Montoya, D.P., Matthews, T.A., Nagorney, D.M., Cunningham, J.M., Smith, D.I., Greene, E.L., Shridhar, V. and Roberts, L.R. (2004b) 'hSulf1 Sulfatase promotes apoptosis of hepatocellular cancer cells by decreasing heparin-binding growth factor signaling', *Gastroenterology*, 126(1), pp. 231-48.

Lai, J.P., Sandhu, D.S., Yu, C., Han, T., Moser, C.D., Jackson, K.K., Guerrero, R.B., Aderca, I., Isomoto, H., Garrity-Park, M.M., Zou, H., Shire, A.M., Nagorney, D.M., Sanderson, S.O., Adjei, A.A., Lee, J.S., Thorgeirsson, S.S. and Roberts, L.R. (2008a) 'Sulfatase 2 up-regulates glypican 3, promotes fibroblast growth factor signaling, and decreases survival in hepatocellular carcinoma', *Hepatology*, 47(4), pp. 1211-22.

Lai, J.P., Thompson, J.R., Sandhu, D.S. and Roberts, L.R. (2008b) 'Heparin-degrading sulfatases in hepatocellular carcinoma: roles in pathogenesis and therapy targets', *Future Oncol*, 4(6), pp. 803-14.

Lamanna, W.C., Baldwin, R.J., Padva, M., Kalus, I., Ten Dam, G., van Kuppevelt, T.H., Gallagher, J.T., von Figura, K., Dierks, T. and Merry, C.L. (2006) 'Heparan sulfate 6-O-endosulfatases: discrete in vivo activities and functional co-operativity', *Biochem J*, 400(1), pp. 63-73.

Lamanna, W.C., Frese, M.A., Balleininger, M. and Dierks, T. (2008) 'Sulf loss influences N-, 2-O-, and 6-O-sulfation of multiple heparan sulfate proteoglycans and modulates fibroblast growth factor signaling', *Journal of Biological Chemistry*, 283(41), pp. 27724-35.

Lamanna, W.C., Kalus, I., Padva, M., Baldwin, R.J., Merry, C.L. and Dierks, T. (2007) 'The heparanome--the enigma of encoding and decoding heparan sulfate sulfation', *J Biotechnol*, 129(2), pp. 290-307.

Lan, H.Y. (2003) 'Tubular epithelial-myofibroblast transdifferentiation mechanisms in proximal tubule cells', *Curr Opin Nephrol Hypertens*, 12(1), pp. 25-9.

Lander, A.D., Stipp, C.S. and Ivins, J.K. (1996) 'The glypican family of heparan sulfate proteoglycans: major cell-surface proteoglycans of the developing nervous system', *Perspect Dev Neurobiol*, 3(4), pp. 347-58.

Le Moine, A., Goldman, M. and Abramowicz, D. (2002) 'Multiple pathways to allograft rejection', *Transplantation*, 73(9), pp. 1373-81.

Lemjabbar-Alaoui, H., van Zante, A., Singer, M.S., Xue, Q., Wang, Y.Q., Tsay, D., He, B., Jablons, D.M. and Rosen, S.D. (2010) 'Sulf-2, a heparan sulfate endosulfatase, promotes human lung carcinogenesis', *Oncogene*, 29(5), pp. 635-46.

Lensen, J.F., Rops, A.L., Wijnhoven, T.J., Hafmans, T., Feitz, W.F., Oosterwijk, E., Banas, B., Bindels, R.J., van den Heuvel, L.P., van der Vlag, J., Berden, J.H. and van Kuppevelt, T.H. (2005) 'Localization and functional characterization of glycosaminoglycan domains in the normal human kidney as revealed by phage display-derived single chain antibodies', *J Am Soc Nephrol*, 16(5), pp. 1279-88.

Leteux, C., Chai, W., Nagai, K., Herbert, C.G., Lawson, A.M. and Feizi, T. (2001) '10E4 antigen of Scrapie lesions contains an unusual nonsulfated heparan motif', *J Biol Chem*, 276(16), pp. 12539-45.

Ley, K., Laudanna, C., Cybulsky, M.I. and Nourshargh, S. (2007) 'Getting to the site of inflammation: the leukocyte adhesion cascade updated', *Nat Rev Immunol*, 7(9), pp. 678-89.

Li, J., Hagner-McWhirter, A., Kjellen, L., Palgi, J., Jalkanen, M. and Lindahl, U. (1997) 'Biosynthesis of heparin/heparan sulfate. cDNA cloning and expression of D-glucuronyl C5-epimerase from bovine lung', *J Biol Chem*, 272(44), pp. 28158-63.

Li, J.P., Gong, F., Hagner-McWhirter, A., Forsberg, E., Abrink, M., Kisilevsky, R., Zhang, X. and Lindahl, U. (2003) 'Targeted disruption of a murine glucuronyl C5-epimerase gene results in heparan sulfate lacking L-iduronic acid and in neonatal lethality', *Journal of Biological Chemistry*, 278(31), pp. 28363-6.

Li, Q., Park, P.W., Wilson, C.L. and Parks, W.C. (2002) 'Matrilysin shedding of syndecan-1 regulates chemokine mobilization and transepithelial efflux of neutrophils in acute lung injury', *Cell*, 111(5), pp. 635-46.

Lin, X. (2004) 'Functions of heparan sulfate proteoglycans in cell signaling during development', *Development*, 131(24), pp. 6009-21.

Lin, X., Buff, E.M., Perrimon, N. and Michelson, A.M. (1999) 'Heparan sulfate proteoglycans are essential for FGF receptor signaling during Drosophila embryonic development', *Development*, 126(17), pp. 3715-23.

Lin, X., Wei, G., Shi, Z., Dryer, L., Esko, J.D., Wells, D.E. and Matzuk, M.M. (2000) 'Disruption of gastrulation and heparan sulfate biosynthesis in EXT1-deficient mice', *Developmental Biology*, 224(2), pp. 299-311.

Lind, T.T., F.McCormick, C., Lindahl, U. and Lidholt, K. (1998) 'The putative tumor suppressors EXT1 and EXT2 are glycosyltransferases required for the biosynthesis of heparan sulfate', *Journal of Biological Chemistry*, 273(41), pp. 26265-8.

Lindahl, U. (2007) 'Heparan sulfate-protein interactions--a concept for drug design?', *Thromb Haemost*, 98(1), pp. 109-15.

Lindahl, U., Kusche-Gullberg, M. and Kjellen, L. (1998) 'Regulated diversity of heparan sulfate', *Journal of Biological Chemistry*, 273(39), pp. 24979-82.

Lindahl, U.K.-G., M. and Kjellen, L. (1998) 'Regulated diversity of heparan sulfate', *Journal of Biological Chemistry*, 273(39), pp. 24979-82.

Liu, J., Shriver, Z., Blaiklock, P., Yoshida, K., Sasisekharan, R. and Rosenberg, R.D. (1999a) 'Heparan sulfate D-glucosaminyl 3-O-sulfotransferase-3A sulfates N-unsubstituted glucosamine residues', *J Biol Chem*, 274(53), pp. 38155-62.

Liu, J., Shworak, N.W., Sinay, P., Schwartz, J.J., Zhang, L., Fritze, L.M. and Rosenberg, R.D. (1999b) 'Expression of heparan sulfate D-glucosaminyl 3-O-sulfotransferase isoforms reveals novel substrate specificities', *J Biol Chem*, 274(8), pp. 5185-92.

Lohse, D.L. and Linhardt, R.J. (1992) 'Purification and characterization of heparin lyases from Flavobacterium heparinum', *Journal of Biological Chemistry*, 267(34), pp. 24347-55.

Lonnemann, G., Shapiro, L., Engler-Blum, G., Muller, G.A., Koch, K.M. and Dinarello, C.A. (1995) 'Cytokines in human renal interstitial fibrosis. I. Interleukin-1 is a paracrine growth factor for cultured fibrosis-derived kidney fibroblasts', *Kidney Int*, 47(3), pp. 837-44.

Loo, B.M., Kreuger, J., Jalkanen, M., Lindahl, U. and Salmivirta, M. (2001) 'Binding of heparin/heparan sulfate to fibroblast growth factor receptor 4', *Journal of Biological Chemistry*, 276(20), pp. 16868-76.

Loo, B.M. and Salmivirta, M. (2002) 'Heparin/Heparan sulfate domains in binding and signaling of fibroblast growth factor 8b', *Journal of Biological Chemistry*, 277(36), pp. 32616-23.

Lortat-Jacob, H. (2006) 'Interferon and heparan sulphate', *Biochemical Society Transactions*, 34(Pt 3), pp. 461-4.

Lortat-Jacob, H., Grosdidier, A. and Imberty, A. (2002) 'Structural diversity of heparan sulfate binding domains in chemokines', *Proc Natl Acad Sci U S A*, 99(3), pp. 1229-34.

Lortat-Jacob, H., Turnbull, J.E. and Grimaud, J.A. (1995) 'Molecular organization of the interferon gamma-binding domain in heparan sulphate', *Biochem J*, 310 (Pt 2), pp. 497-505.

Lowe, J.B. (2003) 'Glycan-dependent leukocyte adhesion and recruitment in inflammation', *Curr Opin Cell Biol*, 15(5), pp. 531-8.

Lum, D.H., Tan, J., Rosen, S.D. and Werb, Z. (2007) 'Gene trap disruption of the mouse heparan sulfate 6-O-endosulfatase gene, Sulf2', *Mol Cell Biol*, 27(2), pp. 678-88.

Lundin, L., Larsson, H., Kreuger, J., Kanda, S., Lindahl, U., Salmivirta, M. and Claesson-Welsh, L. (2000) 'Selectively desulfated heparin inhibits fibroblast growth factor-induced mitogenicity and angiogenesis', *J Biol Chem*, 275(32), pp. 24653-60.

Lyon, M., Deakin, J.A. and Gallagher, J.T. (1994a) 'Liver heparan sulfate structure. A novel molecular design', *Journal of Biological Chemistry*, 269(15), pp. 11208-15.

Lyon, M., Deakin, J.A., Mizuno, K., Nakamura, T. and Gallagher, J.T. (1994b) 'Interaction of hepatocyte growth factor with heparan sulfate. Elucidation of the major heparan sulfate structural determinants', *Journal of Biological Chemistry*, 269(15), pp. 11216-23.

Lyon, M. and Gallagher, J.T. (1998) 'Bio-specific sequences and domains in heparan sulphate and the regulation of cell growth and adhesion', *Matrix Biol*, 17(7), pp. 485-93.

Lyon, M., Rushton, G. and Gallagher, J.T. (1997) 'The interaction of the transforming growth factor-betas with heparin/heparan sulfate is isoform-specific', *Journal of Biological Chemistry*, 272(29), pp. 18000-6.

Maccarana, M., Casu, B. and Lindahl, U. (1993) 'Minimal sequence in heparin/heparan sulfate required for binding of basic fibroblast growth factor', *Journal of Biological Chemistry*, 268(32), pp. 23898-905.

Mach, H., Volkin, D.B., Burke, C.J., Middaugh, C.R., Linhardt, R.J., Fromm, J.R., Loganathan, D. and Mattsson, L. (1993) 'Nature of the interaction of heparin with acidic fibroblast growth factor', *Biochemistry*, 32(20), pp. 5480-9.

Masola, V., Gambaro, G., Tibaldi, E., Brunati, A.M., Gastaldello, A., D'Angelo, A., Onisto, M. and Lupo, A. (2012) 'Heparanase and syndecan-1 interplay orchestrates fibroblast growth factor-2-induced epithelial-mesenchymal transition in renal tubular cells', *Journal of Biological Chemistry*, 287(2), pp. 1478-88.

Massena, S., Christoffersson, G., Hjertstrom, E., Zcharia, E., Vlodavsky, I., Ausmees, N., Rolny, C., Li, J.P. and Phillipson, M. (2010) 'A chemotactic gradient sequestered on endothelial heparan sulfate induces directional intraluminal crawling of neutrophils', *Blood*, 116(11), pp. 1924-31.

McCaffrey, T.A., Falcone, D.J., Vicente, D., Du, B., Consigli, S. and Borth, W. (1994) 'Protection of transforming growth factor-beta 1 activity by heparin and fucoidan', *J Cell Physiol*, 159(1), pp. 51-9.

McCormick, C., Duncan, G., Goutsos, K.T. and Tufaro, F. (2000) 'The putative tumor suppressors EXT1 and EXT2 form a stable complex that accumulates in the Golgi

apparatus and catalyzes the synthesis of heparan sulfate', *Proc Natl Acad Sci U S A*, 97(2), pp. 668-73.

McCormick, C., Leduc, Y., Martindale, D., Mattison, K., Esford, L.E., Dyer, A.P. and Tufaro, F. (1998) 'The putative tumour suppressor EXT1 alters the expression of cell-surface heparan sulfate', *Nat Genet*, 19(2), pp. 158-61.

Middleton, J., Neil, S., Wintle, J., Clark-Lewis, I., Moore, H., Lam, C., Auer, M., Hub, E. and Rot, A. (1997) 'Transcytosis and surface presentation of IL-8 by venular endothelial cells', *Cell*, 91(3), pp. 385-95.

Middleton, J., Patterson, A.M., Gardner, L., Schmutz, C. and Ashton, B.A. (2002) 'Leukocyte extravasation: chemokine transport and presentation by the endothelium', *Blood*, 100(12), pp. 3853-60.

Misseri, R., Meldrum, D.R., Dagher, P., Hile, K., Rink, R.C. and Meldrum, K.K. (2004) 'Unilateral ureteral obstruction induces renal tubular cell production of tumor necrosis factor-alpha independent of inflammatory cell infiltration', *J Urol*, 172(4 Pt 2), pp. 1595-9; discussion 1599.

Misseri, R., Meldrum, D.R., Dinarello, C.A., Dagher, P., Hile, K.L., Rink, R.C. and Meldrum, K.K. (2005) 'TNF-alpha mediates obstruction-induced renal tubular cell apoptosis and proapoptotic signaling', *Am J Physiol Renal Physiol*, 288(2), pp. F406-11.

Mohamed, M.A., Robertson, H., Booth, T.A., Balupuri, S., Kirby, J.A. and Talbot, D. (2000) 'TGF-beta expression in renal transplant biopsies: a comparative study between cyclosporin-A and tacrolimus', *Transplantation*, 69(5), pp. 1002-5.

Morimoto-Tomita, M., Uchimura, K., Bistrup, A., Lum, D.H., Egeblad, M., Boudreau, N., Werb, Z. and Rosen, S.D. (2005) 'Sulf-2, a proangiogenic heparan sulfate endosulfatase, is upregulated in breast cancer', *Neoplasia*, 7(11), pp. 1001-10.

Morimoto-Tomita, M., Uchimura, K., Werb, Z., Hemmerich, S. and Rosen, S.D. (2002) 'Cloning and characterization of two extracellular heparin-degrading endosulfatases in mice and humans', *J Biol Chem*, 277(51), pp. 49175-85.

Morita, H., David, G., Mizutani, A., Shinzato, T., Habuchi, H., Maeda, K. and Kimata, K. (1994a) 'Heparan sulfate proteoglycans in the human sclerosing and scarring kidney. Changes in heparan sulfate moiety', *Contrib Nephrol*, 107, pp. 174-9.

Morita, H., Shinzato, T., David, G., Mizutani, A., Habuchi, H., Fujita, Y., Ito, M., Asai, J., Maeda, K. and Kimata, K. (1994b) 'Basic fibroblast growth factor-binding domain of heparan sulfate in the human glomerulosclerosis and renal tubulointerstitial fibrosis', *Lab Invest*, 71(4), pp. 528-35.

Mulloy, B. and Forster, M.J. (2000) 'Conformation and dynamics of heparin and heparan sulfate', *Glycobiology*, 10(11), pp. 1147-56.

Mulloy, B. and Rider, C.C. (2006) 'Cytokines and proteoglycans: an introductory overview', *Biochemical Society Transactions*, 34(Pt 3), pp. 409-13.

Munro, S. (1998) 'Localization of proteins to the Golgi apparatus', *Trends in Cell Biology*, 8(1), pp. 11-5.

Murdoch, C. and Finn, A. (2000) 'Chemokine receptors and their role in inflammation and infectious diseases', *Blood*, 95(10), pp. 3032-43.

Murphy-Ullrich, J.E., Westrick, L.G., Esko, J.D. and Mosher, D.F. (1988) 'Altered metabolism of thrombospondin by Chinese hamster ovary cells defective in glycosaminoglycan synthesis', *J Biol Chem*, 263(13), pp. 6400-6.

Murray, J. (2002) 'Interview with Dr Joseph Murray (by Francis L Delmonico)', *Am J Transplant*, 2(9), pp. 803-6.

Nasser, N.J. (2008) 'Heparanase involvement in physiology and disease', *Cell Mol Life Sci*, 65(11), pp. 1706-15.

Nath, K.A. (1998) 'The tubulointerstitium in progressive renal disease', *Kidney Int*, 54(3), pp. 992-4.

Ng, Y.Y., Huang, T.P., Yang, W.C., Chen, Z.P., Yang, A.H., Mu, W., Nikolic-Paterson, D.J., Atkins, R.C. and Lan, H.Y. (1998) 'Tubular epithelial-myofibroblast transdifferentiation in progressive tubulointerstitial fibrosis in 5/6 nephrectomized rats', *Kidney Int*, 54(3), pp. 864-76.

Ning, S., Bin, C., Na, H., Peng, S., Yi, D., Xiang-hua, Y., Fang-yin, Z., Da-yong, Z. and Rong-cheng, L. (2012) 'Glypican-3, a novel prognostic marker of hepatocellular cancer, is related with postoperative metastasis and recurrence in hepatocellular cancer patients', *Mol Biol Rep*, 39(1), pp. 351-7.

Nogami, K., Suzuki, H., Habuchi, H., Ishiguro, N., Iwata, H. and Kimata, K. (2004) 'Distinctive expression patterns of heparan sulfate O-sulfotransferases and regional differences in heparan sulfate structure in chick limb buds', *J Biol Chem*, 279(9), pp. 8219-29.

Noonan, D.M. and Hassell, J.R. (1993) 'Perlecan, the large low-density proteoglycan of basement membranes: structure and variant forms', *Kidney Int*, 43(1), pp. 53-60.

O'Riordan, E., Orlova, T.N., Mendelev, N., Patschan, D., Kemp, R., Chander, P.N., Hu, R., Hao, G., Gross, S.S., Iozzo, R.V., Delaney, V. and Goligorsky, M.S. (2008) 'Urinary proteomic analysis of chronic allograft nephropathy', *Proteomics Clin Appl*, 2(7-8), pp. 1025-35.

Okada, H., Danoff, T.M., Kalluri, R. and Neilson, E.G. (1997) 'Early role of Fsp1 in epithelial-mesenchymal transformation', *Am J Physiol*, 273(4 Pt 2), pp. F563-74.

Okada, H., Inoue, T., Suzuki, H., Strutz, F. and Neilson, E.G. (2000) 'Epithelial-mesenchymal transformation of renal tubular epithelial cells in vitro and in vivo', *Nephrol Dial Transplant*, 15 Suppl 6, pp. 44-6.

Okada, H., Strutz, F., Danoff, T.M., Kalluri, R. and Neilson, E.G. (1996) 'Possible mechanisms of renal fibrosis', *Contrib Nephrol*, 118, pp. 147-54.

Okada, Y., Yamada, S., Toyoshima, M., Dong, J., Nakajima, M. and Sugahara, K. (2002) 'Structural recognition by recombinant human heparanase that plays critical roles in tumor metastasis. Hierarchical sulfate groups with different effects and the essential target disulfated trisaccharide sequence', *Journal of Biological Chemistry*, 277(45), pp. 42488-95.

Olsen, S.K., Garbi, M., Zampieri, N., Eliseenkova, A.V., Ornitz, D.M., Goldfarb, M. and Mohammadi, M. (2003) 'Fibroblast growth factor (FGF) homologous factors share structural but not functional homology with FGFs', *J Biol Chem*, 278(36), pp. 34226-36.

Orellana, A., Hirschberg, C.B., Wei, Z., Swiedler, S.J. and Ishihara, M. (1994) 'Molecular cloning and expression of a glycosaminoglycan N-acetylglucosaminyl N-deacetylase/N-sulfotransferase from a heparin-producing cell line', *J Biol Chem*, 269(3), pp. 2270-6.

Ornitz, D.M. (2000) 'FGFs, heparan sulfate and FGFRs: complex interactions essential for development', *Bioessays*, 22(2), pp. 108-12.

Ornitz, D.M., Herr, A.B., Nilsson, M., Westman, J., Svahn, C.M. and Waksman, G. (1995) 'FGF binding and FGF receptor activation by synthetic heparan-derived di- and trisaccharides', *Science*, 268(5209), pp. 432-6.

Pankonin, M.S., Gallagher, J.T. and Loeb, J.A. (2005) 'Specific structural features of heparan sulfate proteoglycans potentiate neuregulin-1 signaling', *Journal of Biological Chemistry*, 280(1), pp. 383-8.

Parish, C.R., Freeman, C. and Hulett, M.D. (2001) 'Heparanase: a key enzyme involved in cell invasion', *Biochim Biophys Acta*, 1471(3), pp. M99-108.

Parthasarathy, N., Goldberg, I.J., Sivaram, P., Mulloy, B., Flory, D.M. and Wagner, W.D. (1994) 'Oligosaccharide sequences of endothelial cell surface heparan sulfate proteoglycan with affinity for lipoprotein lipase', *Journal of Biological Chemistry*, 269(35), pp. 22391-6.

Patterson, A.M., Cartwright, A., David, G., Fitzgerald, O., Bresnihan, B., Ashton, B.A. and Middleton, J. (2008) 'Differential expression of syndecans and glypicans in chronically inflamed synovium', *Ann Rheum Dis*, 67(5), pp. 592-601.

Patterson, A.M., Gardner, L., Shaw, J., David, G., Loreau, E., Aguilar, L., Ashton, B.A. and Middleton, J. (2005) 'Induction of a CXCL8 binding site on endothelial syndecan-3 in rheumatoid synovium', *Arthritis Rheum*, 52(8), pp. 2331-42.

Pellegrini, L., Burke, D.F., von Delft, F., Mulloy, B. and Blundell, T.L. (2000) 'Crystal structure of fibroblast growth factor receptor ectodomain bound to ligand and heparin', *Nature*, 407(6807), pp. 1029-34.

Pereira, R.F., O'Hara, M.D., Laptev, A.V., Halford, K.W., Pollard, M.D., Class, R., Simon, D., Livezey, K. and Prockop, D.J. (1998) 'Marrow stromal cells as a source of progenitor cells for nonhematopoietic tissues in transgenic mice with a phenotype of osteogenesis imperfecta', *Proc Natl Acad Sci U S A*, 95(3), pp. 1142-7.

Petitou, M., Casu, B. and Lindahl, U. (2003) '1976-1983, a critical period in the history of heparin: the discovery of the antithrombin binding site', *Biochimie*, 85(1-2), pp. 83-9.

Phillips, A.O., Topley, N., Morrisey, K., Williams, J.D. and Steadman, R. (1997) 'Basic fibroblast growth factor stimulates the release of preformed transforming growth factor beta 1 from human proximal tubular cells in the absence of de novo gene transcription or mRNA translation', *Lab Invest*, 76(4), pp. 591-600.

Phillips, A.O., Topley, N., Steadman, R., Morrisey, K. and Williams, J.D. (1996) 'Induction of TGF-beta 1 synthesis in D-glucose primed human proximal tubular cells by IL-1 beta and TNF alpha', *Kidney Int*, 50(5), pp. 1546-54.

Pikas, D.S., Eriksson, I. and Kjellen, L. (2000) 'Overexpression of different isoforms of glucosaminyl N-deacetylase/N-sulfotransferase results in distinct heparan sulfate N-sulfation patterns', *Biochemistry*, 39(15), pp. 4552-8.

Pikas, D.S., Li, J.P., Vlodavsky, I. and Lindahl, U. (1998) 'Substrate specificity of heparanases from human hepatoma and platelets', *Journal of Biological Chemistry*, 273(30), pp. 18770-7.

Pober, J.S., Orosz, C.G., Rose, M.L. and Savage, C.O. (1996) 'Can graft endothelial cells initiate a host anti-graft immune response?', *Transplantation*, 61(3), pp. 343-9.

Potenta, S., Zeisberg, E. and Kalluri, R. (2008) 'The role of endothelial-to-mesenchymal transition in cancer progression', *Br J Cancer*, 99(9), pp. 1375-9.

Pribylova-Hribova, P., Kotsch, K., Lodererova, A., Viklicky, O., Vitko, S., Volk, H.D. and Lacha, J. (2006) 'TGF-beta1 mRNA upregulation influences chronic renal allograft dysfunction', *Kidney Int*, 69(10), pp. 1872-9.

Properzi, F., Lin, R., Kwok, J., Naidu, M., van Kuppevelt, T.H., Ten Dam, G.B., Camargo, L.M., Raha-Chowdhury, R., Furukawa, Y., Mikami, T., Sugahara, K. and Fawcett, J.W. (2008) 'Heparan sulphate proteoglycans in glia and in the normal and injured CNS: expression of sulphotransferases and changes in sulphation', *Eur J Neurosci*, 27(3), pp. 593-604.

Proudfoot, A.E., Fritchley, S., Borlat, F., Shaw, J.P., Vilbois, F., Zwahlen, C., Trkola, A., Marchant, D., Clapham, P.R. and Wells, T.N. (2001) 'The BBXB motif of RANTES is the principal site for heparin binding and controls receptor selectivity', *J Biol Chem*, 276(14), pp. 10620-6.

Proudfoot, A.E., Handel, T.M., Johnson, Z., Lau, E.K., LiWang, P., Clark-Lewis, I., Borlat, F., Wells, T.N. and Kosco-Vilbois, M.H. (2003) 'Glycosaminoglycan binding and oligomerization are essential for the in vivo activity of certain chemokines', *Proc Natl Acad Sci U S A*, 100(4), pp. 1885-90.

Pye, D.A., Vives, R.R., Hyde, P. and Gallagher, J.T. (2000) 'Regulation of FGF-1 mitogenic activity by heparan sulfate oligosaccharides is dependent on specific structural features: differential requirements for the modulation of FGF-1 and FGF-2', *Glycobiology*, 10(11), pp. 1183-92.

Pye, D.A., Vives, R.R., Turnbull, J.E., Hyde, P. and Gallagher, J.T. (1998) 'Heparan sulfate oligosaccharides require 6-O-sulfation for promotion of basic fibroblast growth factor mitogenic activity', *J Biol Chem*, 273(36), pp. 22936-42.

Raats, C.J., Van Den Born, J. and Berden, J.H. (2000) 'Glomerular heparan sulfate alterations: mechanisms and relevance for proteinuria', *Kidney Int*, 57(2), pp. 385-400.

Racusen, L.C., Monteil, C., Sgrignoli, A., Lucskay, M., Marouillat, S., Rhim, J.G. and Morin, J.P. (1997) 'Cell lines with extended in vitro growth potential from human renal proximal tubule: characterization, response to inducers, and comparison with established cell lines', *J Lab Clin Med*, 129(3), pp. 318-29.

Racusen, L.C., Solez, K. and Colvin, R. (2002) 'Fibrosis and atrophy in the renal allograft: interim report and new directions', *Am J Transplant*, 2(3), pp. 203-6.

Rapraeger, A.C., Krufka, A. and Olwin, B.B. (1991) 'Requirement of heparan sulfate for bFGF-mediated fibroblast growth and myoblast differentiation', *Science*, 252(5013), pp. 1705-8.

Rapraeger, A.C. and Ott, V.L. (1998) 'Molecular interactions of the syndecan core proteins', *Curr Opin Cell Biol*, 10(5), pp. 620-8.

Rek, A., Brandner, B., Geretti, E. and Kungl, A.J. (2009) 'A biophysical insight into the RANTES-glycosaminoglycan interaction', *Biochim Biophys Acta*, 1794(4), pp. 577-82.

Remuzzi, G. and Bertani, T. (1998) 'Pathophysiology of progressive nephropathies', *N Engl J Med*, 339(20), pp. 1448-56.

Roberts, I.S., Burrows, C., Shanks, J.H., Venning, M. and McWilliam, L.J. (1997) 'Interstitial myofibroblasts: predictors of progression in membranous nephropathy', *J Clin Pathol*, 50(2), pp. 123-7.

Robertson, H., Ali, S., McDonnell, B.J., Burt, A.D. and Kirby, J.A. (2004) 'Chronic renal allograft dysfunction: the role of T cell-mediated tubular epithelial to mesenchymal cell transition', *J Am Soc Nephrol*, 15(2), pp. 390-7.

Robertson, H. and Kirby, J.A. (2003) 'Post-transplant renal tubulitis: the recruitment, differentiation and persistence of intra-epithelial T cells', *Am J Transplant*, 3(1), pp. 3-10.

Robertson, H., Morley, A.R., Talbot, D., Callanan, K. and Kirby, J.A. (2000) 'Renal allograft rejection: beta-chemokine involvement in the development of tubulitis', *Transplantation*, 69(4), pp. 684-7.

Robertson, H., Wong, W.K., Talbot, D., Burt, A.D. and Kirby, J.A. (2001) 'Tubulitis after renal transplantation: demonstration of an association between CD103+ T cells, transforming growth factor beta1 expression and rejection grade', *Transplantation*, 71(2), pp. 306-13.

Roghani, M., Mansukhani, A., Dell'Era, P., Bellosta, P., Basilico, C., Rifkin, D.B. and Moscatelli, D. (1994) 'Heparin increases the affinity of basic fibroblast growth factor for its receptor but is not required for binding', *J Biol Chem*, 269(6), pp. 3976-84.

Rong, J., Habuchi, H., Kimata, K., Lindahl, U. and Kusche-Gullberg, M. (2001) 'Substrate specificity of the heparan sulfate hexuronic acid 2-O-sulfotransferase', *Biochemistry*, 40(18), pp. 5548-55.

Rops, A.L., van den Hoven, M.J., Bakker, M.A., Lensen, J.F., Wijnhoven, T.J., van den Heuvel, L.P., van Kuppevelt, T.H., van der Vlag, J. and Berden, J.H. (2007) 'Expression of glomerular heparan sulphate domains in murine and human lupus nephritis', *Nephrol Dial Transplant*, 22(7), pp. 1891-902.

Rops, A.L., van den Hoven, M.J., Baselmans, M.M., Lensen, J.F., Wijnhoven, T.J., van den Heuvel, L.P., van Kuppevelt, T.H., Berden, J.H. and van der Vlag, J. (2008) 'Heparan sulfate domains on cultured activated glomerular endothelial cells mediate leukocyte trafficking', *Kidney Int*, 73(1), pp. 52-62.

Rosen, S.D. and Lemjabbar-Alaoui, H. (2007) 'Sulf-2: an extracellular modulator of cell signaling and a cancer target candidate', *Expert Opin Ther Targets*, 27, pp. 678-688.

Rosenberg, R.D., Shworak, N.W., Liu, J., Schwartz, J.J. and Zhang, L. (1997) 'Heparan sulfate proteoglycans of the cardiovascular system. Specific structures emerge but how is synthesis regulated?', *Journal of Clinical Investigation*, 100(11 Suppl), pp. S67-75.

Rot, A. and von Andrian, U.H. (2004) 'Chemokines in innate and adaptive host defense: basic chemokinese grammar for immune cells', *Annu Rev Immunol*, 22, pp. 891-928.

Roy-Chaudhury, P., Wu, B., King, G., Campbell, M., Macleod, A.M., Haites, N.E., Simpson, J.G. and Power, D.A. (1996) 'Adhesion molecule interactions in human glomerulonephritis: importance of the tubulointerstitium', *Kidney Int*, 49(1), pp. 127-34.

Ruiz-Ortega, M. and Egido, J. (1997) 'Angiotensin II modulates cell growth-related events and synthesis of matrix proteins in renal interstitial fibroblasts', *Kidney Int*, 52(6), pp. 1497-510.

Ryan, M.J., Johnson, G., Kirk, J., Fuerstenberg, S.M., Zager, R.A. and Torok-Storb, B. (1994) 'HK-2: an immortalized proximal tubule epithelial cell line from normal adult human kidney', *Kidney Int*, 45(1), pp. 48-57.

Rygiel, K.A., Robertson, H., Willet, J.D., Brain, J.G., Burt, A.D., Jones, D.E. and Kirby, J.A. (2010) 'T cell-mediated biliary epithelial-to-mesenchymal transition in liver allograft rejection', *Liver Transpl*, 16(5), pp. 567-76.

Safaiyan, F., Kolset, S.O., Prydz, K., Gottfridsson, E., Lindahl, U. and Salmivirta, M. (1999) 'Selective effects of sodium chlorate treatment on the sulfation of heparan sulfate', *Journal of Biological Chemistry*, 274(51), pp. 36267-73.

Safaiyan, F., Lindahl, U. and Salmivirta, M. (2000) 'Structural diversity of N-sulfated heparan sulfate domains: distinct modes of glucuronyl C5 epimerization, iduronic acid 2-O-sulfation, and glucosamine 6-O-sulfation', *Biochemistry*, 39(35), pp. 10823-30.

Salmivirta, M., Lidholt, K. and Lindahl, U. (1996) 'Heparan sulfate: a piece of information', *Faseb J*, 10(11), pp. 1270-9.

Saoncella, S., Echtermeyer, F., Denhez, F., Nowlen, J.K., Mosher, D.F., Robinson, S.D., Hynes, R.O. and Goetinck, P.F. (1999) 'Syndecan-4 signals cooperatively with integrins in a Rho-dependent manner in the assembly of focal adhesions and actin stress fibers', *Proc Natl Acad Sci U S A*, 96(6), pp. 2805-10.

Sardiello, M., Annunziata, I., Roma, G. and Ballabio, A. (2005) 'Sulfatases and sulfatase modifying factors: an exclusive and promiscuous relationship', *Hum Mol Genet*, 14(21), pp. 3203-17.

Sarrazin, S., Lamanna, W.C. and Esko, J.D. (2011) 'Heparan sulfate proteoglycans', *Cold Spring Harb Perspect Biol*, 3(7).

Sasisekharan, R., Ernst, S. and Venkataraman, G. (1997) 'On the regulation of fibroblast growth factor activity by heparin-like glycosaminoglycans', *Angiogenesis*, 1(1), pp. 45-54.

Schaaf, G.J., Nijmeijer, S.M., Maas, R.F., Roestenberg, P., de Groene, E.M. and Fink-Gremmels, J. (2002) 'The role of oxidative stress in the ochratoxin A-mediated toxicity in proximal tubular cells', *Biochim Biophys Acta*, 1588(2), pp. 149-58.

Schenauer, M.R., Yu, Y., Sweeney, M.D. and Leary, J.A. (2007) 'CCR2 chemokines bind selectively to acetylated heparan sulfate octasaccharides', *Journal of Biological Chemistry*, 282(35), pp. 25182-8.

Schlessinger, J. (1988) 'Signal transduction by allosteric receptor oligomerization', *Trends Biochem Sci*, 13(11), pp. 443-7.

Schlessinger, J., Plotnikov, A.N., Ibrahimi, O.A., Eliseenkova, A.V., Yeh, B.K., Yayon, A., Linhardt, R.J. and Mohammadi, M. (2000) 'Crystal structure of a ternary FGF-FGFR-

heparin complex reveals a dual role for heparin in FGFR binding and dimerization', *Mol Cell*, 6(3), pp. 743-50.

Scholz, D., Cai, W.J. and Schaper, W. (2001) 'Arteriogenesis, a new concept of vascular adaptation in occlusive disease', *Angiogenesis*, 4(4), pp. 247-57.

Sedita, J., Izvolsky, K. and Cardoso, W.V. (2004) 'Differential expression of heparan sulfate 6-O-sulfotransferase isoforms in the mouse embryo suggests distinctive roles during organogenesis', *Dev Dyn*, 231(4), pp. 782-94.

Sharma, A.K., Mauer, S.M., Kim, Y. and Michael, A.F. (1993) 'Interstitial fibrosis in obstructive nephropathy', *Kidney Int*, 44(4), pp. 774-88.

Shaw, J.P., Johnson, Z., Borlat, F., Zwahlen, C., Kungl, A., Roulin, K., Harrenga, A., Wells, T.N. and Proudfoot, A.E. (2004) 'The X-ray structure of RANTES: heparin-derived disaccharides allows the rational design of chemokine inhibitors', *Structure*, 12(11), pp. 2081-93.

Shimizu, K., Libby, P., Shubiki, R., Sakuma, M., Wang, Y., Asano, K., Mitchell, R.N. and Simon, D.I. (2008) 'Leukocyte integrin Mac-1 promotes acute cardiac allograft rejection', *Circulation*, 117(15), pp. 1997-2008.

Shirwan, H. (1999) 'Chronic allograft rejection. Do the Th2 cells preferentially induced by indirect alloantigen recognition play a dominant role?', *Transplantation*, 68(6), pp. 715-26.

Shukla, D., Liu, J., Blaiklock, P., Shworak, N.W., Bai, X., Esko, J.D., Cohen, G.H., Eisenberg, R.J., Rosenberg, R.D. and Spear, P.G. (1999) 'A novel role for 3-O-sulfated heparan sulfate in herpes simplex virus 1 entry', *Cell*, 99(1), pp. 13-22.

Shulman, Z., Cohen, S.J., Roediger, B., Kalchenko, V., Jain, R., Grabovsky, V., Klein, E., Shinder, V., Stoler-Barak, L., Feigelson, S.W., Meshel, T., Nurmi, S.M., Goldstein, I., Hartley, O., Gahmberg, C.G., Etzioni, A., Weninger, W., Ben-Baruch, A. and Alon, R. (2012) 'Transendothelial migration of lymphocytes mediated by intraendothelial vesicle stores rather than by extracellular chemokine depots', *Nat Immunol*, 13(1), pp. 67-76.

Shworak, N.W., HajMohammadi, S., de Agostini, A.I. and Rosenberg, R.D. (2002) 'Mice deficient in heparan sulfate 3-O-sulfotransferase-1: normal hemostasis with unexpected perinatal phenotypes', *Glycoconj J*, 19(4-5), pp. 355-61.

Shworak, N.W., Liu, J., Petros, L.M., Zhang, L., Kobayashi, M., Copeland, N.G., Jenkins, N.A. and Rosenberg, R.D. (1999) 'Multiple isoforms of heparan sulfate D-glucosaminyl 3-O-sulfotransferase. Isolation, characterization, and expression of human cdnas and identification of distinct genomic loci', *Journal of Biological Chemistry*, 274(8), pp. 5170-84.

Shworak, N.W., Shirakawa, M., Mulligan, R.C. and Rosenberg, R.D. (1994) 'Characterization of ryudocan glycosaminoglycan acceptor sites', *J Biol Chem*, 269(33), pp. 21204-14.

Smeds, E., Habuchi, H., Do, A.-T., Hjertson, E., Grundberg, H., Kimata, K., Lindahl, U. and Kusche-Gullberg, M. (2003) 'Substrate specificities of mouse heparan sulphate glucosaminyl 6-O-sulphotransferases', *Biochemical Journal*, 372(Pt 2), pp. 371-80.

Smits, N.C., Lensen, J.F., Wijnhoven, T.J., Ten Dam, G.B., Jenniskens, G.J. and van Kuppevelt, T.H. (2006) 'Phage display-derived human antibodies against specific glycosaminoglycan epitopes', *Methods Enzymol*, 416, pp. 61-87.

Solez, K., Colvin, R.B., Racusen, L.C., Sis, B., Halloran, P.F., Birk, P.E., Campbell, P.M., Cascalho, M., Collins, A.B., Demetris, A.J., Drachenberg, C.B., Gibson, I.W., Grimm, P.C., Haas, M., Lerut, E., Liapis, H., Mannon, R.B., Marcus, P.B., Mengel, M., Mihatsch, M.J., Nankivell, B.J., Nickeleit, V., Papadimitriou, J.C., Platt, J.L., Randhawa, P., Roberts, I., Salinas-Madriga, L., Salomon, D.R., Seron, D., Sheaff, M. and Weening, J.J. (2007) 'Banff '05 Meeting Report: differential diagnosis of chronic allograft injury and elimination of chronic allograft nephropathy ('CAN')', *Am J Transplant*, 7(3), pp. 518-26.

Sorensson, J., Bjornson, A., Ohlson, M., Ballermann, B.J. and Haraldsson, B. (2003) 'Synthesis of sulfated proteoglycans by bovine glomerular endothelial cells in culture', *Am J Physiol Renal Physiol*, 284(2), pp. F373-80.

Soulez, M., Pilon, E.A., Dieude, M., Cardinal, H., Brassard, N., Qi, S., Wu, S.J., Durocher, Y., Madore, F., Perreault, C. and Hebert, M.J. (2012) 'The perlecan fragment LG3 is a novel regulator of obliterative remodeling associated with allograft vascular rejection', *Circ Res*, 110(1), pp. 94-104.

Stark, G.R., Kerr, I.M., Williams, B.R., Silverman, R.H. and Schreiber, R.D. (1998) 'How cells respond to interferons', *Annu Rev Biochem*, 67, pp. 227-64.

Stringer, S.E. (2006) 'The role of heparan sulphate proteoglycans in angiogenesis', *Biochemical Society Transactions*, 34(Pt 3), pp. 451-3.

Strutz, F. and Neilson, E.G. (1994) 'The role of lymphocytes in the progression of interstitial disease', *Kidney Int Suppl*, 45, pp. S106-10.

Strutz, F. and Neilson, E.G. (2003) 'New insights into mechanisms of fibrosis in immune renal injury', *Springer Semin Immunopathol*, 24(4), pp. 459-76.

Strutz, F., Okada, H., Lo, C.W., Danoff, T., Carone, R.L., Tomaszewski, J.E. and Neilson, E.G. (1995) 'Identification and characterization of a fibroblast marker: FSP1', *J Cell Biol*, 130(2), pp. 393-405.

Strutz, F. and Zeisberg, M. (2006) 'Renal fibroblasts and myofibroblasts in chronic kidney disease', *J Am Soc Nephrol*, 17(11), pp. 2992-8.

Strutz, F., Zeisberg, M., Hemmerlein, B., Sattler, B., Hummel, K., Becker, V. and Muller, G.A. (2000) 'Basic fibroblast growth factor expression is increased in human renal fibrogenesis and may mediate autocrine fibroblast proliferation', *Kidney Int*, 57(4), pp. 1521-38.

Strutz, F., Zeisberg, M., Renziehausen, A., Raschke, B., Becker, V., van Kooten, C. and Muller, G. (2001) 'TGF-beta 1 induces proliferation in human renal fibroblasts via induction of basic fibroblast growth factor (FGF-2)', *Kidney Int*, 59(2), pp. 579-92.

Strutz, F., Zeisberg, M., Ziyadeh, F.N., Yang, C.Q., Kalluri, R., Muller, G.A. and Neilson, E.G. (2002) 'Role of basic fibroblast growth factor-2 in epithelial-mesenchymal transformation', *Kidney Int*, 61(5), pp. 1714-28.

Sugaya, N., Habuchi, H., Nagai, N., Ashikari-Hada, S. and Kimata, K. (2008) '6-O-sulfation of heparan sulfate differentially regulates various fibroblast growth factor-dependent signalings in culture', *Journal of Biological Chemistry*, 283(16), pp. 10366-76.

Sumitran-Holgersson, S. (2001) 'HLA-specific alloantibodies and renal graft outcome', *Nephrol Dial Transplant*, 16(5), pp. 897-904.

Sunami, R., Sugiyama, H., Wang, D.H., Kobayashi, M., Maeshima, Y., Yamasaki, Y., Masuoka, N., Ogawa, N., Kira, S. and Makino, H. (2004) 'Acatalasemia sensitizes renal tubular epithelial cells to apoptosis and exacerbates renal fibrosis after unilateral ureteral obstruction', *Am J Physiol Renal Physiol*, 286(6), pp. F1030-8.

Tatrai, P., Egedi, K., Somoracz, A., van Kuppevelt, T.H., Ten Dam, G., Lyon, M., Deakin, J.A., Kiss, A., Schaff, Z. and Kovalszky, I. (2010) 'Quantitative and qualitative alterations of heparan sulfate in fibrogenic liver diseases and hepatocellular cancer', *J Histochem Cytochem*, 58(5), pp. 429-41.

Ten Dam, G.B., Kurup, S., van de Westerlo, E.M., Versteeg, E.M., Lindahl, U., Spillmann, D. and van Kuppevelt, T.H. (2006) '3-O-sulfated oligosaccharide structures are recognized by anti-heparan sulfate antibody HS4C3', *J Biol Chem*, 281(8), pp. 4654-62.

Terasaki, P.I. (2003) 'Humoral theory of transplantation', *Am J Transplant*, 3(6), pp. 665-73.

Terasaki, P.I. and Cai, J. (2008) 'Human leukocyte antigen antibodies and chronic rejection: from association to causation', *Transplantation*, 86(3), pp. 377-83.

Tessler, S., Rockwell, P., Hicklin, D., Cohen, T., Levi, B.Z., Witte, L., Lemischka, I.R. and Neufeld, G. (1994) 'Heparin modulates the interaction of VEGF165 with soluble and cell associated flk-1 receptors', *Journal of Biological Chemistry*, 269(17), pp. 12456-61.

Thiery, J.P. (2002) 'Epithelial-mesenchymal transitions in tumour progression', *Nat Rev Cancer*, 2(6), pp. 442-54.

Thompson, L.D., Pantoliano, M.W. and Springer, B.A. (1994) 'Energetic characterization of the basic fibroblast growth factor-heparin interaction: identification of the heparin binding domain', *Biochemistry*, 33(13), pp. 3831-40.

Toma, L., Berninsone, P. and Hirschberg, C.B. (1998) 'The putative heparin-specific N-acetylglucosaminyl N-Deacetylase/N-sulfotransferase also occurs in non-heparin-producing cells', *J Biol Chem*, 273(35), pp. 22458-65.

Tumova, S., Woods, A. and Couchman, J.R. (2000) 'Heparan sulfate proteoglycans on the cell surface: versatile coordinators of cellular functions', *Int J Biochem Cell Biol*, 32(3), pp. 269-88.

Turnbull, J.E., Fernig, D.G., Ke, Y., Wilkinson, M.C. and Gallagher, J.T. (1992) 'Identification of the basic fibroblast growth factor binding sequence in fibroblast heparan sulfate', *J Biol Chem*, 267(15), pp. 10337-41.

Turnbull, J.E. and Gallagher, J.T. (1991) 'Sequence analysis of heparan sulphate indicates defined location of N-sulphated glucosamine and iduronate 2-sulphate residues proximal to the protein-linkage region', *Biochem J*, 277 (Pt 2), pp. 297-303.

Tyrrell, D.J., Ishihara, M., Rao, N., Horne, A., Kiefer, M.C., Stauber, G.B., Lam, L.H. and Stack, R.J. (1993) 'Structure and biological activities of a heparin-derived hexasaccharide with high affinity for basic fibroblast growth factor', *Journal of Biological Chemistry*, 268(7), pp. 4684-9.

Uchimura, K., Morimoto-Tomita, M., Bistrup, A., Li, J., Lyon, M., Gallagher, J., Werb, Z. and Rosen, S.D. (2006) 'HSulf-2, an extracellular endoglucosamine-6-sulfatase, selectively mobilizes heparin-bound growth factors and chemokines: effects on VEGF, FGF-1, and SDF-1', *BMC Biochem*, 7, p. 2.

Valles, S., Tsoi, C., Huang, W.Y., Wyllie, D., Carlotti, F., Askari, J.A., Humphries, M.J., Dower, S.K. and Qwarnstrom, E.E. (1999) 'Recruitment of a heparan sulfate subunit to the interleukin-1 receptor complex. Regulation by fibronectin attachment', *Journal of Biological Chemistry*, 274(29), pp. 20103-9.

van de Westerlo, E.M., Smetsers, T.F., Dennissen, M.A., Linhardt, R.J., Veerkamp, J.H., van Muijen, G.N. and van Kuppevelt, T.H. (2002) 'Human single chain antibodies against heparin: selection, characterization, and effect on coagulation', *Blood*, 99(7), pp. 2427-33.

van den Born, J., Salmivirta, K., Henttinen, T., Ostman, N., Ishimaru, T., Miyaura, S., Yoshida, K. and Salmivirta, M. (2005) 'Novel heparan sulfate structures revealed by monoclonal antibodies', *J Biol Chem*, 280(21), pp. 20516-23.

van Kuppevelt, T.H., Dennissen, M.A., van Venrooij, W.J., Hoet, R.M. and Veerkamp, J.H. (1998) 'Generation and application of type-specific anti-heparan sulfate antibodies using phage display technology. Further evidence for heparan sulfate heterogeneity in the kidney', *Journal of Biological Chemistry*, 273(21), pp. 12960-6.

Vaughan, E.D., Jr., Marion, D., Poppas, D.P. and Felsen, D. (2004) 'Pathophysiology of unilateral ureteral obstruction: studies from Charlottesville to New York', *J Urol*, 172(6 Pt 2), pp. 2563-9.

Venkatachalam, K.V., Akita, H. and Strott, C.A. (1998) 'Molecular cloning, expression, and characterization of human bifunctional 3'-phosphoadenosine 5'-phosphosulfate synthase and its functional domains', *Journal of Biological Chemistry*, 273(30), pp. 19311-20.

Vives, R.R., Sadir, R., Imberty, A., Rencurosi, A. and Lortat-Jacob, H. (2002) 'A kinetics and modeling study of RANTES(9-68) binding to heparin reveals a mechanism of cooperative oligomerization', *Biochemistry*, 41(50), pp. 14779-89.

Vlodavsky, I. and Friedmann, Y. (2001) 'Molecular properties and involvement of heparanase in cancer metastasis and angiogenesis', *Journal of Clinical Investigation*, 108(3), pp. 341-7.

Vlodavsky, I., Friedmann, Y., Elkin, M., Aingorn, H., Atzmon, R., Ishai-Michaeli, R., Bitan, M., Pappo, O., Peretz, T., Michal, I., Spector, L. and Pecker, I. (1999) 'Mammalian heparanase: gene cloning, expression and function in tumor progression and metastasis', *Nat Med*, 5(7), pp. 793-802.

Waaga, A.M., Gasser, M., Laskowski, I. and Tilney, N.L. (2000) 'Mechanisms of chronic rejection', *Curr Opin Immunol*, 12(5), pp. 517-21.

Waaga, A.M., Rocha, A. and Tilney, N.L. 11 (1997) 'Eartly risk factors contributing to the evolution of long-term allograft dysfunction' *Transplantation rev.*, pp. 208-216.

Waksman, G. and Herr, A.B. (1998) 'New insights into heparin-induced FGF oligomerization', *Nat Struct Biol*, 5(7), pp. 527-30.

Walker, A., Turnbull, J.E. and Gallagher, J.T. (1994) 'Specific heparan sulfate saccharides mediate the activity of basic fibroblast growth factor', *Journal of Biological Chemistry*, 269(2), pp. 931-5.

Wang, L., Brown, J.R., Varki, A. and Esko, J.D. (2002) 'Heparin's anti-inflammatory effects require glucosamine 6-O-sulfation and are mediated by blockade of L- and P-selectins', *J Clin Invest*, 110(1), pp. 127-36.

Wang, L., Fuster, M., Sriramarao, P. and Esko, J.D. (2005) 'Endothelial heparan sulfate deficiency impairs L-selectin- and chemokine-mediated neutrophil trafficking during inflammatory responses', *Nat Immunol*, 6(9), pp. 902-10.

Wang, L., Park, H., Chhim, S., Ding, Y., Jiang, W., Queen, C. and Kim, K.J. (2012) 'A Novel Monoclonal Antibody to Fibroblast Growth Factor 2 Effectively Inhibits Growth of Hepatocellular Carcinoma Xenografts', *Mol Cancer Ther*.

Wang, S., Ai, X., Freeman, S.D., Pownall, M.E., Lu, Q., Kessler, D.S. and Emerson, C.P., Jr. (2004) 'QSulf1, a heparan sulfate 6-O-endosulfatase, inhibits fibroblast growth factor signaling in mesoderm induction and angiogenesis', *Proc Natl Acad Sci U S A*, 101(14), pp. 4833-8.

Ward, S.G., Bacon, K. and Westwick, J. (1998) 'Chemokines and T lymphocytes: more than an attraction', *Immunity*, 9(1), pp. 1-11.

Webb, L.M., Ehrengruber, M.U., Clark-Lewis, I., Baggiolini, M. and Rot, A. (1993) 'Binding to heparan sulfate or heparin enhances neutrophil responses to interleukin 8', *Proc Natl Acad Sci U S A*, 90(15), pp. 7158-62.

Wei, G., Bai, X., Gabb, M.M., Bame, K.J., Koshy, T.I., Spear, P.G. and Esko, J.D. (2000) 'Location of the glucuronosyltransferase domain in the heparan sulfate copolymerase EXT1 by analysis of Chinese hamster ovary cell mutants', *Journal of Biological Chemistry*, 275(36), pp. 27733-40.

Whitelock, J.M. and Iozzo, R.V. (2005) 'Heparan sulfate: a complex polymer charged with biological activity', *Chem Rev*, 105(7), pp. 2745-64.

Wight, T.N., Kinsella, M.G. and Qwarnstrom, E.E. (1992) 'The role of proteoglycans in cell adhesion, migration and proliferation', *Curr Opin Cell Biol*, 4(5), pp. 793-801.

Win, T.S. and Pettigrew, G.J. (2010) 'Humoral autoimmunity and transplant vasculopathy: when allo is not enough', *Transplantation*, 90(2), pp. 113-20.

Wlad, H., Maccarana, M., Eriksson, I., Kjellen, L. and Lindahl, U. (1994) 'Biosynthesis of heparin. Different molecular forms of O-sulfotransferases', *J Biol Chem*, 269(40), pp. 24538-41.

Wright, E.J., McCaffrey, T.A., Robertson, A.P., Vaughan, E.D., Jr. and Felsen, D. (1996) 'Chronic unilateral ureteral obstruction is associated with interstitial fibrosis and tubular expression of transforming growth factor-beta', *Lab Invest*, 74(2), pp. 528-37.

Wuthrich, R.P., Glimcher, L.H., Yui, M.A., Jevnikar, A.M., Dumas, S.E. and Kelley, V.E. (1990) 'MHC class II, antigen presentation and tumor necrosis factor in renal tubular epithelial cells', *Kidney Int*, 37(2), pp. 783-92.

Wuthrich, R.P., Yui, M.A., Mazoujian, G., Nabavi, N., Glimcher, L.H. and Kelley, V.E. (1989) 'Enhanced MHC class II expression in renal proximal tubules precedes loss of renal function in MRL/lpr mice with lupus nephritis', *Am J Pathol*, 134(1), pp. 45-51.

Xu, D., Tiwari, V., Xia, G., Clement, C., Shukla, D. and Liu, J. (2005) 'Characterization of heparan sulphate 3-O-sulphotransferase isoform 6 and its role in assisting the entry of herpes simplex virus type 1', *Biochem J*, 385(Pt 2), pp. 451-9.

Xu, J., Liu, Z. and Ornitz, D.M. (2000) 'Temporal and spatial gradients of Fgf8 and Fgf17 regulate proliferation and differentiation of midline cerebellar structures', *Development*, 127(9), pp. 1833-43.

Yadav, R., Larbi, K.Y., Young, R.E. and Nourshargh, S. (2003) 'Migration of leukocytes through the vessel wall and beyond', *Thromb Haemost*, 90(4), pp. 598-606.

Yamaguchi, K., Tamaki, H. and Fukui, S. (2006) 'Detection of oligosaccharide ligands for hepatocyte growth factor/scatter factor (HGF/SF), keratinocyte growth factor (KGF/FGF-7), RANTES and heparin cofactor II by neoglycolipid microarrays of glycosaminoglycan-derived oligosaccharide fragments', *Glycoconj J*, 23(7-8), pp. 513-23.

Yanagishita, M. (1992) 'Metabolic labeling of glycosylphosphatidylinositol-anchor of heparan sulfate proteoglycans in rat ovarian granulosa cells', *Journal of Biological Chemistry*, 267(14), pp. 9499-504.

Yang, Y., Macleod, V., Miao, H.Q., Theus, A., Zhan, F., Shaughnessy, J.D., Jr., Sawyer, J., Li, J.P., Zcharia, E., Vlodavsky, I. and Sanderson, R.D. (2007) 'Heparanase enhances syndecan-1 shedding: a novel mechanism for stimulation of tumor growth and metastasis', *Journal of Biological Chemistry*, 282(18), pp. 13326-33.

Ysebaert, D.K., De Greef, K.E., Vercauteren, S.R., Ghielli, M., Verpooten, G.A., Eyskens, E.J. and De Broe, M.E. (2000) 'Identification and kinetics of leukocytes after severe ischaemia/reperfusion renal injury', *Nephrol Dial Transplant*, 15(10), pp. 1562-74.

Yuan, B., Liang, M., Yang, Z., Rute, E., Taylor, N., Olivier, M. and Cowley, A.W., Jr. (2003) 'Gene expression reveals vulnerability to oxidative stress and interstitial fibrosis of renal outer medulla to nonhypertensive elevations of ANG II', *Am J Physiol Regul Integr Comp Physiol*, 284(5), pp. R1219-30.

Yue, X., Li, X., Nguyen, H.T., Chin, D.R., Sullivan, D.E. and Lasky, J.A. (2008) 'Transforming growth factor-beta1 induces heparan sulfate 6-O-endosulfatase 1 expression in vitro and in vivo', *Journal of Biological Chemistry*, 283(29), pp. 20397-407.

Zavadil, J. and Bottinger, E.P. (2005) 'TGF-beta and epithelial-to-mesenchymal transitions', *Oncogene*, 24(37), pp. 5764-74.

Zeisberg, E.M., Potenta, S.E., Sugimoto, H., Zeisberg, M. and Kalluri, R. (2008) 'Fibroblasts in kidney fibrosis emerge via endothelial-to-mesenchymal transition', *J Am Soc Nephrol*, 19(12), pp. 2282-7.

Zeisberg, E.M., Tarnavski, O., Zeisberg, M., Dorfman, A.L., McMullen, J.R., Gustafsson, E., Chandraker, A., Yuan, X., Pu, W.T., Roberts, A.B., Neilson, E.G., Sayegh, M.H., Izumo, S. and Kalluri, R. (2007a) 'Endothelial-to-mesenchymal transition contributes to cardiac fibrosis', *Nat Med*, 13(8), pp. 952-61.

Zeisberg, M., Hanai, J., Sugimoto, H., Mammoto, T., Charytan, D., Strutz, F. and Kalluri, R. (2003) 'BMP-7 counteracts TGF-beta1-induced epithelial-to-mesenchymal transition and reverses chronic renal injury', *Nat Med*, 9(7), pp. 964-8.

Zeisberg, M. and Neilson, E.G. (2009) 'Biomarkers for epithelial-mesenchymal transitions', *Journal of Clinical Investigation*, 119(6), pp. 1429-37.

Zeisberg, M., Yang, C., Martino, M., Duncan, M.B., Rieder, F., Tanjore, H. and Kalluri, R. (2007b) 'Fibroblasts derive from hepatocytes in liver fibrosis via epithelial to mesenchymal transition', *Journal of Biological Chemistry*, 282(32), pp. 23337-47.

Zhang, G.H., Ichimura, T., Wallin, A., Kan, M. and Stevens, J.L. (1991) 'Regulation of rat proximal tubule epithelial cell growth by fibroblast growth factors, insulin-like growth factor-1 and transforming growth factor-beta, and analysis of fibroblast growth factors in rat kidney', *J Cell Physiol*, 148(2), pp. 295-305.

Zlotnik, A. and Yoshie, O. (2000) 'Chemokines: a new classification system and their role in immunity', *Immunity*, 12(2), pp. 121-7.

Appendices

A. Verification of HS6ST1 sequence cloned in vector with HS6ST1 transfectants using reverse BGH primers

Score = 1652 bits (859), Expect = 0.0, Identities = 917/933 (98%), Gaps = 5/933 (0%) Strand=Plus/Minus

```
Que 570 ACTACATCACCCTGCTACGAGACCCCGTGTCCCGCTACCTGAGCGAGTGGCGGCATGTGC 629
        ||||||||||| |||||||||||   ||||| |||||||||||||||||||||||||
Sbj 986 ACTACATCACCN-GCTACGAGACCCCNNNTCCCGNTACCTGAGCGAGTGGCGGCATGTGC 928
Que 630 AGAGGGGTGCCACGTGGAAGACGTCGTTGCATATGTGTGATGGGCGCACGCCCACGCCTG 689
        |||||||| |||||| |||||||||||||||||||||||||||||||||||||||  |
Sbj 927 AGAGGGTN--CACGNG-AAGACGTCGTTGCATATGTGTGATGGGCGCACGCCCACGNN-G 872
Que 690 AGGAGCTGCCGCCCTGCTACGAGGGCACGGACTGGTCGGGCTGCACGCTACAGGAGTTCA 749
        ||||||||||||||||||||||||||||||||||||||||||||||||||||||||||||
Sbj 871 AGGAGCTGCCGCCCTGCTACGAGGGCACGGACTGGTCGGGCTGCACGCTACAGGAGTTCA 812
Que 750 TGGACTGCCCGTACAACCTGGCCAACAACCGCCAGGTGCGCATGCTGGCCGACCTGAGCC 809
        |||||||||||||||||||||||||||||||||||||||||||||||| ||||||
Sbj 811 TGGACTGCCCGTACAACCTGGCCAACAACCGCCAGGTGCGCATGCTGGCCGACNTGAGCC 752
Que 810 TGGTGGGCTGCTACAACCTGTCCTTCATCCCCGAGGGCAAGCGGGCCCAGCTGCTGCTCG 869
        ||||||||||||||||||||||||||||||||||||||||||||||||||||||||||||
Sbj 751 TGGTGGGCTGCTACAACCTGTCCTTCATCCCCGAGGGCAAGCGGGCCCAGCTGCTGCTCG 692
Que 870 AGAGCGCCAAGAAGAACCTGCGGGGCATGGCCTTCTTCGGCCTGACCGAGTTCCAGCGCA 929
        ||||||||||||||||||||||||||||||||||||||||||||||||||||||||||||
Sbj 691 AGAGCGCCAAGAAGAACCTGCGGGGCATGGCCTTCTTCGGCCTGACCGAGTTCCAGCGCA 632
Que 930 AGACGCAGTACCTGTTCGAGCGGACGTTCAACCTCAAGTTCATCCGGCCCTTCATGCAGT 989
        ||||||||||||||||||||||||||||||||||||||||||||||||||||||||||||
Sbj 631 AGACGCAGTACCTGTTCGAGCGGACGTTCAACCTCAAGTTCATCCGGCCCTTCATGCAGT 572
Que 990 ACAATAGCACGCGGGCGGGCGGCGTGGAGGTGGATGAAGACACCATCCGGCGCATCGAGG 1049
        ||||||||||||||||||||||||||||||||||||||||||||||||||||||||||||
Sbj 571 ACAATAGCACGCGGGCGGGCGGCGTGGAGGTGGATGAAGACACCATCCGGCGCATCGAGG 512
```

```
Que 1050 AGCTCAACGACCTGGACATGCAGCTGTACGACTACGCCAAGGACCTCTTCCAGCAGCGCT 1109
         ||||||||||||||||||||||||||||||||||||||||||||||||||||||||||||
Sbj 511 AGCTCAACGACCTGGACATGCAGCTGTACGACTACGCCAAGGACCTCTTCCAGCAGCGCT  452
Que 1110 ACCAGTACAAGCGGCAGCTGGAGCGCAGGGAGCAGCGCCTGAGGAGCCGCGAGGAGCGTC 1169
         ||||||||||||||||||||||||||||||||||||||||||||||||||||||||||||
Sbj 451 ACCAGTACAAGCGGCAGCTGGAGCGCAGGGAGCAGCGCCTGAGGAGCCGCGAGGAGCGTC 392
Que 1170 TGCTGCACCGGGCCAAGGAGGCACTGCCGCGGGAGGATGCCGACGAGCCGGGCCGCGTGC 1229
         ||||||||||||||||||||||||||||||||||||||||||||||||||||||||||||
Sbj 391 TGCTGCACCGGGCCAAGGAGGCACTGCCGCGGGAGGATGCCGACGAGCCGGGCCGCGTGC 332
Que 1230 CCACCGAGGACTACATGAGCCACATCATTGAGAAGTGGTAGTGGCGGTGGTGGCCACGGG 1289
         ||||||||||||||||||||||||||||||||||||||||||||||||||||||||||||
Sbj 331  CCACCGAGGACTACATGAGCCACATCATTGAGAAGTGGTAGTGGCGGTGGTGGCCACGGG 272
Que 1290 GAGGCCTCTTGGGGGGTGTGGGGGATAAAACAGGACAGACGACAGGTCCACCCAAGACTG 1349
         ||||||||||||||||||||||||||||||||||||||||||||||||||||||||||||
Sbj 271 GAGGCCTCTTGGGGGGTGTGGGGGATAAAACAGGACAGACGACAGGTCCACCCAAGACTG 212
Quey 1350 TCAAGGGATGAGCATCCCAAACCTGCTCCACAGAGGTAGCTGCGTCCTGAAAAAAAACAG 1409
          ||||||||||||||||||||||||||||||||||||||||||||||||||||||||||||
Sbjc 211 TCAAGGGATGAGCATCCCAAACCTGCTCCACAGAGGTAGCTGCGTCCTGAAAAAAAACAG 152
Query 1410 AGCAGGGATGTAGTGGGGCTGGGCAGGGATGGGGGCTTGAGAAATCAACAGGTGCAGCCC 1469
           ||||||||||||||||||||||||||||||||||||||||||||||||||||||||||||
Sbjct 151 AGCAGGGATGTAGTGGGGCTGGGCAGGGATGGGGGCTTGAGAAATCAACAGGTGCAGCCC 92
Query 1470 AGTGGGTCAGAGGAAAGCGTGCTCGAAGGATGC 1502
           ||||||||||||||||||||||||||||||||
Sbjct 91   AGTGGGTCAGAGGAAAGCGTGCTCGAAGGATGC 59
CPU time:     0.05 user secs.     0.03 sys. secs           0.08 total secs.
```

B. Insert SULF2 align with human SULF2 using –bGHR

Score = 1749 bits (947), Expect = 0.0, Identities = 998/1028 (97%), Gaps = 13/1028 (1%)

Strand=Plus/Plus, >lcl|62673, Length=1071

```
Que 2 GGGCCCCCCGAGCCTCGTGCTGTGCTTGCTGTCCGCAACTGTGTTCTCCCTGCTGGGTGG 61
      ||||||||||||||||||||||||||||||||||||||||||||||||||||||||||||||
Sbj 34 GGGCCCCCCGAGCCTCGTGCTGTGCTTGCTGTCCGCAACTGTGTTCTCCCTGCTGGGTGG 93
  Que  62  AAGCTCGGCCTTCCTGTCGCACCACCGCCTGAAAGGCAGGTTTCAGAGGGACCGCAGGAA  121
           ||||||||||||||||||||||||||||||||||||||||||||||||||||||||||||||
Sbj 94 AAGCTCGGCCTTCCTGTCGCACCACCGCCTGAAAGGCAGGTTTCAGAGGGACCGCAGGAA 153
  Que 122  CATCCGCCCCAACATCATCCTGGTGCTGACGGACGACCAGGATGTGGAGCTGGGTTCCAT  181
           ||||||||||||||||||||||||||||||||||||||||||||||||||||||||||||||
Sbj 154 CATCCGCCCCAACATCATCCTGGTGCTGACGGACGACCAGGATGTGGAGCTGGGTTCCAT 213
  Que 182  GCAGGTGATGAACAAGACCCGGCGCATCATGGAGCAGGGCGGGGCGCACTTCATCAACGC  241
           ||||||||||||||||||||||||||||||||||||||||||||||||||||||||||||||
Sbj 214 GCAGGTGATGAACAAGACCCGGCGCATCATGGAGCAGGGCGGGGCGCACTTCATCAACGC 273
Que 242 CTTCGTGACCACACCCATGTGCTGCCCCTCACGCTCCTCCATCCTCACTGGCAAGTACGT 301
          |||||||||||||||||||||||||||||||||||||||||||||| ||||||||||
Sbj 274 CTTCGTGACCACACCCATGTGCTGCCCCTCACGCTCCTCCATCCTCACCGGCAAGTACGT 333
Que 302 CCACAACCACAACACCTACACCAACAATGAGAACTGCTCCTCGCCCTCCTGGCAGGCACA 361
        ||||||||||||||||||||||||||||||||||||||||||||||||||||||||||||||
Sbj 334 CCACAACCACAACACCTACACCAACAATGAGAACTGCTCCTCGCCCTCCTGGCAGGCACA 393
Que 362 GCACGAGAGCCGCACCTTTGCCGTGTACCTCAATAGCACTGGCTACCGGACAGCTTTCTT 421
        ||||||||||||||||||||||||||||||||||||||||||||||||||||||||||||||
Sbj 394 GCACGAGAGCCGCACCTTTGCCGTGTACCTCAATAGCACTGGCTACCGGACAGCTTTCTT 453
Que 422 CGGGAAGTATCTTAATGAATACAACGGCTCCTACGTGCCACCCGGCTGGAAGGAGTGGGT 481
        ||||||||||||||||||||||||||||||||||||||||||||||||||||||||||||||
Sb 454 CGGGAAGTATCTTAATGAATACAACGGCTCCTACGTGCCACCCGGCTGGAAGGAGTGGGT 513
Que 482 CGGACTCCTTAAAAACTCCCGCTTTTATAACTACACGCTGTGTCGGAACGGGGTGAAAGA 541
        ||||||||||||||||||||||||||||||||||||||||||||||||||||||||||||||
Sbj 514 CGGACTCCTTAAAAACTCCCGCTTTTATAACTACACGCTGTGTCGGAACGGGGTGAAAGA 573
```

```
Que 542 GAAGCACGGCTCCGACTACTCCAAGGATTACCTCACAGACCTCATCACCAATGACAGCGT 601
        ||||||||||||||||||||||||||||||||||||||||||||||||||||||||||||
Sbj 574 GAAGCACGGCTCCGACTACTCCAAGGATTACCTCACAGACCTCATCACCAATGACAGCGT 633
Que 602 GAGCTTCTTCCGCACGTCCAAGAAGATGTACCCGCACAGGCCAGTCCTCATGGTCATCAG 661
        ||||||||||||||||||||||||||||||||||||||||||||||||||||||||||||
Sbj 634 GAGCTTCTTCCGCACGTCCAAGAAGATGTACCCGCACAGGCCAGTCCTCATGGTCATCAG 693
Que 662 CCATGCAGCCCCCCACGGCCCTGAGGATTCAGCCCCACAATATTCACGCCTCTTCCCAAA 721
        ||||||||||||||||||||||||||||||||||||||||||||||||||||||||||||
Sbj 694 CCATGCAGCCCCCCACGGCCCTGAGGATTCAGCCCCACAATATTCACGCCTCTTCCCAAA 753
Que 722 CGCATCTCAGCACATCACGCCGAGCTACAACTACGCGCCCAACCCGGACAAACACTGGAT 781
        ||||||||||||||||||||||||||||||||||||||||||||||||||||||||||||
Sbj 754 CGCATCTCAGCACATCACGCCGAGCTACAACTACGCGCCCAACCCGGACAAACACTGGAT 813
Que 782 CATGCGCTACACGGGGCCCATGAAGCCCATCCACATGGAATTCACCAACATGCTCCAGCG 841
        ||||||||||||||||||||||||||||||||||||||||||||||||||||||||||||
Sbj 814 CATGCGCTACACGGGGCCCATGAAGCCCATCCACATGGAATTCACCAACATGCTCCAGCG 873
Que 842 GAAGCGCTTGCAGACCCTCATGTCGGTGGACGACTCCATGGAGACGATTTACAACATGCT 901
        |||||||||||||||||||||||||||||||||||||||||||| ||||||||||||||
Sbj 874 GAAGCGCTTGCAGACCCTCATGTCGGTGGACGACTCCATGGAGACNATTTACAACATGCT 933
Que 902 GG-TTGAGACGGGCGAGCT-GGACAACACGTACATCGTATACACCGCCGACCACGGTTAC 959
        || |||||| ||||||||| ||| |  ||||||||||||||||||||||||||     |
Sbj 934 GGNTTGAGANGGGCGAGCTNGGANAN-ACGTACATCGTATACACCGCCGACCACNNN--C 990
Qu 960 CACATCGGCCAGTTTGGCCTGGTGAAAGGGAAATCCATGCCATATGAGTTTGAC ATCAG 1018
          ||||| |    ||||     |  |||||| |||||||||||||||||||  ||  ||| |
Sb 991 CACATNGNN--GTTTNNN--GN-GAAAGG-AAATCCATGCCATATGAGTT-GANNATCNG 1043
Query 1019 GGTCCCGT 1026
           ||||||||
Sbjct 1044 GGTCCCGT 1051
```

C. HS structure analysis (S^{35})

Gel filtration
Superose 12

before and after degradation of chondroitinsulfate with chase ABC

Superose 12 0.5 M NH_4HCO_3. 0.5 ml/min/ fraktion
5/1 -11
Sample 1, ca 10000 cpm

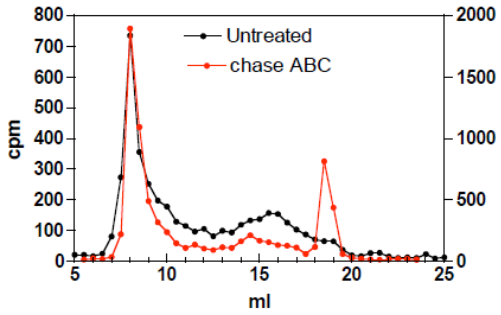

Superose 12 0.5 M NH_4HCO_3. 0.5 ml/min/ fraktion
10/1 -11
Sample 2, 10000 cpm

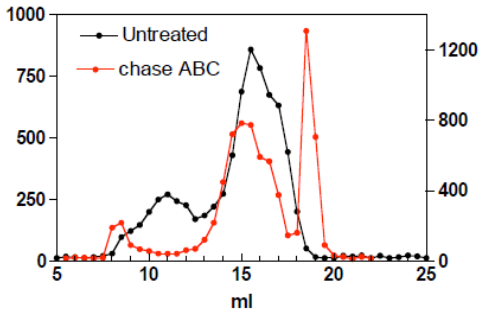

Superose 12 0.5 M NH_4HCO_3. 0.5 ml/min/ fraktion
10/1 -11
Sample 3, 10000 cpm chase ABC

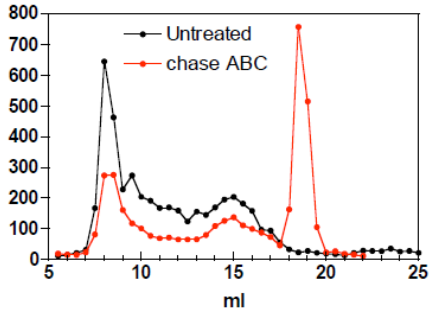

Superose 12 0.5 M NH_4HCO_3. 0.5 ml/min/ fraktion
10/1 -11
Sample 4, 10000 cpm chase ABC

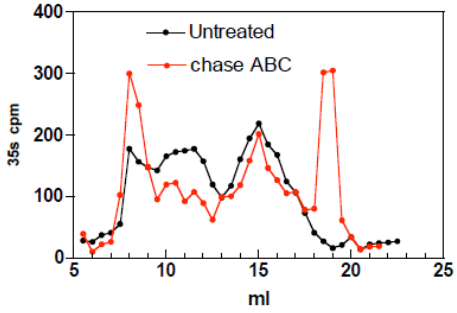

Nitrous acid deamination/$NaBH_4$ reduction
Preparative G15 gel chromatography
to isolate disaccharides for compositional analysis

Sample 1, 200000 cpm HNO_2 pH1.5/$NaBH_4$
G15 0.2 M NH_4HCO_3. ~1.6 ml/10min/ fraktion
16/1 -11

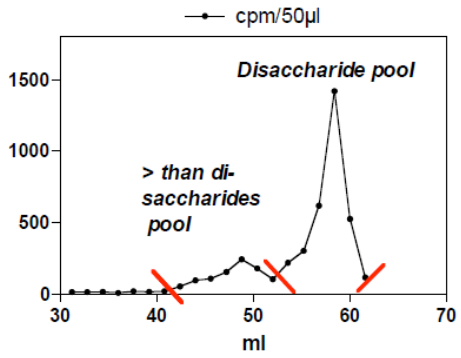

Sample 2, 850000 cpm HNO_2 pH1.5/$NaBH_4$
G15 0.2 M NH_4HCO_3. ~1.6 ml/10min/ fraktion
17/1 -11

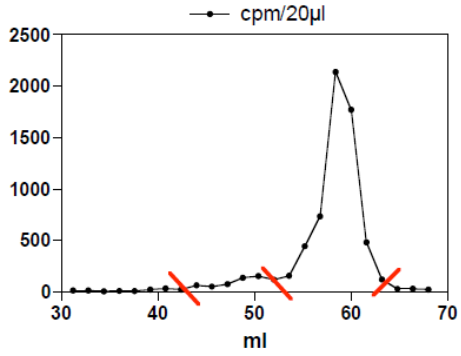

Sample 3, 290000 cpm HNO_2 pH1.5/$NaBH_4$
G15 0.2 M NH_4HCO_3. ~1.6 ml/10min/ fraction
26/1 -11

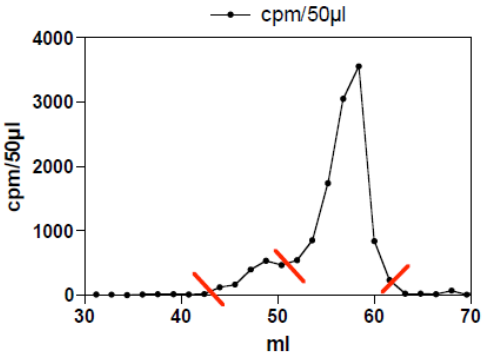

Sample 4, 650000 cpm HNO_2 pH1.5/$NaBH_4$
G15 0.2 M NH_4HCO_3. ~1.7 ml/10min/ fraktion
31/1 -11

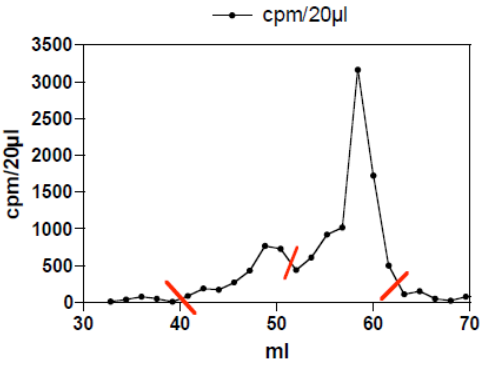

heparan sulfate disaccharide
compositional analysis on a strong anion-exchange column

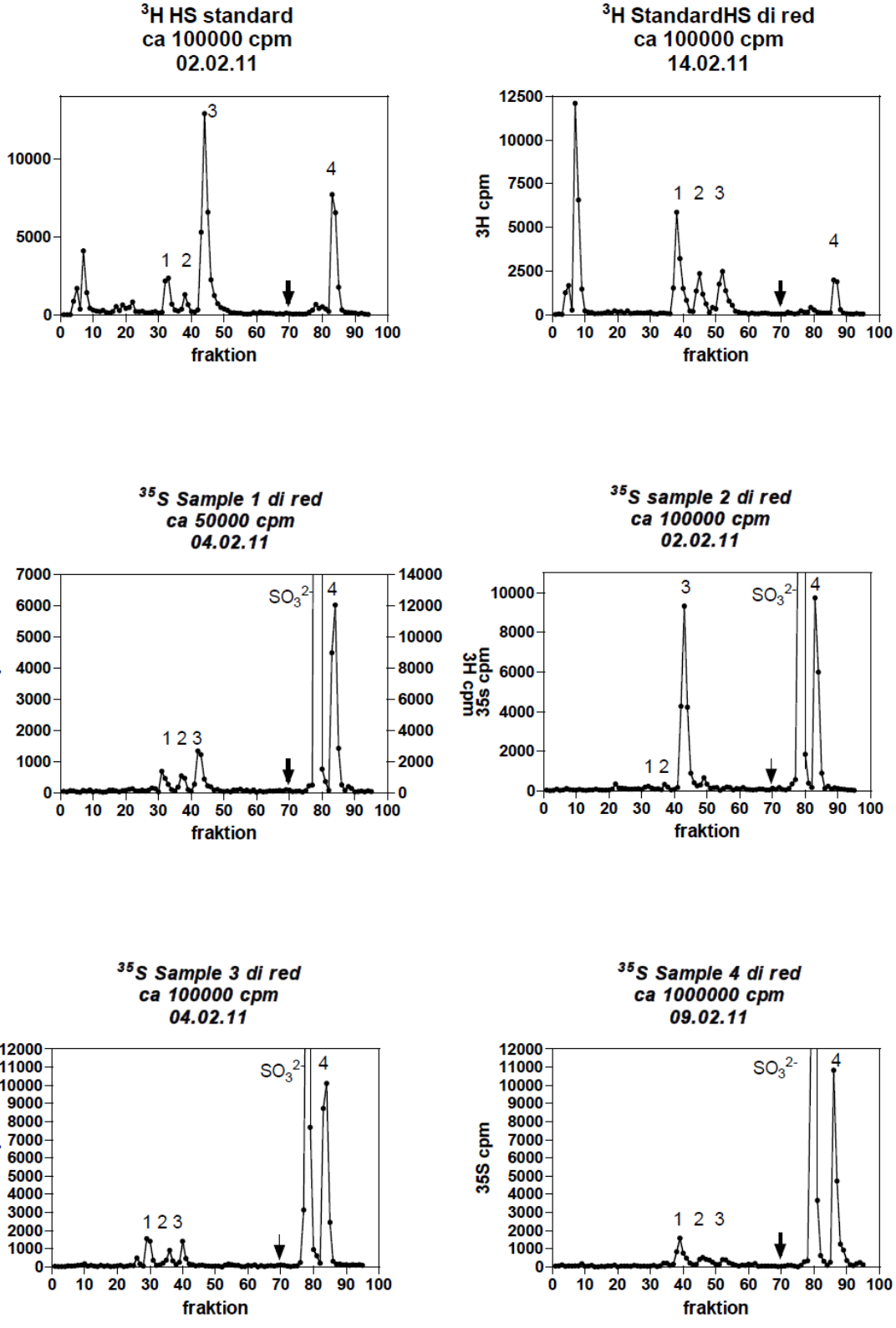

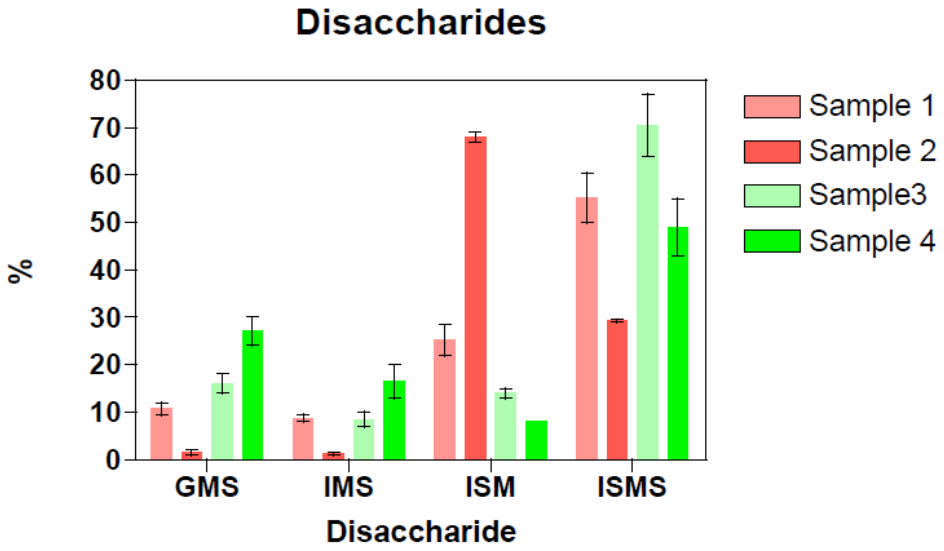

Disaccharide	*SULF2C*	*SULF2+*	*6OST1C*	*6OST1+*
		% of O-^{35}S labeled disaccharides		
GMS	***13 ± 1***	***1.5 ± 0.5***	***16 ± 2***	***27 ± 3***
IMS	***10 ± 1***	***1.3 ± 0.2***	***8.5 ± 1.5***	***16.5 ± 3.5***
ISM	***30 ± 2***	***68 ± 1***	***14 ± 1***	***8 ± 0***
ISMS	***46.5 ± 3.5***	***29 ± 0.3***	***70.5 ± 6.5***	***49 ± 6***

	SULF2C	SULF2+	6OST1C	6OST1+
	% of O-^{35}S labeled disaccharides			
2-O containing disaccharides	***76***	***97***	***84***	***57***
6-O containing disaccharides	***69***	***32***	***95***	***92***

C, mock transfected

+, overexpressing cells

D. HS6ST1 transfectants binding to CCL5

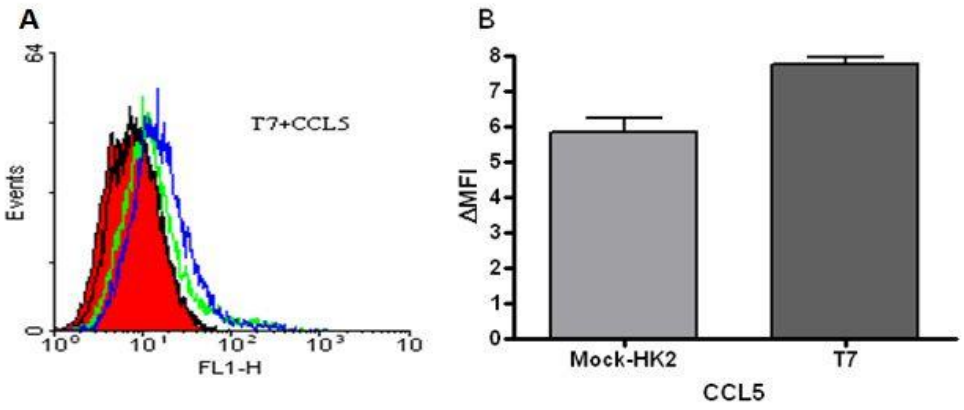

E. Publication arising from this study

a. Oral presentation

b. Abd A. Alhasan, Julia Spielhofer, Marion Kusche-Gullberg, Simi Ali, John A. Kirby. "The role of heparan sulphate sulphation pattern in renal chronic rejection". The 7th international conference on proteoglycans, October 2011, Sydney, Australia.

c. Abd Alhasan, Simi Ali, John Kirby "Examination of the role of heparan sulphate as a key regulator of allograft inflammation" North east postgraduate conference (NEPG), Newcastle, 2009, UK.

b. Published abstracts

1. Abd. A. Alhasan, Marion Kusch-Gullberg, Simi Ali, John Kirby, "The role of Heparan Sulphate sulphation pattern in renal chronic rejection" British Society for Matrix Biology (MSMB) Conference, Newcastle Upon Tyne, September 2011, UK (poster)
2. Abd A. Alhasan, Simi Ali, John Kirby "Examination of the role of heparan sulphate as a key regulator of allograft inflammation and remodelling" British society of immunology (BSI) conference, Liverpool, December 2010, UK (poster)
3. Abd Alhasan, Simi Ali, John Kirby "The Role of heparan sulphate 6-O sulphotransferase (HS6ST1) in inflammatory response" the 6th proteoglycan international conference, September 2009, France (poster).

F. Prizes

Abd A. Alhasan, Julia Spielhofer, Simi Ali, John Kirby "Examination of the role of heparan sulphate as a key regulator of allograft inflammation and remodelling". Poster prize, Poster session in the institute of cellular medicine (ICM), Newcastle University, 2010, UK